



University
of Glasgow

Tonn, Daniela (2010) *Intracellular trafficking of Leishmania major peptidases*. PhD thesis.

<http://theses.gla.ac.uk/1649/>

Copyright and moral rights for this thesis are retained by the author

A copy can be downloaded for personal non-commercial research or study, without prior permission or charge

This thesis cannot be reproduced or quoted extensively from without first obtaining permission in writing from the Author

The content must not be changed in any way or sold commercially in any format or medium without the formal permission of the Author

When referring to this work, full bibliographic details including the author, title, awarding institution and date of the thesis must be given

Intracellular trafficking of *Leishmania major* peptidases

Daniela Tonn
Dipl.-Biol.

**Submitted in fulfilment of the requirements
for the Degree of PhD**

**Division of Infection and Immunity
Faculty of Biomedical and Life Sciences
University of Glasgow**

December 2009

Abstract

Leishmania resides inside mammalian macrophages, from where it is thought to manipulate the host immune system by releasing virulence factors. The cysteine peptidase CPB has been shown to be secreted by the parasite and act as such a virulence factor. CPB is released through the flagellar pocket while being trafficked to the lysosome. Thus, in this project, the intracellular localisations of eight other *L. major* peptidases were analysed by fluorescence microscopy, after tagging the enzymes with green fluorescent protein (GFP). The candidate peptidases were chosen by bioinformatics analyses and predictions of N-terminal secretory signal peptides and potential transmembrane domains. The aim was to find a peptidase accumulating in the flagellar pocket of the cell, from where it could be secreted. Five candidate peptidases (a ubiquitin hydrolase, a CaaX prenyl protease, a zinc carboxypeptidase and two rhomboid peptidases) localised to the mitochondrion, which was unexpected. Another, a calpain-like peptidase, localised to the flagellum but not to the flagellar pocket. A serine carboxypeptidase was found very close to the flagellar pocket, possibly in small vesicles budding off or fusing with the pocket membrane, but did not co-localise with a flagellar pocket marker. The bioinformatics predictions differed from the experimental results here and, additionally, using different algorithms to predict protein properties resulted in contradictory predictions in several cases. This suggests that generic protein prediction programmes for mammalian or higher eukaryotic proteins can be unreliable and of limited usefulness for *Leishmania* proteins. This corroborates the notion that *Leishmania* may use novel, non-classical secretory pathways rather than or in addition to those characterised for higher eukaryotes.

The *L. major* Bem46-like serine peptidase (LmjF35.4020) of the Clan SC (Family S9) was the only candidate peptidase that localised to the flagellar pocket when labelled with GFP. This was an indication that this enzyme may be released from the cell and could act as a virulence factor. Alternatively, it may be a resident protein of the flagellar pocket. Deleting the *Bem46* gene in *L. major* did not have a measurable effect on promastigote growth or on footpad lesion development in mice inoculated with *Bem46*-deficient cells, so it does not appear to play a role as a major virulence factor.

Apart from the secretion of virulence factors, rapid protein turnover, e.g. in the lysosome, is important for the infectivity of *Leishmania*. To investigate lysosome structure and function in *L. major*, a potential LMP (lysosomal membrane protein) was identified by bioinformatics. Thus far, no resident membrane proteins of the *Leishmania* lysosome are known and identifying such a protein would provide a useful marker for the closer investigation of this important organelle. In this project, the location and role of the LMP protein LmjF30.2670 was investigated using GFP-tagging and fluorescence microscopy. The experiments showed that LMP is not lysosomal in *L. major*, rather, it could be observed localising to a distinct, elongated and sometimes doughnut-shaped structure in close proximity to the kinetoplast. This structure was not directly associated with the flagellar pocket or the cell membrane, its position in the cell was variable within a certain area alongside the kinetoplast, it appeared to duplicate during cell division and it did not co-localise with the endocytic / lysosomal marker FM4-64. Deletion of the *LMP* gene did not have any effect on promastigote growth in cell culture and only a small and transient slowing effect on the development of mouse footpad lesions after inoculation with LMP-deficient *L. major*. Lysosomal membrane proteins can be targeted to the lysosome by the protein carrier complex AP3, which binds to tyrosine or dileucine motifs in cargo proteins. LMP contains two such tyrosine motifs at its C-terminus, but disruption of these by site-directed mutagenesis did not affect LMP localisation, suggesting that its trafficking is AP3-independent, which is in accordance with the non-lysosomal localisation of LMP.

Finally, the lysosome-like acidocalcisome organelles have previously been shown to rely on the protein carrier complex AP3 for normal structure and function. In AP3-deficient *Leishmania*, the acidocalcisomes are defective and, at the same time, parasite virulence is markedly reduced (Besteiro et al., 2008o). To analyse how AP3 is important for acidocalcisome morphology and function, a proton pump of the acidocalcisomal membrane, the V-H⁺-PPase, was investigated by GFP-labelling and fluorescence microscopy. In wild type *L. major* the V-H⁺-PPase could be shown to localise to the acidocalcisomes, whereas in AP3-deficient cells it was not detectable, suggesting that the protein is mislocalised and likely degraded. The V-H⁺-PPase also contains several tyrosine motifs that may interact with AP3. The two most prominent of these were disrupted by site-directed

mutagenesis, but this did not affect the localisation of the V-H⁺-PPase, suggesting that these two sites are not, or not solely, important for AP3 binding or that the V-H⁺-PPase is not bound by AP3 directly.

Table of Contents

1. Introduction	16
1.1 The <i>Leishmania</i> parasite	16
1.1.1 The <i>Leishmania</i> life cycle	16
1.2 Leishmaniasis and treatment	18
1.2.1 The leishmaniasis	18
1.2.2 Treatment and vaccination	20
1.3 Genomes and genetics	21
1.4 Host-parasite interactions of <i>Leishmania</i>	23
1.4.1 The mammalian immune response	23
1.4.2 <i>Leishmania</i> and its mammalian host cells	24
1.4.3 <i>Leishmania</i> and the sand fly vector	26
1.5 Virulence factors	27
1.5.1 Surface-bound virulence factors	27
1.5.2 Secreted or released virulence factors	28
1.5.3 Intracellular virulence factors ("pathoantigens")	30
1.6 <i>Leishmania</i> peptidases	31
1.6.1 <i>Leishmania</i> cysteine peptidase B (CBP)	32
1.7 The <i>Leishmania</i> cell	34
1.7.1 The flagellar pocket	35
1.7.2 Intracellular protein trafficking	36
1.7.3 The lysosome	39
1.7.4 Protein trafficking to the lysosome	41
1.7.5 The acidocalcisomes	42
1.7.6 The adaptor protein (AP) complexes	44
1.8 Aims of project	46
2. Material and Methods	47
2.1 Bioinformatics	47
2.1.1 Gene DB	47
2.1.2 Vector NTI	47
2.1.3 DNA Sequencing	47
2.1.4 Predictions of protein properties and topologies	47
2.2 Molecular biology	49
2.2.1 Polymerase Chain Reactions (PCRs) and oligonucleotides	49
2.2.2 DNA vectors used in this study	53
2.2.3 Restriction endonuclease digestions	55
2.2.4 Agarose gel electrophoresis	55
2.2.5 Ligations	56
2.2.6 Transformations	56
2.2.7 Site-directed mutageneses of plasmids	57
2.2.8 DNA isolation from bacteria and plasmid preparation for transfections	57
2.2.9 RNA isolation	58
2.2.10 Reverse Transcriptase (RT-) PCR	58
2.2.11 Targeted gene replacement in <i>Leishmania</i>	58

2.2.12	Southern Blotting.....	59
2.3	Bacterial cultures.....	60
2.3.1	<i>E. coli</i> cell lines used in this study	60
2.3.2	Generation of competent <i>E. coli</i> cell lines.....	60
2.3.3	Bacterial cultures	61
2.3.4	Bacterial cell extracts	62
2.4	Protein biochemistry	62
2.4.1	Denaturing polyacrylamide gel electrophoresis (SDS-PAGE)	62
2.4.2	Coomassie staining of SDS-PAGE gel.....	63
2.4.3	Western Blotting.....	63
2.4.4	Protein purifications	64
2.4.5	Protein quantification	65
2.4.6	Antibody production, purification and quality assessment	65
2.5	<i>Leishmania</i> cell culture	66
2.5.1	<i>Leishmania</i> promastigote culture.....	66
2.5.2	Determination of <i>L. major</i> cell densities.....	67
2.5.3	<i>Leishmania</i> stabilates.....	67
2.5.4	Transfection, selection and cloning.....	67
2.5.5	<i>Leishmania</i> DNA isolation	68
2.5.6	<i>Leishmania</i> cell extracts	69
2.5.7	Mouse infections and parasite harvests from foot pads.....	69
2.6	Fluorescence microscopy	70
2.6.1	The DeltaVision System.....	70
2.6.2	Live cell imaging sample preparation	70
2.6.3	Fixing of cells	71
2.6.4	Immunofluorescence analysis (IFA).....	72
2.7	Statistical data analysis.....	72
3.	Screen for peptidases secreted by <i>Leishmania</i>	73
3.1	Introduction.....	73
3.1.1	Secretion of proteins	73
3.1.2	Targeting of proteins to the mitochondrion	74
3.1.3	Bioinformatics prediction of protein properties.....	75
3.2	Results.....	77
3.2.1	Bioinformatics analyses of candidate peptidases	77
3.2.2	Cloning of GFP fusion proteins and fluorescence microscopy.....	86
3.3	Discussion.....	91
4.	The <i>Leishmania</i> Bem46-like serine peptidase	98
4.1	Introduction.....	98
4.1.1	Bem46-like peptidases.....	98
4.1.2	The S9 family of peptidases	99
4.2	Results.....	100
4.2.1	Bioinformatics analyses of <i>L. major</i> Bem46	100
4.2.2	Fluorescence microscopy.....	107
4.2.3	Deletion of <i>Bem46</i> gene in <i>L. major</i>	109
4.2.4	Expression and purification of recombinant Bem46	112
4.2.5	Expression and purification of soluble recombinant Bem46.....	116
4.3	Discussion.....	117

5. Membrane proteins of the <i>Leishmania</i> lysosome and of the lysosome-like acidocalcisomes	121
5.1 Introduction.....	121
5.1.1 The <i>Leishmania</i> lysosome	121
5.1.2 Lysosome-Associated Membrane Proteins (LAMPs).....	122
5.1.3 The protein carrier complex AP3	124
5.1.4 Tyrosine-based protein sorting signals.....	127
5.1.5 The vacuolar pyrophosphatase of the acidocalcisomes	128
5.2 Results: The <i>L. major</i> LAMP-like protein	130
5.2.1 Identification and bioinformatics analysis of <i>L. major</i> LAMP-like protein	130
5.2.2 Cloning and GFP labelling of LAMP-like protein	135
5.2.3 Fluorescence microscopy.....	136
5.2.4 Mutagenesis of tyrosine motifs.....	141
5.2.5 Deletion of LAMP-like gene in <i>L. major</i>	142
5.3 Results: The <i>L. major</i> acidocalcisomal V-H ⁺ -PPase	146
5.3.1 Cloning and GFP labelling of V-H ⁺ -PPase	146
5.3.2 Fluorescence microscopy.....	146
5.3.3 Mutagenesis of tyrosine motifs.....	148
5.3.4 Confirmation of GFP expression in all V-H ⁺ -PPase cell lines	149
5.4 Discussion.....	150
5.4.1 The LAMP-like protein (LMP)	150
5.4.2 The acidocalcisomal V-H ⁺ -PPase	154
6. Final Conclusions.....	157
7. Appendix	162
Publication:	
Besteiro S, Tonn D, Tetley L, Coombs GH and Mottram JC (2008)	
The AP3 adaptor is involved in the transport of membrane proteins to acidocalcisomes of <i>Leishmania</i> . <i>Journal of Cell Science</i> 121 (5)	162
8. References	172

List of Tables

1. Introduction

Table 1-1: Examples of clinically important species of <i>Leishmania</i>	20
--	----

2. Material and Methods

Table 2-1: All protein prediction and sequence analysis tools, algorithms and databases used in this study	48
--	----

Table 2-2: All oligonucleotide primers used in this study	50
---	----

Table 2-3: All plasmids generated and used in this study	54
--	----

3. Screen for peptidases secreted by *Leishmania*

Table 3-1: All analysed putative peptidases from the <i>L. major</i> genome with prediction of signal peptide and status for candidate selection process	81
--	----

Table 3-2: Details of all candidate peptidases	83
--	----

Table 3-3: Predictions of secretory and mitochondrial sorting signals for all candidate peptidases.....	84
---	----

Table 3-4: Predictions of transmembrane domains and GPI anchoring sites for all candidate peptidases.....	85
---	----

4. The *Leishmania* Bem46 serine peptidase

5. Membrane proteins of the *Leishmania* lysosome and of the lysosome-like acidocalcisomes

Table 5-1: Characteristics of <i>L. major</i> LMP gene and protein	135
--	-----

List of Figures

1. Introduction

Figure 1-1: <i>Leishmania</i> life cycle.....	17
Figure 1-2: Female mounted <i>Phlebotomus sp.</i> sand fly.	18
Figure 1-3: Map of worldwide distribution of leishmaniases.....	19
Figure 1-4: Putative mechanisms of <i>Leishmania</i> uptake into macrophages.....	25
Figure 1-5: Clans and families of all identified <i>L. major</i> peptidases.....	32
Figure 1-6: Overview of <i>Leishmania</i> promastigote with organelles.....	34
Figure 1-7: Schematic of acidocalcisome organelle.....	44

2. Material and Methods

3. Screen for peptidases secreted by *Leishmania*

Figure 3-1: Live cell deconvolution microscopy images of five <i>L. major</i> cell lines expressing different GFP-fusion proteins.....	87
Figure 3-2: Deconvolution microscopy images of <i>L. major</i> cell line expressing GFP-tagged calpain.....	88
Figure 3-3: Fixed cell deconvolution microscopy images of <i>L. major</i> cell line expressing GFP-tagged serine carboxypeptidase.	89
Figure 3-4: Fixed cell deconvolution microscopy images of <i>L. major</i> cell line expressing GFP-tagged Bem46 peptidase.	90

4. The *Leishmania* Bem46 serine peptidase

Figure 4-1: S9 peptidase family members including Bem46..	100
Figure 4-2: Sequence alignment of <i>L. major</i> Bem46 with several other Bem46 proteins.....	103
Figure 4-3: Prediction of <i>L. major</i> Bem46 protein topology, predicted using the SOSUI algorithm.....	104
Figure 4-4: Prediction of <i>L. major</i> Bem46 protein topology, predicted using the HMMTOP algorithm and visualised using TMPres2D.....	105
Figure 4-5: Prediction of <i>L. major</i> Bem46 protein topology, predicted using the TMHMM algorithm.....	106
Figure 4-6: Prediction of <i>L. major</i> Bem46 protein topology, predicted using the Phobius algorithm.....	106
Figure 4-7: <i>L. major</i> Bem46 protein sequence with all annotations.....	107

Figure 4-8: Deconvolution fluorescence microscopy image of <i>L. major</i> co-expressing an extrachromosomal Bem46-GFP fusion protein and a red fluorescent HASPB-mCherry fusion protein	108
Figure 4-9: As in figure 4-8, magnification of flagellar pocket area of cell	108
Figure 4-10: Strategy for PCR and Southern blot analyses of potential Δ <i>bem46</i> clones.....	109
Figure 4-11: Analysis of potential Δ <i>bem46</i> mutant clones by PCR and Southern blotting	110
Figure 4-12: <i>In vitro</i> growth curve of promastigote cultures of wild type <i>L. major</i> and Δ <i>bem46</i> cells.....	111
Figure 4-13: Measurements of footpad lesion development of BALB/c mice after infection with wild type <i>L. major</i> and Δ <i>bem46</i> cells	112
Figure 4-14: Protein purification fractions after denaturing urea extraction of recombinant Bem46	113
Figure 4-15: Western immunoblot of recombinant <i>L. major</i> Bem46 and <i>L. major</i> whole cell lysate, probed with anti-Bem46 antibody	114
Figure 4-16: Western immunoblot of <i>L. major</i> whole cell lysates, probed with anti-Bem46 antibody	114
Figure 4-17: Immunofluorescence microscopy of <i>L. major</i> using anti-Bem46 antibody	115
Figure 4-18: Purified truncated recombinant Bem46	116

5. Membrane proteins of the *Leishmania* lysosome and of the lysosome-like acidocalcisomes

Figure 5-1: Schematic of mouse LAMP-2	123
Figure 5-2: Schematic of the AP3 complex	125
Figure 5-3: Prediction of V-H ⁺ -PPase protein topology. Predicted using HMMTOP and visualised with TMPres2D.....	129
Figure 5-4: Alignment of <i>L. major</i> LMP and human LAMP-2A sequences.....	131
Figure 5-5: Prediction of <i>L. major</i> LMP protein topology, predicted using the SOSUI algorithm	132
Figure 5-6: Prediction of <i>L. major</i> LMP protein topology, predicted using the TMHMM algorithm.....	132
Figure 5-7: Prediction of <i>L. major</i> LMP protein topology, predicted using the HMMTOP algorithm and visualised using TMPres2D.....	133
Figure 5-8: Prediction of <i>L. major</i> LMP protein topology, predicted using the Phobius algorithm.....	134
Figure 5-9: <i>L. major</i> LMP protein sequence with annotations	134
Figure 5-10: Live cell deconvolution fluorescence microscopy images of <i>L. major</i> expressing GFP-tagged full-length LMP protein and stained with FM4-64	137
Figure 5-11: Live cell deconvolution fluorescence microscopy images of <i>L. major</i> expressing the "LAMPends" fusion protein	137

Figure 5-12: Live cell deconvolution fluorescence microscopy image of dividing <i>L. major</i> cell expressing the "LAMPends" fusion protein.....	138
Figure 5-13: Live cell deconvolution fluorescence microscopy images of <i>L. major</i> expressing the "LAMPends" fusion protein and stained with FM4-64	138
Figure 5-14: Live cell deconvolution fluorescence microscopy image of <i>L. major</i> co-expressing the "LAMPends" GFP fusion protein and a red fluorescent HASPB-mCherry fusion protein	139
Figure 5-15: Live cell deconvolution fluorescence microscopy images of <i>L. major</i> $\Delta ap3\delta$ cells expressing GFP-tagged full-length LMP	140
Figure 5-16: Live cell deconvolution fluorescence microscopy images of <i>L. major</i> $\Delta ap3\delta$ cells expressing GFP-tagged "LAMPends" fusion protein.	140
Figure 5-17: Live cell deconvolution fluorescence microscopy images of <i>L. major</i> wild type cells expressing GFP-tagged "LAMPends" fusion protein with C-terminal tyrosine motifs mutated.	141
Figure 5-18: Strategy for PCR analysis of potential Δlmp clones	143
Figure 5-19: PCR analysis of potential Δlmp clones BH3, BH4, HB1 and HB4 and a wild type DNA control.....	143
Figure 5-20: Strategy for Southern blot	144
Figure 5-21: Southern blot analysis of Δlmp clones	144
Figure 5-22: <i>In vitro</i> growth curve of promastigote cultures of wild type <i>L. major</i> and Δlmp cells	145
Figure 5-23: Measurements of footpad lesion development of BALB/c mice after infection with wild type <i>L. major</i> and Δlmp cells	145
Figure 5-24: Live cell deconvolution fluorescence microscopy images of <i>L. major</i> expressing GFP-tagged V-H ⁺ -PPase.....	147
Figure 5-25: Live cell deconvolution fluorescence microscopy images of <i>L. major</i> wild type and $\Delta ap3\delta$ mutant cell lines, expressing GFP-tagged V-H ⁺ -PPase	147
Figure 5-26: Live cell deconvolution fluorescence microscopy images of <i>L. major</i> expressing GFP-tagged V-H ⁺ -PPase with mutated tyrosine sites	148
Figure 5-27: Agarose gel of RT-PCR products.	149

Acknowledgements

I would like to thank my supervisor Prof Jeremy Mottram for the opportunity to work in his lab, for his constant support, patience and advice. "JCM lab" has been a great place to work and learn and I have thoroughly enjoyed my time here. I would also like to thank my co-supervisor Prof Graham Coombs for encouraging me to come and work in Glasgow in the first place and for advice throughout the years. And I'm grateful to my assessors Richard McCulloch and Mike Turner for being so helpful and encouraging.

A big thank you goes to Seb Besteiro, who taught me so much and made sure I got off to a good start in the lab, as well as to Lesley Morrison who was a great bench mate and helped me with so many things over the years.

For lots of help and at least as much fun, I'd like to thank the current and previous "Mottramites" Will, Elaine, Kerry, Elmarie, Esther, Nath, Yuk-Chien, Jim H and Jim S, Cathy, Jana, Ben, Nick, Alan, Laurence, Rod, Federico, Raquel, Tatiana and Ana-Paula. As well as the people of the Hammarton, Mueller, Barry, McCulloch, Doerig and Barrett labs and Jane, Glynn, Barbara, Tomas and Svenja who shared the coldest office in the world with me.

More thanks to Mona, Will and Eileen, Dave, Chris, Frank, Johannes, Tobi, the Glasgow Drum Circle and Voicebeat for good times, stem tables, munro-bagging, slack-lining, music, keeping me sane and being such good friends. I will miss you a lot, my time in Glasgow would never have been the same without you. For many years of friendship, heartfelt thanks also go to Leo and Sara, Marion, Sane and Sarah. Thanks so much for staying with me over the years!

And last, but never least, special thanks go to my parents and Jackie. I am only here now because you have made it possible for me, because you have been so incredibly supportive, so encouraging and always there for me. Thank you for all your love and support, for believing in me, as well as for a million phonecalls and parcels... Thank you!

Author's Declaration

The research reported in this thesis is the result of my own original work, except where stated otherwise, and has not been submitted for any other degree.

Daniela Tonn, December 2009

Definitions and abbreviations

aa	amino acid
AP	adaptor protein complex
bp	base pair
BSA	bovine serum albumin
BLEO	bleomycin / phleomycin
CL	cutaneous leishmaniasis
CPA / B / C	cysteine peptidase A / B / C
DABCO	4-diazabicyclo[2.2.2]octane
DAPI	4,6-diamidino-2-phenylindole (nucleic acid stain)
DMSO	dimethyl sulfoxide
DNA	desoxyribonucleic acid
DTT	dithiothreitol
EDTA	ethylene diamine tetra acetic acid
ER	endoplasmic reticulum
ERAD	ER-associated degradation
FM4-64	N-(3-triethylammoniumpropyl)-4-(6-(4-(diethylamino)-phenyl)hexatrienyl) pyridinium dibromide (endocytic stain)
fPPG	filamentous proteophosphoglycan
GFP	green fluorescent protein
GPI	glycosylphosphatidylinositol
HIFCS	heat-inactivated fetal calf serum
HYG	hygromycin B
HRP	horseradish peroxidase
IL	interleukin
IPTG	isopropyl- β -D-thiogalactopyranoside
kb	kilo base
kDa	kilo Dalton
LAMP	lysosome-associated membrane protein
LB	Luria broth medium
LMP	putative LAMP-like protein
LPG	lipophosphoglycan
LROs	lysosome-related organelles
λ (λ_{Ex} / λ_{Em})	wavelength (excitation λ / emission λ)
μ	micro
m	milli / metre
M	molar
Mb	megabasepairs
min / mins	minute / minutes
MCL	muco-cutaneous leishmaniasis
MHC	major histocompatibility complex
mRNA	messenger RNA
MVT	multivesicular tubule
n	nano
NEO	neomycin (G418)
nt	nucleotide
OD	optical density
p	pico
PBS	phosphate buffered saline

PCR	polymerase chain reaction
PSG	parasite secretory gel
RNA	ribonucleic acid
SAP / SAcP	secretory acid phosphatase
SDS-PAGE	sodium dodecyl sulphate polyacrylamide gel electrophoresis
sec	second
SPase I	signal peptide peptidase I
SRP	signal recognition particle
Th1 / 2	T helper cell type 1 / 2
Triton X-100	t-octylphenoxy-polyethoxyl-ethanol
UV	ultra violet
V	volts
V-H ⁺ -PPase	vacuolar proton pyrophosphatase
VL	visceral leishmaniasis
v/v	volume to volume
w/v	weight to volume
WHO	world health organisation
WT	wild type

Amino acid abbreviations used in this study

A	alanine (Ala)
a	an aliphatic amino acid (I, L or V)
C	cysteine (Cys)
D	aspartic acid (Asp)
E	glutamic acid (Glu)
F	phenylalanine (Phe)
G	glycine (Gly)
H	histidine (His)
I	isoleucine (Ile)
K	lysine (Lys)
L	leucine (Leu)
M	methionine (Met)
N	asparagine (Asn)
P	proline (Pro)
Q	glutamine (Gln)
R	arginine (Arg)
S	serine (Ser)
T	threonine (Thr)
V	valine (V)
W	tryptophan (Trp)
X	any amino acid
Y	tyrosine (Tyr)
∅	a bulky hydrophobic amino acid (L, I, F, V or M)

1. Introduction

1.1 The *Leishmania* parasite

Protozoan parasites of the genus *Leishmania* are the causative agent of leishmaniasis in humans and other mammals. They are grouped into the order of Kinetoplastida and the family of Trypanosomatidae, together with parasites of the genus *Trypanosoma*, the causative agents of African Sleeping Sickness (*T. brucei*) and Chagas' disease in South America (*T. cruzi*).

1.1.1 The *Leishmania* life cycle

The transmitting vectors of *Leishmania* are bloodsucking female sand flies (Phlebotominae) of the genera *Phlebotomus* (Old World) (Fig. 1-2) and *Lutzomyia* (New World). After the fly has taken up *Leishmania* with a bloodmeal, the short and ovoid *Leishmania* promastigotes live in the fly gut, where they adhere to the midgut walls and start to replicate. They develop into long, slender nectomonad promastigotes which then migrate to the anterior of the insect gut and become short and broad leptomonad promastigotes. These secrete a gel that consists mainly of filamentous proteophosphoglycan (fPPG) and forms a plug in the gut. This allows the promastigotes to proliferate and develop further into the infective metacyclic promastigotes, which are then transmitted to a mammalian host (Gossage et al., 2003b). Once the sand fly has injected the metacyclic promastigotes into the mammal, the *Leishmania* are quickly taken up into host cells, mainly macrophages, by phagocytosis. They do not remain in the bloodstream for any length of time. They survive within the host cell phagosome and differentiate into round, non-motile amastigotes with only a short flagellum that barely emerges from its pocket. The phagosome fuses with lysosomes to form a mature, acidic phagolysosome (parasitophorous vacuole) and the amastigotes multiply within. The parasites adhere closely to the membrane of the vacuole and their growth rate appears to be slow, possibly so as to not rupture the vacuole too quickly (Chang et al., 2003d). When the

amastigotes have proliferated, they are released from the macrophage and can then invade other host cells. When the infected host is bitten by another sand fly, infected macrophages are taken up into the insect gut, the amastigotes differentiate into procyclic promastigotes and the cycle is repeated (Fig. 1-1) (recently rev in (Banuls et al., 2007)).

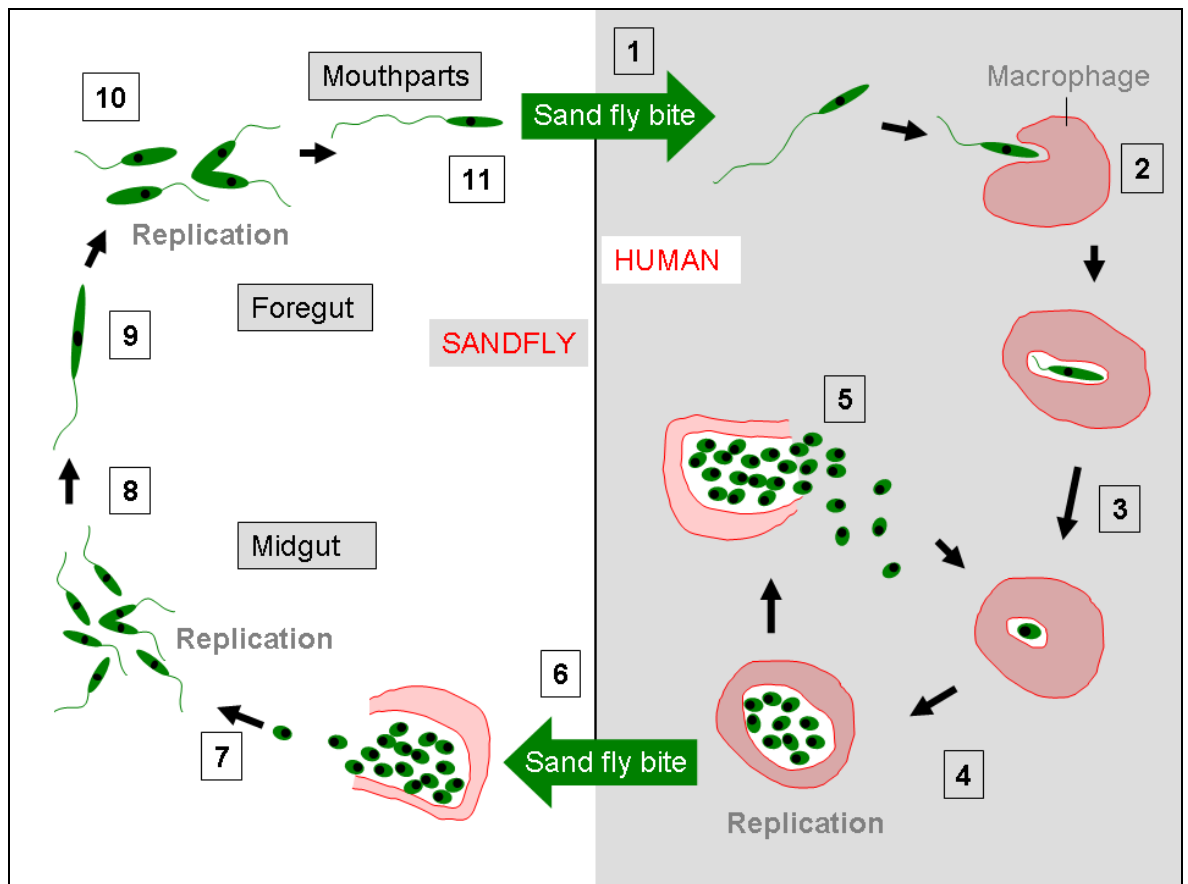


Figure 1-1: *Leishmania* life cycle. (1) Metacyclic promastigotes transmitted into mammalian host by sand fly bite. (2) Phagocytosis of promastigote into host cell (macrophage depicted here) (3) Promastigote develops into intracellular amastigote. (4) Amastigotes proliferate within parasitophorous vacuole. (5) Amastigotes are released from host cell and can infect others. (6) Infected host cells are taken up into sand fly gut with bloodmeal. (7) Amastigotes are released and develop into ovoid procyclic promastigotes in midgut. (8) Promastigotes develop into long, non-dividing nectomonad promastigotes. (9) Nectomonads migrate to anterior gut. (10) Nectomonads become short leptomonad promastigotes. (11) Leptomonads develop into infective metacyclic promastigotes which are then transmitted into the mammalian host by sand fly bite (adapted from (Gossage et al., 2003a)).



Figure 1-2: Female mounted *Phlebotomus* sp. sand fly. Image: CDC Public Health Image Library, from World Health Organisation, Geneva, Switzerland.

1.2 Leishmaniasis and treatment

1.2.1 *The leishmaniases*

The leishmaniases are diseases of the tropics and subtropics, prevalent in the Old World (parts of the Mediterranean, Africa and Asia with the Middle East and India) and the New World (parts of Central and South America) (Fig. 1-3), with varying characteristics, depending on the *Leishmania* species causing the infection (Table 1-1). The three main forms of leishmaniasis are visceral, cutaneous and mucocutaneous.

The visceral, most severe form of the disease (VL, also known as "kala azar") is caused by *L. donovani* and *L. infantum* in the Old World and *L. chagasi* in the New World. Symptoms can include fever, anaemia, organ swelling, intestinal ulcers and oedema and VL is often fatal if not treated. Skin lesions are characteristic of cutaneous leishmaniasis (CL); this type is caused by species of the *L. major*, *L. braziliensis* and *L. mexicana* complexes and symptoms extend from small, localised and self-healing ulcers to large disfiguring lesions that lead to necrosis of the skin and dissemination of the parasites through the body. The muco-cutaneous form of the disease (MCL) is prevalent only in the New World and caused by the *L. Viannia* subgenus, mainly *L. braziliensis*. Symptoms include lesions of nasal and oral tissue and the destruction of facial cartilage and bone.

The broad range of clinical symptoms of the leishmaniases reflects the varying impact of the different *Leishmania* species on the human immune system (Banuls *et al.*, 2007; Murray *et al.*, 2005).

In the year 2000, the WHO estimated that 12 million people are infected with *Leishmania*, in over 88 countries worldwide, and every year around 60000 die of leishmaniasis with around 2 million new infections arising (WHO, Leishmaniasis fact sheet, 2000). These numbers are likely an under-estimate now (PAHO / WHO, Leishmaniasis 2007 update sheet); because of urban-rural migrations and growing poverty, the leishmaniases are spreading and are expected to become more prevalent in the future (Hommel, 1999). Additionally, *Leishmania* co-infection of HIV patients (Fig. 1-3) as well as *Leishmania* transmission through shared use of needles among intravenous drug users is a growing concern (Jhingran *et al.*, 2008; Alvar *et al.*, 1997)

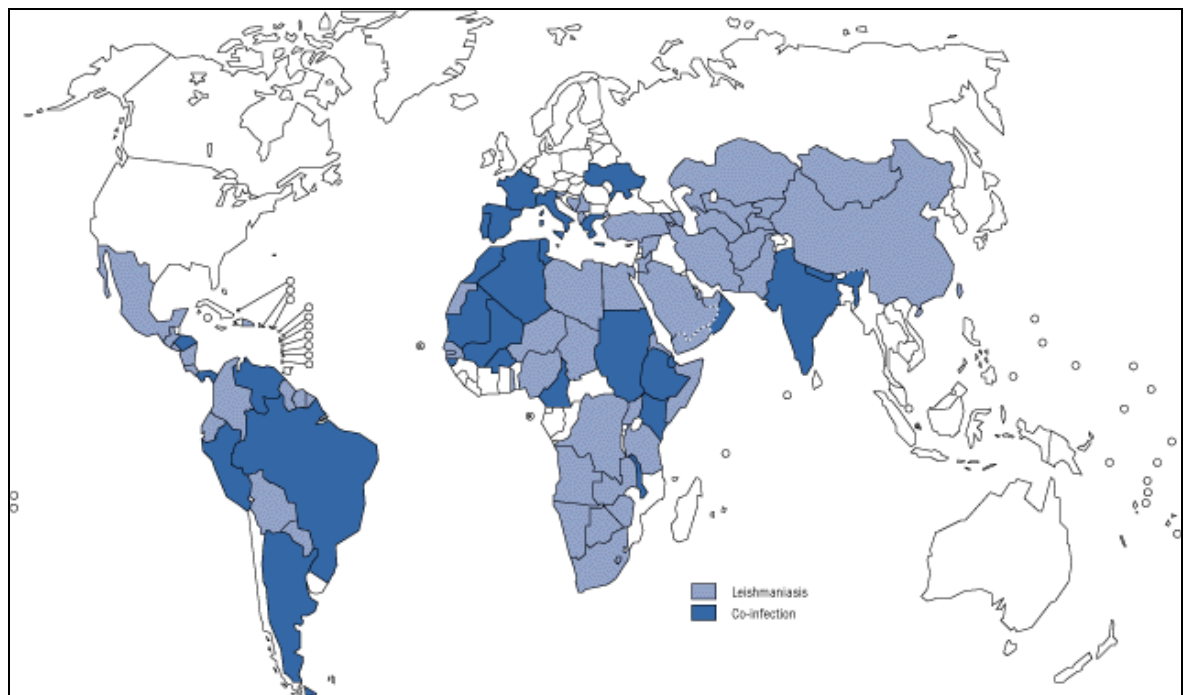


Figure 1-3: Map of worldwide distribution of leishmaniases (reported cases, 1990-1998). Light blue are areas of endemic leishmaniases, dark blue areas are affected by *Leishmania*-HIV co-infection (from WHO “Essential leishmaniasis maps”)

Table 1-1: Examples of clinically important species of *Leishmania*, the type of leishmaniasis they cause (VL = visceral leishmaniasis, LCL = localised cutaneous leishmaniasis, DCL = diffuse cutaneous leishmaniasis, MCL = muco-cutaneous leishmaniasis), and their geographic distribution.

Species	Disease type	Geographic distribution
<i>L. donovani</i>	VL	Old World
<i>L. infantum</i>	VL	Old World
<i>L. chagasi</i>	VL	New World
<i>L. major</i>	LCL	Old World
<i>L. tropica</i>	LCL	Old World
<i>L. aethiopica</i>	LCL, DCL	Old World
<i>L. braziliensis</i>	LCL, MCL	New World
<i>L. panamensis</i>	LCL, MCL	New World
<i>L. peruviana</i>	LCL, MCL	New World
<i>L. mexicana</i>	LCL, DCL	New World
<i>L. amazonensis</i>	LCL, DCL	New World
<i>L. pifanoi</i>	LCL, DCL	New World

1.2.2 Treatment and vaccination

The main drugs for the treatment of leishmaniasis are pentavalent antimonials like sodium stibogluconate ("Pentostam"), which have been used since the 1940s. These drugs can be very effective, but they need to be administered daily for three to four weeks, they can have serious side effects because of the toxicity of antimony, and resistant parasites are becoming more wide-spread. Additionally, leishmaniasis patients with an HIV co-infection cannot be treated well with antimonials and usually relapse. Newly developed drugs are being tested to treat the different forms of the disease. However, both old and new drugs have disadvantages, including high costs (liposomal amphotericin B "AmBisome"), toxicity (pentamidine), teratogenicity (miltefosine), long administration periods of several weeks, emerging drug resistance or unsuitability for treatment in HIV co-infection. Different drugs are more or less useful in different cases and geographical regions; it is unlikely that one optimal treatment will be found for

all leishmaniasis (Berman, 2003; Melby, 2002; Croft and Coombs, 2003; Opperdoes and Michels, 2008; Ouellette *et al.*, 2008).

Currently there still is no effective *Leishmania* vaccine. "Leishmanisation", inoculation with live parasites, has traditionally been used for immunisation in Asia, but this can in some cases lead to a chronic infection. Research has been carried out with heat-inactivated adjuvant-supplemented *Leishmania* or *Leishmania* fractions, with drug-sensitive or genetically attenuated *Leishmania* mutants for live vaccines, as well as with all-defined vaccines like recombinant proteins or DNA vaccines (Khamesipour *et al.*, 2006). Especially a vaccine composed of a recombinant *Leishmania* protein (SMT, a sterol 24-c-methyltransferase) in adjuvant has shown some success (Goto *et al.*, 2007), but further research will be needed before a reliable vaccine can be produced.

1.3 Genomes and genetics

The genome sequence of *L. major* was published in 2005 (Ivens *et al.*, 2005f), *L. braziliensis* and *L. infantum* followed in 2007 (Peacock *et al.*, 2007b) and the *L. mexicana* genome is currently being assembled. The *L. major* genome consists of 32.8 Mb with 8311 putative protein-coding genes, as well as 911 predicted RNA genes. Sequencing the genome has led to a "molecular toolkit" for working with *Leishmania* and analysing genes of interest. The widely used gene silencing technique RNAi (RNA interference) has only been observed to function in *L. braziliensis*; all other investigated species do not appear to contain all the required proteins (Peacock *et al.*, 2007a; Smith *et al.*, 2007). The genomes of *T. brucei* and *T. cruzi* were also published in 2005 (Berriman *et al.*, 2005; El Sayed *et al.*, 2005b). This now allows valuable comparisons among the trypanosomatid species (El Sayed *et al.*, 2005a; Kissinger, 2006; Lynn and McMaster, 2008).

Leishmania is diploid and carries 34 - 36 pairs of chromosomes (*L. major* 36, *L. mexicana* 34, *L. braziliensis* 35), although aneuploidy of several chromosomes has also been observed (Myler, 2008). Additionally, all kinetoplasts contain kDNA, the kinetoplast DNA of the mitochondrion. *Leishmania* contains a single large mitochondrion. Its DNA is contained within the kinetoplast and organised in

mini- and maxicircles (Campbell et al., 2003b; Beverley, 2003). Minicircles (0.8 - 1.6 kb in size, 30 000 - 50 000 copies) encode guide RNA genes for RNA editing processes (Sturm and Simpson, 1990; Corell *et al.*, 1993). The maxicircles (35 - 50 kb in size, 10 - 30 copies per cell) encode the actual mitochondrial genome, which includes mitochondrial rRNA subunits (Simpson and Simpson, 1978; Campbell et al., 2003a).

Most *L. major* genes are arranged in one of 133 directional clusters of up to several hundred genes, which are transcribed as polycistrons (Ivens et al., 2005e; Myler et al., 1999; Worthey et al., 2003). Transcription initiation appears to be controlled by a small number of promoters in the strand-switch regions between two opposing transcription clusters (Martinez-Calvillo *et al.*, 2003; Clayton, 2002; Thomas *et al.*, 2009), although random initiation may also be taking place. The polycistronic transcripts are processed post-transcriptionally to produce monocistronic mRNAs. There is no or only little transcription regulation, most control takes place at the level of mRNA stability. Unwanted mRNAs are degraded after transcription (Clayton and Shapira, 2007a; Haile et al., 2008), while retained mRNAs are cleaved from the precursor transcript and processed by trans-splicing of a 39 nucleotide long spliced leader (SL) sequence to their 5' ends. This sequence is obtained from the SL-RNA (around 100 nt). In parallel to the 5' modification, the 3' end of the mRNA is poly-adenylated (Matthews *et al.*, 1994) (Clayton and Shapira, 2007b). The regulation of gene expression is an area of ongoing research as it shows some unique features in trypanosomatids.

Sexual recombination in a meiosis-like manner has only recently been observed in *Leishmania* promastigotes, which were traditionally thought to be asexual. It appears that, in the sand fly stage, mating can occur between different parasite genotypes, leading to hybrid cells (Akopyants *et al.*, 2009).

1.4 Host-parasite interactions of *Leishmania*

1.4.1 *The mammalian immune response*

An intracellular pathogen like *Leishmania* evades the humoral B-cell response (antibodies) of the host's immune system and it is the T-cell-mediated immune response that is responsible for dealing with intracellular pathogens.

Cytotoxic T-cells attack and kill infected antigen-presenting cells by inducing apoptosis. Antigen-presenting host cells are the dendritic cells, B-cells and macrophages. They present antigens bound to MHC (major histocompatibility complex) molecules on their surfaces. MHC class I proteins present cytosolic antigens to the cytotoxic T-cells. This process activates the T-cells and stimulates their proliferation (Alberts *et al.*, 2002).

The second group of T-cells, the T helper cells, is also induced by antigen-presenting cells, but they do not kill directly, they produce cytokines that activate the infected macrophages to destroy their internal pathogens. Here, MHC class II proteins present the antigens, picked up by endocytosis, to the T helper cells. T helper cells also stimulate B-cells to produce antibodies and cytotoxic T-cells to proliferate. There are two major types of T helper cells, Th1 and Th2. Naïve T helper cells develop into one of these types depending on the cytokines released by the antigen-presenting cells; IL-12 secretion by macrophages or dendritic cells for example triggers a Th1 response (Alberts *et al.*, 2002). Infection with *Leishmania* leads to either a Th1 or a Th2 based immune response, depending on the genetic background and immunological status of the individual host (Alexander and Bryson, 2005b; Rogers *et al.*, 2002a). The parasite has been shown to manipulate cytokine production in host cells, for example inhibiting secretion of IL-12 that is required for an inflammatory (Th1) response (Carrera *et al.*, 1996; Weinheber *et al.*, 1998b).

Th1 helper cells are responsible for activating macrophages and further T-cells; they secrete the cytokines IFN- γ (interferon gamma) and TNF- α (tumor necrosis factor alpha). A Th1-based immune response triggers macrophages to attack and kill their pathogens with hydrolytic enzymes, reactive oxygen species and nitric

oxide, leading to a local inflammation and the elimination of the pathogen (Alberts *et al.*, 2002). Therefore, a Th1 response is useful and protective against intracellular pathogens like *Leishmania* and presents itself in the self-healing cases of leishmaniasis (Alexander and Bryson, 2005c).

Th2 helper cells stimulate B-cells and their antibody production by secreting a Th2-specific set of cytokines, including IL-4. Since antibodies cannot enter cells, this response only targets extracellular pathogens (Alberts *et al.*, 2002), while intracellular pathogens like *Leishmania* can proliferate, establish a severe infection and even lead to the death of the host. A defective Th1 response (as is thought to cause the immunodeficiency of BALB/c mice) has a similar effect (Alexander and Bryson, 2005a).

1.4.2 *Leishmania and its mammalian host cells*

Leishmania are most vulnerable when they have just entered a mammalian host. They have left the insect environment and are not yet inside the host macrophage. Here, the promastigote parasite requires a whole array of strategies to evade the host immune system. The surface-bound display or actual secretion of virulence factors plays an important role at this stage, allowing the parasite to enter the host cell undetected.

Leishmania appear to infect several different types of mammalian leukocytes, including neutrophils and dendritic cells, but it is thought that macrophages harbour the majority of *Leishmania* cells (Gregory and Olivier, 2005). Recent publications have presented evidence for an important role for neutrophils in the infection process. Neutrophils, which are the first phagocytes to arrive at the sand fly bite location, have been shown to ingest *Leishmania*. Infected neutrophils may then act as "Trojan horses" and silently introduce *Leishmania* into macrophages when they are phagocytosed themselves (Laskay *et al.*, 2008). It still appears that macrophages do take up *Leishmania* directly, too, but perhaps neutrophils "rescue" parasites that would otherwise not have entered a macrophage. Or neutrophils release *Leishmania* again, possibly in a more resistant differentiation stage or enclosed in a host cell derived membrane. The released parasite can then be taken up by macrophages (Peters *et al.*, 2008; John and Hunter, 2008a; Jochim and Teixeira, 2009) (Fig. 1-4).

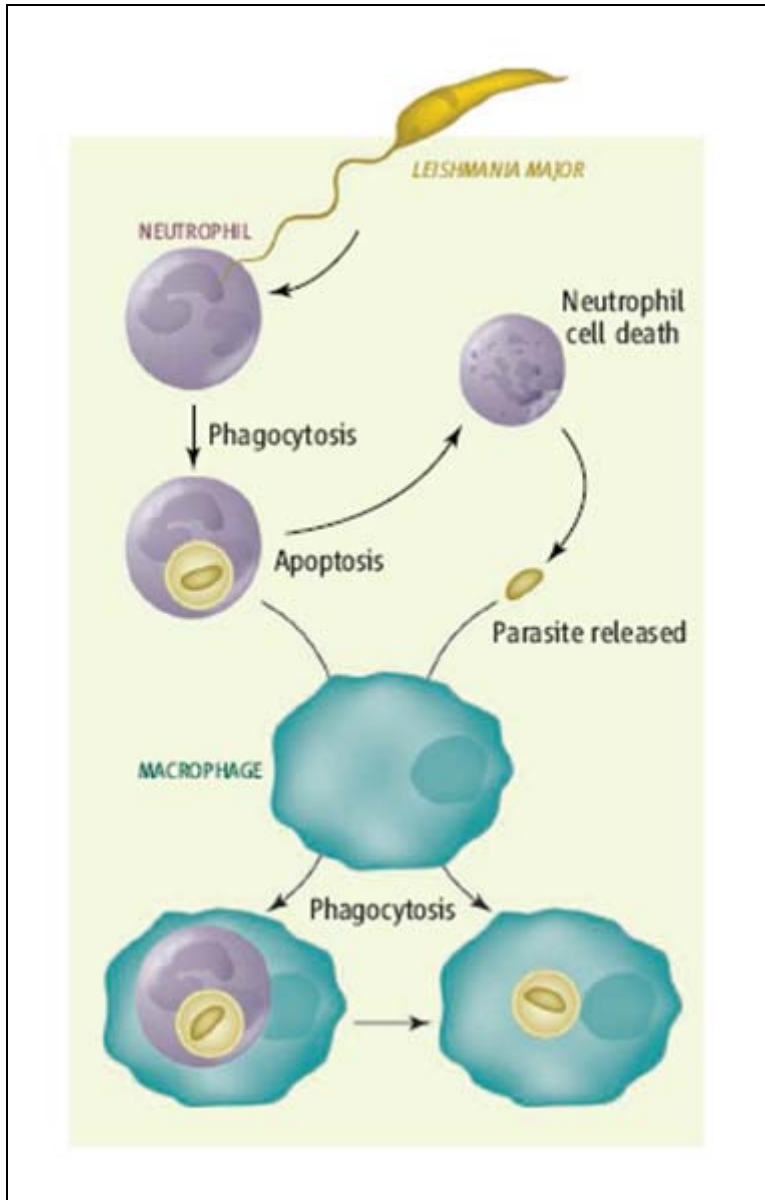


Figure 1-4: Putative mechanisms of *Leishmania* uptake into neutrophils and macrophages at a sand fly bite site in a mammalian host. Left side: Silent entry of *Leishmania* into the macrophage (as “Trojan Horse”); *L. major* is taken up into neutrophil, this undergoes apoptosis and is then phagocytosed by a macrophage. Right side: Alternative mechanism; *L. major* is taken up by a neutrophil, then leaves it and is taken up by a macrophage afterwards. From (John and Hunter, 2008b)

Once inside the macrophage, the parasites change the properties of the phagosome membrane and initially inhibit fusion with other vesicles. This delays vacuole maturation and the accumulation of harsh late endosomal properties until the parasites have developed into amastigotes (Desjardins and Descoteaux, 1997a; Olivier et al., 2005b). *Leishmania* have been shown to downregulate nitric oxide production by downregulating iNOS (cytokine-inducible nitric oxide synthase) expression, to neutralise reactive oxygen species (ROS) and lysosomal

enzymes in the macrophage, and to interfere with the host immune system (Chan et al., 1989; McNeely et al., 1989; Proudfoot et al., 1996; Desjardins and Descoteaux, 1997b; De Souza et al., 1995d; Barr and Gedamu, 2003; Ghosh et al., 2003).

The intracellular amastigote stage is more resistant to the hostile environment of the later phagolysosome and survives well in acidic pH (Burchmore and Barrett, 2001a). It relies on the host cell for a number of nutrients, which it sequesters from the degradative environment of the parasitophorous vacuole, including low molecular weight molecules like sugars, amino acids, lipids and phosphate. The vacuole can acquire further macromolecules and debris through fusion with other phagosomes. Amastigotes endocytose larger molecules from the vacuole lumen and they also have a large repertoire of intramembrane transporters for import of low molecular weight nutrients (Burchmore and Barrett, 2001b; McConville et al., 2007).

Further manipulations of the host cell, such as the secretion of virulence factors and the internalisation and degradation of host MHC complex components (Antoine et al., 1999; De Souza et al., 1995c), enable *Leishmania* amastigotes to establish a persistent macrophage infection and replicate. After proliferation, the amastigotes are released from the host cell and can then infect other phagocytes or be taken up into a sand fly. It is not clear if the release of *Leishmania* involves bursting of the phagocyte or if the parasites are released by an exocytic process (Handman and Bullen, 2002).

1.4.3 *Leishmania and the sand fly vector*

The attachment of some *Leishmania* species, including *L. major*, to the sand fly gut epithelium is facilitated by the lipophosphoglycan LPG, which binds to insect cell surface galectins (Pimenta *et al.*, 1992; Sacks *et al.*, 2000). LPG is not only important for this process, but is also a virulence factor in the mammalian host stage.

Leishmania promastigotes secrete a filamentous proteophosphoglycan (fPPG) that forms a gel-like mass, the parasite secretory gel (PSG) plug, in the anterior sand fly gut. In this environment, the cells can differentiate into infective

metacyclic promastigotes. The PSG plug seems to make feeding more difficult for the sand fly ("blocked fly hypothesis"), leading to an increase in feeding attempts and, therefore, more chances of parasite transmission to a mammal (Stierhof et al., 1999b; Ilg, 2000b; Rogers et al., 2002b).

1.5 Virulence factors

Leishmania virulence factors can be broadly classified into three groups: Surface-bound molecules, secreted / released molecules, and intracellular "pathoantigens" (Chang et al., 2003c). All virulence factors influence the host organism in favour of the parasite; they facilitate infection, propagate survival, persistence or replication of *Leishmania* and promote disease progression.

1.5.1 Surface-bound virulence factors

Surface molecules are exported via the flagellar pocket, where they are thought to be integrated into the pocket membrane and distributed to the surface membrane from there. Surface molecules can remain attached or be cleaved and released.

The lipophosphoglycan LPG is the dominant non-protein surface molecule of most human-infective promastigotes and has been shown to act as a virulence factor in *L. major* (Spath et al., 2000). LPG consists of a polymer of repeating disaccharide-phosphate units with variable side-chain modifications and a neutral oligosaccharide on the end. It is anchored to the membrane by a GPI anchor. Its composition (length, side chain modifications) is specific to each *Leishmania* species and also life-stage dependent (Turco and Descoteaux, 1992). *L. major* LPG structure changes during metacyclogenesis; metacyclic promastigotes carry very long LPG, double the length of the procyclic promastigotes' LPG (Sacks et al., 1990). Amastigote LPG is also larger than that of the promastigote form (in *L. major*) (Turco and Sacks, 1991b) or not detectable at all (in *L. donovani*) (McConville and Blackwell, 1991b).

It appears that the dense LPG coat of metacyclic promastigotes facilitates attachment to the macrophage, shields the cell surface from attacks by the complement cascade, protects from proteolytic attacks in the host cell and

slows down phagosome maturation, thus allowing differentiation into the more resistant amastigote stage (Olivier et al., 2005a). LPG is not always a major virulence factor; some species like *L. mexicana* apparently do not require LPG for virulence (Ilg, 2000a; Turco et al., 2001c).

The most prevalent protein on the surface of *Leishmania* is GP63 (or Leishmanolysin) and it is also a virulence factor. It is a GPI-anchored zinc metallopeptidase and has been found on all analysed *Leishmania* species and stages so far, although its abundance is reduced on amastigote cells in comparison to promastigotes (Frommel et al., 1990; Medina-Acosta et al., 1989). It was found to facilitate migration and binding to host cells, to hydrolyse host peptides, and to confer resistance to complement-mediated lysis, thus protecting the parasite in the mammalian host (Brittingham et al., 1999; Joshi et al., 2002; Russell and Wilhelm, 1986; Sorensen et al., 1994; Joshi et al., 1998; McGwire et al., 2003; Seay et al., 1996). Amastigotes appear to express different types of GP63, without a GPI anchor, that have been observed to accumulate in the flagellar pocket area rather than on the entire surface (Hsiao et al., 2008).

1.5.2 Secreted or released virulence factors

Only a relatively small number of virulence factors secreted by *Leishmania* have been identified and characterised to date.

Secretory acid phosphatase (SACP or SAP), a glycoprotein, is secreted by *Leishmania* promastigotes (Gottlieb and Dwyer, 1982; Bates and Dwyer, 1987a; Bates et al., 1989c; Shakarian and Dwyer, 2000). In New World species like *L. mexicana*, SACP is secreted as polymeric filaments, which may be assembled in the flagellar pocket (Ilg, 2000c). SACP can dephosphorylate a broad range of substrates, possibly allowing it to influence the host in favour of the parasite (Bates and Dwyer, 1987b; Bates et al., 1989b; Doyle and Dwyer, 1993; Shakarian et al., 1997; Joshi et al., 2004a). *L. donovani* SACP is resistant to a range of peptidases, which could contribute to its robust activity in the hydrolytic environment of the parasitophorous vacuole (Joshi et al., 2004b).

Another type of filamentous glycoprotein is also secreted by *Leishmania*, the secretory gel protein fPPG (filamentous proteophosphoglycan). It fills the flagellar pocket with a network of fibrous molecules and then emerges from it to surround the cell with a gel-like mass (Stierhof et al., 1999a). This plays a particular role in the survival of *Leishmania* in the sand fly gut. fPPG is transmitted into the mammalian host together with the parasites and has been shown to exacerbate the infection in the mammal, making it a virulence factor in the sand fly vector as well as in the mammalian host (Rogers et al., 2004).

Certain secreted peptidases of *Leishmania* have also been shown to be important virulence factors (Mottram et al., 2004b). Cysteine peptidases can manipulate interleukin signalling, thereby suppressing a protective Th1 immune response and facilitating parasite survival (Weinheber et al., 1998a; Buxbaum et al., 2003c; Mottram et al., 2004c). Additionally, cysteine peptidases have been observed to degrade components of MHC class II molecules, thus preventing parasite antigens being presented on the macrophage surface (De Souza et al., 1995b).

The *L. major* SIR2rp protein is an NAD-dependent deacetylase and a homologue of the yeast ageing regulator protein SIR2 (silent information regulator 2). In *Leishmania* it has been shown to be released, promote parasite survival and interfere with mammalian cell proliferation (Vergnes et al., 2002; Sereno et al., 2005).

Dwyer and colleagues identified LdNuc, a class I nuclease, as a secreted enzyme of *L. donovani*. It showed broad substrate specificity *in vitro* and may act as a virulence factor by cleaving a range of nucleic acids in the host cell, possibly to provide purines for the parasite metabolism (Joshi and Dwyer, 2007).

Intriguingly, the genome of *L. tarentolae*, a lizard *Leishmania* that is not infective to mammals, contains homologues of several virulence factors from other *Leishmania* species. These include LPG, CPB and GP63 and it appears that either *L. tarentolae* is crucially missing a virulence factor that enables other species to infect mammals or it contains novel factors that prevent pathogenicity (Azizi et al., 2009).

1.5.2.1 The *Leishmania* "secretome"

Elucidation of the *Leishmania* "secretome", the entirety of secreted / released proteins, will allow the identification of further secreted virulence factor candidates. As yet, experimental results are relatively scarce and have to be interpreted carefully. The experimental design for secretome analyses is hampered by technical problems. Efforts have concentrated on analysing promastigote culture supernatants. But promastigotes and amastigotes likely differ in their secretome and as amastigotes are the prevalent stage in mammalian infections, investigation of their secretome is highly relevant, too.

The promastigote secretome will mainly include proteins involved in the insect stages of the life cycle, as well as - at a later stage - virulence factors for evading the mammalian immune system directly after infection and for entering macrophages. Chenik and colleagues (2005) analysed the culture supernatant of *L. major* stationary phase promastigotes and found known secreted proteins including heat shock and ribosomal proteins and the CPB cysteine peptidase, as well as several unknown proteins and ribosomal proteins that were not thought to be secreted (Chenik *et al.*, 2006). More recently, Silverman and colleagues (2008) identified over 150 proteins in the *L. donovani* secretome, including peptidases like oligopeptidase B (OPB), macrophage migration inhibitory factor-like protein (MIF), proteasomal proteins, the small GTPase Rab1, heavy chain clathrin and the LACK antigen. Surprisingly, only two of the 151 proteins contained a classical N-terminal signal peptide, suggesting that *Leishmania* may use alternative, non-canonical secretory signals instead (Silverman *et al.*, 2008).

1.5.3 Intracellular virulence factors ("*pathoantigens*")

Secreted or surface-bound *Leishmania* molecules do not appear to elicit an immune response in mammals; they primarily facilitate establishment and replication of the parasite within phagocytes and are not highly immunogenic (Chang *et al.*, 2003b). The *Leishmania* epitopes that do lead to an immune response are highly conserved intracellular proteins of the parasite cytoplasm, including heat shock proteins, acidic ribosomal proteins, histones and the LACK ("*Leishmania* homologue of receptors for activated C kinase") antigen (Requena *et al.*, 2000b). Some of these antigens are species-specific, for example the

LACK antigen, which is a virulence factor in *L. major* but not in *L. mexicana* (Torrentera *et al.*, 2001). These "pathoantigens" are thought to be released from intracellular amastigotes that have undergone lysis. The antigens are then processed by antigen presenting cells and presented to the immune system on their surface, using the MHC pathways. Is it not clear whether some amastigotes lyse within intact host cells, which could then present the antigens themselves using the MHC class I system, or whether the host cell disintegrates too and the antigenic components are endocytosed by other phagocytes and presented in an MHC class II-dependent manner (Chang *et al.*, 2003a; Requena *et al.*, 2000a).

1.6 *Leishmania* peptidases

Peptidases are enzymes that cleave peptide bonds. There are five major groups of peptidases: aspartic, cysteine, serine, threonine and metallopeptidases. The *L. major* genome encodes at least 154 such proteins, including members of all groups (Fig. 1-5) (Besteiro *et al.*, 2007e; Ivens *et al.*, 2005d). Many of these peptidases have not been characterised as yet. Some of the well-studied *Leishmania* peptidases are known virulence factors, including the surface metallopeptidase GP63 and the cysteine peptidase CPB. The importance of peptidases, especially cysteine peptidases, for parasite virulence makes these enzymes potential drug targets or vaccine components (Mottram *et al.*, 1996c; Selzer *et al.*, 1999; Alexander *et al.*, 1998a; Pollock *et al.*, 2003a).

In mammals, peptidase activity can be controlled by peptidase inhibitors like serpins or cystatins, but none of these are found in the *Leishmania* genome. *Leishmania* does contain two classes of inhibitors, ICPs (cysteine peptidase inhibitors) and ISPs (serine peptidase inhibitors), both of which are thought to be involved in inhibiting host enzymes rather than the parasite's own (Besteiro *et al.*, 2004; Besteiro *et al.*, 2007d; Eschenlauer *et al.*, 2009).

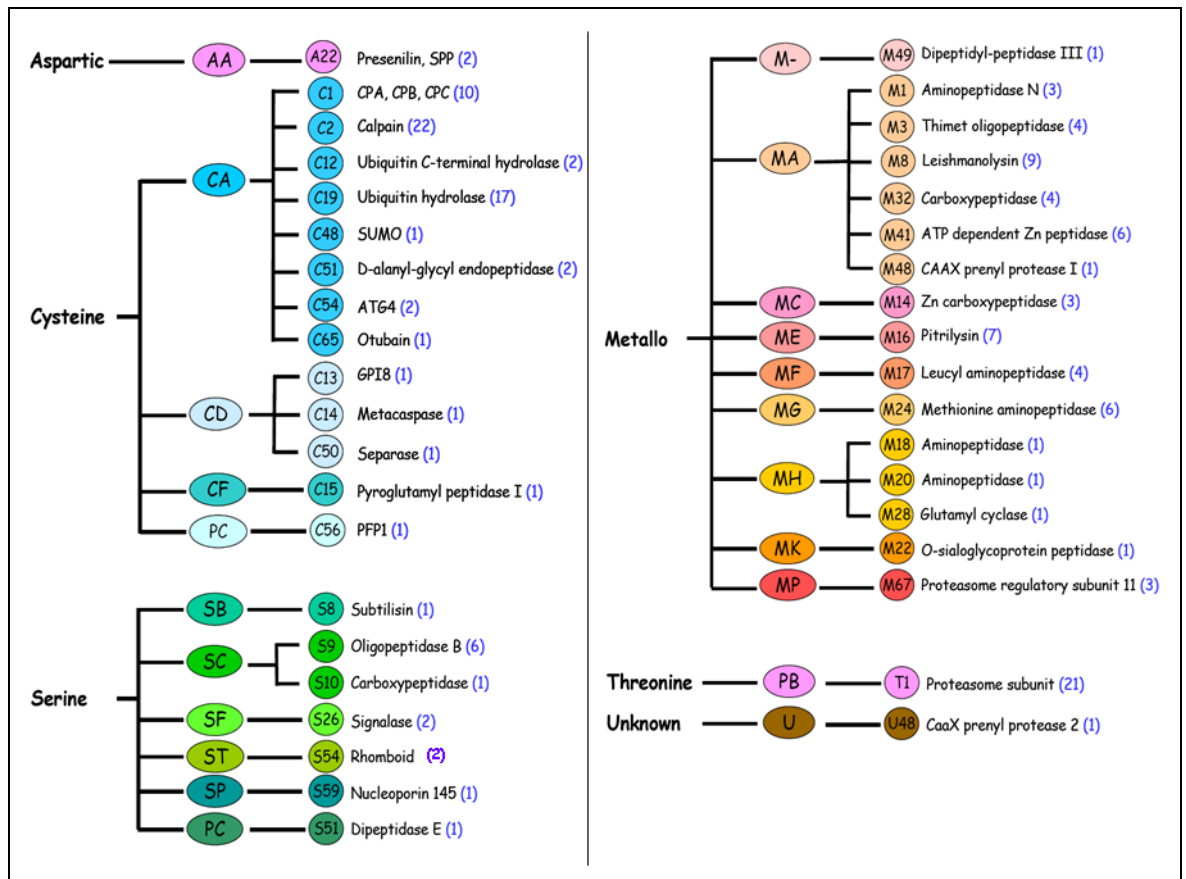


Figure 1-5: Clans and families of all identified *L. major* peptidases. Numbers (blue, in brackets) are putative number of members of each peptidase type. Adapted from (Besteiro et al., 2007c)

1.6.1 *Leishmania cysteine peptidase B (CBP)*

The most extensively studied cysteine peptidases of *Leishmania* are the papain-like enzymes of Clan CA, including the cathepsin L-like cysteine peptidases CPA and CPB and the cathepsin B-like CPC (Besteiro et al., 2007f; Mottram et al., 2004d).

The cysteine peptidase B (CPB) is encoded on several genes in a tandem array (eight genes in *L. major*, 19 in *L. mexicana*). It is a stage-regulated lysosomal peptidase that has been detected mainly in the amastigote megasome, but also in the promastigote MVT (multivesicular tubule)-lysosome. It has been shown to act as a virulence factor. *L. mexicana* CPB-deficient mutants can still infect mouse macrophages, but mouse footpad lesions develop and progress much slower than in a wild type infection or even self-heal, depending on the susceptibility of the mouse strain. An *L. mexicana* double mutant lacking CPA in

addition to CPB shows an even stronger attenuation of virulence with no lesion development, suggesting that CPA also acts as a virulence factor (Buxbaum et al., 2003b; Mottram et al., 1996b; Mottram et al., 1997; Mottram et al., 1998). The effect of CPB appears to depend on the immune status of the host and on the *Leishmania* species, though. In BALB/c mice, CPB actively promotes a Th2 immune response instead of the protective Th1 (Alexander et al., 1998b; Pollock et al., 2003b; Mottram et al., 2004e). In other mice (C3H), *L. mexicana* CPB seems to actively suppress a Th1 response, resulting in persistent and non-healing infection; an *L. major* infection on the other hand is cleared (Buxbaum et al., 2003a). Further investigations have shown that CPB - as well as CPA - is crucial for autophagy in *L. mexicana*. Doubly deficient cells showed an accumulation of non-degraded autophagosomal material, reduced viability and inhibition of metacyclogenesis, which can explain the attenuated virulence of the double mutant (Williams et al., 2006c).

CPB is trafficked to the lysosome, its final destination, along a direct as well as an indirect route. It is synthesised in the ER as an inactive zymogen containing a pre- and a pro-domain. From the ER it is either taken directly to the lysosome or it can be trafficked via the Golgi into the flagellar pocket, where the pre-peptide is cleaved. Some of the enzyme is then released into the parasitophorous vacuole of the macrophage, while the rest is re-endocytosed and transported to the lysosome. The pro-domain is cleaved off after arrival, which activates the enzyme (Brooks et al., 2000a; Mottram et al., 2004g; Huete-Perez et al., 1999b).

Released CPB is thought to degrade NF κ B (nuclear transcription factor kappa B) and I κ B (inhibitory NF κ B) in the macrophage cytoplasm (Cameron *et al.*, 2004). It has been found to be present even outside the host macrophages, in the extracellular matrix (Ilg *et al.*, 1994), and it appears to manipulate the host immune system and induce a Th2 response. It remains unclear how the enzyme is transported across the membranes from the parasitophorous vacuole into the host cell cytoplasm and further on into the extracellular matrix (Mottram et al., 2004f). Another reported function of cysteine peptidases is the degradation of MHC class II complexes in the parasitophorous vacuole, which allows the parasite to prevent antigen presentation and an immune response (De Souza et al., 1995a).

1.7 The *Leishmania* cell

Leishmania promastigotes are about 15 - 20 μm long with a flagellum of at least the same length. Amastigotes on the other hand are rounded with a diameter of only 2 - 4 μm . Both cell types show a polar morphology. They contain a nucleus and an endoplasmic reticulum (ER), one Golgi apparatus, a single large mitochondrion, the peroxisome-related glycosomes, endosomes, a large lysosome and a flagellum at the anterior pole of the cell (Fig. 1-6). The flagellum emerges from the flagellar pocket, an apical invagination of the cell membrane. The shape of the cell and the polarity of endo- and exocytosis are maintained by a crosslinked layer of subpellicular microtubules beneath the plasma membrane, with the exception of the flagellar pocket membrane. A set of large microtubules is also found in the cytoplasm, alongside the tubular lysosome, and it is thought to be important for this organelle's structure (Mullin et al., 2001f; Waller and McConville, 2002d; Weise et al., 2000d).

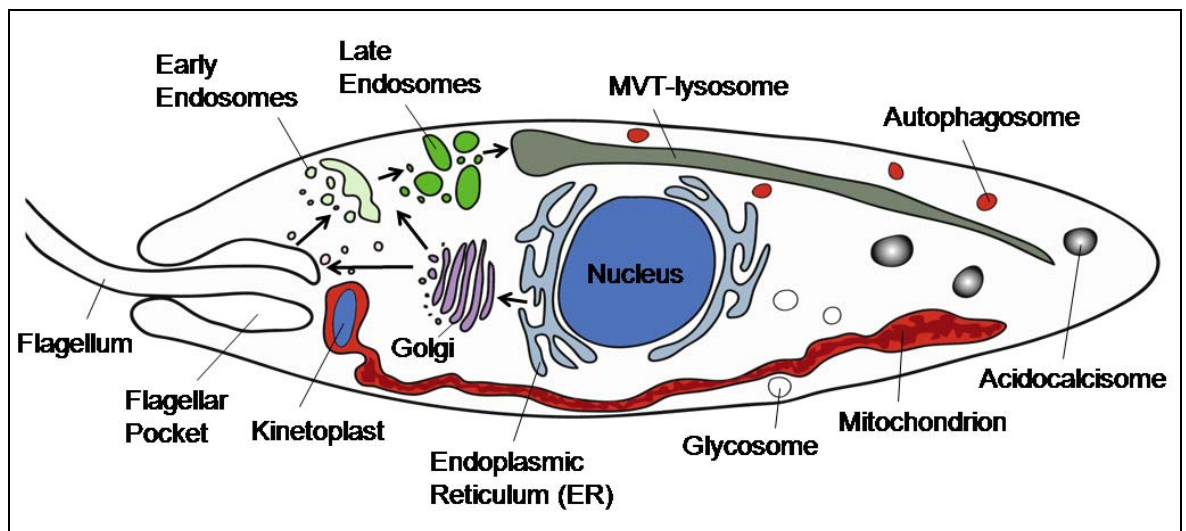


Figure 1-6: Overview of *Leishmania* promastigote with organelles. Black arrows show general endo- and exocytic protein trafficking routes.

The surface membrane of *Leishmania* cells contains some specific and unusual molecules. Non-protein bound GIPLs (glycoinositol phospholipids) and LPG (lipophosphoglycan) form a dense surface coat, together with GPI (glycosylphosphatidyl-inositol)-anchored proteins like GP63 (Naderer et al., 2004; Turco et al., 2001b). GPI anchors are remarkably common on *Leishmania* surface molecules, but the significance of this is as yet not clear. GPI-anchored proteins

appear not to be essential for growth and virulence of the parasite (Hilley *et al.*, 2000). Transmembrane proteins, abundant in the plasma membranes of other eukaryotes, are comparatively rare on the *Leishmania* surface (Ghedini *et al.*, 2001i). The amastigote surface contains no LPG or less than that of promastigotes, and instead mainly free GPIs and glycosphingolipids acquired from the membrane of the parasitophorous vacuole of the host cell (Turco *et al.*, 2001a; Turco and Sacks, 1991a; McConville and Blackwell, 1991a; Winter *et al.*, 1994).

1.7.1 The flagellar pocket

The flagellar pocket is an invagination of membrane around the base of the flagellum, which lacks the subpellicular microtubule scaffold. The pocket lies on the outside of the cell, but is still separated from the environment by desmosome-like junctions around the flagellum. Its membrane composition differs from the cell body surface and it is the sole site of endocytosis and exocytosis, for example for the uptake of nutrients or the secretion of virulence factors (Landfear and Ignatushchenko, 2001a; de Souza, 2002a; McConville *et al.*, 2002i). Only here is the membrane accessible and sufficiently flexible for vesicle fusion and budding (Webster and Russell, 1993). Endocytic and exocytic (secretory) trafficking pathways converge at the pocket and it is an important protein sorting station. Surface molecules like GPI-anchored proteins are distributed to the cell surface from the pocket. Secreted proteins can accumulate in the pocket, be released into the environment directly or be internalised again into the endocytic pathway (McConville *et al.*, 2002h). In promastigotes, the beating of the flagellum may aid a constant efflux out of the pocket (Ghedini *et al.*, 2001h; Bates *et al.*, 1989a).

The flagellum appears to not only be important for motility, adhesion to the sand fly gut (Killick-Kendrick *et al.*, 1974; Warburg *et al.*, 1989) and possibly flagellar pocket function and biogenesis. Recent studies suggest that amastigote flagella interact with the membrane of the parasitophorous vacuole (Gluenz *et al.*, 2009). Furthermore, the flagellum may also play a role as a sensory organelle, similar to sensory cilia in higher eukaryotes, as has been suggested in trypanosomes (Oberholzer *et al.*, 2007; Ralston *et al.*, 2009).

1.7.2 Intracellular protein trafficking

Rapid protein trafficking and degradation are particularly important for a parasite like *Leishmania*, as its different hosts and habitats and the changes between the highly adapted life cycle stages require fast and efficient protein turnover. To ensure this, the organelles of the endocytic and exocytic / secretory pathways like the Golgi and the endosomes are localised close to the flagellar pocket membrane, where endo- and exocytosis take place. This supports a rapid variation of surface molecules and virulence factors, as well as fast changes of cell shape and morphology during the life cycle (Morgan et al., 2002a; Waller and McConville, 2002a).

As in other eukaryotes, the major routes of vesicular traffic, both endocytic and intracellular, are mediated by clathrin-coated vesicles (CCVs) in *Leishmania* (Weise et al., 2000c; de Souza et al., 2009; Denny et al., 2005a). These have an outer coat of clathrin molecules and beneath this a layer of one type of adaptor protein (AP) complex. Such vesicles are formed from clathrin-coated pits in the donor membrane. The pits invaginate, engulf the cargo molecules and bud off as transport vesicles. Upon arrival at the destination membrane, the clathrin coat merges with the target and the cargo is released into the new compartment or the environment (Hirst and Robinson, 1998; Bonifacino and Traub, 2003; Alberts *et al.*, 2002).

Apart from clathrin-coated vesicles, there also are other common vesicle trafficking mechanisms. The COP-I and COP-II (coatamer I and II) vesicle systems function primarily within the Golgi and between the Golgi and the ER; lipid rafts and caveolae (flask-like invaginations of the membrane) are other important pathways. Homologues of many components of these mechanisms, as well as caveolae-like formations and lipid rafts have been found in *Leishmania* (Denny et al., 2001; Morgan et al., 2002b; McConville et al., 2002g). So it seems that most of the eukaryotic membrane transport compartments are conserved in *Leishmania* (McConville et al., 2002f).

A group of SNAREs (soluble N-ethylmaleimide-sensitive factor (NSF) attachment protein (SNAP) receptors) is important for the correct targeting of vesicles to a destination membrane, and also for tethering and fusion. When two cellular

compartments are about to fuse, SNAREs of both membranes interact to promote docking and fusion of vesicle and target membrane (Jahn and Scheller, 2006). 25 proteins with SNARE-domains have been identified in the *L. major* genome. GFP-labelling of several *Leishmania* SNAREs showed that they localise at the Golgi, in late endosomes, lysosomes or near the flagellar pocket. This supports the notion that the endo- and exocytic vesicle transport pathways are important and well-developed in *L. major* (Besteiro et al., 2006b).

For proteins to be recognised as cargo for specific vesicles, they require sorting signals, which are usually short amino acid sequences situated in the cytoplasmic domain of a protein. They are recognised and bound by adaptor protein complexes like APs. A variety of such signals has been studied to date. For membrane proteins, they include tyrosine- and dileucine-based motifs (Bonifacino and Traub, 2003).

1.7.2.1 Protein synthesis

Eukaryotic proteins are synthesised at the ribosomes, which are either free in the cytosol or bound to the endoplasmic reticulum (rough ER). Especially transmembrane proteins and secretory proteins are synthesised in the ER-bound ribosomes and are directly, co-translationally imported into the ER membrane or lumen. An N-terminal ER-signal sequence is essential for this import process. This signal is recognised by the SRP (signal recognition particle), which mediates import into the ER; the ER targeting signal is cleaved after the protein has been translocated. In the ER, proteins can be modified, for example glycosylated, or a GPI anchor can be added. Secretory proteins traffic from the ER to the Golgi apparatus where further modifications can take place, are transferred to the trans-Golgi network (TGN) and then to their final destination, for example the cell surface or organelles like the lysosome or the acidocalcisomes. These transport steps are facilitated by transport vesicles shuttling between compartments (Alberts *et al.*, 2002). *Leishmania* possess much the same general mechanisms of protein synthesis as higher eukaryotes (McConville et al., 2002e).

1.7.2.2 Endo- and exocytosis

In *Leishmania* promastigotes, the endocytic pathway consists of tubular early endosomes near the flagellar pocket, followed by late endosomes (or "multivesicular bodies") with characteristic internal vesicles and one large tubular MVT (multivesicular tubule)-lysosome (Ghedini et al., 2001g; Mullin et al., 2001e; Weise et al., 2000b; Waller and McConville, 2002b). Endocytosed molecules are internalised in clathrin-coated vesicles at the flagellar pocket membrane and passed into the endosomal system. There are several distinct populations of endosomes, characterised by their respective composition of Rab proteins. These are small monomeric GTPases of the Ras superfamily and are important for regulating endocytic processes in eukaryotic cells including kinetoplastids (McConville et al., 2002c; Engstler et al., 2007). Several Rab proteins have been identified in kinetoplastids, including Rab1 in the Golgi (Besteiro et al., 2006a; Dhir et al., 2004b), Rab5 in early endosomes in the flagellar pocket region (Marotta *et al.*, 2006; Singh *et al.*, 2003) and Rab7 in early as well as late endosomes (Patel *et al.*, 2008; Denny *et al.*, 2002). So the *Leishmania* endosome network appears to be similar to that of other organisms, while the single large MVT-lysosome is unusual; mammalian cells contain several smaller lysosomal vesicles. Exocytosis of proteins in kinetoplastids is thought to be mediated by transport vesicles between the Golgi apparatus and the flagellar pocket membrane (McConville *et al.*, 2002b; Engstler *et al.*, 2007).

1.7.2.3 Protein degradation

The main sites of protein degradation in the cell are the lysosome and the proteasome. Intracellular proteins destined for degradation can be targeted to the lysosome through the autophagy pathway. Alternatively they can be targeted to the cytosolic proteasome for degradation. Ubiquitination is an important mechanism for labelling proteins for hydrolysis and *Leishmania* has a number of genes encoding ubiquitination enzymes (Ivens et al., 2005c; Besteiro et al., 2007g). Furthermore, the kinetoplastids are the only eukaryotes found so far that contain not only a conserved eukaryotic 20S proteasome (Wang et al., 2003; Robertson, 1999b), but also a HslVU proteasome of prokaryotic origin in the mitochondrion (Li et al., 2008; Couvreur et al., 2002; Ivens et al., 2005b).

The (macro-) autophagy pathway is a major mechanism of protein delivery to the lysosome. It is active particularly in starvation periods and during cellular differentiation. Autophagosomes, double-membraned vesicles, deliver cytoplasmic proteins and organelles to the lysosome for digestion (Levine and Klionsky, 2004; Luzio et al., 2003b; Yoshimori, 2004). The autophagy pathway requires several autophagy-related (ATG) proteins, which interact in two separate pathways contributing to the autophagy mechanism (Levine and Yuan, 2005). Autophagy in *Leishmania* is dependent on the activity of lysosomal peptidases like CPA and CPB (Williams et al., 2006b; Williams et al., 2009), which are involved in the degradation of autophagosomes and their contents after fusion of autophago- and lysosome. Autophagy appears to be crucial for cell differentiation events like metacyclogenesis and the maturation of metacyclic promastigotes to amastigotes and is, therefore, linked to the parasite's survival and virulence (Besteiro et al., 2006c; Besteiro et al., 2007a; Williams et al., 2006a).

Proteins that are internalised into the cell via endocytosis are also taken to the lysosome for degradation. They pass through the early and late endosomes of the endocytic pathway and the degradation process begins in hybrid compartments that are formed when endosomes and lysosomes exchange content or fuse. After degradation is complete, the resulting amino acids can be exported from the mature lysosomes and used by the cell (Luzio et al., 2003a). It appears that the endocytic pathway of *Leishmania* is generally similar to that of higher eukaryotes and endosomes transport internalised protein cargo to the single large lysosome or - in amastigotes - the megasomes (de Souza et al., 2009; McConville et al., 2002d).

1.7.3 The lysosome

Lysosomes are the most important organelles for protein degradation in a eukaryotic cell. These membrane-bound acidic compartments contain many different acid hydrolases, for example peptidases. They degrade macromolecules, which are transported from endocytic vesicles through early and late endosomes to lysosomes. Content exchange between endo- and lysosomes appears to be mediated by transient "kiss-and-run" contact as well as

by direct fusion and creation of hybrid compartments, where degradation of macromolecules mainly takes place (Bright et al., 2005; Luzio et al., 2007b). In addition, lysosomes can interact with autophagosomes and also with the plasma membrane for exocytic purposes, for example retrograde transport of some surface receptors for recycling after their usage as a carrier into the lysosome. Other lysosome-like compartments have been termed "secretory lysosomes"; they are distinct from "normal lysosomes" and transport newly synthesised secretory proteins to the cell surface. Examples of secretory lysosomes are melanosomes, platelet dense granules and MHC class II compartments (Luzio et al., 2007a; Blott and Griffiths, 2002). There are different lysosome-related organelles (LROs) in various organisms and certain cell types, for example the pigment granules of skin melanocytes and the *Drosophila* eye, as well as the dense granules of blood platelets (Luzio et al., 2003c).

Leishmania cells have a single mature lysosome with a unique morphology. In late promastigote cells, it is the multivesicular tubule (MVT) lysosome, a large tubular structure that stretches along the length of the cell and contains many internal vesicles (Ghedin et al., 2001f; Mullin et al., 2001d; Weise et al., 2000a). The MVT lysosome and the endosomal pathway can be targeted with different endosomal markers like FM4-64 (a red fluorescent live imaging probe), which is endocytosed and passed through the early and late endosomes to the lysosome (Mullin et al., 2001c; Besteiro et al., 2006d). pH-sensitive markers like LysoTracker do not label the lysosome particularly well, suggesting that it is not as acidic in *Leishmania* as in other organisms (Mullin et al., 2001b). In *Leishmania*, LysoTracker preferentially labels acidocalcisomes, which appear to be more acidic than the lysosome in these cells (Ghedin et al., 2001e; Besteiro et al., 2008n). Fixing cells for fluorescent labelling has been shown to disintegrate the MVT, leading to a string of small vesicles instead of one large tubule (Ghedin et al., 2001d). Therefore, live imaging probes are preferable for fluorescence microscopy of the MVT lysosome.

Amastigotes of the *L. mexicana* and *L. donovani* complexes contain different forms of large lysosomes, called megasomes, which can be found in large numbers and occupying up to 15% of the total cell volume (Alexander and Vickerman, 1975; Coombs et al., 1986; Ueda-Nakamura et al., 2001b; de Souza, 2002b).

1.7.4 Protein trafficking to the lysosome

Proteins from the extracellular environment or the parasite surface are delivered to the *Leishmania* lysosome for degradation through the endocytic pathway. Furthermore, intracellular proteins and organelles that require lysosomal degradation can be taken to the lysosome via the autophagy pathway. Proteins are then hydrolysed and the amino acids are used in the parasite's metabolism.

On the other hand, newly synthesised *Leishmania* proteins are also targeted to the lysosome from biosynthetic pathways at the endoplasmic reticulum (ER) and the Golgi. Such proteins can be hydrolases for the lysosomal lumen or integral proteins of the lysosomal membrane. Lysosomal targeting appears to take two alternative routes, either directly from the Golgi to endo- or lysosomes, or indirectly via the cell surface at the flagellar pocket and subsequent re-endocytosis (McConville et al., 2002k).

In mammals, newly synthesised luminal lysosomal hydrolases are targeted to the lysosome from the trans-Golgi network through the mannose-6-phosphate pathway. This involves a mannose-6-phosphate modification of the enzymes after biosynthesis, binding to mannose-6-phosphate receptors (MPRs) and subsequent vesicular transport of the enzymes to endosomes. By definition, absence of MPRs distinguishes lysosomal membranes from all other endosomal membranes in mammals (Luzio et al., 2007c; Bonifacino and Traub, 2003). The mannose-6-phosphate pathway is thought to be absent from kinetoplastids and it is not known what mechanism replaces it, possibly a kinetoplastid-specific pathway (Cazzulo et al., 1990; Brooks et al., 2000b; Allen et al., 2007a). Newly synthesised lysosomal membrane proteins do not require the mannose-6-phosphate pathway but are trafficked by transporters like the multimeric carrier complex AP3, either directly from the trans-Golgi to endo- and lysosomes or along an indirect route via the plasma membrane (Luzio et al., 2007d). Two types of targeting motifs for lysosomal membrane proteins have been studied in detail so far, tyrosine motifs and dileucine motifs in the C-terminal domains of lysosomal membrane proteins. Canonical tyrosine sites consist of a YXXØ motif (with Ø being a bulky hydrophobic residue) or, alternatively, an NPXY motif (for

internalisation of certain membrane proteins). Canonical dileucine sites show a [D/E]XXXL[L/I] or DXXLL motif. Sorting by tyrosine and dileucine signals is thought to depend on recognition and interaction with adaptor protein (AP) complexes (Bonifacino and Traub, 2003). Tyrosine and dileucine signals have been shown to exist and play a role in kinetoplastids' lysosomal trafficking (Tazeh and Bangs, 2007a; Weise et al., 2005).

1.7.5 The acidocalcisomes

Acidocalcisomes are small, acidic organelles that can be found in many eukaryotic cells including *Leishmania* (Vannier-Santos et al., 1999b). They are electron-dense, rounded granules with a diameter of ~ 200 nm (up to 1.2 µm in *L. amazonensis* under certain conditions (Miranda et al., 2004c), and they contain high concentrations of calcium, polyphosphates, magnesium and other ions (Docampo and Moreno, 1999; Docampo and Moreno, 2001b; Miranda et al., 2004b). Kinetoplastid acidocalcisomes have been observed to align, possibly along a cytoskeletal structure, and they can accumulate at the posterior end of the cell (Mullin et al., 2001a; Docampo and Moreno, 2001a; Waller and McConville, 2002c). Their membrane contains proton and calcium pumps, ion exchangers and aquaporins (Fig. 1-7), but their function and their origin are not clear (Docampo et al., 2005c).

Acidocalcisomes were first identified in trypanosomes (Vercesi *et al.*, 1994), but acidocalcisome-like organelles are conserved from bacteria to humans (in blood platelets), so they might have a conserved function (Docampo et al., 2005a). They may act as dynamic storage organelles, especially for polyphosphate and calcium, and contribute to pH- and osmoregulation, adaptation to environmental stress or regulation of calcium levels in signalling (Ruiz et al., 2001; Rohloff and Docampo, 2006; Lefurgey et al., 2005; Moreno and Docampo, 2009a; Miranda et al., 2004a). Recent work on the soluble VPS1 pyrophosphatases of the acidocalcisome lumen in *T. brucei* and *L. amazonensis* indicates that these proteins, or indeed fully functional acidocalcisomes, are required for virulence (Lemerrier *et al.*, 2004; Espiau *et al.*, 2006).

Their acidic pH suggests that the acidocalcisomes are related to the acidic endo- / lysosomal compartments. However, at the same time endocytic markers like

FM4-64 are not passed on from the endocytic pathway to the acidocalcisomes, which suggests they are independent and do not exchange content with endo- or lysosomes (Mullin et al., 2001g; Docampo and Moreno, 2001c; Miranda et al., 2000; Scott et al., 1997). Nevertheless, *Leishmania* treated with sterol biosynthesis inhibitors were observed to accumulate endocytic markers in their acidocalcisomes (Vannier-Santos et al., 1999a), and *Leishmania* mutants with a sphingolipid deficiency have been shown to lack late endosomes as well as acidocalcisomes (Zhang et al., 2005), suggesting a common origin of acidocalcisomes and endo-/lysosomal organelles. However, fractionation experiments have shown that acidocalcisomes and lysosomes differ in size and protein composition (Scott and Docampo, 2000). For fluorescence microscopy analyses, acidocalcisomes can be labelled with the dyes LysoTracker and Acridine Orange (which accumulate in acidic compartments), or DAPI (which labels polyP-enriched compartments) (Ghedini et al., 2001c; Besteiro et al., 2008m).

Apart from acidocalcisomes, there is a variety of other acidic lysosome-related organelles (LROs) in different organisms and cell types, including melanosomes and platelet dense granules of blood platelets. They are distinct from lysosomes in morphology and function, but appear to share certain characteristics like targeting pathways for their membrane proteins (Dell'Angelica et al., 2000a; Cutler, 2002). All LROs may share a common origin of biosynthesis (Moreno and Docampo, 2009b).

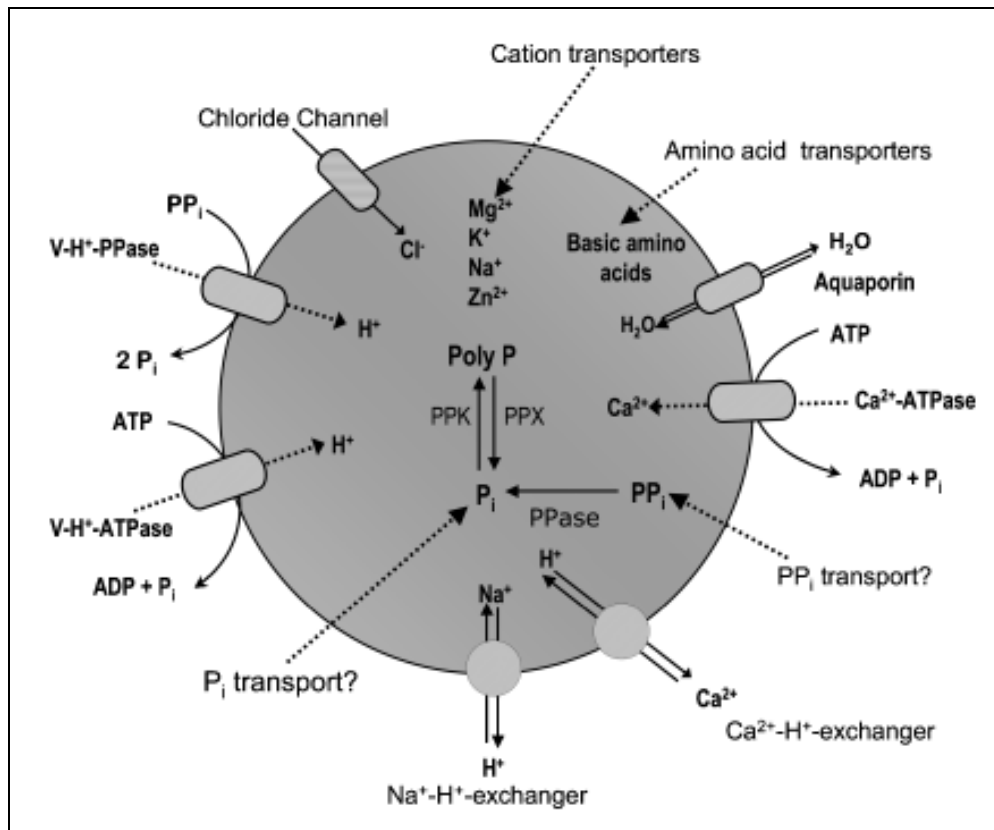


Figure 1-7: Schematic of acidocalcisome organelle with transporters and location of stored molecules (Moreno and Docampo, 2009c).

PP_i: pyrophosphate, P_i: phosphate, poly P: polyphosphate, V-H⁺-PPase: vacuolar proton pyrophosphatase, V-H⁺-ATPase: vacuolar ATPase, PPK: poly P kinase, PPX: exopolyphosphatase, PPase: pyrophosphatase.

1.7.6 The adaptor protein (AP) complexes

Several endo- and exocytic protein trafficking routes depend on a group of cytoplasmic adaptor protein (AP) carriers. These are large multimeric protein complexes that are an important factor in the clathrin-mediated formation and targeting of transport vesicles and the recruitment of cargo molecules (Robinson, 2004b). Four such complexes, AP1, AP2, AP3 and AP4, have been identified in humans to date. *L. major* as well as *Saccharomyces cerevisiae*, *Caenorhabditis elegans* and *Drosophila melanogaster* contain AP1, AP2 and AP3, but lack AP4 (Boehm and Bonifacino, 2001a; Robinson, 2004a; Denny et al., 2005b). This points to the AP carriers as an ancient component of eukaryotic cells and suggests that they were already present before the point of kinetoplastid speciation (Denny et al., 2005c). Each adaptor complex consists of a characteristic combination of four complex-specific subunits or adaptins: β (large), μ (medium) and σ (small), as well as one of γ, α, δ and ε (all large).

The subunits form a rounded shape with two protruding "ears" (Fig. 5-2 in chapter 5).

Different localisations and functions have been observed for the four APs (Boehm and Bonifacino, 2002d). AP1 has been associated with protein traffic between the trans-Golgi network and late endosomes and lysosomes; it interacts with clathrin-coated pits to form vesicles (Gallusser and Kirchhausen, 1993). As does AP2, which is involved in endocytosis from the plasma membrane and has been observed to deliver membrane proteins to the lysosome (Janvier and Bonifacino, 2005). AP3 transports membrane proteins from the trans-Golgi network to lysosomes, apparently also in association with clathrin (Dell'Angelica et al., 1998a). Little is known about the function of AP4; it has been found on the Golgi and on endosomes, it appears to be involved in targeting proteins to the lysosome but it is not clear whether it interacts with clathrin (Barois and Bakke, 2005; Hirst et al., 1999a; Aguilar et al., 2001; Boehm and Bonifacino, 2002c; Dell'Angelica et al., 1999a). To be recognised and trafficked by APs, proteins have to present certain binding motifs. AP1, AP2 and AP3 have been shown to recognise dileucine and tyrosine binding motifs via their μ subunits (Ohno et al., 1996c; Ohno et al., 1998d; Dell'Angelica et al., 1997a; Vowels and Payne, 1998; Bonifacino and Dell'Angelica, 1999).

In mammalian cells, two additional adaptin-like carrier protein families have been found, the GGAs (Golgi-localised γ -ear containing AFR-binding proteins) and the stonins, but these are monomeric and not part of AP complexes (Boehm and Bonifacino, 2001b). Neither GGAs nor stonins have been found in the kinetoplastids (Field and Carrington, 2004).

Aims of project

L. major manipulates its hosts by secreting virulence factors, such as the lysosomal cysteine peptidase CPB. This suggests that other peptidases may also be secreted in a similar way. Additionally, the *Leishmania* lysosome plays a role in parasite virulence and survival by facilitating rapid protein turnover and, therefore, fast differentiation, cell remodelling and adaptation to the different environments during the life cycle. The lysosome-like acidocalcisomes have also been shown to be important for *Leishmania* virulence, but it is not known how.

Thus, this thesis has the following aims:

- 1.) The screening of several *L. major* peptidases for their intracellular localisation, so as to identify a novel peptidase that is secreted and may act as a virulence factor.
- 2.) The identification of an *L. major* LAMP (lysosome-associated membrane protein) which will be useful as a lysosomal marker and allow a closer investigation of the structure and function of this organelle.
- 3.) Further investigation of *L. major* acidocalcisomes by analysing the intracellular localisation and targeting of the acidocalcisomal proton pump V-H⁺-PPase.

2. Material and Methods

2.1 Bioinformatics

2.1.1 Gene DB

The DNA and amino acid sequences for all genes of interest were obtained from the *L. major* genome database on GeneDB (www.genedb.org).

2.1.2 Vector NTI

DNA and amino acid sequence analyses as well as the *in silico* design of plasmids and oligonucleotide primers for PCRs were performed using the Vector NTI software package (Invitrogen), including the sequence alignment tool AlignX (ClustalW algorithm) and the sequencing analysis tool ContigExpress.

2.1.3 DNA Sequencing

All DNA samples (plasmids or PCR products) were sequenced by the Sequencing Service of the University of Dundee (www.dnaseq.co.uk). Sequencing results were analysed using the Vector NTI application ContigExpress (Invitrogen).

2.1.4 Predictions of protein properties and topologies

Properties and topological features of proteins were predicted using several different prediction programmes and websites (Table 2-1).

Table 2-1: All protein prediction and sequence analysis tools, algorithms and databases used in this study, with source and website for access.

Programme	Source / Website
TargetP 1.1	Center for Biological Sequence Analysis (CBS), Technical University of Denmark, Lyngby, Denmark. http://www.cbs.dtu.dk/services/TargetP/
SignalP 2.0 and 3.0	Center for Biological Sequence Analysis (CBS), Technical University of Denmark, Lyngby, Denmark. http://www.cbs.dtu.dk/services/SignalP/
MitoProt II (v1.101)	Helmholtz Center Munich, Institute of Human Genetics, Technical University of Munich, Germany. http://ihg2.helmholtz-muenchen.de/ihg/mitoprot.html
SOSUI 1.11	Dept of Applied Physics, Nagoya University, Japan. http://bp.nuap.nagoya-u.ac.jp/sosui
HMMTOP 2.0	Institute for Enzymology, Hungarian Academy of Sciences, Budapest, Hungary. http://www.enzim.hu/hmmtop/
TMPres2D For visualisation of HMMTOP results.	Biophysics & Bioinformatics Laboratory, University of Athens, Athens, Greece. http://biophysics.biol.uoa.gr/TMRPres2D/index.jsp
TMHMM 2.0	Center for Biological Sequence Analysis (CBS), Technical University of Denmark, Lyngby, Denmark. http://www.cbs.dtu.dk/services/TMHMM/
Phobius	Stockholm Bioinformatics Center, Stockholm, Sweden. http://phobius.sbc.su.se/
big-PI	Institute of Molecular Pathology (IMP), University of Vienna, Vienna, Austria. http://mendel.imp.ac.at/gpi/gpi_server.html
Merops Peptidase Database	Information on all known peptidases and tool for identification of active site residues. At the Wellcome Trust Sanger Institute, Cambridge, UK. http://merops.sanger.ac.uk/
NCBI BLAST	Website for BLAST (Basic Local Alignment Tool) analyses of DNA and protein sequences. At the National Center for Biotechnology Information (NCBI), Bethesda, MD, USA. http://blast.ncbi.nlm.nih.gov/Blast.cgi

2.2 Molecular biology

2.2.1 Polymerase Chain Reactions (PCRs) and oligonucleotides

All oligonucleotide primers were designed using the software Vector NTI (Invitrogen) and obtained from Eurofins MWG Operon (Ebersberg, Germany). For details of all oligonucleotides used in this study, see table 2-2.

PCRs for clonings, site-directed mutageneses or sequencing were performed using high fidelity proof-reading DNA polymerases according to the manufacturers' instructions (*PfuTurbo* DNA Polymerase from Stratagene, TaqPlus Precision DNA Polymerase from Stratagene and Phusion High-Fidelity DNA Polymerase from Finnzymes). PCRs for bacterial colony screens or other analyses that did not require proof-reading activity were performed with *Taq* DNA Polymerase from New England Biolabs according to the manual and using a 10 x PCR mix (1.13 mg ml⁻¹ BSA, 450 mM Tris pH 8.8, 110 mM ammonium sulphate, 45 mM MgCl₂, 68.3 mM β-mercapto-ethanol, 44 μM EDTA pH 8.0, 10 mM dCTP, 10 mM dATP, 10 mM dGTP, 10 mM dTTP, in H₂O) as the reaction buffer. Standard *Taq* polymerase PCRs were typically performed in a 20 μl volume, with approximately 100 ng DNA, 10 pmol of each oligonucleotide primer, 0.5 units of *Taq* polymerase and 2 μl of PCR mix. Concentrations and volumes for proof-reading PCRs were adjusted according to the manufacturers' instructions. PCR conditions (primer annealing temperature and elongation time) were optimised for each reaction. PCRs were typically performed in a Hybaid PCRExpress or PCRSprint thermocycler. Colony PCRs were performed on whole *E. coli* cells picked from colonies on agar plates. In this case, a 10 min cell lysis step was included at the beginning of the PCR programme.

Table 2-2: All oligonucleotide primers used in this study with targeted gene or region, direction, as well as sequence with underlined restriction digestion enzyme binding site or site-directed mutagenesis codons in bold.

Primer ID	Target sequence	Direction	Sequence (restriction sites underlined and mutagenesis codons in bold)
A. Primers for cloning candidate peptidase genes into pNUS-GFPcN vector (pGL1132)			
OL2243	Rhomboid-like serine peptidase, full length (LmjF02.0430)	forward	<u>CCATATGGT</u> GCGTGTGCGATCCAATAT <i>NdeI</i>
OL2244		reverse	TGGTACCGAAACGCGAGCGTGCATACACG <i>KpnI</i>
OL2245	Control Rhomboid-like serine peptidase, full length (LmjF04.0850)	forward	<u>CCATATGCAGCAGCCATGCTTCTTTG</u> <i>NdeI</i>
OL2246		reverse	TGGTACCGAGCGTGGCAGTGAGCTTGTCTG <i>KpnI</i>
OL2247	Ubiquitin hydrolase cysteine peptidase, truncated (LmjF09.0240)	forward	<u>CCATATGCACTTGC</u> GCGTGTGCTGCCAC <i>NdeI</i>
OL2248		reverse	CAGATCTGCTATGAGGCTTGCTGGCTTTA <i>BglII</i>
OL2251	CaaX prenyl protease, full length (LmjF26.2690)	forward	<u>CCATATGTGCTGCCTTGT</u> CAGTGGTG <i>NdeI</i>
OL2252		reverse	TGGTACCGTAGCGCCACAGTGTCCACGCC <i>KpnI</i>
OL2663	Calpain-like cysteine peptidase, full length (LmjF31.0390)	forward	<u>CCATATGTACGTCTGCATCACTTCTG</u> <i>NdeI</i>
OL2664		reverse	TGGTACCAGATCTCTCCTCCAGGATGCCA <i>KpnI</i>
OL2255	Zinc carboxypeptidase, truncated (LmjF33.0200)	forward	<u>CCATATGGTGCAGGGCATGCTGTTCT</u> <i>NdeI</i>
OL2256		reverse	TGGTACCCAGCAGCCGGAACGTTACGGAC <i>KpnI</i>
OL2659	Serine carboxypeptidase, full length (LmjF18.0450)	forward	<u>GATTAATATGGCGTCTTTTCTCTCAACCA</u> <i>AseI</i>
OL2660		reverse	CAGATCTCGCCAAACTCTGGCCGCGCAGG <i>BglII</i>
OL2259	Bem46-like serine peptidase, full length (LmjF35.4020)	forward	<u>CCATATGAGCTTTGGCAGCTTTCTTC</u> <i>NdeI</i>
OL2260		reverse	TGGTACCAACGACAGCAGCAGCTCCGGCG <i>KpnI</i>

B. Primers for “Bem46LONG” protein expression construct			
OL3058	<i>Bem46</i> fragment (LmjF35.4020)	forward	<u>CCATATGGCAGAGCGCGTGTGCGTCACC</u> <i>NdeI</i>
OL3060		reverse	<u>CAAGCTTCTAAACGACAGCAGCAGCTCC</u> <i>HindIII</i>
C. Primers for cloning of Bem46 deletion plasmids			
OL2874	5' deletion flank of <i>Bem46</i> (LmjF35.4020)	forward	<u>AAGCTTCACTGCGTTCGCCCCGCTTTTTT</u> <i>HindIII</i>
OL2875		reverse	<u>GTCGACAAAGGGTGCAGCCGAAGTCA</u> <i>SalI</i>
OL2876	3' deletion flank of <i>Bem46</i> (LmjF35.4020)	forward	<u>CCCGGGGCGGCGACAAAAGGAAAGCAGC</u> <i>SmaI</i>
OL2877		reverse	<u>AGATCTTGAAGGCGACGTGAAGCACATAC</u> <i>BglII</i>
D. Primers for analysing potentially <i>Bem46</i> deficient <i>L. major</i> cell lines			
OL2259	<i>Bem46</i> wild type allele (LmjF35.4020)	forward	<u>CCATATGAGCTTTGGCAGCTTTCTTC</u> <i>NdeI</i>
OL2260		reverse	<u>TGGTACCAACGACAGCAGCAGCTCCGGCG</u> <i>KpnI</i>
OL3278	Southern blot probe sequence in 3' flank of <i>Bem46</i>	forward	GGAGGAAGTGAGAGAGGAGT
OL3279		reverse	CCTACTCTCTACACGTCTC
E. Primers for cloning <i>LMP</i> gene into pNUS-GFPcN vector			
OL2428	<i>LMP</i> gene, full length	forward	<u>CCATATGAGCGACTTTGCCTCTGGGA</u> <i>NdeI</i>
OL2429		reverse	<u>TGGTACCCGAGTAGGAATCATCCGATTC</u> <i>KpnI</i>
OL1973	5' end of <i>LMP</i> gene	reverse	<u>TTCCATATGTACAACCACTTCAGCA</u> <i>NdeI</i>
OL2002	3' end of <i>LMP</i> gene	forward	<u>GATAGATCTGTGCTGCGAAGGCTGC</u> <i>BglII</i>
OL1975		reverse	<u>TTCGGTACCTCACGAGTAGGAATCA</u> <i>KpnI</i>
F. Primers for site-directed mutageneses of <i>LMP</i> tyrosine sites			
OL2690	<i>LMP</i> tyrosine site I	forward	GCAGCGTCTGCGCACAACGCCTACGTTCTCGGC AAGCG
OL2691		reverse	CGCTTGCCGAGAACGTAGGCGTTGTGCGCAGA CGCTGC
OL2692	<i>LMP</i> tyrosine site II	forward	GCAGCGGCACAAGGAGGGGGCCAACCTTTTAC AGAATCC
OL2693		reverse	CGCTTGCCGAGAACGTAGGCGTTGTGCGCAGA CGCTGC
OL3007	Region of tyrosine mutations (sequencing primers)	forward	CGTACTACTTTACCCAGGTGTCTGTG
OL3008		reverse	CCAGTGTGGCCATGGCACAGGGAGC

G. Primers for cloning of <i>LMP</i> deletion plasmids			
OL2323	5' deletion flank of <i>LMP</i> gene (LmjF30.2670)	forward	<u>CAAGCTTGGCGTTTATTTCTGGCCTGGGG</u> <i>HindIII</i>
OL2324		reverse	<u>CGTCGACGAGGCTGAGGCTGGGA</u> ACTGGC <i>Sall</i>
OL2325	3' deletion flank of <i>LMP</i> gene (LmjF30.2670)	forward	<u>CCCCGGGAGTGCCGACGGCCGTACTGACG</u> <i>SmaI</i>
OL2326		reverse	<u>GAGATCTTGT</u> TTGTATCTCTTGAAATTGG <i>BglII</i>
H. Primers for analysis of potentially <i>LMP</i> gene deficient <i>L. major</i> cell lines			
OL13	Hygromycin cassette	reverse	GGTGAGTTCAGGCTTTTTCA
OL2698		forward	CTCGGTGTGAGCGCTCGTCGCCGCT
OL12	Bleomycin cassette	forward	TGGCCGAGGAGCAGGACTGA
OL2699		reverse	CTGAGACTGCTTGCAGGCGTGCCT
OL2428	Wild type <i>LMP</i> allele	forward	CCATATGAGCGACTTTGCCTCTGGGA
OL2429		reverse	TGGTACCCGAGTAGGAATCATCCGGATTC
I. Primers for investigation of acidocalcisomal V-H ⁺ -PPase			
OL2426	V-H ⁺ -PPase, full length (for GFP fusion)	forward	<u>CCATATGGCTGGGAGGATCTTGATTG</u> <i>NdeI</i>
OL2427		reverse	<u>TGGTACCCTCGATGAGGTT</u> CAGCACAATA <i>KpnI</i>
OL2639	GFP cassette (for RT PCR)	forward	TTCACTGGCGTGGTCCCAATTCTCGT
OL2640		reverse	CCATCCTCAATGTTGTGTCTGATCTT
J. Primers for site-directed mutageneses of V-H ⁺ -PPase tyrosine sites			
OL2452	V-H ⁺ -PPase tyrosine site III	forward	TACTACACCTCCAATGCCGCCGCCAGTGCAG GAGATTG
OL2453		reverse	AATCTCCTGCACTGGGCGGGCGGCATTGGAGG TGTAGTAG
OL2454	V-H ⁺ -PPase tyrosine site IV	forward	GCCCTGACGATCGACGCGGCCGCCCTATTTCC GATAAC
OL2455		reverse	GTTATGGGAAATAGGGCCGGCCGCGTCGATCG TCAGGGC

2.2.2 DNA vectors used in this study

All genes of interest were cloned into plasmids for GFP tagging or protein expression (Table 2-3). The PCR-amplified genes were first sub-cloned into a commercial sub-cloning vector (pGEM-T Easy Vector System from Promega or PCR-Script cloning kit from Stratagene) according to the manufacturers' instructions, and subsequently cloned into the final plasmid. The pGEM-T Easy system was used mainly for sub-cloning *Taq* polymerase PCR products, as the standard *Taq* polymerase adds an A-tail (a single adenosine) to the ends of the product after PCR and this A-tail allows ligation with the T (thymidine)-overhangs at the ends of the vector. Alternatively, PCR products from non-A-tailing polymerases can be cloned into the pGEM-T Easy vector after an additional A-tailing step with *Taq* Polymerase (15 mins at 72 °C). The PCR-Script vector has blunt ends without poly-T overhangs and can therefore be used for sub-cloning directly after PCRs with non-A-tailing high-fidelity polymerases, or A-tailed products can be cloned into the blunt ended PCR-Script vector after removing the A-tail by "polishing" the PCR product with *Pfu* Polymerase and polishing buffer from the PCR-Script kit (Stratagene) according to the manufacturer's instructions. For GFP-labelling of proteins, the vectors pNUS-GFPcN (pGL1132, for C-terminal GFP tag) and pNUS-GFPnN (pGL1135, for N-terminal GFP tag) were used (Tetaud et al., 2002b). For the expression of the Bem46 protein with a His-tag, the expression vector pET28a (pGL655) was used. For integration of the mCherry-labelled HASPB surface protein into the 18S rRNA ribosomal locus (GeneDB ID LmjF27.rRNA.06) of the *L. major* genome and expression under the control of the ribosomal (rRNA) pol1 promoter, the vector pRIB (pGL631) was used, which is based on the pFW31 vector (Benzel *et al.*, 2000). The pRIB plasmid containing the HASPB sequence was linearised using *PacI* and *PmeI*, transfected into *L. major* for homologous recombination into the ribosomal locus, and cells were cloned before analysis by fluorescence microscopy. For deletion of the *L. major* Bem46 and LMP genes, the *Leishmania* knock-out vector pGL345 was used, which was originally designed to delete the *L. mexicana* cysteine peptidase B (CPB) array (Mottram et al., 1996a). The CPB flanking regions in the vector were replaced with Bem46 and LMP flanking regions respectively, using double restriction digests (*HindIII* / *Sall* for the 5'flank, *SmaI* / *BglII* for the 3'flank) and the hygromycin resistance marker

contained in pGL345 was exchanged to bleomycin (cassette taken from pGL762) to generate a second knock-out vector with a different antibiotic resistance marker for deletion of the second allele of a gene. The plasmids were linearised using *HindIII* and *BglIII* before transfecting and cloning.

Table 2-3: All plasmids generated and used in this study with plasmid backbone, inserted gene with GeneDB ID, use of the plasmid and resistance markers

Plasmid ID	Plasmid backbone	Gene inserted (with GeneDB ID), plasmid function, antibiotic resistance markers (Amp: ampicillin, Neo: G418, Kan: kanamycin, Bleo: bleomycin)
pGL1569	pNUS-GFPcN	CaaX prenyl protease 2 LmjF26.2690, GFP fusion plasmid, Amp/Neo
pGL1570	pNUS-GFPcN	Zinc carboxypeptidase LmjF33.0200, GFP fusion plasmid, Amp/Neo
pGL1572	pNUS-GFPcN	Rhomboid serine peptidase LmjF02.0430, GFP fusion plasmid, Amp/Neo
pGL1586	pNUS-GFPcN	Ubiquitin hydrolase cysteine peptidase LmjF09.0240, GFP fusion plasmid, Amp/Neo
pGL1588	pNUS-GFPcN	Bem46 serine peptidase LmjF35.4020, GFP fusion plasmid, Amp/Neo
pGL1763	pNUS-GFPcN	Calpain cysteine peptidase LmjF31.0390, GFP fusion plasmid, Amp/Neo
pGL1764	pNUS-GFPcN	Serine carboxypeptidase LmjF18.0450, GFP fusion plasmid, Amp/Neo
pGL1589	pNUS-GFPcN	Rhomboid-like serine peptidase LmjF04.0850 (mitochondrial control), GFP fusion plasmid, Amp/Neo
pGL1577	pET28a (pGL655)	Bem46 peptidase LmjF35.4020 (slight truncation), protein expression construct pBP266, Amp
pGL1578	pET28a (pGL655)	Bem46 peptidase LmjF35.4020 (slight truncation), protein expression construct pBP268, Kan
pGL1954	pET28a (pGL655)	Bem46 peptidase LmjF35.4020 (larger truncation), protein expression construct, Kan
pGL1893	pRIB (pGL631)	mCherry-tagged HASPB, for integration in ribosomal locus, Amp/Hyg
pGL1898	pGL345	Bem46 knock-out vector, Amp/Hyg
pGL1899	pGL345	Bem46 knock-out vector, Amp/Bleo
pGL1682	pNUS-GFPcN	LMP protein LmjF30.2670 (full length), GFP fusion plasmid, Amp/Neo
pGL1683	pNUS-GFPnN	LMP protein LmjF30.2670 (“Lamp ends” construct), GFP fusion plasmid, Amp/Neo
pGL1765	pGL1682	LMP protein LmjF30.2670 (full length), mutated tyrosine site I, GFP fusion plasmid, Amp/Neo
pGL1826	pGL1682	LMP protein LmjF30.2670 (full length), mutated tyrosine site II, GFP fusion plasmid, Amp/Neo

pGL1957	pGL1683	LMP protein LmjF30.2670 (“Lamp ends” construct), mutated tyrosine site I, GFP fusion plasmid, Amp/Neo
pGL1958	pGL1683	LMP protein LmjF30.2670 (“Lamp ends” construct), mutated tyrosine site II, GFP fusion plasmid, Amp/Neo
pGL1705	pGL345	LMP knock-out vector, Amp/Hyg
pGL1707	pGL345	LMP knock-out vector, Amp/Bleo
pGL1681	pNUS-GFPcN	V-H ⁺ -PPase LmjF31.1220, GFP fusion plasmid, Amp/Neo
pGL1702	pGL1681	V-H ⁺ -PPase LmjF31.1220, mutated tyrosine site III, GFP fusion plasmid, Amp/Neo
pGL1703	pGL1681	V-H ⁺ -PPase LmjF31.1220, mutated tyrosine site IV, GFP fusion plasmid, Amp/Neo
pGL1704	pGL1681	V-H ⁺ -PPase LmjF31.1220, tyrosine sites III and IV mutated, GFP fusion plasmid, Amp/Neo

2.2.3 Restriction endonuclease digestions

All restriction endonucleases used were obtained from New England Biolabs (NEB) and used with their specific buffers in 20 - 50 µl volumes according to the manufacturer's instructions. To digest large amounts of DNA, the volume was increased and digests occasionally carried out overnight. Double digests using two enzymes were done simultaneously when possible, or sequentially with a purification and buffer exchange step. Digested DNA was visualised by agarose gel electrophoresis.

2.2.4 Agarose gel electrophoresis

DNA was visualised by agarose gel electrophoresis, using UltraPure agarose powder (Invitrogen) at 1 % (w/v) in 0.5 x TBE buffer (20 mM Tris, 20 mM boric acid, 0.5 mM EDTA, pH 7.2). For small fragments (< 500 bp) the concentration was increased to 1.5 or 1.8 % and for large fragments (> 2 kb) it was decreased to 0.8 %. The agarose was solubilised in the buffer by boiling in the microwave and cast after addition of SYBR-Safe DNA stain (Invitrogen, used at 1 in 5000 dilution). Gel electrophoreses were performed in LifeTechnologies Horizon gel chambers. DNA samples were prepared with 6 x DNA loading dye (0.25 % (w/v) bromophenol blue, 0.25 % (w/v) xylene cyanol FF, 30 % (v/v) glycerol, in H₂O) and run at around 100 V, depending on the size and concentration of the gel and

the size of the DNA fragments. A 1 kb molecular weight marker (Invitrogen 1 Kb Ladder) was used at a concentration of 0.5 µg per lane to determine the size of the analysed DNA fragments. Gels were viewed under UV light, using a BioRad Gel-Doc imager with Quantity One software, or a DarkReader blue light transilluminator (Clare Chemical Research) for excising DNA from a gel. DNA extractions from agarose gels were performed using a Gel Extraction kit (Qiagen) according to the manufacturer's instructions.

2.2.5 Ligations

Ligations were performed with T4 DNA ligase and T4 ligase buffer (New England Biolabs), according to the manufacturer's instructions. Typically, purified digested plasmid and DNA insert were used at a ratio of 1:3 in a 10 µl reaction volume, and incubated overnight in a 16 °C water bath. Especially for blunt-ended ligations, digested vectors were treated with CIP (calf intestinal alkaline phosphatase, from New England Biolabs) according to the manufacturer's instructions, to dephosphorylate the DNA ends and prevent self-ligation, and then purified using a PCR purification kit (Qiagen). Ligations into the commercial sub-cloning vectors pGEM-T Easy (Promega) or PCR-Script (Stratagene) were performed according to the manufacturers' instructions. After ligations, the ligated plasmids were transformed into *Escherichia coli* competent cells and verified either by bacterial colony PCR or by plasmid purification and subsequent restriction digest analysis.

2.2.6 Transformations

Plasmids were introduced into bacterial cells for replication by heat shock transformation. For this, 50 µl of competent *E. coli* cells (thawed on ice) were mixed with 1 µl of isolated plasmid or 10 µl of a ligation reaction mix, kept on ice for 20 mins, heat-shocked in a water bath at 42 °C for 45 sec, and then transferred back on to ice for 5 to 10 mins before plating the cells out on agar plates containing the appropriate antibiotics for selection of positive transformants. Cells transformed with a kanamycin resistance cassette-containing plasmid, like pET28a, were incubated in 1 ml of warm LB medium

without antibiotics on a shaker for 30 - 45 mins at 37 °C before plating out, to allow the cells to recover and develop kanamycin resistance.

2.2.7 Site-directed mutageneses of plasmids

Site-directed mutageneses of individual amino acids were performed using the "QuikChange Mutagenesis" kit (Stratagene) according to the manufacturer's instructions. All site-directed mutageneses in this study were targeted at tyrosine motifs, changing a tyrosine (DNA codons TAT or TAC) to an alanine (codon GCC). These mutageneses were performed on the respective gene after cloning it into the GFP fusion plasmids pNUS-GFPcN or pNUS-GFPnN. To obtain double mutants with two tyrosine sites disrupted within one protein, the two sites were mutated sequentially. The mutated plasmids were confirmed by sequencing and then used for *L. major* transfections and fluorescence microscopy.

2.2.8 DNA isolation from bacteria and plasmid preparation for transfections

Plasmid DNA was purified from bacterial cells using a QIAprep Spin Miniprep kit (Qiagen), either on the benchtop or in the QIAcube machine (Qiagen), according to the manufacturer's instructions. For transfections of *Leishmania*, as well as for the preparation of DNA sequencing samples, plasmid DNA was quantified and concentrated by ethanol precipitation. Quantifications were carried out using an Eppendorf BioPhotometer and measuring the absorption at 260 nm (A_{260}) to estimate DNA concentration as well as the ratio A_{260} to A_{280} (absorption of DNA at 260 nm to absorption of contaminating proteins at 280 nm, ideally between 1.8 and 2) to estimate purity. For ethanol precipitations, DNA samples were mixed with 2 volumes of 100 % ethanol and 1/10 volume of 3 M sodium acetate at pH 5.2, frozen for least one hour (at -20 °C) and centrifuged at 13 000 x g and 4 °C for 20 mins. The DNA pellet was washed once with 70 % ethanol, dried and then resuspended in sterile H₂O to the appropriate concentration.

2.2.9 RNA isolation

Total RNA was isolated from *L. major* cell lines with Trizol reagent (Invitrogen), according to the manufacturer's instructions. All equipment was cleaned with DEPC (diethylpyrocarbonate)-treated water (0.01 % (v/v) DEPC) before handling RNA samples, to avoid contamination with RNases. The RNA was visualised on a 1 % agarose RNA gel made with UltraPure TAE buffer (Invitrogen) and stained with ethidium bromide, before use in further experiments.

2.2.10 Reverse Transcriptase (RT-) PCR

To prepare cDNA for RT-PCRs, RNA samples were first treated with RQ1 RNase-free DNase (Promega). Then the cDNA was synthesised from the mRNA contained in the total RNA, using random hexamer primers and SuperScript Reverse Transcriptase III (both Invitrogen) according to the manufacturer's instructions. Control samples without Reverse Transcriptase ("-RT") were also included. Using the cDNA as the template, a 500 bp fragment of the GFP cassette in the transgenic cell lines was PCR-amplified, using specific primers (OL2639 and OL2640) and standard *Taq* DNA polymerase (New England Biolabs).

2.2.11 Targeted gene replacement in Leishmania

L. major genes were deleted by replacing both alleles with the antibiotic resistance markers hygromycin and bleomycin respectively, by homologous recombination. For this, vectors were cloned, based on the *Leishmania* knock-out vector pGL345, to include specific 5' and 3' flanking regions (500 - 900 bp each) of the gene of interest up- and downstream of the antibiotic marker cassettes. The vectors were linearised with *Hind*III and *Bgl*III and transfected into *L. major* wild type cells for integration into the genome, sequentially replacing both alleles. Transfectants were cloned and doubly resistant cells were selected using hygromycin and bleomycin. Whole genomic DNA was isolated from potential knock-out clones and analysed for successful gene deletion by PCR and Southern Blot.

2.2.12 Southern Blotting

Southern Blotting was used to analyse *L. major* whole genomic DNA after targeted gene replacement to confirm the deletion of a gene. For each cell line, 4 to 5 µg of DNA were digested overnight in the appropriate buffer for the respective enzyme(s). The enzymes were chosen to allow probing and visualisation of different sized fragments in order to distinguish between wild type and heterozygous as well as homozygous knock-out cell lines. The digested DNA was electrophoresed through a large, thick 0.8 % agarose gel with large wells, stained with SYBR-Safe DNA stain (Invitrogen) and was photographed alongside a fluorescent ruler to determine the position of the DNA ladder relative to the DNA smear and the length of the gel. The gel was washed first with depurination buffer (0.25 M HCl) for 10 mins on a shaker and rinsed with dH₂O, then washed with denaturation buffer (1.5 M NaCl, 0.5 M NaOH) for 15 - 30 mins on a shaker, rinsed with dH₂O, and finally washed with neutralisation buffer (3 M NaCl, 0.5 M Tris-HCl, pH 7.0) for 15 - 30 mins and rinsed with dH₂O. The DNA was then transferred from the gel onto a membrane overnight, using capillary forces. The gel was placed on a blotting paper wick, the ends of which were placed in a chamber filled with 20 x SSC buffer (3 M NaCl, 0.3 M sodium citrate, pH 7.0). The membrane (Hybond-N nylon membrane, GE Healthcare Amersham) was pre-soaked first in dH₂O and then in 20 x SSC buffer, then placed on the gel, followed by two layers of blotting paper, a thick stack of paper towels, a plastic plate to distribute the pressure and a weight. After the overnight transfer, the membrane was washed for 10 to 20 mins in 2 x SSC buffer and then the DNA was covalently attached to the membrane in a UV Stratalinker 2400 crosslinker (Stratagene) at 1200 mJoules. The blot was kept dry until probing. Blots were probed using the Gene Images AlkPhos Direct Labelling and Detection System (GE Healthcare Amersham) according to the manual, to generate a fluorescence-labelled DNA probe, allow this to bind to the membrane-linked DNA and visualise it on photographic film after incubation with a chemiluminescence substrate. The DNA probe was generated by a standard *Taq* DNA polymerase PCR reaction, amplifying a suitable region of ~ 500 bp within one of the flanking regions of the gene and purifying the DNA from an agarose gel.

2.3 Bacterial cultures

2.3.1 *E. coli* cell lines used in this study

For high-copy replication of plasmid DNA and subsequent DNA isolation from the bacterial cells, competent *E. coli* XL1-Blue cells were used (genotype *recA1 endA1 gyrA96 thi-1 hsdR17 supE44 relA1 lac*, tetracycline-resistant, original batch from Stratagene, subsequently re-cultured in the lab).

Four different *E. coli* strains were used in protein expression experiments, depending on which yielded the best results for the respective plasmids: *E. coli* BL21 (DE3), *E. coli* BL21 (DE3) pLysS, *E. coli* BL21 (DE3) Rosetta and *E. coli* BL21 (DE3) Rosetta-gami. *E. coli* BL21 (DE3) carries the DE3 prophage with the T7 RNA polymerase gene and the *lacI^q* lac-repressor protein overexpression site. Plasmids that contain a T7 promoter for expression of the inserted protein of interest (e.g. pET vector based constructs) are repressed until expression is induced by the addition of IPTG and subsequent activation of T7 polymerase from a lac promoter. The pLysS strain of BL21 (DE3) carries an additional plasmid (pLysS) which encodes the T7 phage lysozyme. This inhibits the T7 polymerase and further suppresses T7 polymerase activity, and therefore the expression of the protein of interest, until induction with IPTG. The pLysS plasmid confers chloramphenicol resistance. The BL21 (DE3) Rosetta strain (original batch from Novagen) is derived from the BL21 (DE3) strain and optimised for expression of eukaryotic proteins with rare codon usage. It carries an additional plasmid which encodes tRNAs for codons that are rare in *E. coli* and also confers chloramphenicol resistance. The BL21 (DE3) Rosetta-gami strain (original batch from Novagen) has all features of the Rosetta strain and, additionally, is optimised to support the correct folding of the expressed target protein in the bacterial cytoplasm. All these bacterial cell lines were made competent by chemical treatment in the lab.

2.3.2 Generation of competent *E. coli* cell lines

All batches of competent cells used were made using a rubidium chloride method. A single colony of the respective *E. coli* strain was used to inoculate

2 ml of LB (Luria Broth) medium for an overnight culture at 37 °C. 0.5 ml of this culture was diluted into 100 ml LB broth and cultured for ~ three hours until an optical density (OD, measured at wavelength of 600 nm) of 0.4 - 0.6 was reached. The culture was incubated on ice for 10 mins, then centrifuged at 1000 x g for 15 mins at 4 °C in two 50 ml conical flasks. The cell pellet was resuspended in 33 ml cold RF1 buffer (100 mM RbCl, 50 mM MnCl₂ · 4H₂O, 30 mM potassium acetate pH 7.5, 10 mM CaCl₂ (dihydrate), 15 % (w/v) glycerol, pH adjusted to 5.8 with 0.2 M acetic acid, filter-sterilised), incubated for 15 mins on ice and centrifuged as before. The pellet was resuspended in 8 ml cold RF2 buffer (10 mM MOPS pH 6.8, 10 mM RbCl, 75 mM CaCl₂ (dihydrate), 15 % (w/v) glycerol, pH adjusted to 6.8 with NaOH, filter-sterilised) and incubated on ice for one hour. The suspension was aliquoted for single use and snap-frozen in ethanol on dry ice; aliquots were stored at - 80 °C.

2.3.3 Bacterial cultures

E. coli cells were spread onto agar plates containing the appropriate antibiotics (ampicillin at 100 µg ml⁻¹, kanamycin at 50 µg ml⁻¹ or chloramphenicol at 38 µg ml⁻¹) after transformation, using a sterile glass spreader. Plates were incubated at 37 °C overnight, then sealed with parafilm and maintained at 4 °C for up to one month. Single colonies were used to inoculate liquid cultures. For long term storage, *E. coli* cultures were mixed with an equal volume of 2 % (w/v) peptone and 40 % (v/v) glycerol solution in 1 ml aliquots and stored at -80 °C. Liquid bacterial cultures for replication and isolation of plasmid DNA were grown in Luria Broth (LB) medium at 37 °C, shaking overnight. Appropriate antibiotics were added to the cultures and cells were harvested for plasmid DNA purification. Cultures for protein expression experiments were grown in LB medium. Large cultures (typically 100 ml for a small scale test, 1 litre for a large protein expression culture) were inoculated with up to 15 ml of a fresh overnight culture, in a baffled Erlenmeyer flask of at least twice the volume of the culture and with appropriate antibiotics. Large cultures were grown at 37 °C in a shaker (~ 180 rpm) to an OD_{600nm} of ~ 0.6 and then induced by adding IPTG (isopropyl β-D-1-thiogalactopyranoside) and culturing further at the required temperature, usually overnight. New protein expression constructs were typically tested under

the following overnight culturing conditions: temperatures of 20 °C, 25 °C and 37 °C, induction with different IPTG concentrations between 0.1 and 1 mM.

2.3.4 Bacterial cell extracts

Recombinant protein was expressed in *E. coli* as described above. After harvesting the *E. coli* cells (typically 20 mins at 5000 x g), they were lysed using B-Per Bacterial Protein Extraction Reagent (Pierce) according to the manufacturer's instructions and adding DNase I (10 µg ml⁻¹) during an extended lysis step on ice for 10 mins. After centrifugation (typically 30 mins at 15000 x g) and separation of the insoluble components, the soluble fraction could be subjected to protein purification procedures.

2.4 Protein biochemistry

2.4.1 Denaturing polyacrylamide gel electrophoresis (SDS-PAGE)

Whole cell extracts and purified proteins were separated and visualised by SDS-PAGE (sodium dodecyl phosphate polyacrylamide gel electrophoresis), typically using 12 % (w/v) polyacrylamide gels cast in plastic casting cassettes (Invitrogen) according to the manufacturer's instructions. Gels were made with 30 % acrylamide-bis solution (Bio-Rad). A 5 % stacking gel was cast over the 12 % resolving gel to initially focus the proteins before separation. Samples were mixed with SDS-PAGE loading buffer (2 x loading buffer: 20 % (v/v) glycerol, 2.5 % (w/v) SDS, 0.05 % (w/v) bromophenol blue, 0.2 M Tris-HCl pH 6.8, 10 % DTT in H₂O) and boiled for ~ 5 mins at 100 °C. For the electrophoresis, XCell SureLock Mini Cell chambers (Invitrogen) were used with 1 x SDS-PAGE running buffer (10 x running buffer: 25 mM Tris, 192 mM glycine, 0.1 % (w/v) SDS), initially at 90 V through the stacking gel, then at ~ 150 V through the resolving gel until the protein dye front reached the bottom of the gel. A protein marker (Pre-stained Protein Marker Broad Range, New England Biolabs) was run alongside the protein samples at a concentration of 1 - 2 µg per lane to determine the size of the analysed proteins.

2.4.2 Coomassie staining of SDS-PAGE gel

After electrophoresis, polyacrylamide gels were stained with Coomassie stain (2.5 % (w/v) Coomassie Brilliant Blue R-250, 45 % (v/v) methanol, 10 % (v/v) glacial acetic acid, in H₂O) for one hour at room temperature under agitation. Gels were then treated with destaining solution (10 % (v/v) methanol, 10 % (v/v) glacial acetic acid, in H₂O) for several hours or overnight, at room temperature under agitation. The destaining solution was changed several times during this process and a paper tissue was placed in the solution next to the gel to absorb stain.

2.4.3 Western Blotting

For Western blotting, proteins were transferred from an SDS-PAGE gel (not Coomassie-stained) onto a nitrocellulose membrane (Hybond-C, GE Healthcare Amersham). The transfer was carried out using a semi-dry blotting chamber (Bio-Rad Trans-Blot SD Semi-Dry Transfer Cell) with transfer buffer (20 % (v/v) methanol, 20 mM Tris-HCl, 15 mM glycine, in H₂O) and at 20 V for 30 mins. After the transfer, the membrane was incubated in a blocking solution of 5 % (w/v) milk powder (Marvel) in TBST buffer (25 mM Tris-HCl pH 8.0, 120 mM NaCl, 0.1 % Tween-20) for one hour at room temperature or overnight at 4 °C on a shaker. After blocking, the membrane was incubated with the primary antibody (diluted in fresh blocking solution) for the appropriate time (one hour up to overnight) at room temperature or at 4 °C. In this study, the anti-His primary antibody (Qiagen Tetra-His Mouse IgG) was usually used at a 1 in 1000 dilution and the anti-Bem46 antibody (rabbit polyclonal antibody) at varying concentrations in the different experiments. After incubation with the primary antibody, the membrane was rinsed 3 x 10 mins with TBST buffer and then incubated with HRP (horseradish peroxidase)-conjugated secondary antibody for one hour at room temperature. The anti-mouse secondary antibody (Promega goat anti-mouse IgG HRP) required for the anti-His primary antibody was used at a 1 in 5000 dilution. The anti-rabbit secondary antibody (Sigma goat anti-rabbit IgG HRP) required for the anti-Bem46 primary antibody was used at a 1 in 10000 dilution. The secondary antibody was followed by 3 x 10 mins TBST washes, treatment of the membrane with ECL (enhanced chemiluminescence) substrate (SuperSignal West

Pico Chemiluminescent Substrate or West Femto Maximum Sensitivity Substrate, Pierce ThermoScientific) according to the manufacturer's instructions and exposure of the Western blot on photographic film or using a chemiluminescence detector (Bio-Rad Chemi-Doc XRS).

2.4.4 Protein purifications

Recombinant His-tagged protein was purified by metal ion affinity chromatography under native or denaturing conditions.

Small scale native purifications were carried out by incubating the filtered soluble fraction of bacterial protein extracts with Ni-NTA (nickel-nitrilotriacetic acid) agarose beads (Qiagen), preparing a small column (Disposable 2 ml Polystyrene Columns, Pierce ThermoScientific) with this slurry and washing the column with wash buffer (50 mM NaH₂PO₄, 300 mM NaCl, 20 to 50 mM imidazole, pH 8.0). The protein was then eluted with elution buffer (50 mM NaH₂PO₄, 300 mM NaCl, 500 mM imidazole, pH 8.0) into several fractions.

Large scale native purifications were performed using an IMAC (immobilised metal-ion affinity) column packed with MC-20 matrix (Poros) on a BioLogic Duo-Flow purification (Bio-Rad) system. The column was equilibrated with equilibration buffer (50 mM NaH₂PO₄, 300 mM NaCl, 0.5 mM imidazole, pH 8.0), the filtered soluble fraction of a bacterial extract was loaded onto the column, washed with wash buffer (50 mM NaH₂PO₄, 300 mM NaCl, 20 to 50 mM imidazole, pH 8.0) and eluted into several fractions with elution buffer (50 mM NaH₂PO₄, 300 mM NaCl, 500 mM imidazole, pH 8.0).

For denaturing protein purification, bacterial cells were lysed with urea buffer (8 M urea, 100 mM NaH₂PO₄, 10 mM Tris pH 8.0) with DNase I (10 µg ml⁻¹) and lysozyme (100 µg ml⁻¹), incubated at room temperature overnight on a roller, sonicated (10 x 10 sec), centrifuged (typically 30 mins at 15000 x g), and the soluble fraction filtered before loading onto the column. The affinity chromatography was carried out using an IMAC (immobilised metal-ion affinity) column packed with MC-20 matrix (Poros) on a Bio-CAD purification system (Applied Biosystems). The column was first equilibrated with urea buffer (as used for cell lysis), loaded with the protein extract, washed with urea buffer

adjusted to pH 6.2 and flow-through collected, washed with urea buffer adjusted to pH 5.2 and flow-through collected; finally the denatured protein was eluted with urea buffer adjusted to pH 4.5. Before using denatured protein for antibody production, the urea buffer was removed by dialysis into PBS, using a Slide-A-Lyzer 10 K dialysis cassette (10000 MWCO, Pierce ThermoScientific) to dialyse 3 ml protein solution in 2 litres PBS for ~ 20 hours, changing the PBS once during this time. Potentially forming protein precipitate can still be used for animal inoculation for antibody production.

2.4.5 Protein quantification

Protein concentrations were determined by Bradford assays, using Bradford reagent (Sigma, undiluted or at 1 in 5 dilution) according to the manufacturer's instructions. Assays were set up in 96-well plates; the standard curve was produced using nine BSA solutions with concentrations ranging from 0 to 2 mg ml⁻¹. The results were read at a wavelength of 592 nm in a Versamax microplate reader (Molecular Devices) with SoftMaxPro software.

2.4.6 Antibody production, purification and quality assessment

A specific polyclonal antiserum against *L. major* Bem46 was raised in a rabbit, using the almost full-length recombinant protein as an antigen. The recombinant protein was expressed with a C-terminal 6 x histidine-tag in *E. coli* using the pET28a-based plasmid pGL1577, purified by urea extraction and dialysis as described above. A rabbit was immunised with the protein (4 inoculations with 250 µl of 1 mg ml⁻¹ protein over the course of three months) at the Scottish National Blood Transfusion Service (Penicuik, Midlothian) and three bleeds as well as the pre-immune serum were obtained.

The antibody was purified using an affinity-purification column with bound recombinant (his-tagged) Bem46. For this, recombinant Bem46 was first exchanged into a coupling buffer (4 M guanidine hydrochloride (Sigma), 100 mM sodium phosphate, 0.05 % sodium azide, pH 6.4, in H₂O) to allow binding to the affinity column. For this buffer exchange, a Bio-Rad pre-packed 10 ml buffer exchange column was used; the column was washed with 20 ml coupling buffer, loaded with up to 3 ml protein solution (purification fractions), the flow-through

discarded and finally 4 ml coupling buffer were added and the flow-through (4 ml buffer-exchanged recombinant protein) collected. Next, this collected protein was bound to the beads for the affinity purification column; it was covalently linked to 2 ml AminoLink Coupling Gel (Pierce) on a disposable 5 ml column (Pierce), following the manufacturer's instructions and using 400 µl AminoLink reductant solution (Pierce). This coupling process was carried out for six hours at room temperature or overnight at 4 °C on a roller, then the beads were allowed to settle for ~ 30 mins, before draining the column, washing it with 5 ml coupling buffer, blocking it by adding 2 ml 1 M Tris (pH 7.5) and further 200 µl AminoLink reductant solution, incubating for 30 mins at room temperature on a roller, then allowing the beads to settle for 30 mins. The column was washed with 15 ml 1 M NaCl, followed by 5 ml PBS with 0.05 % sodium azide. 750 µl antiserum were applied to the column and let flow through. This was repeated several times to purify a useful amount of antibody, always allowing the entire 750 µl to flow through before applying more. Afterwards, 100 µl of PBS with sodium azide were applied and allowed to enter the resin, the column was capped at the bottom, further 500 µl were added, the column capped at the top and incubated standing at room temperature for one hour. It was washed with 12 ml azide-free PBS and drained. To elute the bound antibody, 4 ml elution buffer (100 mM glycine-HCl pH 2.7) were applied and 0.5 ml elution fractions were collected. The fractions were pH neutralised immediately by adding 50 µl 1M Tris-HCl (pH 7.5) to each. Antibody concentrations of the fractions were determined by Bradford assay and the best fractions were buffer-exchanged into PBS and sodium azide (final concentration 0.02 %) for use.

2.5 Leishmania cell culture

2.5.1 Leishmania promastigote culture

Leishmania major promastigote parasites (*L. major* MHOM/IL/80/Friedlin, WHO designation MHOM/JL/81/Friedlin) were grown and maintained in HOMEM medium (Invitrogen or PAA) supplemented with 10 % (v/v) heat-inactivated foetal calf serum (HIFCS), at 25 °C in lidded flasks (Corning 25 cm² canted neck culture flasks with phenol-style cap). Cells were subpassaged into fresh medium

every three to four days and usually only used for experiments up to subpassage 20. The following antibiotics were added if appropriate for selection of transfected cells: G418 (Calbiochem) at $50 \mu\text{g ml}^{-1}$ (neomycin resistance cassette confers G418 resistance), bleomycin (phleomycin, from InvivoGen) at $20 \mu\text{g ml}^{-1}$, puromycin (Calbiochem) at $50 \mu\text{g ml}^{-1}$ and hygromycin B (Calbiochem) at $50 \mu\text{g ml}^{-1}$. To prevent bacterial contaminations, penicillin-streptomycin (Sigma) was added to cultures occasionally (at 1 % (v/v)).

2.5.2 Determination of *L. major* cell densities

L. major cell culture densities were determined using an Improved Neubauer haemocytometer counting chamber (Weber Scientific) under a light microscope (at 200 x magnification). Before counting, cells were fixed in an equal volume of 2 % (v/v) paraformaldehyde solution (in PBS). For growth curves, cultures were started at 1×10^5 cells ml^{-1} and cell densities were determined daily at the same time for seven to nine days.

2.5.3 Leishmania stabilates

Stabilates of *L. major* cell lines were prepared with 10 % cryoprotectant DMSO (dimethyl sulfoxide) and 20 % HIFCS in HOMEM medium, using mid-log phase dividing promastigotes. They were gradually frozen, in cryovials (AlphaLaboratories, Feel the Seal 1 ml or 1.2 ml tubes) protected with cotton wool, at $-80 \text{ }^\circ\text{C}$ overnight and then transferred into liquid nitrogen for long-term storage.

2.5.4 Transfection, selection and cloning

L. major cells were transfected by electroporation, either with Cytomix buffer in a Bio-Rad electroporator (Gene Pulser II with Capacitance Extender II) or with the Amaxa transfection system and the Human T-cell Nucleofector kit (Lonza Biologics). For the Cytomix protocol, 5×10^7 cells were pelleted at $1000 \times g$ for 5 mins, resuspended in half the volume of ice cold Cytomix buffer (120 mM KCl, 0.15 mM CaCl_2 , 10 mM K_2HPO_4 , 25 mM HEPES, 2 mM EDTA, 2 mM MgCl_2 , pH 7.6), pelleted again and resuspended in ice cold Cytomix buffer to a final concentration of 1×10^8 cells ml^{-1} . Approximately $20 \mu\text{g}$ DNA (ethanol-

precipitated and resuspended in 20 µl sterile dH₂O) was pipetted into a chilled electroporation cuvette, 400 µl of cells in buffer were added and electroporated once at 0.45 kV and capacitance 500 µF. The cells were left on ice for 10 mins to recover, then transferred into 10 ml fresh HOMEM medium supplemented with FCS and warmed to culturing temperature. This method was used for all the transfections in chapter 3 (screen of potentially secreted *L. major* peptidases). The transfections described in chapters 4 and 5 were performed using the Amaxa system, again with 5×10^7 cells per transfection. Cells were pelleted at 1000 x g for 10 mins and resuspended in 100 µl Amaxa Human T-cell Nucleofactor buffer and mixed with 10 µg ethanol-precipitated DNA (in 20 µl sterile dH₂O) in an Amaxa cuvette. Samples were electroporated in the Amaxa instrument, using the set programme U-033, and then transferred onto ice for several mins before transferring the cells into 10 ml fresh HOMEM medium supplemented with HIFCS and warmed to culturing temperature. All transfected populations were cultured at 25 °C overnight to recover. A non-transfected control culture was always included for each transfection, to assure un-transfected cells did not exhibit antibiotic resistance in the selection process. If populations required cloning out, the transfected cells were immediately split into two separate 5 ml cultures. One day after transfection, the appropriate antibiotics were added to the cultures to select for positive transfectants, depending on which antibiotic resistance cassette was introduced into the cells on the transfected plasmid. Cells were grown for at least two weeks for the selection to be complete and the plasmids to be established in the lines. If clonal populations were required, the transfected populations were transferred into 96-well plates in three serial dilutions (1 in 5, 1 in 50 and 1 in 500) one day after transfections, after adding antibiotics. The plates were sealed with parafilm to avoid drying out and were incubated at 25 °C over several weeks to allow cultures to grow. Based on the calculated transfection efficiencies, an average of 20 clones should be obtained from the 1 in 50 dilution, and 2 from 1 in 500 (Protocols for handling and working with *Leishmania*, Mottram laboratory, 2008).

2.5.5 *Leishmania* DNA isolation

Whole genomic DNA was prepared from *Leishmania* cell lines using the DNeasy Blood & Tissue kit (Qiagen) according to the “Cultured animal cells” protocol, on

the bench top or using the QIAcube machine (Qiagen). 10 ml of mid to late log *L. major* culture were pelleted at 2000 x g for 5 mins, resuspended in a small remainder of the supernatant, transferred to a 1.5 ml eppendorf tube, pelleted again (3000 x g for 1 min) and resuspended in 200 µl PBS (100 µl when using the QIAcube). 20 µl proteinase K (from Qiagen kit) and 4 µl RNase A (100 mg ml⁻¹ solution) were added, vortexed and incubated for 2 mins at room temperature. From here, the kit was used according to the manufacturer's instructions.

2.5.6 Leishmania cell extracts

Whole cell extracts of *Leishmania* were prepared with lysis buffer containing 2 % SDS (sodium dodecyl sulphate) (w/v) in PBS with protease inhibitors, usually Complete Protease Inhibitor Cocktail (Roche), used according to the manufacturer's instructions. Typically, 5 to 10 ml of mid or late log *L. major* cells were pelleted at 1000 x g for 5 mins, washed twice with sterile PBS, resuspended in 100 - 200 µl cold lysis buffer, incubated on ice for ~ 15 mins and then boiled for 5 mins.

2.5.7 Mouse infections and parasite harvests from foot pads

BALB/c mice were injected into the footpad with 20 µl stationary-phase *L. major* promastigote cultures at a concentration of 5 x 10⁷ cells ml⁻¹ in sterile PBS. To generate an infection progression curve, six mice were used per cell line and lesion growth of the footpad was measured weekly until the footpad had swollen to 5 mm and the mice were culled. Amastigote parasites were harvested from the footpad by excising the lesion from the foot using a scalpel and transferring fragments of the infected tissue into HOMEM buffer with 10 % HIFCS and the antibiotic gentamycin (Sigma) at 10 µg ml⁻¹. Incubation in this medium at 25 °C leads to differentiation of the harvested amastigotes into culture promastigotes.

2.6 Fluorescence microscopy

2.6.1 The DeltaVision System

All fluorescence microscopy was performed on a DeltaVision Deconvolution microscopy system (Applied Precision), fitted with a CoolSnap HQ camera. The system was operated and images were captured and processed using the software SoftWoRx, running on a Linux system. Fluorescent cells were imaged with a FITC filter (λ_{Ex} : 490 nm / λ_{Em} : 528 nm) for GFP fluorescence, a RD-TR-PE filter (λ_{Ex} : 555 nm / λ_{Em} : 617 nm) for mCherry, MitoTracker, LysoTracker and FM4-64 fluorescence and a DAPI filter (λ_{Ex} : 360 nm / λ_{Em} : 457 nm) for DAPI (4',6-diamidino-2-phenylindole) staining of nuclei and kinetoplasts. Reference images were obtained under brightfield illumination. Images were typically obtained at an exposure time of 1 sec and with transmission levels (% T) of the neutral density filter adjusted to the respective intensity of the fluorescence. All images were taken at a 1000 x magnification using a 100 x oil immersion objective. Usually, 20 Z-stacks were taken for each image. They were deconvolved using a "conservative ratio setting" with 10 iterations. For figures, either the best Z-stack image was chosen, or several Z-stacks were projected into one image. Images of two or more fluorescence channels and / or brightfield were merged using Adobe Photoshop CS.

2.6.2 Live cell imaging sample preparation

For imaging of live cells, the cells were harvested by centrifugation (1 min at 1000 x g), usually ~200 μl of mid-log phase cells per slide or adjusted volumes for cultures of lower or higher density. Cells were washed twice or - if treated with a stain - three times with ice-cold PBS, resuspended in ~40 μl PBS per slide and applied to a glass slide with a large cover slip (24 x 63 mm). The cover slip was sealed onto the slide with clear nail varnish to prevent leakage or drying of the sample. To decrease the cells' movement and therefore facilitate imaging, the slides were usually cooled for ~10 mins at 4 °C before microscopy. Several different molecular stains were used to fluorescently label different components of the cells: DAPI (4',6-diamidino-2-phenylindole) was used to stain nucleus and kinetoplast. DAPI permeates membranes and binds to DNA. It is excited at a

wavelength of 358 nm and emits at around 461 nm. In this study, DAPI was made up to a stock solution of 10 mg ml⁻¹ in H₂O and was used at a final concentration of 1 µg ml⁻¹, cells were incubated for 5 to 10 mins at room temperature and then washed with PBS and prepared as described above. LysoTracker Red DND-99 stain (Invitrogen Molecular Probes) was used to target acidic organelles like the lysosome and (in *Leishmania*) particularly the acidocalcisomes. Its absorption peaks at 577 nm and it emits at 592 nm. The stain was made up to a 1 mM stock solution and used at a final concentration of 10 µM. Cells were incubated for ~30 mins at 25 °C and then washed three times with PBS and prepared as described above. The mitochondrion was stained with MitoTracker Red CMXRos stain (Invitrogen Molecular Probes). This stain is excitable at 578 nm and emits at 599 nm. It was made up to a 1 mM stock solution and then a 10 µM working solution in PBS and used at a final concentration of 1 - 2 nM. Cells were incubated for 2 mins at 25 °C and then washed three times with PBS and prepared as described above. The lipophilic molecular dye FM4-64 (Invitrogen Molecular Probes) was used as a red fluorescent endocytic marker; it is excited at 558 nm and emits at 734 nm. In *Leishmania*, it labels the flagellar pocket of the cell within the first minutes of staining, then enters the endocytic pathway and later labels the lysosome (after 30 to 45 mins). The stock solution was made up to 12 mM in DMSO and used at a final concentration of 40 µM. Cells were incubated with FM4-64 for 15 mins at 4 °C and then washed, resuspended in fresh HOMEM medium and incubated at 25 °C for various times, depending on the desired staining.

2.6.3 Fixing of cells

Cells were fixed for counting and for fluorescence microscopy in 1 % (v/v) paraformaldehyde in PBS. For the fluorescence microscopy in this study, most cell lines were fixable while still retaining their GFP or mCherry signals as well as all of the molecular stains, at least if analysed directly (within one or two hours). This also applies to the stains MitoTracker and FM4-64 which are described as non-fixable in the manufacturer's manuals.

2.6.4 Immunofluorescence analysis (IFA)

For immunostaining and fluorescence microscopy, 200 μ l *L. major* cells were first washed twice in PBS and fixed in paraformaldehyde as described above. After 30 mins, cells were permeabilised with 20 μ l 1 % Triton X-100 (in PBS) for 10 mins, and then 20 μ l of 1 M glycine / PBS were added for 10 mins in order to neutralise free aldehyde groups from the fixation and reduce background fluorescence. The cells were washed twice and resuspended in 200 - 400 μ l fresh PBS. Glass slides were washed in 70 % ethanol, coated with 0.01 % poly-L-lysine (Sigma) and dried. The fixed cells (~ 50 μ l per slide) were allowed to adhere to the slides (confined by a square of nail varnish) for 15 - 30 mins in a dark box containing PBS-soaked tissue to prevent drying. The slides were then incubated with blocking buffer TB (0.1 % Triton X-100, 0.1 % BSA, in PBS) for at least 5 mins. Primary antibodies were diluted in TB buffer and incubated with the cells for one hour at room temperature, or overnight at 4 °C. Approximately 150 μ l antibody solution were used per slide. Cells were washed carefully three times with at least 10 ml PBS, and excess liquid was removed by blotting with a tissue at the corner of the slide. Alexa Fluor 594 (red)-conjugated anti-rabbit secondary antibody (Molecular Probes) was diluted 1 in 2000 in TB buffer and incubated with the cells in the dark for one hour at room temperature. DAPI (4',6-diamidino-2-phenylindole, 10 mg ml⁻¹ stock solution) was diluted in TB buffer at 0.5 μ g ml⁻¹ and incubated with the cells for one min, then the slides were washed 3 x with 10 ml PBS and excess liquid as well as remains of the nail varnish square were removed. Approximately 50 μ l of mounting solution (2.5 % DABCO in 50 % glycerol and PBS) were applied to a 20 x 64 mm coverslip; this was placed on the slide and sealed with nail varnish. Until microscopy, slides were kept in a moist box in the dark, to prevent drying.

2.7 Statistical data analysis

Data from promastigote culture growth curves as well as mouse footpad lesion measurements were expressed as means \pm standard deviation from the mean. P-values were calculated by unpaired, two-tailed Student's T-tests, using Microsoft Excel. Differences were considered significant at a p-value of < 0.05.

3. Screen for peptidases secreted by *Leishmania*

3.1 Introduction

Leishmania is known to release virulence factors which are either secreted into the host environment or are attached to the *Leishmania* surface, from where they can interact with the host or be cleaved and released. An example of a well-studied *Leishmania* virulence factor is the cysteine peptidase B (CPB), which is a degradative hydrolase of the lysosome. A proportion of CPB molecules is not trafficked directly from biosynthesis in the ER to the lysosome, but is exocytosed into the flagellar pocket, re-endocytosed and then transported to the lysosome via the endocytic pathway. During this process, some CPB is released from the flagellar pocket and acts as a virulence factor and manipulate the immune system (Mottram et al., 2004a). Other *Leishmania* peptidases may be released in a similar manner and could be active as virulence factors, for example cleaving components of the host immune defence machinery.

3.1.1 Secretion of proteins

The flagellar pocket is the sole site of exocytosis in *Leishmania*. To be released from the cell, all molecules, including virulence factor proteins, have to be targeted into the flagellar pocket first.

Classical targeting signals that direct proteins into the secretory pathway after biosynthesis are located at the N-terminus of a protein (Blobel and Dobberstein, 1975) and are typically around 15 - 30 residues long. Such "signal peptides" are cleaved after trafficking of the protein. There is no signal peptide consensus sequence, but they usually consist of a positively charged N-terminal part (n-region) followed by a hydrophobic stretch (h-region) and polar uncharged amino acids at the C-terminal end (c-region) of the peptide (Emanuelsson et al., 2007;

Tobin and Wirth, 1993a). It appears that this type of signal is widely conserved; experiments have shown that a mammalian signal peptide elicits correct secretory targeting in *Leishmania* (Tobin and Wirth, 1993b), suggesting conservation of some secretory mechanisms. Alternatively to a signal peptide, a protein can be targeted into the secretory pathway and then anchored in a membrane by a "signal anchor" which is not cleaved but forms a transmembrane helix. It is worth noting that not all proteins with a signal peptide are secreted; they can be retained in the ER, the Golgi or in vesicles along the way. Also not all secreted proteins contain a classical signal peptide (Emanuelsson *et al.*, 2007). Non-classical secretion pathways are an alternative type of protein secretion in eukaryotes, targeting proteins to the cell surface independently of the ER /Golgi network and without a canonical N-terminal secretory signal (Bendtsen *et al.*, 2004a). This takes place via secretory lysosomes, polypeptide export through ABC transporters or by budding of the plasma membrane itself (Rubartelli *et al.*, 1990; Mehul and Hughes, 1997; McConville *et al.*, 2002j). In *Leishmania*, the surface protein HASPB (previously named Gene B Protein) is an example of a secreted surface protein that does not exhibit a classical N-terminal signal peptide (Rangarajan *et al.*, 1995b). Its N-terminus contains a myristoylation and a palmitoylation site and dual acylation at these sites appears to be crucial for secretory targeting via a novel and conserved pathway (Denny *et al.*, 2000).

3.1.2 Targeting of proteins to the mitochondrion

Non-secretory proteins can be targeted to different intracellular destinations and organelles. This usually requires a particular sorting signal and some of these signals have been identified in eukaryotes.

Targeting of proteins into the mitochondrion requires a complex mitochondrial targeting signal. This does not consist of a particular conserved amino acid sequence, but common features are an N-terminal amphipathic anti-helix and an unusual enrichment in arginine, alanine and serine. The length of such a signal is highly variable from only a few to over 80 residues (Emanuelsson *et al.*, 2007; von Heijne *et al.*, 1989b). Import into the mitochondrion is a more complex process than for other organelles because of this organelle's double membrane.

Proteins can be translocated across one or both membranes, for integration into either of these or - for soluble proteins - release into the intermembrane space or the inner matrix (Hannavy *et al.*, 1993; Costa-Pinto *et al.*, 2001).

3.1.3 Bioinformatics prediction of protein properties

Many features and topological properties of proteins can be predicted using programmes available online. These differ in their approach, their species- and cell type specificity and outputs are generally not directly comparable.

Proteins of an eukaryote as divergent as *Leishmania* may be difficult to characterise using general or eukaryotic protein prediction software, as the underlying patterns and trafficking motifs may vary considerably in this species, in comparison to higher eukaryotes. Nevertheless, prediction programmes can be powerful tools to gain a first insight into a protein's solubility, anchoring and target compartment *in silico*.

A specific N-terminal signalling domain is an indicator of possible secretion and can target a protein into the secretory pathway. Transmembrane domains point to a localisation of the protein in an organellar membrane or at the cell surface. Transmembrane proteins on the cell surface can interact with the environment from there, or be released by cleavage. Additionally, an N-terminal mitochondrial targeting motif is identifiable with suitable predictors, as are potential GPI anchoring sites. To predict N-terminal secretory or mitochondrial signals, the prediction programmes TargetP, SignalP and MitoProt were used. The SOSUI, TMHMM, HMMTOP and Phobius algorithms were employed for the prediction of transmembrane domains and big-PI predicted potential GPI anchoring sites. Guidelines and information on the available prediction tools and their optimal usage have been collected and reviewed in (Emanuelsson *et al.*, 2007).

TargetP 1.1 (CBS, Technical University of Denmark) gives an initial indication of the kind of N-terminal signal present in an amino acid sequence. It differentiates between a secretory signal peptide (SP), a mitochondrial targeting peptide (mTP) and "others" and it provides a reliability coefficient (RC) for each prediction, between 1 (very reliable) and 5 (unreliable) (Emanuelsson *et al.*,

2000; Nielsen *et al.*, 1997). Following the TargetP prediction, more detailed predictions of signal or mitochondrial targeting peptides can be obtained with the programmes SignalP and MitoProt.

SignalP 2.0 and 3.0 (CBS, Technical University of Denmark) provides a more in-depth analysis of the likelihood of a secretory signal peptide or a signal anchor, and additionally predicts cleavage sites for signal peptidase I (SPase I). Predictions are made using Neural Networks (SignalP-NN) or Hidden Markov Models (SignalP-HMM) trained on eukaryotic sequences (Bendtsen *et al.*, 2004b).

SignalP-NN analyses the amino acid sequence as a series of overlapping windows, using two separate Neural Networks for predicting the actual signal peptide and predicting the SPase I cleavage site. Five different scores are estimated by SignalP-NN: the S-score (likelihood of residue belonging to a signal peptide), the C-score (likelihood of residue being the first residue of a mature protein, which should coincide with a change in the S-score), the Y-score (geometric average of C-score and smoothed slope of S-score for a better estimation of cleavage site) and the D-score (average of maximal Y-score and mean S-score for an optimised combined result). The output includes a graph as well as a table of the results and a prediction of the most likely cleavage site within the protein sequence.

In contrast, SignalP-HMM predicts the probability of a signal peptide by fitting the entire amino acid sequence onto a model of a signal peptide-containing protein. It distinguishes between a signal peptide, a signal anchor and "other" N-terminal signals. If a signal peptide is predicted, the programme identifies the n-region, h-region and c-region of the peptide, as well as the most likely cleavage site.

MitoProt II (Helmholtz Center Munich) can be used to predict the probability of an N-terminal mitochondrial targeting sequence. This prediction is based on the analysis of 47 parameters that have been correlated with mitochondrial targeting and the programme has been trained and validated using a database of over 13 000 proteins (Claros and Vincens, 1996). It analyses the sequence of up to 40 amino acids from the N-terminus of a protein and calculates the probability of import to the mitochondrion.

Several different programmes are available for the prediction of transmembrane domains in proteins by analysing the hydropathy of the amino acid sequence as well as the length of hydrophobic stretches.

Transmembrane domain predictors used in this study were SOSUI (University of Nagoya; (Hirokawa *et al.*, 1998), TMHMM 2.0 (CBS, Technical University of Denmark; (Krogh *et al.*, 2001), HMMTOP 2.0 (Hungarian Academy of Sciences; (Tusnady and Simon, 2001; Tusnady and Simon, 1998) and Phobius (Stockholm Bioinformatics Centre), which is a combined predictor of transmembrane domains and signal peptides with a better discrimination between the two than SignalP (Kall *et al.*, 2004a). The output files of all programmes contain a table of results with the predicted number of transmembrane domains and their positions as well as a graphical representation. It is important to note that a predicted transmembrane domain at the far N-terminus may be a false positive and actually a signal peptide (Lao *et al.*, 2002b).

The programme big-PI (IMP, University of Vienna) was employed for the prediction of a GPI-anchoring site at the C-terminus of the mature protein (Eisenhaber *et al.*, 1999), which can indicate the positioning of a protein in the cell membrane, from where it can potentially be cleaved.

3.2 Results

3.2.1 Bioinformatics analyses of candidate peptidases

Bioinformatics analyses were carried out on all 160 proteins identified as peptidases in the *L. major* genome project (Ivens *et al.*, 2005a). They were initially identified as peptidases by comparison to the Merops database of all known peptidases (<http://merops.sanger.ac.uk>).

As a first indicator of intracellular localisation, signal peptide predictions for the 160 putative *L. major* peptidases were obtained from the genome database GeneDB. These predictions had been generated with version 2.0 of the SignalP-HMM algorithm. In this initial analysis, 38 were predicted to contain a secretory signal peptide (Table 3-1). These were analysed further by re-evaluating the SignalP predictions with TargetP and the updated version 3.0

SignalP algorithms, as well as by predicting mitochondrial targeting signals using MitoProt, transmembrane domains using SOSUI, TMHMM, HMMTOP and Phobius and potential GPI-anchoring sites using big-PI.

Proteins of known function, those known to be currently under investigation elsewhere or those that were unlikely to be secreted (e.g. predicted to be mitochondrial) were excluded from the list of candidates (Table 3-1). Finally, seven new candidate peptidases and one potential mitochondrial control were selected for more detailed analysis.

The eight candidate peptidases contained diverse members from the different peptidase groups (Table 3-2). Three cysteine peptidases were included: a calpain-like cysteine peptidase, a ubiquitin hydrolase cysteine peptidase and a CaaX prenyl protease with an unknown catalytic mechanism. From the serine peptidase group, four candidates were chosen: two rhomboid-like serine peptidases, one of which was included as a mitochondrial control, the only *L. major* serine carboxypeptidase and a Bem46-like serine peptidase. The only metallopeptidase included was a zinc carboxypeptidase of unknown function. No aspartic or threonine peptidases were selected. All candidate peptidases had homologues in other *Leishmania* species, with shared synteny in almost all cases. The Bem46-like serine peptidase was the only candidate where the *L. infantum* and *L. braziliensis* genes were not both located on the same chromosome as in *L. major*; the *L. braziliensis* Bem46 was located on chromosome 34 instead of 35. All candidate peptidases also had homologues in *T. brucei* and *T. cruzi*. Additionally, it should be mentioned that no homologues of the selected *L. major* peptidases were present in the *L. donovani* "secretome" as previously published by Silverman and co-workers (Silverman *et al.*, 2008). The predictions of secretory and mitochondrial targeting signals for all candidate peptidases are shown in Table 3-2 and those of transmembrane domains and GPI anchoring sites in Table 3-3.

The calpain-like cysteine peptidase (LmjF31.0390) was predicted to be a soluble protein without transmembrane domains or a mitochondrial targeting signal, featuring a secretory signal peptide that is most likely cleaved after residue 17. The predictions from different programmes were consistent and strong for the calpain-like cysteine peptidase.

The ubiquitin hydrolase cysteine peptidase (LmjF09.0240) was also predicted to be a soluble protein without transmembrane domains. SignalP and Phobius assigned a secretory signal peptide with a cleavage site after residue 28, whereas TargetP and MitoProt predicted a mitochondrial targeting peptide instead of a secretory signal.

The CaaX prenyl protease (LmjF26.2690) was predicted to contain two to four transmembrane domains, depending on the algorithm. A secretory signal peptide with a cleavage site after residue 48 was predicted by SignalP when using the Hidden Markov Model (HMM) algorithm. However, SignalP Neural Networks (NN) and TargetP predicted a low probability of a signal peptide, a potential cleavage site after residue 15 and, in accordance with the MitoProt result, a high probability of import into the mitochondrion.

The first rhomboid-like serine peptidase (LmjF02.0430) was predicted to have either none or up to four transmembrane domains, depending on the algorithm. A secretory signal was calculated as highly likely, but the most likely cleavage site was placed after residue 18 by version 2.0 of SignalP and after residue 27 by the updated version 3.0. Predictions agreed on a very low probability of mitochondrial import.

The second rhomboid-like serine peptidase (LmjF04.0850), which was included as a mitochondrial control, received very high probability values for import into the mitochondrion. TargetP as well as Phobius and SignalP-NN did not predict a secretory signal peptide. However, SignalP-HMM did predict such a signal, with a calculated cleavage site after residue 63 in SignalP version 2.0 and after residue 36 in version 3.0. This peptidase was predicted to contain three to five transmembrane domains.

The serine carboxypeptidase (LmjF18.0450) was predicted to contain none or one transmembrane domain. The latter was predicted at the very N-terminus of the protein, which can be a false positive and correspond to a secretory signal peptide instead (Emanuelsson *et al.*, 2007). The probability values for a secretory signal were high across all used algorithms, with a consistently calculated cleavage site after residue 29. TargetP predicted no mitochondrial

targeting sequence, whereas MitoProt gave a medium probability value of 0.6 for mitochondrial import.

The Bem46-like serine peptidase (LmjF35.4020) also was predicted to have one transmembrane domain at its N-terminus, which may be a signal peptide. The calculated probabilities of a secretory signal peptide varied widely between different programmes, from SignalP version 2.0 and Phobius predicting no signal peptide, to TargetP assigning a high likelihood value of 0.95 with a high reliability coefficient. The cleavage site of a potential signal peptide was positioned after residue 29 by SignalP version 3.0. No mitochondrial import was predicted.

Finally, the analysis of the largest protein, the zinc carboxypeptidase (LmjF33.0200) yielded the most varying and contradictory results. SOSUI and TMHMM predicted it to be soluble with no transmembrane domains, whereas HMMTOP and Phobius assigned four transmembrane domains. Predictions for a secretory signal peptide ranged from unlikely in TargetP (which assigned this prediction a very poor reliability coefficient of 5) to a reasonably high likelihood (0.79) and a potential cleavage site after residue 18 in SignalP-HMM version 3.0. Import to the mitochondrion was calculated unlikely.

None of the analysed proteins were predicted to contain a GPI-anchoring site.

Table 3-1: All 160 analysed putative peptidases from the *L. major* genome with prediction of signal peptide (SignalP 2.0) and evaluation status for candidate selection process. CP: cysteine peptidase, SP: serine peptidase, MP: metallo-peptidase, TP: threonine peptidase. "Selected" peptidases are the candidates chosen for investigation here. Peptidases "previously characterised" or "under investigation" are or have been investigated elsewhere.

Peptidase	Signal peptide	Status
Cysteine peptidases (CP)		
Calpain-like CPs (28 genes)	26 no, 2 yes	1 selected
Ubiquitin hydrolase-like CPs (19 genes)	16 no, 3 yes	1 selected
CPA	Yes	previously characterised
CPB (8 gene array)	Yes	previously characterised
CPC	Yes	previously characterised
GPI8 CP	Yes	previously characterised
SUMO1/Ulp2 CP	No	-
ATG4-like CP (2 genes)	No	-
D-alanyl-glycyl endopeptidase-like CP (2 genes)	No	-
Otubain-like CP	No	-
Metacaspase CP	No	-
Separase CP	No	-
Pyroglutamyl peptidase I CP	No	-
Pfpl/DJ-1-like CP	No	-
Metallopeptidases (MP)		
Zinc carboxypeptidase-like MP (3 genes)	2 no, 1 yes	1 selected
GP63-like MP (6 genes)	Yes	previously characterised
Mitochondrial intermediate peptidase-like MP	Yes	probably mitochondrial
Mitochondrial processing MP, alpha subunit (3 genes)	2 no, 1 yes	probably mitochondrial
Mitochondrial processing MP, beta subunit (2 genes)	1 no, 1 yes	probably mitochondrial
ATP-dependent zinc MP (5 genes)	4 no, 1 yes	-
Aminopeptidase P1-like MP (4 genes)	3 no, 1 yes	-
Metallopeptidase clan ME family M16	Yes	-
Caax prenyl protease 1 MP	No	-
Dipeptidyl peptidase-III-like MP	No	-
Aminopeptidase-like MP (10 genes)	No	-
Peptidyl dipeptidase-like MP (2 genes)	No	-
Thimet oligopeptidase-like MP	No	-
Carboxypeptidase-like MP (4 genes)	No	-
Mitochondrial ATP-dependent zinc MP (2 genes)	No	-
Pitriylsin-like MP	No	-
Metallopeptidase clan MP family M67 (2 genes)	No	-
Methionine aminopeptidase-like MP	No	-
Glutamamyl carboxypeptidase-like MP	No	-
Aspartyl aminopeptidase-like MP	No	-
O-sialoglycoprotein-like MP	No	-
Proteasome regulatory non-ATPase subunit 11-like MP	No	-

Peptidase	Signal peptide	Status
Aspartic peptidases (AP)		
Presenilin-like AP	No	-
Signal peptide peptidase	No	-
Serine peptidases (SP)		
Serine carboxypeptidase CBP1-like SP	Yes	selected
Bem46-like SP	No*	selected
Rhomboid-like SP (2 genes)	Yes	2 selected [#]
Mitochondrial inner membrane signal peptidase	Yes	probably mitochondrial
Subtilisin-like SP (2 genes)	1 no, 1 yes	under investigation
ATP-dependent Clp protease subunit (5 genes)	3 no, 2 yes	-
OPB-like SP (2 genes)	No	-
Prolyl oligopeptidases-like SP	No	-
Dipeptidyl peptidase-8-like SP	No	-
Signal peptidase I-like SP	No	-
Serine peptidase, Clan SC, family S9D	No	-
26S Protease Regulatory Subunit-like SP	No	-
Nucleoporin-like SP	No	-
Threonine peptidases (TP)		
HslVU complex proteolytic subunit-like TP	Yes	likely mitochondrial
Several proteasome subunit TPs (20 genes)	No	-
Unclassified peptidases		
Caax prenyl protease 2	Yes	selected

* has hydrophobic domain close to N-terminus

[#] one of these was chosen as a mitochondrial control

Table 3-2: Details of all candidate peptidases. *L. major* gene IDs from www.genedb.org. CP: cysteine peptidase, SP: serine peptidase, MP: metallopeptidase

Peptidase name	<i>L. major</i> gene ID	Size of gene (bp / kb) and protein (kDa)	GFP fusion protein	pNUS-GFP fusion plasmid ID
Calpain-like cysteine peptidase (CP), clan CA, family C2	LmjF31.0390	2.6 kb 97 kDa	full length C-terminal fusion	pGL1763
Ubiquitin hydrolase cysteine peptidase (CP), clan CA, family C19	LmjF09.0240	2.8 kb 105 kDa	truncated to 2.4 kb, C-terminal fusion	pGL1586
CaaX prenyl protease 2 family U48 (unknown catalytic mechanism)	LmjF26.2690	375 bp 25 kDa	full length C-terminal fusion	pGL1569
Rhomboid-like serine peptidase (SP), clan ST, family S54	LmjF02.0430	1.1 kb 40 kDa	full length C-terminal fusion	pGL1572
Rhomboid-like serine peptidase (SP) (mitochondrial control), clan ST, family S54	LmjF04.0850	1.2 kb 44 kDa	full length C-terminal fusion	pGL1589
Serine carboxypeptidase (SP), clan SC, family S10	LmjF18.0450	1.4 kb 52 kDa	full length C-terminal fusion	pGL1764
Bem46-like serine peptidase (SP), clan SC, family S09X	LmjF35.4020	1.2 kb 43 kDa	full length C-terminal fusion	pGL1588
Zinc carboxypeptidase (MP), clan MC, family M14	LmjF33.0200	4.5 kb 161 kDa	truncated to 600 bp, C-terminal fusion	pGL1570

Table 3-3: Predictions of secretory and mitochondrial sorting signals for all candidate peptidases.

L: likelihood, P: probability, SP: signal peptide, mTP: mitochondrial targeting peptide, SA: signal anchor, CS: most likely SPase I cleavage site, aa: amino acid residue, RC: TargetP reliability coefficient (from 1 - very reliable to 5 - not reliable), D-Score: best indicator of signal peptide probability from SignalP.

Peptidase name	<i>L. major</i> gene ID	Prediction programme results for N-terminal secretory and mitochondrial signal peptides				
		TargetP	SignalP-HMM version 2.0	SignalP-HMM version 3.0	SignalP-NN version 3.0	MitoProt
Calpain-like cysteine peptidase	LmjF31.0390	SP L = 0.93 mTP L = 0.03 RC: 1	SP P = 0.99 SA P = 0.001 CS: after aa 17	SP P = 0.99 SA P = 0.001 CS: after aa 17	SP P = 0.59 (D-Score) CS: after aa 17	Mitochondrial import P = 0.04
Ubiquitin hydrolase cysteine peptidase	LmjF09.0240	SP L = 0.18 mTP L = 0.89 RC: 2	SP P = 0.95 SA P = 0.05 CS: after aa 28	SP P = 0.94 SA P = 0.05 CS: after aa 28	SP P = 0.54 (D-Score) CS: after aa 28	Mitochondrial import P = 0.93
CaaX prenyl protease 2	LmjF26.2690	SP L = 0.09 mTP L = 0.87 RC: 2	SP P = 0.92 SA P = 0.03 CS: after aa 48	SP P = 0.92 SA P = 0.03 CS: after aa 48	SP P = 0.29 (D-Score) CS: after aa 15	Mitochondrial import P = 0.96
Rhomboid-like serine peptidase	LmjF02.0430	SP L = 0.96 mTP L = 0.02 RC: 1	SP P = 0.87 SA P = 0.00 CS: after aa 18	SP P = 0.92 SA P = 0.02 CS: after aa 27	SP P = 0.54 (D-Score) CS: after aa 27	Mitochondrial import P = 0.05
Rhomboid-like serine peptidase (mitochondrial control)	LmjF04.0850	SP L = 0.02 mTP L = 0.93 RC: 1	SP P = 0.93 SA P = 0.003 CS: after aa 63	SP P = 0.82 SA P = 0.01 CS: after aa 36	SP P = 0.25 (D-Score) CS: none	Mitochondrial import P = 0.99
Serine carboxypeptidase	LmjF18.0450	SP L = 0.99 mTP L = 0.05 RC: 1	SP P = 1.00 SA P = 0.00 CS: after aa 29	SP P = 0.99 SA P = 0.001 CS: after aa 29	SP P = 0.84 (D-Score) CS: after aa 29	Mitochondrial import P = 0.60
Bem46-like serine peptidase	LmjF35.4020	SP L = 0.95 mTP L = 0.03 RC: 1	SP: none SA: none CS: none	SP P = 0.27 SA P = 0.73 CS: after aa 29	SP P = 0.65 (D-Score) CS: after aa 29	Mitochondrial import P = 0.08
Zinc carboxypeptidase	LmjF33.0200	SP L = 0.18 mTP L = 0.33 RC: 5	SP P = 0.76 SA P = 0.00 CS: after aa 18	SP P = 0.79 SA P = 0.00 CS: after aa 18	SP P = 0.27 (D-Score) CS: none	Mitochondrial import P = 0.07

Table 3-4: Predictions of transmembrane domains and GPI anchoring sites for all candidate peptidases.
 TM: transmembrane, GPI: potential glycosylphosphatidylinositol anchoring site, SP: secretory signal peptide

Peptidase name	<i>L. major</i> gene ID	Prediction programme results for transmembrane domains and GPI anchoring sites				
		SOSUI	TMHMM	HMMTOP	Phobius	big-PI
Calpain-like cysteine peptidase	LmjF31.0390	TM domains: 0	TM domains: 0	TM domains: 0	TM domains: 0 SP: yes	No GPI
Ubiquitin hydrolase cysteine peptidase	LmjF09.0240	TM domains: 0	TM domains: 0	TM domains: 0	TM domains: 0 SP: yes	No GPI
CaaX prenyl protease 2	LmjF26.2690	TM domains: 4	TM domains: 2	TM domains: 4	TM domains: 4 SP: yes	No GPI
Rhomboid-like serine peptidase	LmjF02.0430	TM domains: 0	TM domains: 3-4	TM domains: 3	TM domains: 3 SP: yes	No GPI
Rhomboid-like serine peptidase (mitochondrial control)	LmjF04.0850	TM domains: 3	TM domains: 4	TM domains: 7	TM domains: 5 SP: no	No GPI
Serine carboxypeptidase	LmjF18.0450	TM domains: 1 (at N-terminus)	TM domains: 1 (at N-terminus)	TM domains: 1 (at N-terminus)	TM domains: 0 SP: yes	No GPI
Bem46-like serine peptidase	LmjF35.4020	TM domains: 1 (at N-terminus)	TM domains: 1 (at N-terminus)	TM domains: 3 (one at N-terminus)	TM domains: 1 (at N-terminus) SP: no	No GPI
Zinc carboxypeptidase	LmjF33.0200	TM domains: 0	TM domains: 0	TM domains: 4	TM domains: 4 SP: yes	No GPI

3.2.2 Cloning of GFP fusion proteins and fluorescence microscopy

The candidate peptidases selected by bioinformatics were cloned and fused to GFP at their C-terminus, using the pNUS-GFPcN vector (pGL1132) (Tetaud et al., 2002a). Six of the eight peptidases were cloned full-length. Only the ubiquitin hydrolase and the zinc carboxypeptidase, which are very large genes, were truncated at their 3' end to facilitate cloning (Table 3-2). For all peptidases, the N-termini were left unmodified to allow targeting of the protein through its N-terminal secretory or mitochondrial signal. *L. major* wild type promastigotes were transfected with the eight different GFP fusion plasmids and the plasmids were maintained extrachromosomally in the cell lines by culturing the cells under constant antibiotic selection pressure. After allowing two to three weeks for the GFP fluorescence to be established at a detectable level, the eight cell lines were examined by fluorescence microscopy using the DeltaVision deconvolution microscope system. The cells were analysed at different phases of growth to detect possible changes of protein distribution or trafficking, but all eight candidate peptidases displayed unchanging patterns of GFP fusion protein localisations throughout their promastigote life cycle. The fluorescence patterns described in the following section were always observed in the majority of cells (> 50 %) of a sample. When appropriate, cells were stained with the red endocytic dye FM4-64, which stains the flagellar pocket when incubated for a short period of time, or with MitoTracker Red, which stains the mitochondrion. Live cells and lightly (30 %) paraformaldehyde-fixed cells exhibited the same fluorescence patterns and intensities, for GFP as well as for all stains used (if imaged directly after staining), so figures in this chapter contain live as well as fixed cell microscopy images.

Five of the eight GFP-fused candidate peptidases appeared to localise to the single large mitochondrion: the ubiquitin hydrolase, the CaaX prenyl protease, the zinc carboxypeptidase as well as both rhomboids (Fig. 3-1). This is consistent with high likelihood values for mitochondrial import for one of the rhomboids, the ubiquitin hydrolase and the CaaX prenyl protease. Mitochondrial targeting was not predicted for the zinc carboxypeptidase and the second rhomboid-like serine peptidase (Tables 3-3 and 3-4).

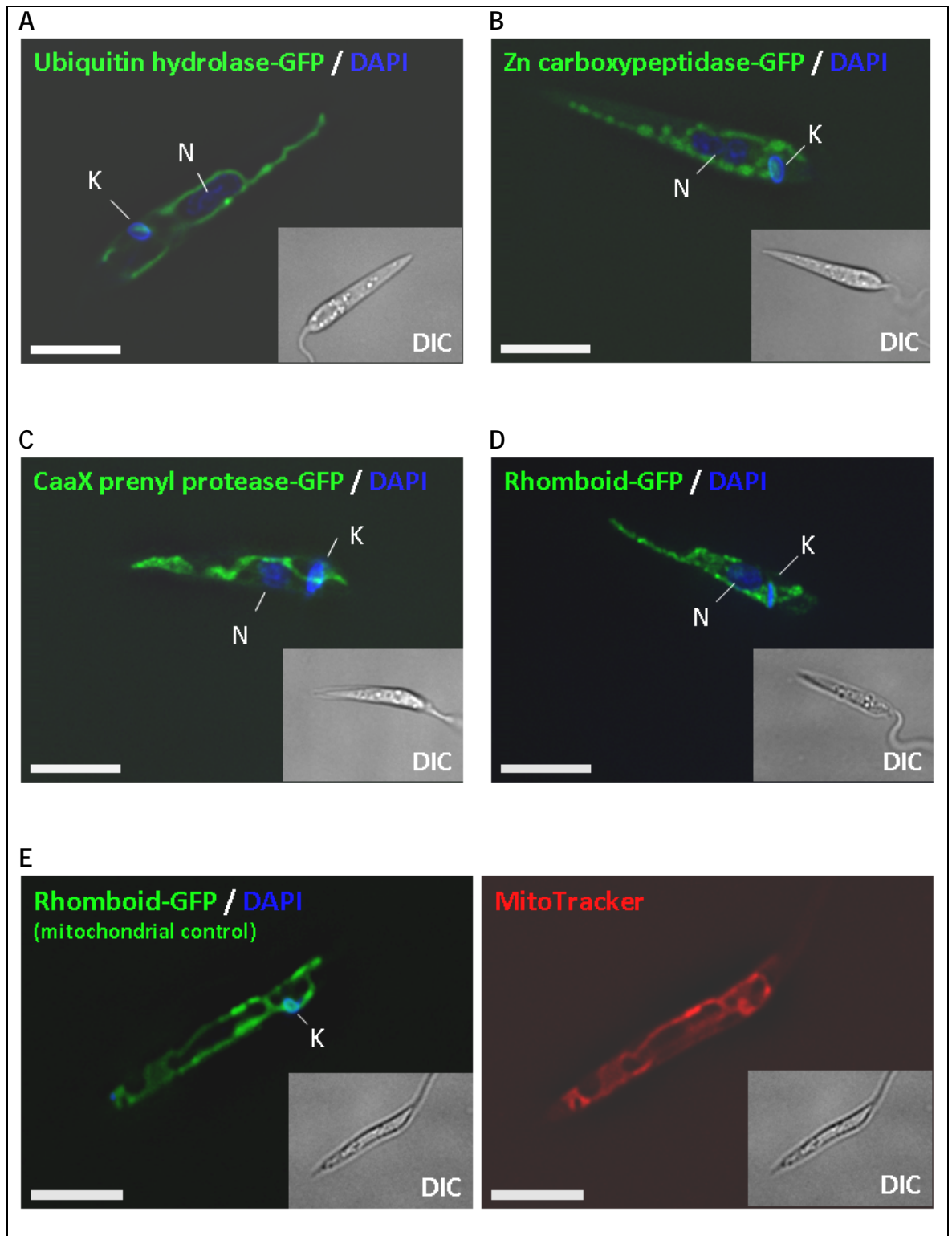


Figure 3-1: Live cell deconvolution microscopy images of five *L. major* cell lines expressing different GFP-fusion proteins with the GFP signal pattern corresponding to the mitochondrion. Kinetoplasts (K) and nuclei (N) stained with DAPI. DIC images of cells shown as insets. Scale bar = 10 µm.

(A) Cell expressing GFP-tagged ubiquitin hydrolase (LmjF09.0240) (B) Cell expressing GFP-tagged zinc carboxypeptidase (LmjF33.4020) (C) Cell expressing GFP-tagged CaaX prenyl protease (LmjF26.2690) (D) Cell expressing GFP-tagged rhomboid peptidase (LmjF02.0430) (E) Left panel: cell expressing GFP-tagged mitochondrial control rhomboid peptidase (LmjF04.0850); right panel: image of the same cell stained with red fluorescent MitoTracker dye.

The calpain-like peptidase showed a flagellar localisation. The GFP fusion protein appeared to accumulate in the flagellum outside the cell body, and the intensity of the signal decreased towards the tip of the flagellum. The GFP signal could not be detected in the flagellar pocket (Fig. 3-2).

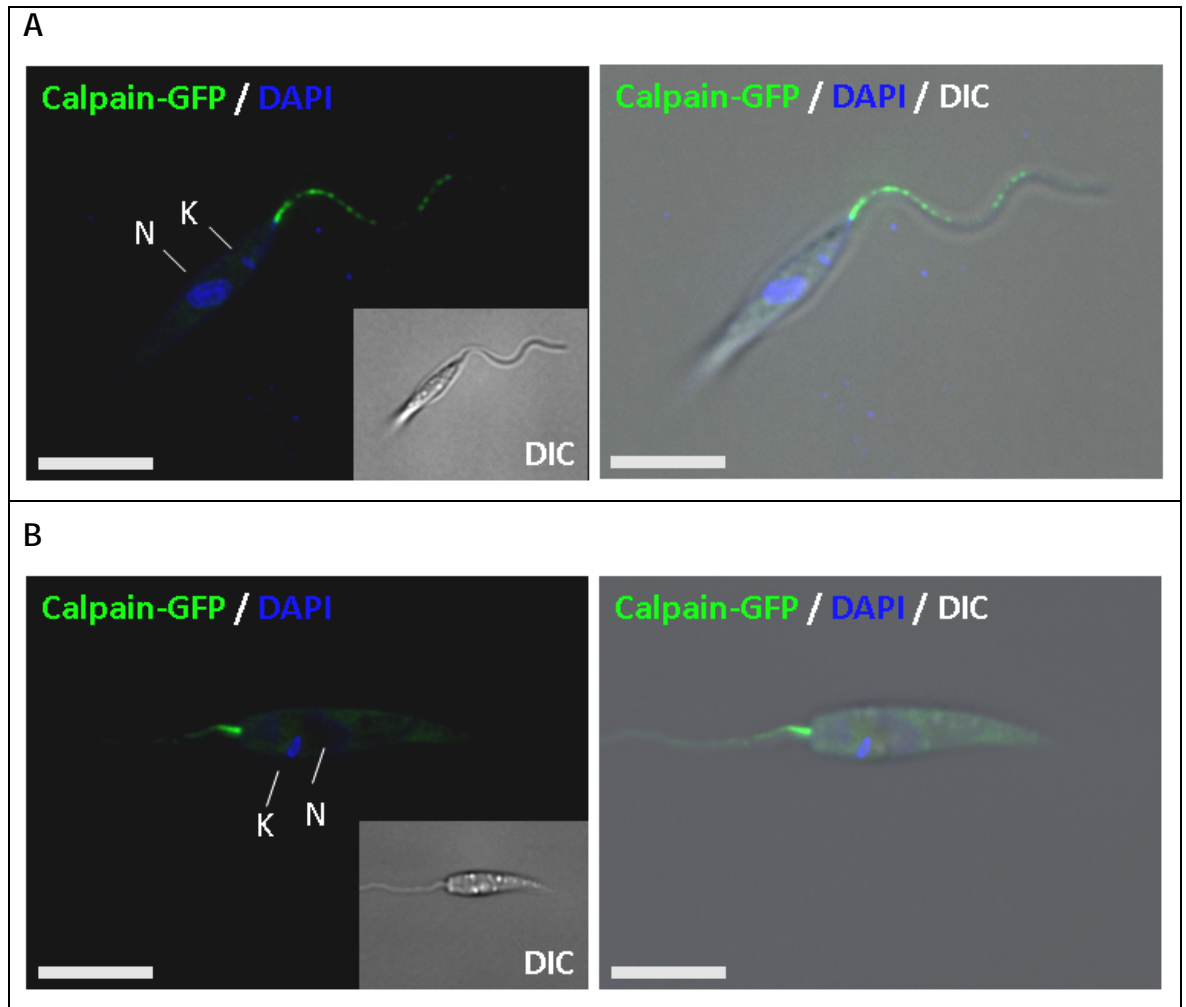


Figure 3-2: Deconvolution microscopy images of *L. major* cell line expressing GFP-tagged calpain. Kinetoplasts (K) and nuclei (N) stained with DAPI. Brightfield (DIC) images of cells shown as insets. Scale bar = 10 μ m.
 (A) Scattered GFP fluorescence signal decreasing along the length of the flagellum; left panel: GFP and DAPI signals, fixed cell; right panel: overlay with brightfield (DIC) image to outline the cell.
 (B) GFP fluorescence concentrated in the portion of the flagellum close to the cell body outside the flagellar pocket; left panel: GFP and DAPI signals, live cell; right panel: image overlay with brightfield (DIC) image to outline the cell.

The serine carboxypeptidase appeared to localise to punctate structures surrounding the flagellar pocket. The GFP signal did not co-localise with the red fluorescent flagellar pocket stain FM4-64 (Fig. 3-3).

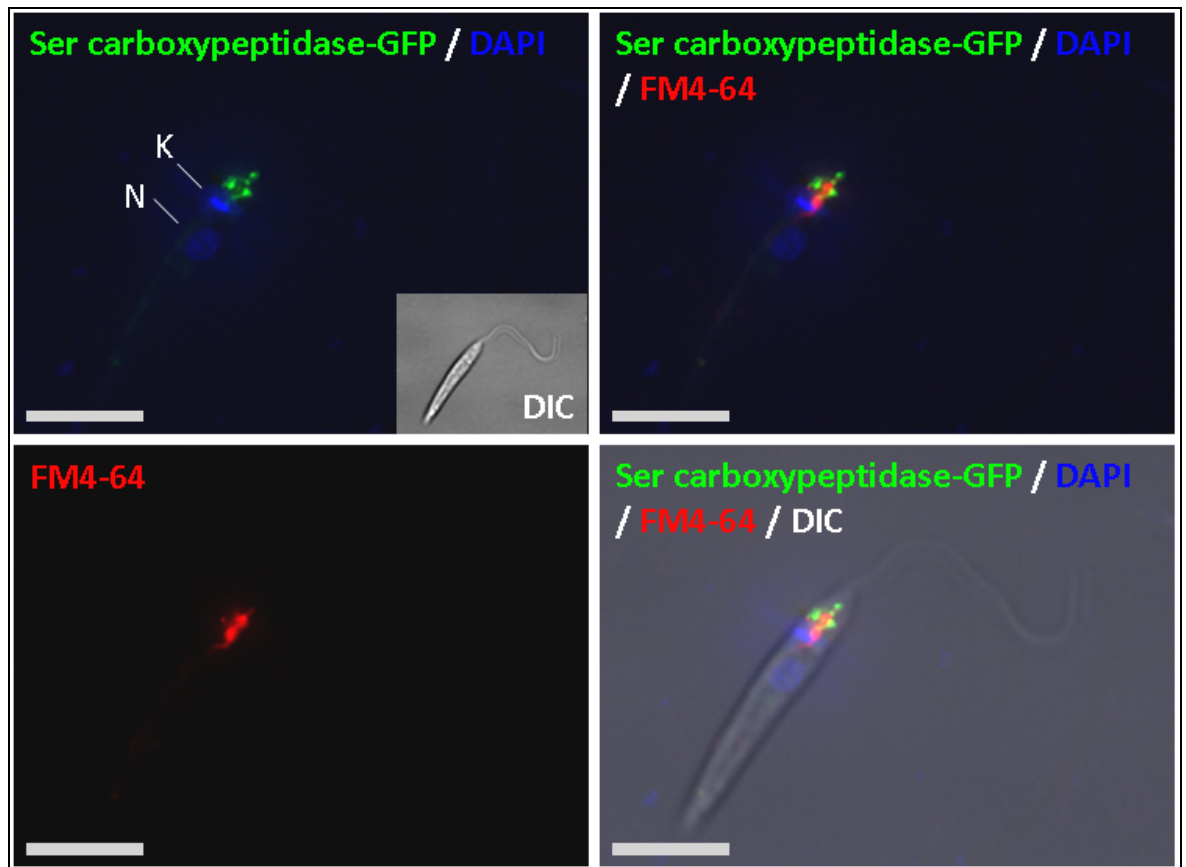


Figure 3-3: Fixed cell deconvolution microscopy images of *L. major* cell line expressing GFP-tagged serine carboxypeptidase (LmjF18.0450) and stained with the red flagellar pocket stain FM4-64. Kinetoplast (K) and nucleus (N) stained with DAPI. DIC image of cell shown as inset. Scale bar = 10 μ m. Top left: GFP and DAPI fluorescence image; bottom left: FM4-64 red fluorescent molecular dye staining the flagellar pocket; top right: merged image of GFP, DAPI and FM4-64 signals with no visible co-localisation; bottom right: merged image of GFP, DAPI and FM4-64 with brightfield (DIC) image to give outline of cell.

The GFP-labelled Bem46 localised to the flagellar pocket. The GFP signal largely co-localised with the red fluorescent flagellar pocket stain FM4-64 (Fig. 3-4).

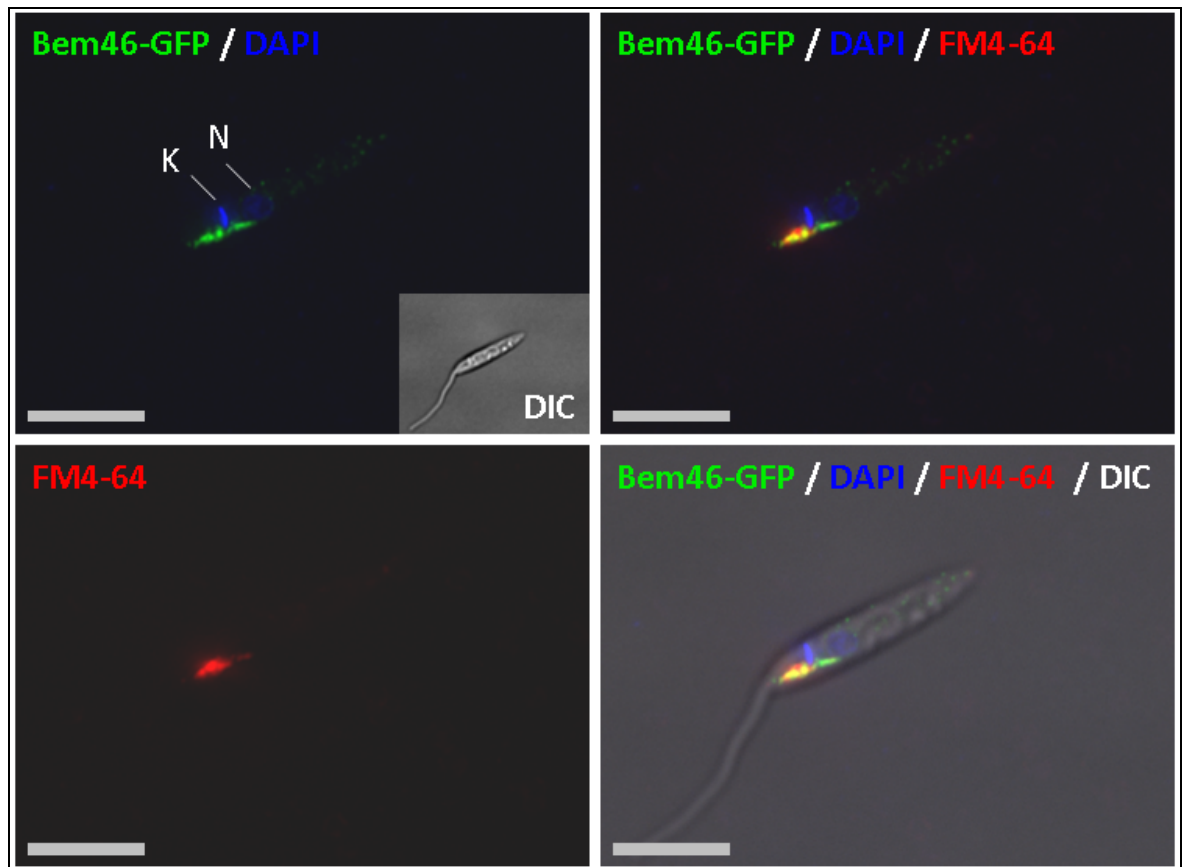


Figure 3-4: Fixed cell deconvolution microscopy images of *L. major* cell line expressing GFP-tagged Bem46 peptidase (LmjF35.4020) with the GFP signal pattern co-localising with the red flagellar pocket stain FM4-64. Kinetoplast (K) and nucleus (N) stained with DAPI. Brightfield (DIC) image of cell shown as inset. Scale bar = 10 μ m.

Top left: GFP and DAPI fluorescence image; bottom left: FM4-64 red fluorescent molecular dye staining the flagellar pocket; top right: merged image of GFP, DAPI and FM4-64 signals with co-localisation of GFP and FM4-64 in flagellar pocket; bottom right: merged image of GFP, DAPI and FM4-64 with brightfield (DIC) image to give outline of cell.

3.3 Discussion

The generation of GFP-fusion proteins of the eight selected *L. major* peptidases was successful and the GFP fluorescence could be tracked *in vivo* by fluorescence microscopy to determine the intracellular localisation of each fusion protein.

It is remarkable that five of the eight candidate peptidases were trafficked to the mitochondrion in *L. major* when tagged with GFP. The *in silico* predictions of mitochondrial targeting motifs as opposed to secretory signal peptides yielded ambiguous results for the ubiquitin hydrolase and the CaaX prenyl protease and clearly non-mitochondrial results for the zinc carboxypeptidase and one of the rhomboids. So the observed mitochondrial localisation was unanticipated for these. The second rhomboid was expected to be targeted to the mitochondrion, and the pattern of its localisation in this organelle supports the conclusion that the reticulated GFP-labelled structure visible in all five candidates was indeed the mitochondrion. The identification of this organelle was further corroborated by the fact that the DAPI-stained kinetoplast was always closely associated with or incorporated in the GFP pattern, as well as by staining experiments with the MitoTracker Red molecular stain, which co-localised with the GFP fluorescence pattern.

It is not apparent why these proteins localised to the mitochondrion. Mistargeting to the mitochondrion due to misfolding or overexpression of the fusion proteins is unlikely, because misfolded or surplus protein would be expected to accumulate in the cytoplasm, be trafficked to the lysosome or the proteasome for degradation (Goldberg, 2003b; Katayama et al., 2008) or possibly be targeted into the flagellar pocket for exocytosis from the cell. Protein import to the mitochondrion is a directed process and requires distinct targeting motifs (von Heijne et al., 1989a). Consequently the observed localisation of a protein in this compartment is most likely genuine. The fact that not all eight fusion proteins localised to the mitochondrion, which could point to a systematic mistake or a fault with the DNA vector used, additionally supports the notion that the mitochondrial localisation was not an artefact.

Very little data is available on the candidate peptidases analysed in this study; they are mostly putative enzymes that have not been investigated in kinetoplastids. Therefore, conclusions regarding their function and reasons for their mitochondrial localisation are speculative.

Ubiquitin hydrolase cysteine peptidases are de-ubiquitinating enzymes and are involved in the non-lysosomal protein degradation process at the proteasome, where they cleave ubiquitin molecules from ubiquitinated proteins. Poly-ubiquitination labels a protein for proteasomal degradation and de-ubiquitination takes place to rescue proteins from the degradation pathway, to modify the ubiquitin signal or to recycle ubiquitin. Ubiquitin hydrolase peptidases specifically cleave bonds involving the C-terminal glycine of ubiquitin, either bound to another ubiquitin or to a different protein (Alberts *et al.*, 2002; Bonifacino and Weissman, 1998). Nineteen ubiquitin hydrolase cysteine peptidases are found in the *L. major* genome and the clan CA / family C19 group of proteins is one of the largest peptidase families. Ubiquitination in mitochondria has not been broadly investigated to date. However, there are examples of ubiquitinated proteins in mitochondria (Sun *et al.*, 2009; Thompson *et al.*, 2003), as well as a ubiquitin ligase and a ubiquitin hydrolase located in the outer membrane of human mitochondria (Yonashiro *et al.*, 2006; Nakamura and Hirose, 2008b). So there is evidence for a ubiquitination machinery in the mitochondria of higher eukaryotes (Germain, 2008) and it has been suggested that a human ubiquitin hydrolase is involved in the maintenance of mitochondrial morphology (Nakamura and Hirose, 2008a). The ubiquitin hydrolase investigated here may be part of a similar system in *Leishmania*.

The CaaX prenyl protease is a peptidase which cleaves C-terminal CaaX sequences (whereby a is an aliphatic amino acid) of membrane proteins during prenylation. First, the CaaX sequence is prenylated (farnesylated or geranylgeranylated, depending on the nature of the X residue) at the cysteine residue, then a CaaX prenyl protease cleaves the aaX tripeptide, leaving the cysteine as the new C-terminus, which is then methylated by a specific methyltransferase. After these modifications, the prenylated protein can insert into and function within a membrane (Otto *et al.*, 1999). The activity of CaaX prenyl proteases is membrane-associated and there are often only one or two such enzymes found in any organism, which then play a major role in the processing of proteins. Two

CaaX prenyl proteases have been found in the *L. major* genome (Besteiro et al., 2007b), one of which was investigated in this project. Its catalytic mechanism has not been elucidated; therefore it is not classed into one of the five types of peptidases yet. A *T. cruzi* homologue as well as some prenyl proteases in other organisms have been found to localise to the ER membrane with their active site in the cytosol (Porcel et al., 2000). It is possible that the *L. major* prenyl protease studied here functions in a similar way, but is inserted into the mitochondrial outer membrane with its C-terminus, exposing the active site to the cytosol. This would explain the mitochondrial location of the GFP fusion protein.

Rhomboid-like serine peptidases are polytopic type II intramembrane proteins that cleave other proteins within the membrane. The membrane lipid bilayer is an unusual site for proteolysis, but the active site of rhomboids contains a water-filled indentation which allows hydrolytic cleavage to take place in an otherwise hydrophobic environment. Rhomboids play a role in several cellular processes like signalling cascades and are widely conserved, from bacteria to humans (Lemberg and Freeman, 2007b; McQuibban et al., 2003). It is thought that eukaryotic cells contain at least two rhomboids, one of which is found in the mitochondrion. Some species contain more than two, for example *Drosophila* with seven rhomboids (Koonin et al., 2003). Accordingly, the *L. major* genome contains two predicted rhomboid-like serine peptidases, a mitochondrial and a non-mitochondrial one, and both were investigated in this study. The predicted mitochondrial rhomboid was used as a mitochondrial control protein and its GFP fusion protein co-localised with the MitoTracker stain in a mitochondrion-shaped pattern as expected. Surprisingly, the second rhomboid showed the same pattern when fused to GFP, suggesting that it is mitochondrial as well and the reason for this is not clear. The *L. major* rhomboids do not have close homologues in other species outside of the kinetoplastids and they differ from the rhomboids of higher eukaryotes in that they are largely predicted to have fewer transmembrane domains than the usual six or seven (Lemberg and Freeman, 2007a). Interestingly, loss of the mitochondrial rhomboid in yeast causes a growth defect and abnormal mitochondria (Freeman, 2004). It is worth noting that the *L. major* cell line transfected with the GFP-fused mitochondrial

control rhomboid here showed a consistently reduced growth rate too, which may have been due to over-expression in the mitochondrion.

The zinc carboxypeptidase had a very low prediction to be mitochondrial, but its GFP fusion protein clearly localised there. Since this protein has not yet been investigated in detail, its enzymatic properties are only putative. It does not have close homologues in other organisms outside the *Leishmania* species. It is interesting to note that the bioinformatics predictions for the large full length zinc carboxypeptidase were of lower reliability and consistency than those for the other seven candidate peptidases, which may point to a potential decrease in prediction accuracy with increasing protein size and, therefore, structural complexity. Additionally, this protein was truncated for the GFP fusion and only a small region from the N-terminal end was cloned into the GFP vector. The fact that it was nevertheless targeted to the mitochondrion suggests that the N-terminus alone is sufficient for correct trafficking by an N-terminal mitochondrial targeting motif. However, it is possible that a full length fusion protein would traffic in a different way and that the GFP pattern observed in this study was caused by the truncation.

Apart from these five mitochondrial peptidases, the remaining three candidates exhibited more interesting and distinct GFP fusion protein fluorescence patterns.

The calpain-like peptidase clearly localised to the flagellum with a concentration of GFP in the flagellum outside the cell body and a decrease of fluorescence towards the distal tip. The GFP-fusion protein was not visible in the flagellar pocket. Calpains (*Calcium-dependent papain-like cysteine peptidases*) are thought to be involved in signal transduction pathways, the function of the cytoskeleton and a broad range of other cellular processes (Evans and Turner, 2007a). They are usually intracellular but non-lysosomal and require calcium for activity. They often cleave their highly specific substrates only partially, leading to modification rather than breakdown (Evans and Turner, 2007b; Croall and Ersfeld, 2007). Kinetoplastid calpains seem to differ from animal calpains. They do not show the classical calpain structure including an EF-hand calcium binding site and they are classified into five groups according to their domains and their resemblance with mammalian calpains. The *L. major* calpain analysed here is a

class I calpain; these have the highest similarity to mammalian calpains in comparison to other kinetoplastids' calpain-like proteins (Croall and Ersfeld, 2007). The first trypanosomatid calpain-like protein that was investigated was *T. brucei* CAP5.5, which is associated with the cytoskeleton (Hertz-Fowler *et al.*, 2001) and was also identified as a component of the *T. brucei* flagellar proteome (Broadhead *et al.*, 2006). Overall, six calpain-like proteins were found in the “flagellome” of *T. brucei*, all with conserved *L. major* homologues but not including the calpain analysed here. Since the *Leishmania* “flagellome” has not been analysed yet, it is possible that this calpain is specific for the *L. major* flagellum and differs in localisation from its *Trypanosoma* homologue. Another possibility is that the *T. brucei* “flagellome” analysis is not comprehensive. The calpain investigated here seemed not to be expressed along the whole flagellum, but only in a short area close to the flagellar pocket. So its expression level relative to the whole flagellum may be below the significance threshold for the identification of distinct flagellar proteins. It will be interesting to investigate the localisation of this calpain in the amastigote stage of *L. major*, where the flagellum does not protrude from the pocket, to see whether the calpain remains associated with the short flagellum within the pocket or is redistributed elsewhere in the cell.

The two peptidases that did localise to the flagellar pocket area and might be secreted are Bem46 and the serine carboxypeptidase.

The serine carboxypeptidase GFP fusion protein appeared to localise to small punctate or elongated structures in close proximity to the flagellar pocket. It is possible that the protein accumulated in small vesicles budding off or fusing with the flagellar pocket membrane. The GFP signal did not co-localise with the endocytic stain FM4-64, neither at the flagellar pocket nor further into the endocytic pathway or at the lysosome. Therefore it seems that the protein was either not released into the pocket or only at undetectable levels or may have been released from the pocket too rapidly for detection. The transmembrane domain predictions calculated only one transmembrane helix for this peptidase, at the N-terminus, which may be a signal peptide. Even if it is a genuine transmembrane domain, it may anchor the protein in the membrane until it is cleaved, so it is feasible for it to be released into the flagellar pocket in a soluble form. Generally, serine carboxypeptidases of clan SC, family S10 are

located in lysosomes in animals and in the vacuole in plants and fungi (Parussini et al., 2003c), so it is unexpected that the *L. major* serine carboxypeptidase was not found in the lysosome. However, there is a possibility that it normally is targeted to the lysosome, perhaps via the flagellar pocket like CPB, but was here retained in vesicles along the way. A reason for this could be an interference of GFP with targeting signals. Carboxypeptidases function by cleaving the C-terminal amino acid of proteins. A *T. cruzi* homologue of the *L. major* serine carboxypeptidase has been characterised by Cazzulo and co-workers (Parussini et al., 2003b) and is thought to be lysosomal. Like other serine carboxypeptidases of the S10 family it was shown to be a glycoprotein with two or three N-glycosylation sites. Apart from an N-terminal signal peptide, it seems also likely that there is a short pro-peptide, as in many other serine carboxypeptidases (Parussini et al., 2003a). All in all, a similar structure could be expected for the *L. major* peptidase, but since it shows only 47 % similarity with its closest homologue, the *T. cruzi* serine carboxypeptidase, it may have evolved *L. major* specific characteristics, functions or intracellular destinations. Again, there is a possibility that the GFP tagging and overexpression interfered with correct folding and that the observed localisation is an artefact and possibly a route of disposal of surplus or misfolded protein.

Finally, the Bem46-like serine peptidase GFP fusion protein showed a clear localisation to the flagellar pocket and a good co-localisation with the flagellar pocket stain FM4-64. This pattern was observed in most cells. A few cells showed a different pattern with strong GFP expression throughout the cytosol. This may indicate that the flagellar pocket localisation seen in most cells was a true observation and not due to over-expression of the GFP fusion protein, as large amounts of GFP seemed to accumulate in the cytosol of some cells without being exported into the flagellar pocket as a “detoxification” route. Bem46 belongs to the S9 serine peptidase family which also includes the membrane-bound oligopeptidase B (OPB), which has been well characterised in kinetoplastids and which cleaves small peptides (Matos Guedes *et al.*, 2007; Coetzer *et al.*, 2008), but Bem46 seems to be a highly divergent member of the family. It does not contain the β -propeller domain which restricts substrate size for other family members. Bem46 peptidases have not been investigated in much detail in other organisms, but some research on plants and fungi suggests an involvement of the

protein in maintenance of cell polarity (Mercker et al., 2009d; Mochizuki et al., 2005c). The *L. major* Bem46 was predicted to contain a transmembrane domain at the N-terminus, which may be a signal peptide. Depending on the algorithm, one or two other transmembrane domains are found in this protein, which would make a crucial difference to the ability of the protein to be secreted. An N-terminal transmembrane domain or signal peptide may target the protein into the flagellar pocket membrane where it could be cleaved and released as a soluble enzyme and, potentially, act as a virulence factor. If one or both of the other potential transmembrane domains are real, they could prevent release and the protein may remain in the membrane. Assuming the observed flagellar pocket localisation is not an artefact created by GFP-tagging or overexpression, the peptidase may be an integral protein of the pocket membrane. No resident proteins of the *Leishmania* flagellar pocket membrane are known to date, so it will be worth investigating the role of Bem46 in this compartment and its potential usefulness as a marker protein.

To conclude, the bioinformatics predictions and the *in vivo* GFP-labelling results did not correspond consistently. There were striking ambiguities within the predictions for some proteins, for example two algorithms predicting no signal peptide for Bem46 and two other algorithms confidently suggesting a signal peptide. Two of the five mitochondrial peptidases were not identified as mitochondrial proteins according to the predictions; three peptidases yielded similarly strong predictions for N-terminal secretory signals and mitochondrial signals, which should be mutually exclusive.

4. The *Leishmania*

Bem46-like serine peptidase

4.1 Introduction

4.1.1 Bem46-like peptidases

The first Bem46 protein described was a temperature-sensitive Bem1/Bud5 suppressor ("Bud EMergence") protein identified in the yeast *Schizosaccharomyces pombe* (Valencik and Pringle 1995, unpublished, Uniprot database accession P54069). It appears that Bem46 is involved in the interaction of the small G protein Bem1 and the activator Bud5 (a GDP-GTP exchange factor), which is important for the establishment of cellular polarity and the initiation of bud formation through reorganisation of the actin cytoskeleton (Cabib *et al.*, 1998).

Many other organisms including mammals, invertebrates, protozoans and prokaryotes carry Bem46 homologues, but these proteins have thus far only been studied in detail in the fly *Drosophila melanogaster*, the fungus *Neurospora crassa* and the plant *Arabidopsis thaliana*. In *D. melanogaster* there is evidence that BEM46 may interact with an activator (GDP-GTP exchange factor) of a G protein that is involved in the asymmetrical cell division of larval neuroblasts, but it is not essential (Giot *et al.*, 2003; Parmentier *et al.*, 2000). The *N. crassa* BEM46 was found to be essential for maintaining cell polarity of hyphae germinating from ascospores, and facilitating their directional growth. BEM46 was differentially expressed, localising to the perinuclear endoplasmic reticulum and close to the cell membrane, depending on the cell type. It contains a secretory signal peptide and apparently no ER retention signal, so may not permanently reside in the ER. It was also expressed differentially in different tissues (Mercker *et al.*, 2009c). The *A. thaliana* BEM46 (or WAV2) was found to be highly expressed in the plant root tip area and to suppress root bending by

inhibiting root tip rotation. The protein appears to be membrane-bound and mainly expressed on the cell surface. Some evidence suggests it may influence microtubule organisation (Mochizuki et al., 2005b).

In general, Bem46-like proteins are conserved proteins found in many different organisms. They are usually predicted to have at least one transmembrane domain towards the N-terminus, an alpha/beta-hydrolase domain and often an N-terminal signal peptide (Mercker et al., 2009b). Results from functional studies suggest a role for Bem46 in signal transduction and the maintenance of cell polarity, with a possible involvement in the modulation of the cytoskeleton.

4.1.2 The S9 family of peptidases

Bem46 proteins are serine peptidases with an alpha/beta-hydrolase domain and are classified into clan SC, prolyl oligopeptidase family S9, subfamily S9X (unassigned peptidases). Members of the S9 family of peptidases are usually oligopeptidases with a restricted substrate size specificity. This is conferred by an N-terminal eight-bladed beta-propeller domain, which restricts entry of larger peptides into the active site (Fulop et al., 1998a). Substrate specificity varies; many S9 peptidases cleave prolyl bonds, but not all. The oligopeptidase B (OPB) preferentially cleaves arginine and lysine bonds (Polgar, 2002a; Pacaud and Richaud, 1975a). The active site of S9 peptidases is a catalytic triad positioned in the C-terminal domain and consists of the active site residues serine, aspartic acid and histidine, in this order. The fold of the catalytic domain is a characteristic alpha/beta-hydrolase fold with an alpha-beta-alpha sandwich structure consisting of eight beta-sheets connected by alpha-helices (Rawlings *et al.*, 2008; Ollis *et al.*, 1992). The *L. major* Bem46 is a divergent member of the S9 family. It has a conserved catalytic triad in its alpha/beta-hydrolase domain, but the overall sequence identity to other members like OPB is not very high. It also lacks the N-terminal beta-propeller domain, which may allow Bem46 to cleave larger substrates or a broader range of substrates than other S9 peptidases (Fig. 4-1).

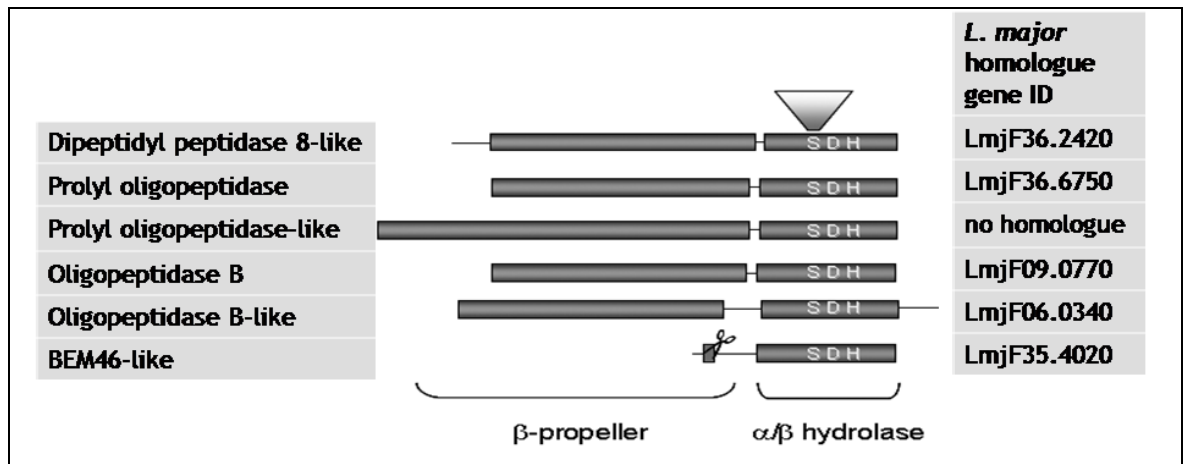


Figure 4-1: S9 peptidase family members including Bem46-like serine peptidase. Comparison of protein length and domain structure. Catalytic domain with catalytic triad SDH present in all members, Bem46-like peptidase lacking N-terminal beta-propeller domain. Scissor symbol shows cleavage site downstream of Bem46 signal peptide / N-terminal transmembrane domain. Adapted from a figure by Cathy Moss.

4.2 Results

4.2.1 Bioinformatics analyses of *L. major* Bem46-like peptidase

4.2.1.1 Phylogenetic analysis

BLAST analyses of the *L. major* Bem46 (LmjF35.4020) sequence did not reveal any highly identical homologues of the protein outside the kinetoplastids; Bem46 proteins of non-kinetoplastids show below 30 % sequence identity to *L. major* Bem46. Nevertheless, it can be aligned with Bem46 homologues from a broad range of other organisms, and the alignment shows some sequence conservation and a similarity in length, as well as a conservation of all three residues of the active site in all aligned species but the mammal (rat) (Fig. 4-2).

Similarity of Bem46 proteins is higher among the kinetoplastids. *L. major* Bem46 is highly identical to its *L. infantum* (identity 94 %, e-value 0.0) and *L. braziliensis* (identity 83 %, e-value 5e-180) homologues, but the identity is already markedly reduced in the other kinetoplastids species *T. brucei* (identity 43 %, e-value 4e-74) and *T. cruzi* (identity 43 %, e-value 1e-81). All these species carry only one respective *Bem46* gene.

The closest non-kinetoplastid proteins that were revealed by BLAST analysis were Bem46 proteins of many different *Drosophila* species and hypothetical proteins from a broad range of organisms (including fungi, invertebrates, *Xenopus*, yeast and prokaryotes), as well as orthologues of the vertebrate alpha/beta-hydrolase-containing protein 13 from the S33 peptidase family, but identity with the *L. major* Bem46 is below 40 % for these (with e-values above $5e-38$).

The *Bem46* gene LmjF35.4020 encodes the only Bem46-like protein in the *L. major* genome; its closest homologue (LmjF33.0400, another putative S9 family serine peptidase) only shows 28 % identity, with an e-value of $9.7e-09$.

The *L. major* Bem46 can be aligned with Bem46-like proteins from other kinetoplastids, *Drosophila*, yeast, bacteria and other organisms, and the active site residues appear conserved and can be aligned. Such alignment is not readily achievable for the *L. major* Bem46 and other members of the *L. major* S9 peptidase family like the oligopeptidase B (OPB), which differ substantially and appear to feature a different active site position.

```

1                               80
L. major      (1) MSFGSFLLSAGLYLVLVAVFVSLFLHIMSRYRYSQQNQLLYPHIPPESREVCEDPVALGIPYAERVCVTTADK VRLWGY
S. pombe      (1) ---MLVLHHPSLRFQAAFSLFQDSENPLSLPTLLIFHHPIVYLRVYIHPS-FISFLDMAGSLSSA FNVLKYSGMA SLAV
D. melanogaster (1) -----MKEVGIALPKSR-GVGVGVLA AFLLCF FYYFYGGY TLALF
E. histolytica (1) -----M IWEI IAGATALI V
R. norvegicus (1) -----M VLRNLR LFPCL CSAL
M. tuberculosis (1) -----MS LKRCRALPVVA IVAL
A. thaliana    (1) -----M VTYVSALFY FFGI
Consensus     (1)                               IV      MA  AL

```

```

81                               160
L. major      (81) MLWPAPAPSAEKSNGNASVPDSIGR LSSNVA L AEGGMHVEV L APGSAT DST SASNMVSGSSRSV L MSSGMPSFV M L YFHCN
S. pombe      (77) T L I A L GFLYKY O K T L V Y P S A F P Q G S R E N V P L P K E F N M E Y E R L E L R T R D K V L D S L M L Q S E S P E S R --- P T L L Y F H A N
D. melanogaster (42) A G I I L L F Y Y A Q D L L Y H P D L P A N S R I Y L P I P T M H N L P H I T V S I K T P D D V L H A L W V T Q P E E R S K S S --- P T L L Y F H C N
E. histolytica (15) V L S G I Y L F T H Q Y E I V F Y P T R S L P V E E T T Q T F Q L P F E L K V S I F T N D N N I Y L A C L K - E P S K --- H I T L L L F Q S N
R. norvegicus (17) G R K I A A E Y R S F T S K S K E H I V P L M N M M I Y L N C L T V K F P L L V D L K R P E T K I A H T V N F F L R S E P G V --- L - - L G I -
M. tuberculosis (18) V A S G V I M F I W S Q Q R --- R - L Y F P S A G P V P S A S S V L P A G R D V V V E T Q D G M R L G G Y F P H T S G G S G --- P A V L V C N G N
A. thaliana    (16) V V A G V A L L V A F Q E K L V Y V P V L P G L S K S Y P I P A R L N L I Y E D I W L Q S D G V R L H A M F I K M P F E C R G --- P T L L F F Q E N
Consensus     (81) V L G L L F Q L L Y L P S I T D V L T D V T L H W E S P T L L Y F G N

```

```

161                               240
L. major      (161) A G N V G H R L P L A Q A F V T H L K C A V M M V D Y R G F G L S D D S E Q L Q E T L E L D A Q A C F D Y L W Q D P R V P R D R I I V M C T S L G G A V S T H L
S. pombe      (152) A G N M G H R L P L A R V F S A L N M N V F L I S Y R G Y G K S T G - S P S E A G L K I D S Q T A L E Y L M E H P I C S K T K I V V Y Q S I G G A V A I A L
D. melanogaster (118) A G N M G H R M Q N V W G I V H H L H C N V L M V E Y R G Y G L S T G - V P T E R G L V T D A R A A I D Y L H T R H D L D H S Q L I L F G R S L G G A V V D V
E. histolytica (89) A G T V L D R I E M A K K Y E L C D V N F V L A V Y R G F D K S T G - I P E V T M A N D V E K Y F S L E S - L G V D M N N I V V I C R S I G A S M A L K L
R. norvegicus (86) -----W H T V P S C R G E E A K G K C R C W Y K A A L R D G N P I L V Y L H G - - S A E H R S S L F Y R V A T N A A R A L E A
M. tuberculosis (88) A G D R S M R A E L A V A L H G - L G L S V L L F D Y R G Y G G N P C - R P S E Q G L A A D A R A A Q E W L S G Q S D V D P A R I A Y F C E S L G A A V A V G L
A. thaliana    (90) A G N I A H R L E N V R I M I Q K L K C N V F M L S Y R G Y G A S E G - Y P S Q Q G I I K D A Q A A L D H L S G R T D L D T S R I V V F G R S L G G A V C A V L
Consensus     (161) A G N M G H R L L A Y L N V L M V Y R G Y G S G P S E G L D A Q A A I D Y L V D R I V V F G S L G G A V A I L

```

```

241                               320
L. major      (241) A A N E R Y G R R I A A V I E N S F S S I S D M A S A I S R P I L T K L A S R C P D L A V G I F E Y Y V K P L A L R I S W N S A Q K I T K V V - - V P M L F L
S. pombe      (231) T A K N Q - - D R I S A L I L E N T F T S I K D M I P T V F Y G G S I I S R - - - - - F C T E I W S Q D E I R K L K K - L P V L F L
D. melanogaster (197) A A D T V Y G Q K L M C A I V E N T F S S I P E M A V E V H P A V K Y L P N - - - - - L L F K N K Y H S M S K I G K C S - - V P F L E I
E. histolytica (167) Y N K K N - - - C K G L I L E N G F T L L D V G K I L M P A I S F F P - - - - - W L I K D K W D N L N E I K Q V Q G K R I L R C
R. norvegicus (144) K G G Y P - - - V D A I V L E A P F T N M W V A S I N Y P L L K L Y E I A R - - - - - S A Y R N - K D R Y K M V V - - - F P -
M. tuberculosis (166) A V Q R P - - - P A A L V L R S P F T S L A E V G A V H Y P W L P L R R - - - - - L I L D H Y P S I E R I A S V H - - A P V L V I
A. thaliana    (169) T K N N P - - D K V S A L I L E N T F T S I L D M A G V L L P F L K W F I G G S G T K S L K - - - - - L L N F V V R S P W K T I D A A E I K - Q F V L F L
Consensus     (241) A K I A A L I L E N T F T S I D M A L P I I I L L K W S I D K I V P V L F L

```


4.2.1.2 Prediction of protein topology

The bioinformatics analysis described in chapter 3 allowed a preliminary characterisation of Bem46. It was predicted that the protein is not targeted to the mitochondrion and contains a secretory signal peptide, which may be an uncleaved signal anchor that could retain Bem46 in a membrane. Topology algorithms predicted a highly likely transmembrane domain at the N-terminus, which may be a misinterpretation of the signal peptide or anchor sequence, and one or two further transmembrane domains, depending on the algorithm used. The Phobius algorithm was developed to distinguish better between signal peptides and transmembrane domains at the N-terminus and can therefore be more accurate than other algorithms (Emanuelsson et al., 2007; Kall et al., 2004b). While SOSUI (Fig. 4-3), TMHMM (Fig. 4-5) and Phobius (Fig. 4-6) predicted only one transmembrane domain, HMMTOP predicted up to three (Fig. 4-4). The active site lies in the C-terminal half of the protein (Fig 4-7) and the active site residues S 231 (serine), D 323 (aspartic acid) and H 365 (histidine) were identified by Merops Blast (<http://merops.sanger.ac.uk>). Additionally, Bem46 contains one non-conserved asparagine site (⁹⁴NAS⁹⁶) that could be N-glycosylated.

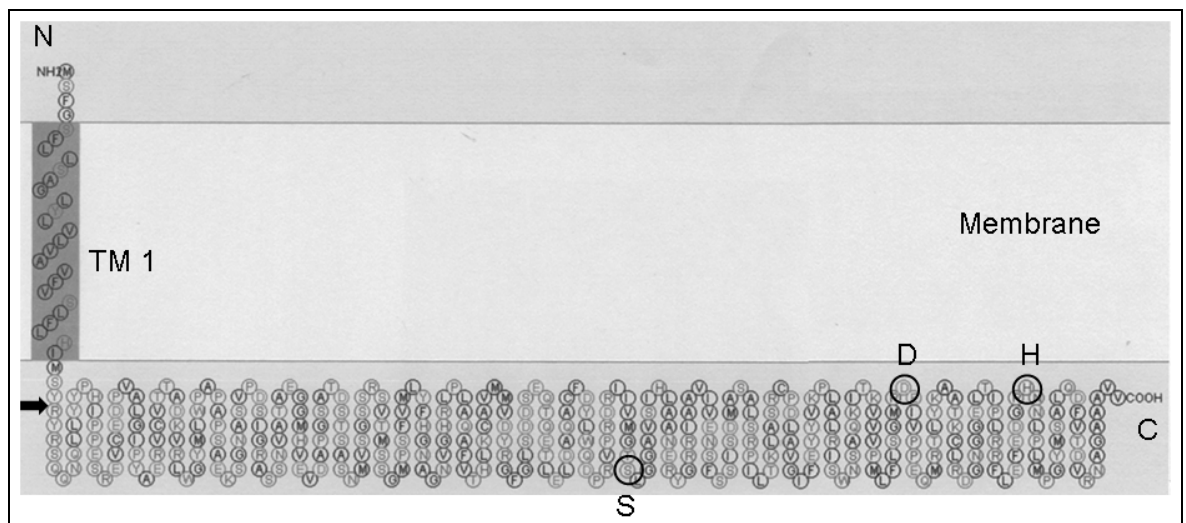


Figure 4-3: Prediction of *L. major* Bem46 protein topology, predicted using the SOSUI algorithm. N: N-terminus, C: C-terminus, TM1: transmembrane domain 1. Residues in circles: active site residues S (Ser), D (Asp) and H (His). Black arrow: potential cleavage site.

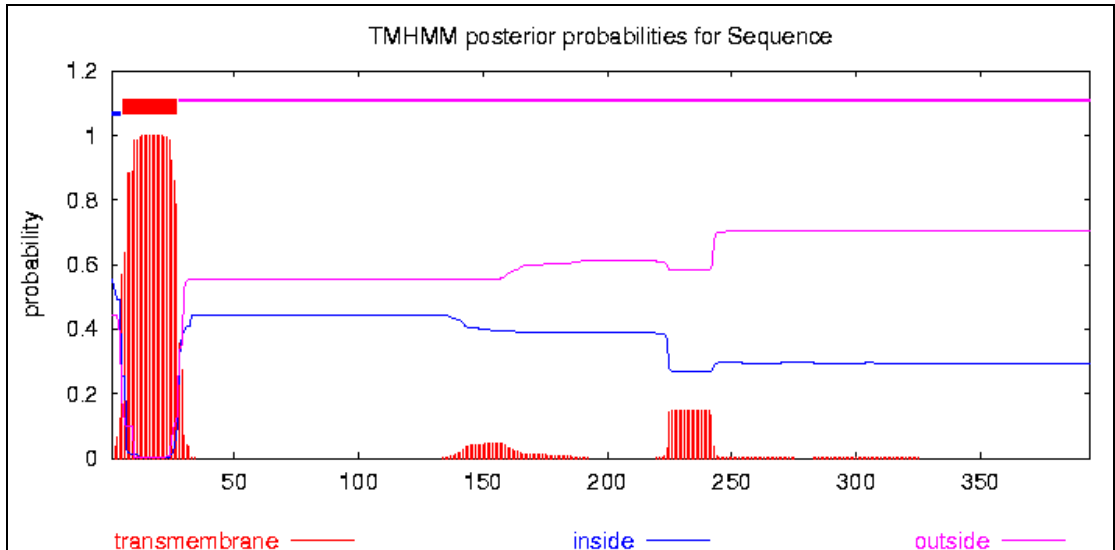


Figure 4-5: Prediction of *L. major* Bem46 protein topology, predicted using the TMHMM algorithm. Red: probability of transmembrane domain. Orientation in the membrane not determinable (probability of “inside” localisation of N-terminus: 0.5).

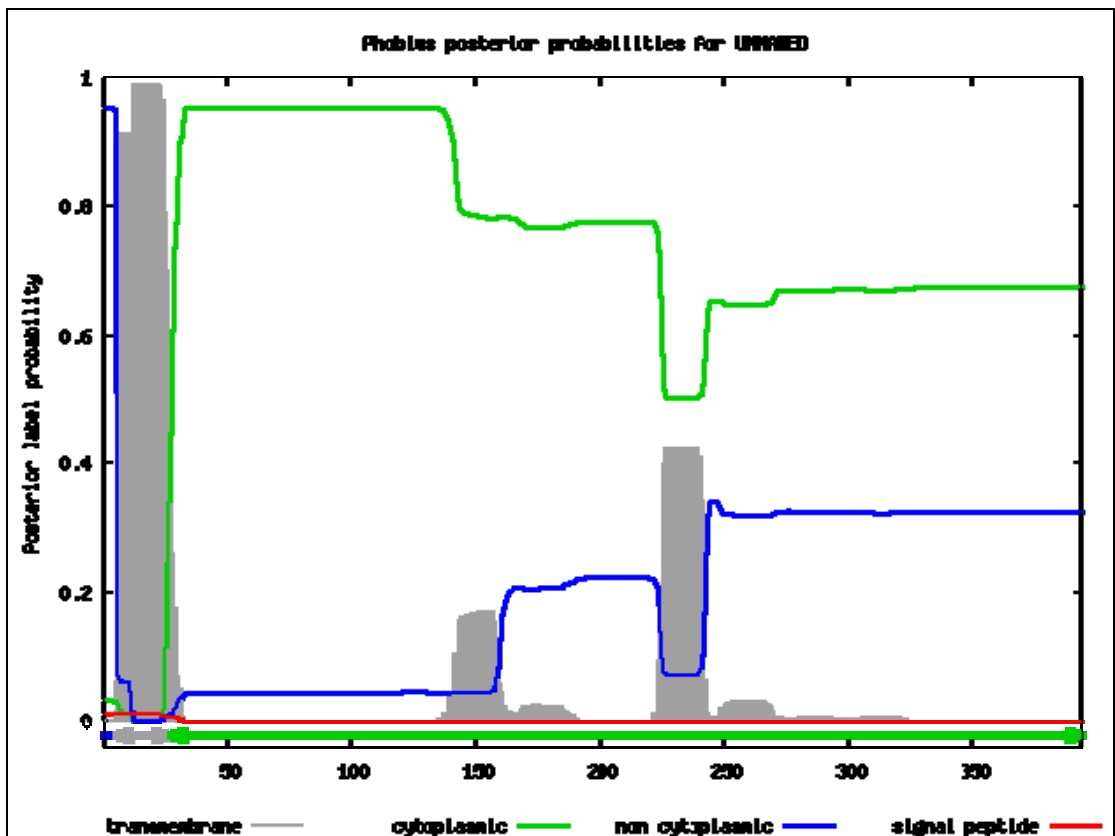


Figure 4-6: Prediction of *L. major* Bem46 protein topology, predicted using the Phobius algorithm. Red line: probability of a signal peptide, grey peak at N-terminus: predicted transmembrane domain.

```

MSFGSSFLLSAGLYLVLVAVFVSL *FLHIMS↓YRYRSQQNQQLLYPHIPPESRVCEDPVALGIP
Y *AERVCVTTADKVRLWGYMLWPAPAPSAEKSGNASVPDGRASSNVATAEGGMHVEVDA
PGSATDSTSASNMVSGSSRSVTMSSGMPSFVMLYFHGNAGNVGHRPLAQAQFVTHLKAVM
MVDYRGFGLSDDSEQTQETLELDAQACFDYLWQDPRVPRDRIIVMGS SLGGAVSIHLAANER
YGRRIAAVIVENSFSSISDMASALSRPILTKLASRCPDAVGIFEYVVKPLALRISWNSAQKITKV
VPMLFLSGMR DEIVPPEQMRTLYKATKCLRDGNGGELTIPLRRFLEFEDGR HNNLPLMPGY
MSALQDFVTDVRNGAAAVV

```

Figure 4-7: *L. major* Bem46 protein sequence with annotations.

Yellow: most likely transmembrane domain, black arrow: potential cleavage site, blue star: truncation point for long expression construct (used for antibody production, truncated by 23 amino acids), red star: truncation point for shorter protein expression construct (used to enhance solubility, truncated by 62 amino acids), red: active site residues, grey: potential N-glycosylation site.

4.2.2 Fluorescence microscopy

GFP-labelled Bem46 could be shown to localise to the flagellar pocket of promastigote *L. major*, as was described in chapter 3. To obtain additional information on the localisation of GFP-tagged Bem46 in *L. major*, it was co-expressed with a fusion protein of the surface protein HASPB (previously named Gene B Protein, (Rangarajan et al., 1995a) and the red fluorescent tag mCherry (Shaner *et al.*, 2004). This fusion protein construct was generated by Elmarie Myburgh using the pRIB vector, and the HASPB-mCherry sequence was integrated into the ribosomal locus of the *L. major* genome to ensure stable gene expression under the control of the ribosomal promoter. Transfected cells were serially diluted and selected for expression of both fluorescent marker proteins.

The mCherry-labelled HASPB was mainly visible at the cell surface in the initial two to three days of a promastigote culture. It appeared that cell lines with a strong expression of HASPB-mCherry exhibited a low expression level of Bem46-GFP and *vice versa*. Cells expressing both constructs at a sufficiently high level for deconvolution fluorescence microscopy were not abundant. The surface-labelling HASPB-mCherry protein particularly labelled the flagellar membrane, thus also outlining the position of the flagellum within the flagellar pocket. The GFP-labelled Bem46 did not co-localise with the red fluorescent signal, but was visible in close proximity, confined to the flagellar pocket area and surrounding the flagellum (Fig. 4-8 and 4-9).

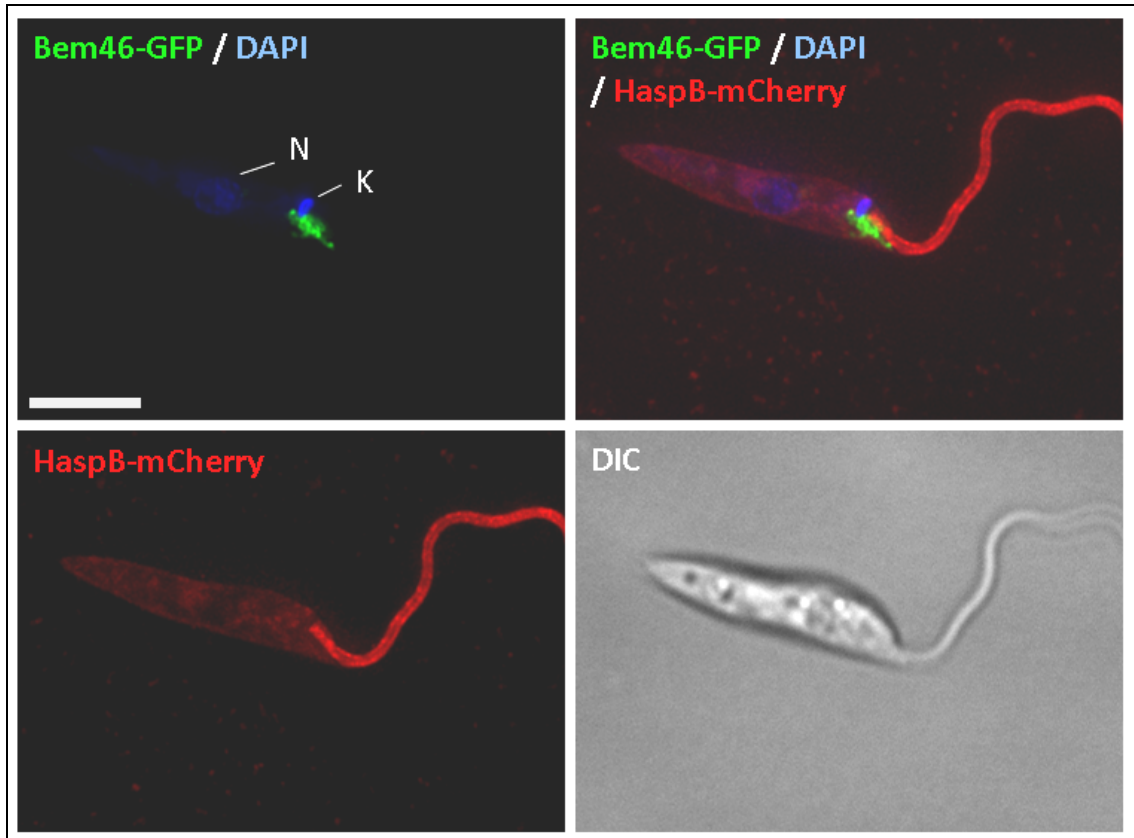


Figure 4-8: Deconvolution fluorescence microscopy image of *L. major* co-expressing an extrachromosomal Bem46-GFP fusion protein and a red fluorescent HASPB-mCherry fusion protein labelling the cell surface; fixed cell. Nucleus (N) and kinetoplast (K) stained blue with DAPI. Brightfield image (DIC) for reference. Scale bar: 10 μ m.

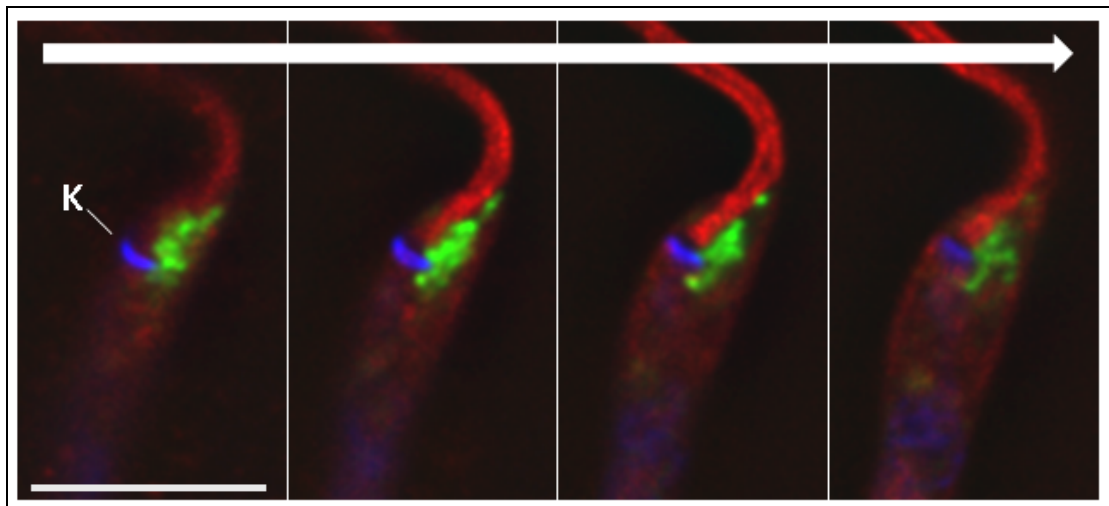


Figure 4-9: As in figure 4-8 (see above). Magnification of flagellar pocket area of cell. Shown are four consecutive deconvolution microscopy Z-stacks (from left to right: stack 8, 10, 12 and 14) to allow a view of the fluorescence pattern in different focal planes. Scale bar: 10 μ m.

4.2.3 Deletion of *Bem46* gene in *L. major*

L. major cell lines deficient in *Bem46* ($\Delta bem46$) were generated by deleting both alleles of the wild type gene locus and replacing them sequentially with the antibiotic resistance marker cassettes for hygromycin and bleomycin. The initial round of transfection was carried out with both hygromycin and bleomycin resistance marker plasmids separately, yielding heterozygous cell lines resistant to the respective antibiotic. These were subsequently transfected again, to add the respective other antibiotic marker, in replacement of the second allele of the *Bem46* gene. This second transfection was more successful for bleomycin resistant cells being transfected with hygromycin than *vice versa*. In the following section, all cell lines mentioned had been initially transfected with the bleomycin marker and then with hygromycin. Doubly resistant parasite cell lines were obtained after cloning transfectants under antibiotic pressure. They were analysed for correct *Bem46* gene deletion by PCR and Southern blot analysis (Fig. 4-10 and 4-11).

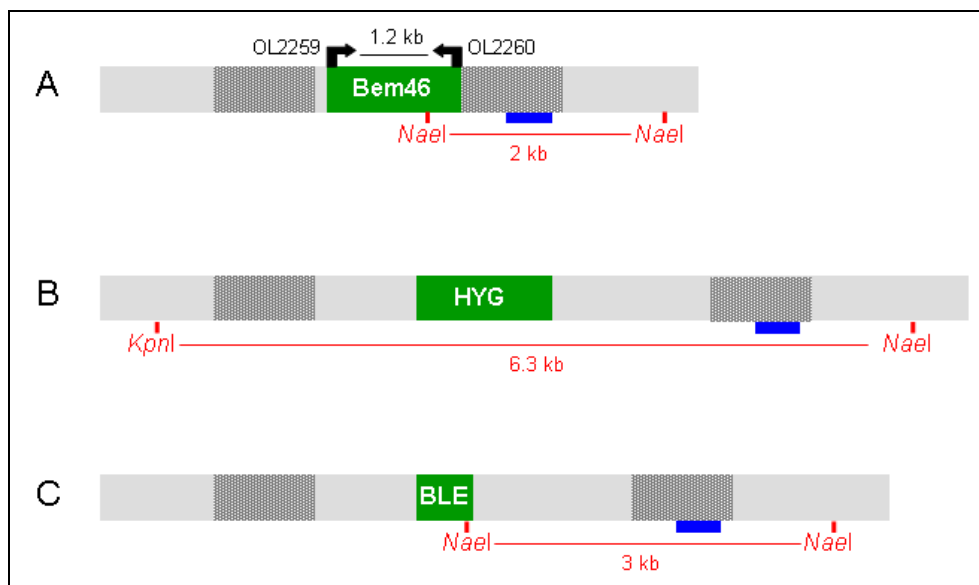


Figure 4-10: Strategy for PCR and Southern blot analyses of potential $\Delta bem46$ clones. (A) *L. major* *Bem46* locus. (B) Hygromycin cassette integrated in *Bem46*. (C) Bleomycin cassette integrated in *Bem46*. Green: open reading frames; light grey: surrounding DNA sequence; dark grey: 5' and 3' gene deletion flanks; arrows: primer binding sites, annotated with PCR product size in black. OL numbers: primer numbers for PCR. Blue box: binding site for Southern blot probe. Red: relevant *KpnI* and *NaeI* restriction sites for Southern blot, with restriction digest fragment sizes in red.

PCRs were performed with primers targeting the wild type *Bem46* allele, resulting in a PCR product of 1.2 kb in wild type and heterozygote cell lines and no PCR product in $\Delta bem46$ lines. Four of six doubly resistant clonal cell lines did not show a PCR product (Fig. 4-11 A). Of these four, three clones were confirmed to be *Bem46* deficient mutants ($\Delta bem46$) by Southern blot. Southern blots were performed on *NaeI*-/*KpnI*-digested genomic DNA after agarose gel electrophoresis. The DNA was transferred from the gel onto a membrane and hybridised with a probe specific for the 3' flank of *Bem46*. The detected fragments differed in size, depending on the *Bem46* alleles or integrated antibiotic markers present in the respective cell line (Fig. 4-10). The three positive clones (clones 3, 4 and 5) showed correct integration of both antibiotic resistance cassettes and a loss of the wild type allele (Fig. 4-11 B).

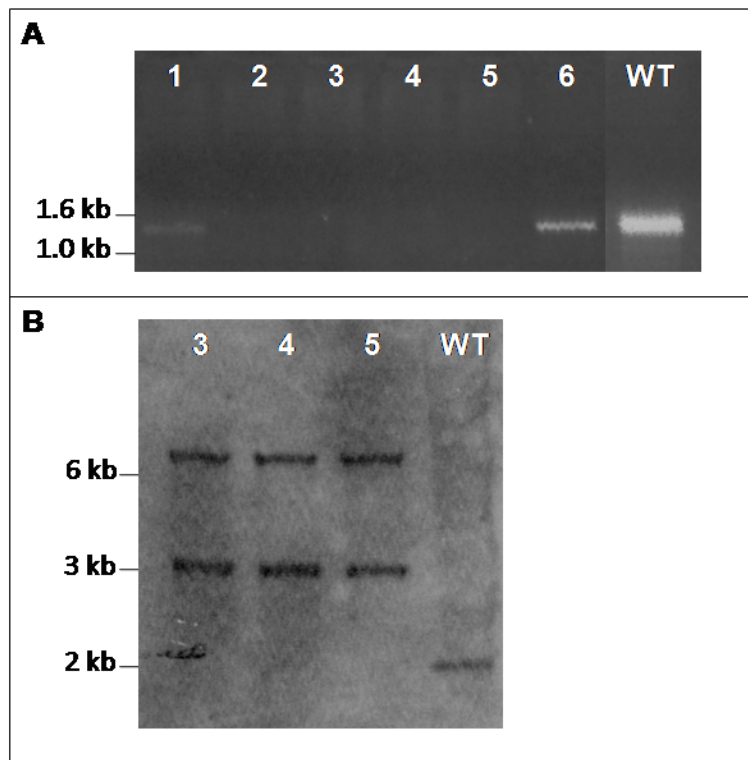


Figure 4-11: Analysis of potential $\Delta bem46$ mutant clones by PCR and Southern blotting. (A) PCR of the wild type *Bem46* gene locus. 1-6: potential $\Delta bem46$ cell lines 1-6, WT: control PCR using wild type DNA. Expected size of PCR product: 1.2 kb. (Fig. 4-10) (B) Southern blot of potential $\Delta bem46$ clones 3, 4 and 5, as well as wild type DNA (WT). Blot probed for the 3' flanking region of the gene locus after digest with *NaeI* and *KpnI*. Wild type locus fragment size 2 kb. Bleomycin cassette integration site fragment size 3 kb. Hygromycin cassette integration site fragment size 6.3 kb (Fig. 4-10).

The generated Bem46 gene deficient cell line $\Delta bem46$ (clone 3) was analysed for promastigote growth *in vitro* and infectivity in mice by inoculation into the footpad and monitoring of lesion development.

$\Delta bem46$ promastigote growth in cell culture was assessed daily over a period of seven days. The *L. major* $\Delta bem46$ cells exhibited a normal growth rate in culture (Fig. 4-12), albeit with a trend of slightly slower growth than the wild type after culture day 4. However, unpaired T-tests showed there was no significant difference in growth between the two cell lines, with all p-values above 0.2.

BALB/c mice were inoculated with $\Delta bem46$ and wild type parasites, and footpad lesion development was monitored weekly over a period of four weeks with six mice per *L. major* cell line (Fig. 4-13). As in the promastigote culture, there was a small lag in lesion growth for $\Delta bem46$. Unpaired t-tests showed that there was a significant difference between the two cell lines in week 3 ($p = 0.04$), but measurements in all other weeks did not differ significantly (p values above 0.1).

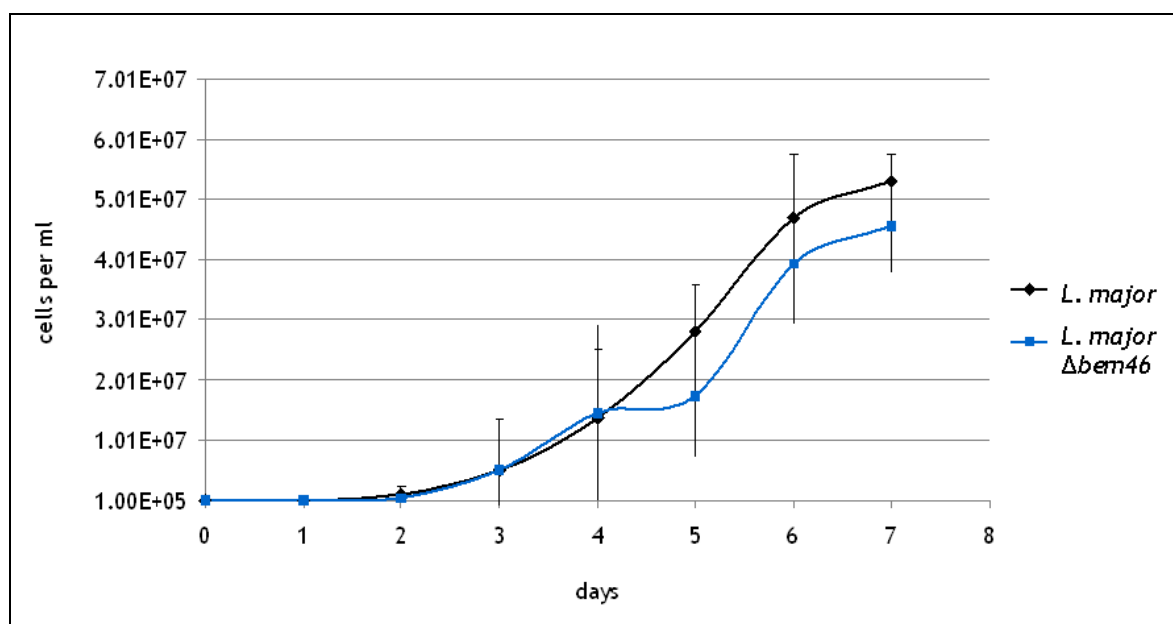


Figure 4-12: *In vitro* growth curve of promastigote cultures of wild type *L. major* and $\Delta bem46$ cells. Daily cell counts, experiments done in triplicates. Error bars show +/- standard deviation of the mean.

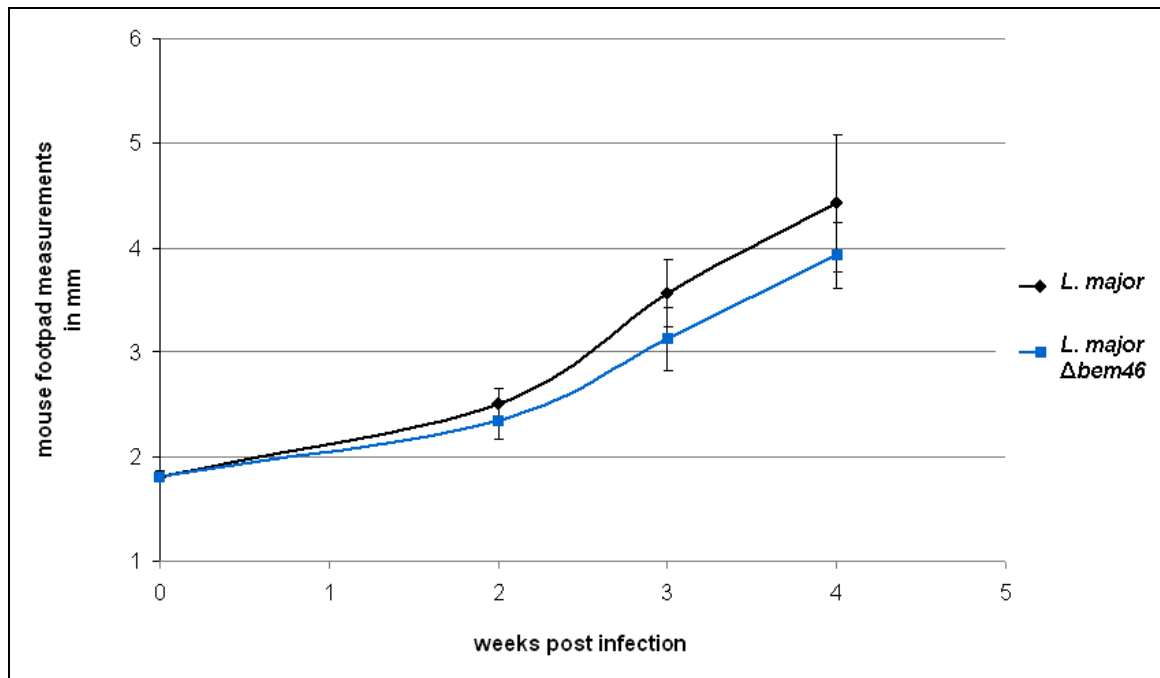


Figure 4-13: Measurements of footpad lesion development of BALB/c mice after infection with wild type *L. major* and Δ *bem46* cells. Weekly measurements of footpad swelling in mm. Measurements of six mice per cell line. Error bars show +/- standard deviation of the mean.

4.2.4 Expression and purification of recombinant Bem46-like peptidase for antibody production

The localisation of the GFP-tagged Bem46 was a first indication that this protein is trafficked to the flagellar pocket, but additional evidence could support the results, such as immunofluorescence staining and further fluorescence microscopy. For the production of a specific antibody, recombinant Bem46 protein was expressed in bacteria, purified and injected into a rabbit for polyclonal antibodies to be produced.

The nearly full-length Bem46 was expressed in *E. coli* to obtain and purify the protein for antibody production. The gene was truncated by 69 bp (23 amino acids) at its N-terminus, where a transmembrane domain was predicted, in order to try and enhance solubility. It was cloned into the pET28a vector, which added a C-terminal His-tag (6 histidine residues) to the protein sequence. This cloning work was done by Gareth Westrop, resulting in plasmid pGL1577 (originally named pBP266, carries ampicillin resistance cassette). Different *E. coli* cell lines and different expression conditions and media were assessed in order to obtain a

high yield of recombinant protein as well as good solubility (for details of conditions tested see material and methods, section 2.3.2). The recombinant Bem46 was largely detected in the insoluble pellet fraction in all conditions tested. The best yield was obtained by culturing transformed BL21 (DE3) pLysS cells overnight (~ 16 hours), at 15 °C in LB medium supplemented with ampicillin and chloramphenicol and by inducing expression with 1 mM IPTG.

As most of the protein remained insoluble, it was purified by denaturing urea extraction (elution peak at pH 5.3) using the BioCAD system. The elution fractions obtained were analysed by SDS-PAGE and Western immunoblot using an anti-His antibody (Fig. 4-14). Protein yield was quantified by Bradford assay. Before the recombinant protein could be used for raising an antibody, it was dialysed with PBS to remove the high concentration of urea in the samples. Dialysis caused it to precipitate in fine crystals. The precipitate was used for antibody production in a rabbit. The rabbit serum from three bleeds, as well as the pre-immune serum, was affinity-purified using recombinant protein bound to a column, and tested by Western immunoblotting and by immunofluorescence microscopy.

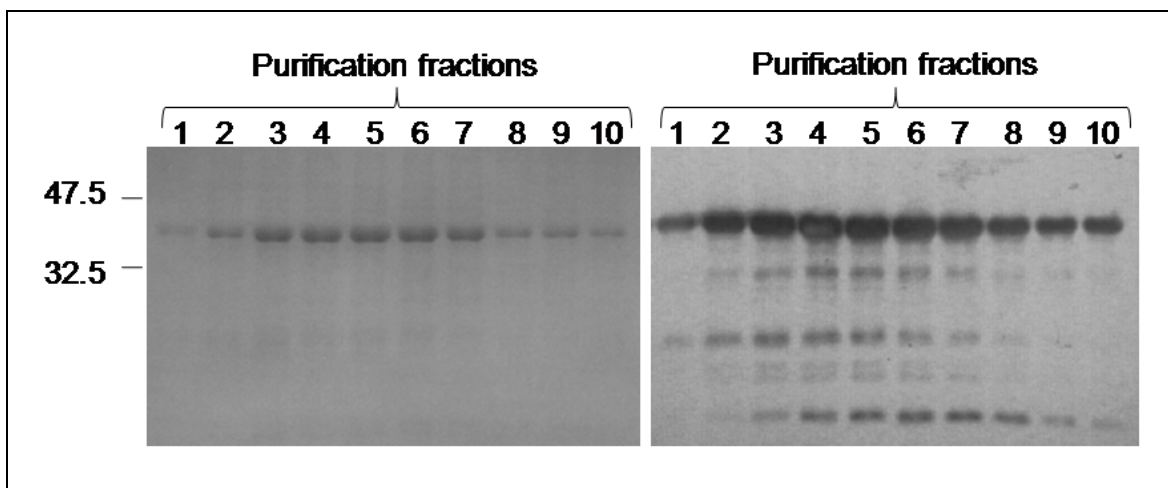


Figure 4-14: Protein purification fractions 1-10 after denaturing urea extraction of recombinant Bem46 (expected size: ~ 41 kDa). Left: Coomassie blue-stained 12 % SDS-PAGE gel of Bem46 elution fractions. Right: Western immunoblot of the same gel, using an anti-His-tag antibody.

On Western immunoblots, the anti-Bem46 antibody detected recombinant *L. major* Bem46 with no contaminating cross-reactions with other proteins (Fig. 4-15); detection of recombinant protein was possible with 100 µg of antibody.

However, on blots of *L. major* whole cell lysates, the anti-Bem46 antibody bound to several proteins, one of which was the correct size for the wild type Bem46 (43 kDa) (arrowed in Fig. 4-16) and which did not seem to appear in $\Delta bem46$ lysate. To detect the endogenous Bem46, the antibody had to be used at a higher concentration (2 mg). On blots of lysates of cell lines carrying an extrachromosomal overexpression plasmid for the GFP-tagged Bem46, the anti-Bem46 antibody detected the overexpressed fusion protein at 70 kDa, in addition to the apparent endogenous Bem46 and the contaminating proteins (Fig. 4-16).

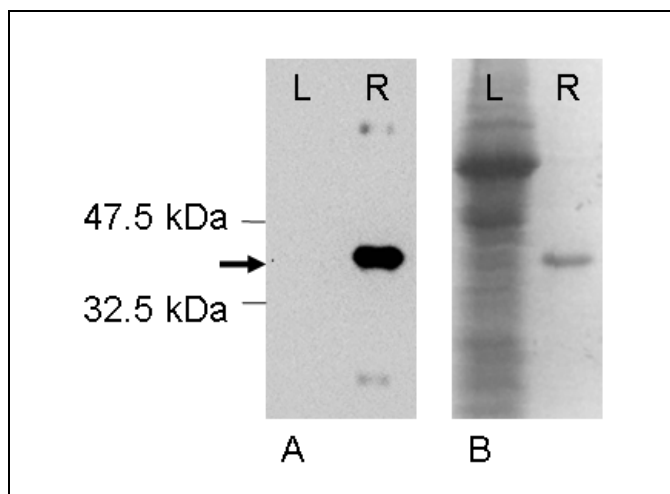


Figure 4-15: Western immunoblot of recombinant *L. major* Bem46 (R) and *L. major* whole cell lysate (L), probed with 100 μ g of anti-Bem46 antibody. Arrow: Recombinant Bem46 (~ 41 kDa). (A) Western blot. (B) Corresponding Coomassie-stained SDS polyacrylamide gel.

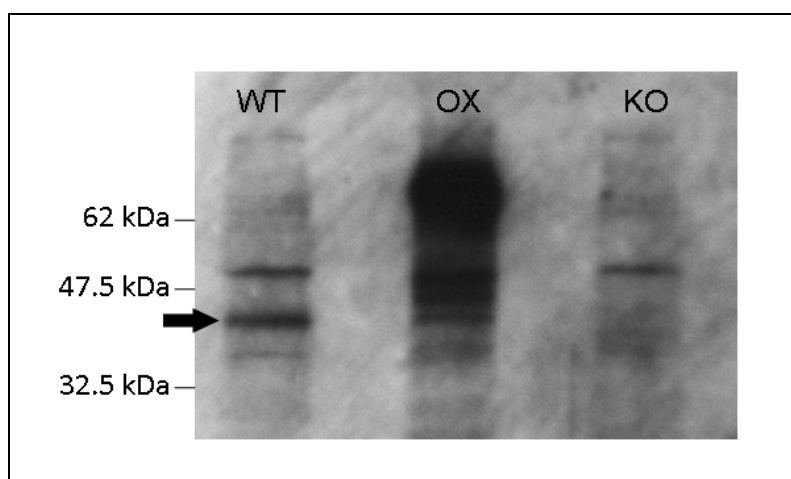


Figure 4-16: Western immunoblot of *L. major* whole cell lysates, probed with 2 mg of anti-Bem46 antibody. Cell lines used: wild type (WT), wild type expressing Bem46-GFP extrachromosomal overexpression plasmid (OX), $\Delta bem46$ (KO). Arrow: Putative Bem46 protein of correct size (43 kDa).

Immunofluorescence analysis (IFA) of *L. major* cells using the anti-Bem46 antibody (1 mg antibody per slide) did not yield consistent results. Fluorescent punctate structures could be detected by fluorescence microscopy in all samples, while control samples without secondary antibody showed no fluorescence. Cells carrying the extrachromosomal overexpression plasmid for the GFP-tagged Bem46 showed a higher intensity of fluorescence in the flagellar pocket area and the immunostaining fluorescence pattern largely co-localised with the GFP fluorescence signal. Wild type cells showed a similar pattern with fluorescent punctae throughout the cell and often an accumulation towards the flagellar pocket area. The $\Delta bem46$ cells showed a similar fluorescence pattern with notably more punctae along the length of the flagellum and no apparent larger punctae at the flagellar pocket (Fig 4-17).

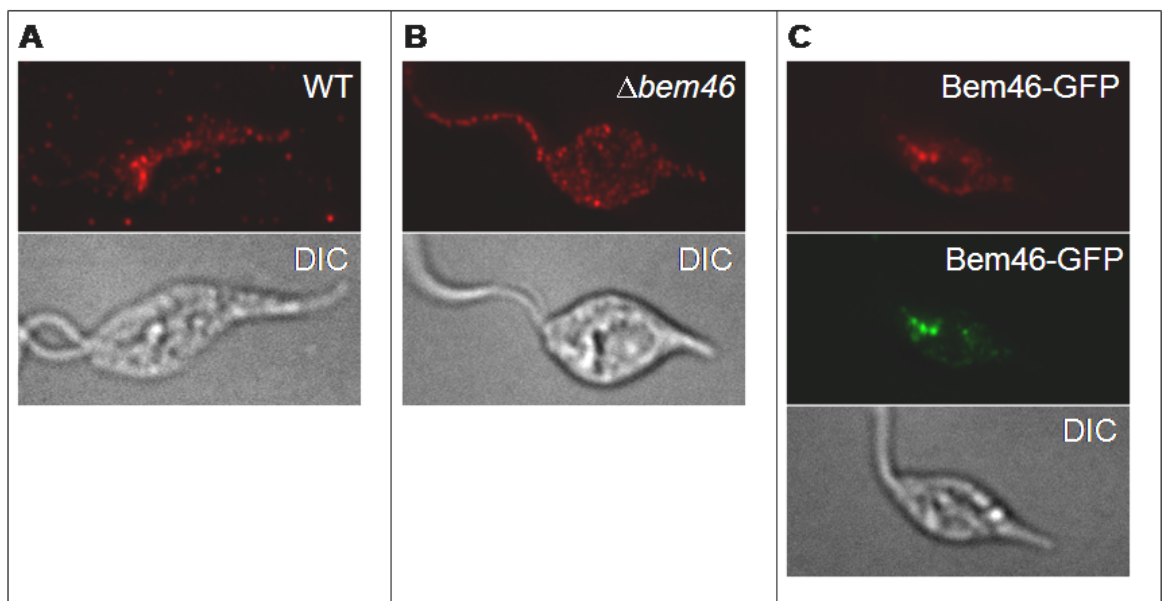


Figure 4-17: Immunofluorescence microscopy of *L. major* using anti-Bem46 antibody (dilution 1 in 200). Cells fixed, brightfield (DIC) images shown for reference. (A) Wild type *L. major* stained with anti-Bem46 antibody (B) $\Delta bem46$ stained with anti-Bem46 antibody (C) Wild type *L. major* overexpressing GFP-labelled Bem46 and stained with anti-Bem46 antibody. Top panel: red fluorescence filter image, anti-Bem46 antibody fluorescence pattern. Middle panel: green fluorescence filter image, GFP fluorescence pattern. Bottom panel: Brightfield (DIC) reference image.

4.2.5 Expression and purification of soluble recombinant

Bem46-like peptidase

A second, further truncated protein expression construct was generated for obtaining soluble recombinant Bem46. 62 amino acids (186 bp) were deleted from the N-terminus of the sequence, including the predicted transmembrane domain, in order to try and enhance solubility (Fig. 4-7). The truncated gene sequence was cloned and fused to a His-tag at the N-terminus using the vector pET28a. The fusion protein was expressed in *E. coli* as before. Again, different expression conditions were explored. It was established that using *E. coli* BL21 (DE3) cells in LB medium, with expression induced with 0.5 M IPTG at 20 °C resulted in the highest yield of soluble protein of all tested conditions. The recombinant protein was purified using a small-scale bench top His-tag affinity purification system and analysed by SDS-PAGE and Western immunoblot (Fig. 4-18). This showed that a large proportion of the protein remained in the insoluble fraction; some was soluble but had not bound to the affinity column and passed through during column loading. Nevertheless the purified elution fractions contained protein of the correct size (37.5 kDa) and with few contaminations. The earliest fractions (E1 to 3) showed a small smear of lower molecular weight protein below the Bem46 protein band, probably degradation.

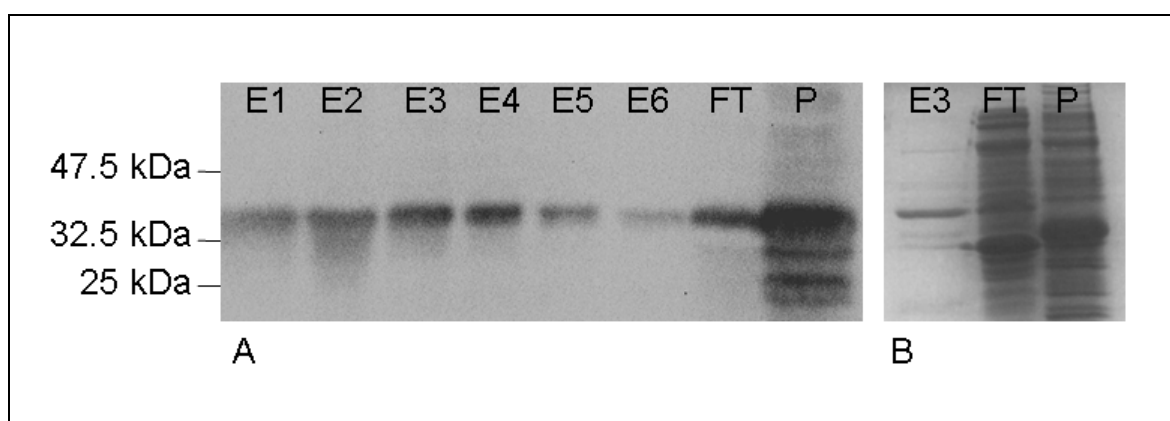


Figure 4-18: Purified truncated recombinant Bem46 (protein size 37.5 kDa). (A) Western immunoblot. Soluble fractions (E1 to E6) after His-tag affinity purification, column flow-through fraction (FT) and insoluble pellet (P). Blot probed with anti-His-tag antibody. (B) Corresponding Coomassie-stained SDS polyacrylamide gel of fraction E3, flow-through (FT) and pellet (P) fractions.

4.3 Discussion

It could be shown by fluorescence microscopy and co-localisation with the flagellar pocket stain FM4-64 that the *L. major* Bem46 accumulated in the flagellar pocket of promastigotes when tagged with GFP (see chapter 3). Additional labelling of the cell and flagellum membrane with a red fluorescent surface protein (HASPb-mCherry) revealed that Bem46-GFP was directly surrounding the flagellum within the flagellar pocket. From here, Bem46 may be released into the host environment, where it could act as a virulence factor and degrade host molecules.

However, bioinformatics predictions of the Bem46 topology predicted at least one transmembrane domain, at the protein's N-terminus. This suggests that Bem46 could be anchored to the flagellar pocket membrane. A single, N-terminal transmembrane domain could be cleaved and the protein may still be released. Alternatively, Bem46 may be a resident protein of the pocket membrane and not released into the environment at all. The composition of the flagellar pocket is not well-studied. This compartment is not an extracellular environment, but rather a semi-confined space and exchange with the outside environment is probably regulated (Landfear and Ignatushchenko, 2001b). The pocket membrane is a region of high endo- and exocytic activity, so a peptidase that is particularly abundant here, like possibly Bem46, could play an important role. It could process proteins that are being exported through the pocket, or exogenous proteins that are being imported from the environment for degradation. The notion that Bem46 may be retained in the pocket is supported by the fact that two recent studies on the *L. donovani* and *L. braziliensis* secretomes did not find Bem46 homologues to be secreted (Silverman et al., 2008; Cuervo et al., 2009c). The finding that recombinant Bem46 expressed as an insoluble protein, even after truncation of the predicted transmembrane domain at the N-terminus, adds to the evidence that Bem46 may be membrane-bound, perhaps by more than one transmembrane domain. No flagellar pocket-specific membrane proteins of *Leishmania* are known to date, so it will be worth analysing the localisation and function of Bem46 in this compartment in more detail. If the flagellar pocket membrane localisation can be confirmed, Bem46 could be useful as a protein marker for the *Leishmania* flagellar pocket. Finally,

it is possible that Bem46 is distributed along the entire cell surface, not solely in the pocket, but at a lower abundance that was not readily detected by fluorescence microscopy.

Deletion of the *Bem46* gene in *L. major* had neither a significant effect on promastigote growth in culture, nor on the establishment and progression of footpad infections in BALB/c mice. Consequently, Bem46 does not appear to be a major virulence factor in *L. major*. This finding supports the notion that Bem46 may not be secreted but retained in the flagellar pocket membrane. Promastigote $\Delta bem46$ cells appear morphologically normal under light microscopy, suggesting that Bem46 is not an essential structural component of the flagellar pocket membrane or matrix composition. Loss of Bem46 may have caused a more subtle phenotype in the cells, which was not readily detected. Alternatively, other enzymes, for example other S9 serine peptidases, may have compensated for the lack of Bem46. Promastigote cultures and BALB/c mouse infections were performed as initial experiments, but other options like infections of more immuno-competent mouse strains like C57/BL6 as well as *in vitro* macrophage infections can be explored to reveal more subtle phenotypic changes. Additionally, electron microscopy (EM) of the flagellar pocket area may allow the detection of morphological changes in $\Delta bem46$ cells that were not visible under light microscopy. Immuno-EM with the anti-Bem46 antibody that was raised in this study would be useful to confirm the flagellar pocket localisation shown by GFP-tagging. However, additional antibody purification steps may be required to enhance the specificity and decrease the cross-reactivity of the generated antibody for use in immuno-EM. Labelling Bem46 with a multiple HA (hemagglutinin)-tag, expressing this construct from the ribosomal locus of the *L. major* genome, and using an anti-HA antibody for immuno-EM is an alternative option.

In other organisms, Bem46 peptidases play a role in the maintenance of cell polarity. Downregulation of Bem46 peptidases leads to loss-of-polarity phenotypes, expressed by undirected budding site establishment in yeast (Valencik and Pringle 1995, unpublished, Uniprot database accession P54069), uninhibited bending of growing root tips in *Arabidopsis* (Mochizuki et al., 2005a), and undirected hyphae growth in the fungus *Neurospora* (Mercker et al., 2009a).

Maintenance of cell polarity is highly important for *Leishmania*, with the flagellar pocket and flagellum positioned at the anterior end of the cell, and an asymmetrical distribution of organelles and trafficking pathways, some of which converge at the flagellar pocket. The fact that Bem46-GFP accumulated at one end of the cell may indicate that Bem46 plays a role for *Leishmania* cell polarity. This notion makes it even more interesting to analyse the morphology of $\Delta bem46$ cells in more detail by electron microscopy.

Bem46 is classified as an S9 serine peptidase. However, it appears to differ markedly from other members of the S9 family like oligopeptidase B (OPB), not only in its sequence but also in its structure, as Bem46 lacks the entire N-terminal beta-propeller domain that restricts substrate size for other S9 peptidases (Fulop et al., 1998b). Consequently, Bem46 may not have a specific substrate size limit and may be able to cleave relatively large peptides.

Different members of the S9 family have different substrate specificities and cellular localisations; the S9 type peptidase POP (prolyl oligopeptidase), for example, cleaves substrates after proline, whereas OPB preferentially cleaves after basic residues (arginine and lysine) (Polgar, 2002b; Pacaud and Richaud, 1975b; Fulop et al., 1998c). Consequently, possible properties and substrate preferences of Bem46 can not be easily inferred from what is known about other S9 peptidases, and Bem46 may differ substantially. If expression of soluble and active recombinant Bem46 can be achieved, screening a library of different peptides may be most useful in order to determine which amino acids Bem46 cleaves, and whether it is an endopeptidase that cleaves within peptide sequences, or an exopeptidase that cleaves only terminal amino acids.

All experiments were performed on promastigote stage cells. It will be interesting to analyse the localisation of Bem46 in amastigotes, which is the intracellular stage in the mammalian host. Amastigotes are distinctly smaller and their flagellum barely protrudes from the flagellar pocket. Pro- and amastigotes exhibit some morphological and biochemical differences, and expression, trafficking and localisation of Bem46 may undergo changes during differentiation. If Bem46 is in fact released from promastigotes it may play a role during the infection and proliferation stages within the sand fly host, or during the initial phase of a mammalian infection. However, the situation in

amastigotes may be different and Bem46 could be downregulated, re-routed to a different subcellular destination, or membrane-bound in promastigotes while released in amastigotes or *vice versa*. To elucidate the localisation of Bem46 in amastigote cells, macrophages can be infected with Bem46-GFP-expressing metacyclic promastigotes and changes in the GFP fluorescence patterns can be tracked within the macrophage.

5. Membrane proteins of the *Leishmania* lysosome and of the lysosome-like acidocalcisomes

5.1 Introduction

5.1.1 The *Leishmania* lysosome

The protein composition of the *Leishmania* lysosome has not yet been characterised in detail. Several hydrolytic enzymes of the lysosomal lumen are known, for example the cysteine peptidase CPB (Huete-Perez et al., 1999a). However, no integral proteins of the lysosomal membrane in *Leishmania* have been identified to date. Such transmembrane proteins likely contribute to the morphology of the lysosome, which changes considerably during the *Leishmania* life cycle, from a small compartment in early promastigotes to the long tubular MVT lysosome in metacyclic promastigotes and the large megasomes of amastigotes (Ghedini et al., 2001b; Ueda-Nakamura et al., 2001a). Lysosomal membrane proteins are also important for lysosomal function, for example the acidification of the lumen or the export of amino acids, fatty acids and carbohydrates after degradation of macromolecules. Additionally, they probably play a role in the interaction and fusion with late endosomes and autophagosomes, act as receptors for molecule import into the lysosome and may stabilise and protect the inside of the membrane from the harsh, acidic conditions of the lysosome lumen and its degradative enzymes (Eskelinen *et al.*, 2002; Granger *et al.*, 1990; Fukuda, 1991; Cuervo and Dice, 1996).

In higher eukaryotes, the lysosomal membrane contains various transporters and integral proteins, most importantly LAMPs (lysosome associated membrane proteins) and LIMPs (lysosome integral membrane proteins) (Luzio et al., 2003d).

Identifying a lysosomal membrane protein in *Leishmania* will allow further investigations into lysosomal structure and function. Establishing a reliable marker membrane protein for this organelle may be very useful for fluorescence microscopy as well as other cell biology applications; marker proteins have been identified for other organelles and are now routinely used, for example the molecular chaperone BiP of the endoplasmic reticulum (Bangs *et al.*, 1993), the mitochondrial marker protein CS (citrate synthase, (Castro *et al.*, 2008), the glycosome marker proteins GAPDH (glyceraldehyde-3-phosphate dehydrogenase, (Hart and Opperdoes, 1984; Plewes *et al.*, 2003) and PFK (phosphofructokinase, (Lopez *et al.*, 2002), as well as the proteins Rab1 (Dhir *et al.*, 2004a), GM-130 (Golgi matrix protein, (Nakamura *et al.*, 1995) and GRIP (McConville *et al.*, 2002a) of the Golgi apparatus.

5.1.2 Lysosome-Associated Membrane Proteins (LAMPs)

In many organisms, LAMPs are an important and abundant component of the lysosomal membrane. In mammals there are two different forms, LAMP-1 and LAMP-2. In mice, deficiency in LAMP-1 leads only to mild defects, possibly because LAMP-2 can compensate for its function. Lack of LAMP-2 has more severe consequences, including a pathological accumulation of autophagosomes in several organs, muscles and other tissues and often death after 20 - 40 days. Doubly deficient mice, lacking both LAMPs, show even more autophagosome accumulation, a change in lysosomal appearance and defects in cholesterol metabolism, leading to death within 16 days. Surprisingly, it was shown that the overall protein degradation and also the acidity of the lysosome are not strongly affected by the deletion of either or both LAMP genes (Eskelinen, 2006; Eskelinen *et al.*, 2004b). In humans, LAMP-2 deficiency leads to a rare and severe disorder, Danon disease, a lysosomal glycogen storage defect that is associated with cardiomyopathy, muscle weakness and mental retardation (Nishino *et al.*, 2000).

Mammalian LAMPs are type I transmembrane proteins with one transmembrane domain, a short C-terminal tail in the cytosol and a long luminal N-terminus (Fig. 5-1). The luminal domain is heavily glycosylated, with 16 - 23 N-glycosylation sites, depending on the organism. Both LAMP-1 and LAMP-2 are

additionally O-glycosylated in the "hinge" region of the luminal domain. The heavy glycosylation may play a role in protecting the LAMPs from the hydrolytic environment of the lysosomal lumen. But LAMP-deficient cells as well as cells with deglycosylated LAMPs still contain intact lysosomes, so LAMPs are not essential for the maintenance of these organelles (Eskelinen et al., 2004a; Eskelinen et al., 2005a; Kundra and Kornfeld, 1999). It has been suggested that mammalian LAMPs are required for the motility and subsequent fusion of phagosomes and the compartments of the endosomal system (Huynh *et al.*, 2007). Mammalian LAMPs are targeted to the lysosomes via two pathways, a direct route from the ER and trans-Golgi to the late endosomes and lysosomes, as well as an indirect route via the plasma membrane and early endosomes before internalisation into late endosomes and lysosomes (Hunziker and Geuze, 1996). A specific C-terminal tyrosine-based sorting signal (GYXXØ) has been shown to be required for lysosomal targeting, whereby the bulky hydrophobic C-terminal amino acid Ø (V, L, I, M or F) plays an important role (Gough et al., 1999b).

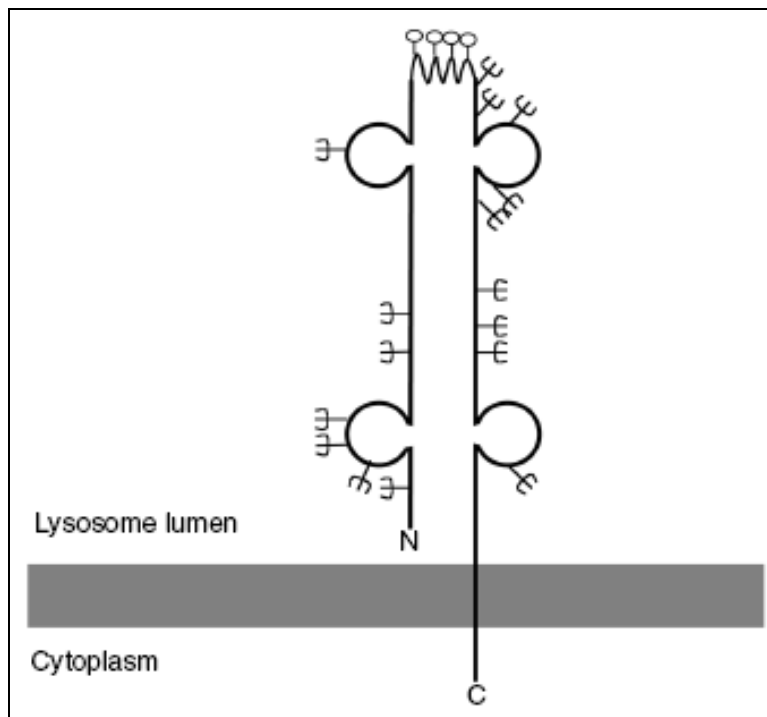


Figure 5-1: Schematic of mouse LAMP-2. The four loops are formed by disulfide bridges, zig-zag at the top denotes proline-rich hinge region, forks represent N-glycosylation sites, rings represent O-glycosylation sites in hinge region. LAMP-1 has a very similar structure. Image from (Eskelinen et al., 2005b)

T. brucei contains one LAMP-like protein, the type I transmembrane protein p67, which is encoded at multiple gene loci. It is not a sequence homologue of mammalian LAMPs, but it shows a strong structural resemblance, with a highly glycosylated long N-terminal domain in the lysosomal lumen, one transmembrane domain and a cytosolic C-terminal tail. It localises to the lysosome in both life cycle stages of *T. brucei* (Alexander *et al.*, 2002; Kelley *et al.*, 1999). The function of p67 is not known, it may play a role analogous to that of mammalian LAMPs, but this has not been elucidated in detail. It has been shown that p67 is essential in *T. brucei* bloodstream form cells and that loss of p67 severely affects lysosomal morphology. p67 is sorted to the lysosomal membrane of *T. brucei* by two dileucine targeting motifs in the C-terminal domain which are crucial for targeting (Tazeh and Bangs, 2007b; Peck *et al.*, 2008); this is thought to depend on AP3- or AP4-mediated vesicle transport (Allen *et al.*, 2007b). *Leishmania* does not have a close homologue of p67.

5.1.3 The protein carrier complex AP3

The adaptor complex AP3 is a multimeric protein complex consisting of the subunits $\beta 3$, $\mu 3$, $\sigma 3$ and δ (Fig. 5-2) (Odorizzi *et al.*, 1998c). It is involved in sorting and carrying newly synthesised membrane proteins to the lysosome (Nakatsu and Ohno, 2003a), as experiments on yeast, fly and mammalian cells have shown (Dell'Angelica *et al.*, 1999f; Cowles *et al.*, 1997a; Rozenfeld and Devi, 2008; Luzio *et al.*, 2003e). However, as yet, it is not clear whether AP3 trafficks proteins from the trans-Golgi network to the lysosome or, alternatively, from early endosomes, or probably both (Peden *et al.*, 2004b; Ihrke *et al.*, 2004a).

AP3 recruits cargo proteins with specific tyrosine-based and dileucine-based motifs as sorting signals (Dell'Angelica *et al.*, 1997b; Ohno *et al.*, 1998c; Wen *et al.*, 2006; Honing *et al.*, 1998; Nakatsu and Ohno, 2003b). It is thought to bind and interact with clathrin through its "clathrin-box" site on the β subunit (Dell'Angelica *et al.*, 1998b; Newell-Litwa *et al.*, 2007; Peden *et al.*, 2004a; Drake *et al.*, 2000). Two isoforms of the subunits $\beta 3$ and $\mu 3$ - and therefore two differing AP3 complexes - are expressed in mammals, one ubiquitously (AP3A) and one solely in neurons (AP3B) (Yang *et al.*, 2000b; Simpson *et al.*, 1997).

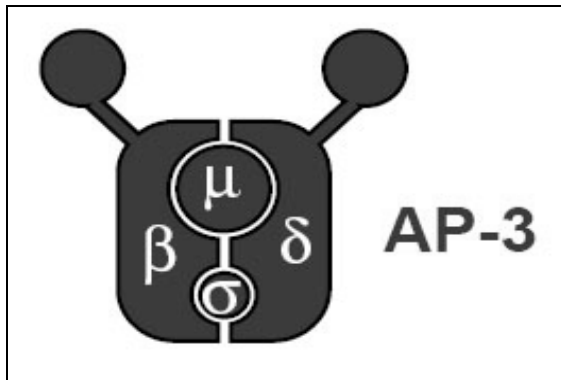


Figure 5-2: Schematic of the AP3 complex with its subunits (Odorizzi et al., 1998b).

When AP3 is defective, yeast cells exhibit a mislocalisation of the alkaline phosphatase ALP and the t-SNARE Vam3p to cytoplasmic vesicles instead of the vacuole (Cowles et al., 1997b). The *Drosophila* pigmentation mutants *garnet*, *ruby*, *carmine* and *orange* each carry a mutation in one of the four AP3 subunits. These fly mutants exhibit pigmentation defects, particularly of the eyes. A likely explanation for this is that the proteins required for synthesis, transport or storage of the pigments are not delivered to the lysosome-like pigment granules by the AP3 carrier properly (Boehm and Bonifacino, 2002a).

In mammalian cells, lack of AP3 can have severe consequences, too. A distinct human disease, Hermansky-Pudlak syndrome type 2 (HPS2, OMIM 233300), has been linked to AP3 defects. HPS2 patients exhibit albinism, prolonged bleeding time (platelet storage pool deficiency), lysosomal storage disorders and an increase in lysosome and melanosome sizes (HERMANSKY and PUDLAK, 1959; Dell'Angelica et al., 1999e). HPS2 corresponds to the mouse mutants *mocha* and *pearl*. The *mocha* mouse has a defect in the AP3 δ subunit, while the *pearl* mouse carries a mutation of the β 3 subunit. Both show prolonged bleeding time (platelet storage pool deficiency), pigmentation defects / albinism (melanosomal storage defect) and lysosomal storage defects (Kantheti et al., 1998c; Feng et al., 1999; Odorizzi et al., 1998a; Boehm and Bonifacino, 2002b). AP3 deficient mouse mutants show a mislocalisation of the lysosomal membrane

proteins LAMP-1 and LAMP-2, which contain tyrosine-based AP3 binding motifs, and LIMP-2, which contains dileucine-based AP3 binding motifs (Yang et al., 2000a; Le Borgne et al., 1998). In the wild type these proteins are thought to be transported from the ER to endosomes and then to lysosomes along two pathways: directly through AP3-vesicles or indirectly through the secretory pathway via the plasma membrane. LAMPs have been observed to accumulate in endosomal AP3-vesicle buds (Peden et al., 2004c). In mutants lacking AP3, the LAMP proteins are found on the lysosomes as usual, but also clustered on the cell surface. This indicates that only the indirect, possibly AP2-mediated pathway to the lysosome is active in the mutant; with the AP3 pathway not functioning, there is too much LAMP-1 and LAMP-2 to be processed through the indirect pathway, so they accumulate on the plasma membrane (Dell'Angelica et al., 2000b; Dell'Angelica et al., 1999d; Yang et al., 2000c; Peden et al., 2004d). This effect has also been observed for other mammalian lysosomal proteins, for example endolyn (Ihrke et al., 2004b) and CD63 (Rous *et al.*, 2002). AP3 appears to be important but not essential for the lysosomal targeting of several membrane proteins.

All these findings suggest that AP3 is involved in protein traffic to lysosomes and LROs (lysosome-related organelles) like melanosomes and platelet dense granules (Boehm and Bonifacino, 2002e; Dell'Angelica et al., 1999c; Kantheti et al., 1998b). The latter resemble the acidocalcisomes of *Leishmania* in their size, acidity and polyphosphate content (Besteiro et al., 2008l; Ruiz et al., 2004).

Recent experiments from the Mottram laboratory have provided evidence that the protein carrier complex AP3 appears to be involved in protein trafficking to the acidocalcisomes of *Leishmania* (Besteiro et al., 2008k). AP3 null mutants of *L. major* ($\Delta ap3\delta$) were created by deleting the δ -subunit of the AP3 complex, which should abolish the function of the entire AP3 complex (Kantheti et al., 1998a). The $\Delta ap3\delta$ cells were viable, but cell growth rates were reduced. The appearance of the MVT lysosome in the mutants was not visibly different from that in wild type parasites (as analysed by fluorescence microscopy with the marker dye FM4-64). Surprisingly, however, the acidocalcisomes were much less acidic than in wild type cells, had lost their polyphosphate content and seemed to be less prevalent or less detectable, likely because they were empty or otherwise compromised. This is the first evidence that AP3 may also be involved

in the targeting of proteins to the acidocalcisomes, e.g. intramembrane proton pumps like the V-H⁺-PPase and V-H⁺-ATPase. Infection experiments with mice showed that parasites lacking AP3 were capable of invading macrophages, but they did not proliferate as well as wild type parasites and they did not produce any skin lesions in mice (Besteiro et al., 2008j). These findings are supported by results previously reported for the V-H⁺-PPase of *T. brucei*. RNAi silencing of this protein led to a loss of acidocalcisome acidity and polyphosphate content, as well as a cell growth defect in procyclic and bloodstream form cells (Lemercier et al., 2002c). These findings point to a so far unknown involvement of the acidocalcisomes and potentially the AP3 carrier in parasite virulence.

5.1.4 Tyrosine-based protein sorting signals

Canonical tyrosine-based sorting signals consist of the amino acids YXXØ, whereby Ø is a bulky hydrophobic residue like L, I, F, V or M (Ohno et al., 1996b). Such YXXØ signals are conserved throughout the eukaryotes, from protozoans to mammals (Bonifacino and Traub, 2003). It appears that many proteins that are sorted by a YXXØ motif are at least partly or transiently targeted to the plasma membrane and YXXØ is an important signal for the rapid internalisation of proteins from the surface. YXXØ is known to be important for sorting of proteins to the endo- and lysosomal compartments. YXXØ motifs involved in lysosomal targeting are usually preceded by a glycine residue and are positioned within 9 residues of the protein's C-terminus (Gough et al., 1999a; Williams and Fukuda, 1990; Harter and Mellman, 1992; Bonifacino and Traub, 2003).

Different YXXØ motifs are known to be recognised by one or more of the respective μ subunits of the adaptor complexes AP1, AP2, AP3 and AP4 (Ohno et al., 1995; Ohno et al., 1996a; Ohno et al., 1998b; Hirst et al., 1999b). Recognition by μ subunits of AP3 is strongest for YXXØ motifs with acidic residues before and after the tyrosine (Ohno et al., 1998a) and the evidence suggests that AP3 mainly recognises YXXØ motifs for lysosomal targeting. YXXØ motifs that are folded inside the protein are unlikely to be active signals (Bonifacino and Traub, 2003).

5.1.5 The vacuolar proton pyrophosphatase of the acidocalcisomal membrane

Several proteins of the kinetoplastid acidocalcisomes have been identified (Docampo et al., 2005b), including the intramembrane proton pump V-H⁺-PPase (vacuolar-type proton-translocating pyrophosphatase). If the AP3 carrier is indeed involved in transporting membrane proteins to the acidocalcisomes, the V-H⁺-PPase is a potential cargo candidate. It was initially known as a component of the plant vacuole membrane and was later discovered as an active enzyme and an acidocalcisomal marker in kinetoplastids (Scott et al., 1998; Rodrigues et al., 1999a; Rodrigues et al., 1999b; Lemercier et al., 2002b). Its activity couples the energy-releasing hydrolysis of pyrophosphate with translocation of protons into the acidocalcisome lumen for maintenance of acidity.

The *L. major* V-H⁺-PPase (gene ID LmjF31.1220) is an intramembrane protein with 16 predicted transmembrane domains (Fig. 5-3). It is a relatively large protein with 803 amino acids and a molecular weight of 83.5 kDa. It contains an inorganic H⁺-pyrophosphatase domain and is thought to function as a proton pump in the acidocalcisome membrane, like its homologues in other organisms (Lemercier et al., 2002a). There are six canonical YXXØ tyrosine motifs in the V-H⁺-PPase sequence, which are candidate binding sites for a possible interaction with the carrier complex AP3. Of the six tyrosine sites, two (sites V and VI) lie within the predicted transmembrane domains on the luminal side of the membrane and are therefore unlikely to be accessible for interactions with cytosolic proteins. Tyrosine sites I to IV are positioned in the cytosolic loops of the V-H⁺-PPase and may interact with cytosolic proteins, but site I is the least highly conserved of the four sites and does not appear in trypanosome V-H⁺-PPases (Fig. 5-3). Site II is located very closely to the membrane and less accessible than the others. Hence, tyrosine sites III (YRPV, Tyr-Arg-Pro-Val) and IV (YGPI, Tyr-Gly-Pro-Ile) may be the most likely candidates for an interaction with AP3 or another carrier (Besteiro et al., 2008i).

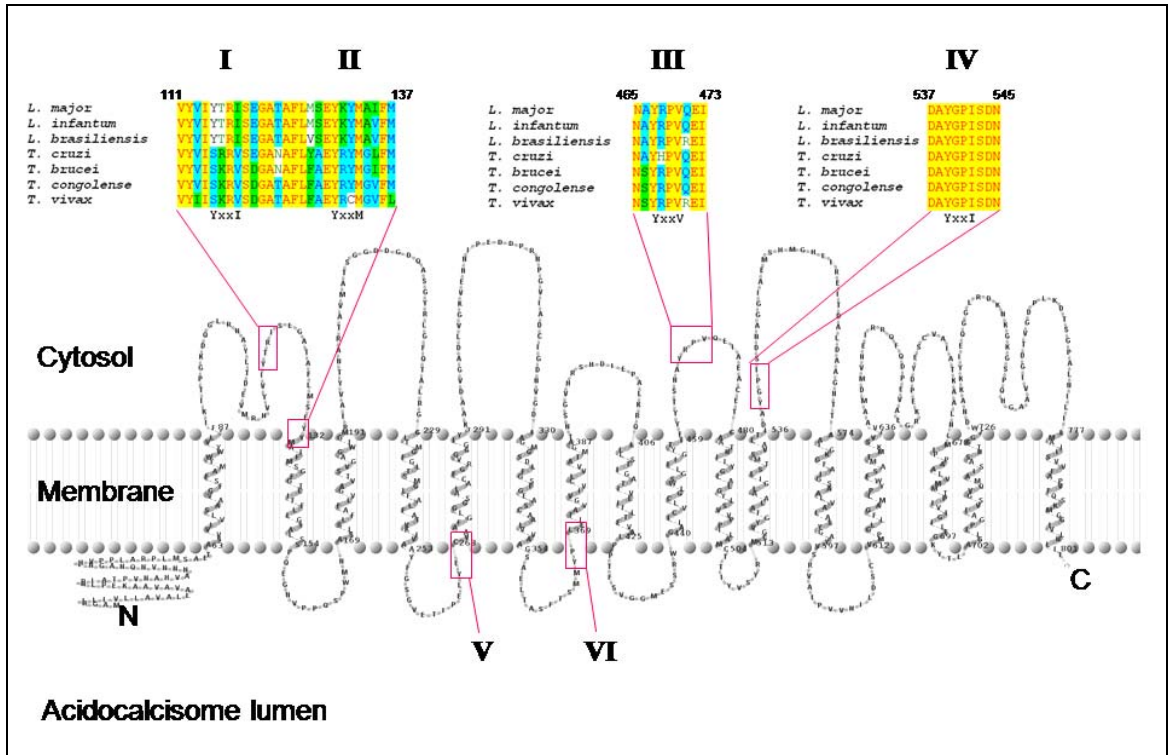


Figure 5-3: Prediction of V-H⁺-PPase protein topology. Predicted using HMMTOP and visualised with TMPres2D. Image: Sebastien Besteiro.

5.2 Results: The *L. major* LAMP-like protein

5.2.1 Identification and bioinformatics analysis of *L. major* LAMP-like protein

A *Leishmania* genome BLAST search with mammalian LAMP sequences yielded no significant results, indicating that *L. major* does not have a sequence homologue of mammalian LAMP proteins or p67 from *T. brucei*. Nevertheless, the *L. major* lysosomal membrane should - as in mammals - contain different membrane proteins that contribute to and maintain lysosome structure, morphology and function. No such proteins have been identified thus far.

Since the AP3 carrier complex is known to transport membrane proteins to the lysosome in other organisms by binding to canonical tyrosine or dileucine motifs, the initial approach to finding a membrane protein of the *Leishmania* lysosome was to search the *L. major* genome database for a transmembrane protein containing such motifs. This work was done by Sebastien Besteiro, who conducted a double query search on the GeneDB database for proteins with either of the two AP3 binding motifs as well as transmembrane domains. From the resulting proteins, LmjF30.2670 was chosen as a candidate LAMP-like protein (LMP), because it was predicted to contain one or two transmembrane domains like the mammalian LAMPs. It shows only around 12 % identity with human LAMP-2A and can be poorly aligned with this protein (Fig. 5-4); it also contains two putative tyrosine motifs towards its C-terminus (see Table 5-1 for summary of LmjF30.2670 characteristics). It is important to note that LmjF30.2670 does not show a high sequence homology to mammalian LAMPs, but may be a structural homologue. The *L. major* LMP and the human LAMP-2A are similar in length (Fig. 5-4) and possibly in topology. Notably, the GY residues of the C-terminal lysosomal targeting motif of the human LAMP (Gough et al., 1999c) are conserved in *L. major*, although the rest of the tyrosine motif is different (GYKQF in humans, GYNSL followed by eight further amino acids before the C-terminus in *L. major*).

The *L. major* LMP is conserved among the kinetoplastids with identity values of 61 to 69 % in *Leishmania* species (with an e-value of $7e-171$ for *L. infantum* and

an e-value of $5e-123$ for *L. braziliensis*) and 50 % for *T. brucei* and *T. cruzi* (with e-values $2e-36$ and $6e-41$ respectively), so may have an important function. It does not share sequence identity with the trypanosome LAMP-like protein p67. BLAST search results did not show any vertebrate homologues of the protein, merely weak homologies with a small number of bacterial, yeast and invertebrate proteins, all with e-values above 6.0.

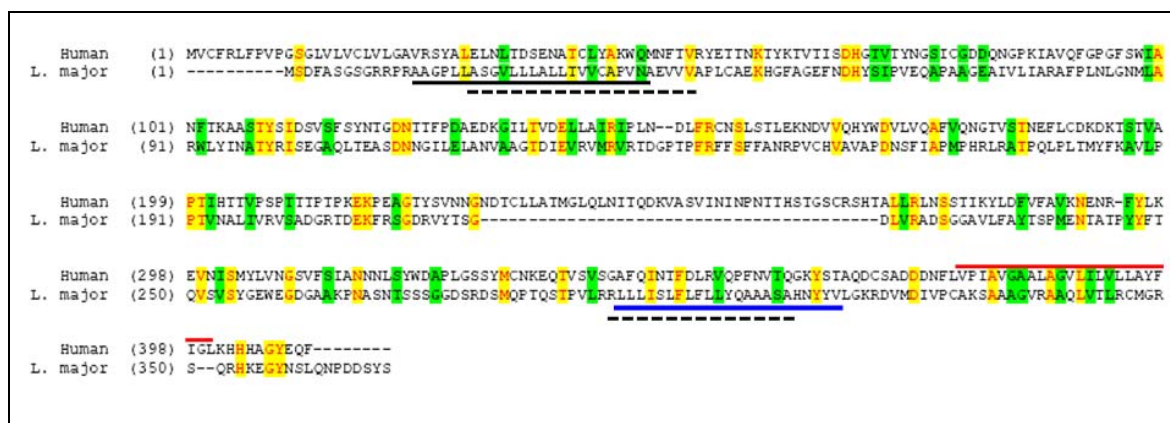


Figure 5-4: Alignment of *L. major* LMP and human LAMP-2A sequences. Red line: human LAMP transmembrane domain; black line: HMMTOP predicted *L. major* transmembrane domain; blue line: TMHMM predicted *L. major* transmembrane domain; dashed lines: SOSUI predicted *L. major* transmembrane domains.

5.2.1.1 Prediction of protein topology and features

The protein topology of the *L. major* LMP was predicted using the programmes SOSUI, TMHMM, HMMTOP and Phobius. The results of these predictions differed, with SOSUI predicting two transmembrane domains at the N- and the C-terminus (Fig 5-5), HMMTOP predicting one transmembrane domain near the N-terminus (same position as in SOSUI) (Fig. 5-7), and TMHMM as well as Phobius predicting one at the C-terminus (same position as in SOSUI) (Fig. 5-6 and 5-8). It is worth noting that the N-terminal transmembrane domain predicted by SOSUI and HMMTOP may be a misinterpretation of an N-terminal signal peptide. The Phobius algorithm was developed to distinguish better between signal peptides and transmembrane domains at the N-terminus and may therefore be more accurate (Emanuelsson et al., 2007; Kall et al., 2004c). The N-terminal transmembrane domain predicted by HMMTOP does not coincide with the transmembrane domain of mammalian LAMPs; it lies further upstream (Fig. 5-4).

Two tyrosine motifs (YXXØ) were identified manually in the sequence. Additionally there is one canonical dileucine motif ([D/E]XXX[LL/LI]) as well as two potential N-glycosylation sites (Fig. 5-9).

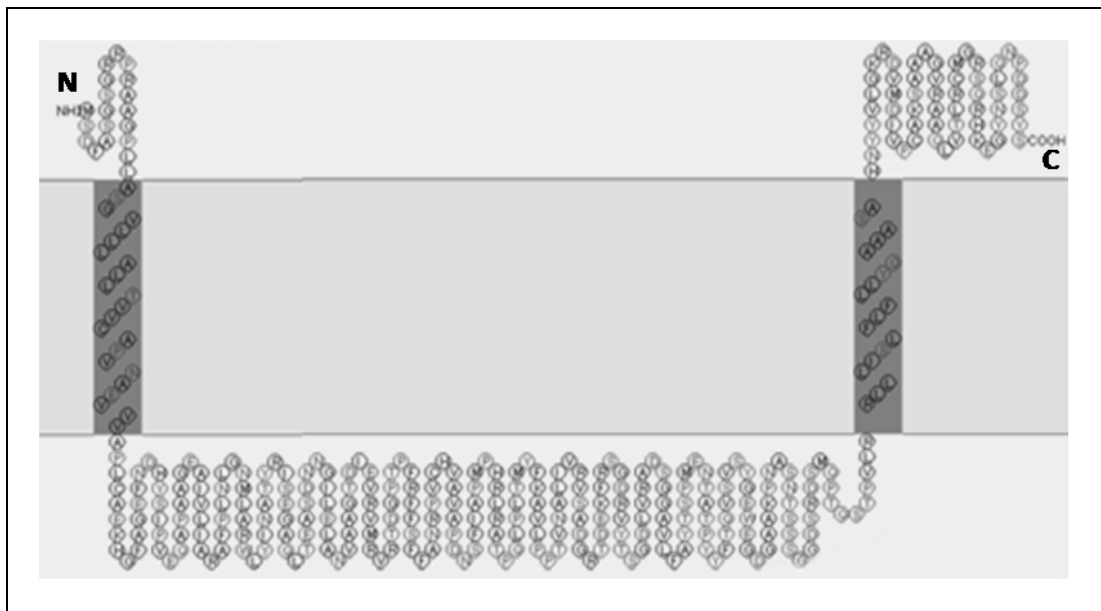


Figure 5-5: Prediction of *L. major* LMP protein topology, predicted using the SOSUI algorithm. N: N-terminus, C: C-terminus. Predicted two transmembrane domains at amino acids 20-42 and 293-311.

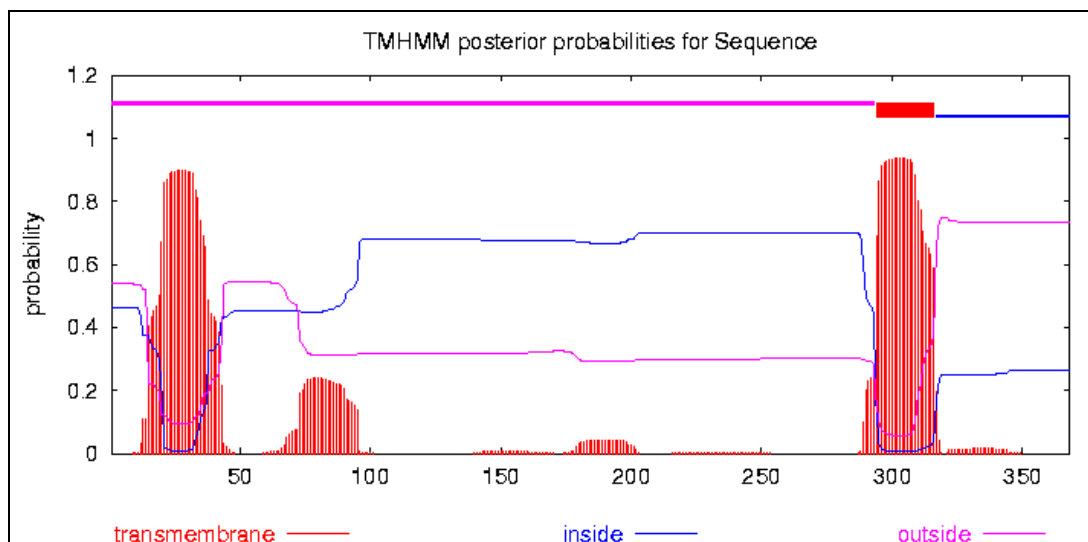


Figure 5-6: Prediction of *L. major* LMP protein topology, predicted using the TMHMM algorithm. Red: probability of transmembrane domain. Predicted one transmembrane domain at amino acids 294-316 and a potential second transmembrane or signal peptide domain at the N-terminus.

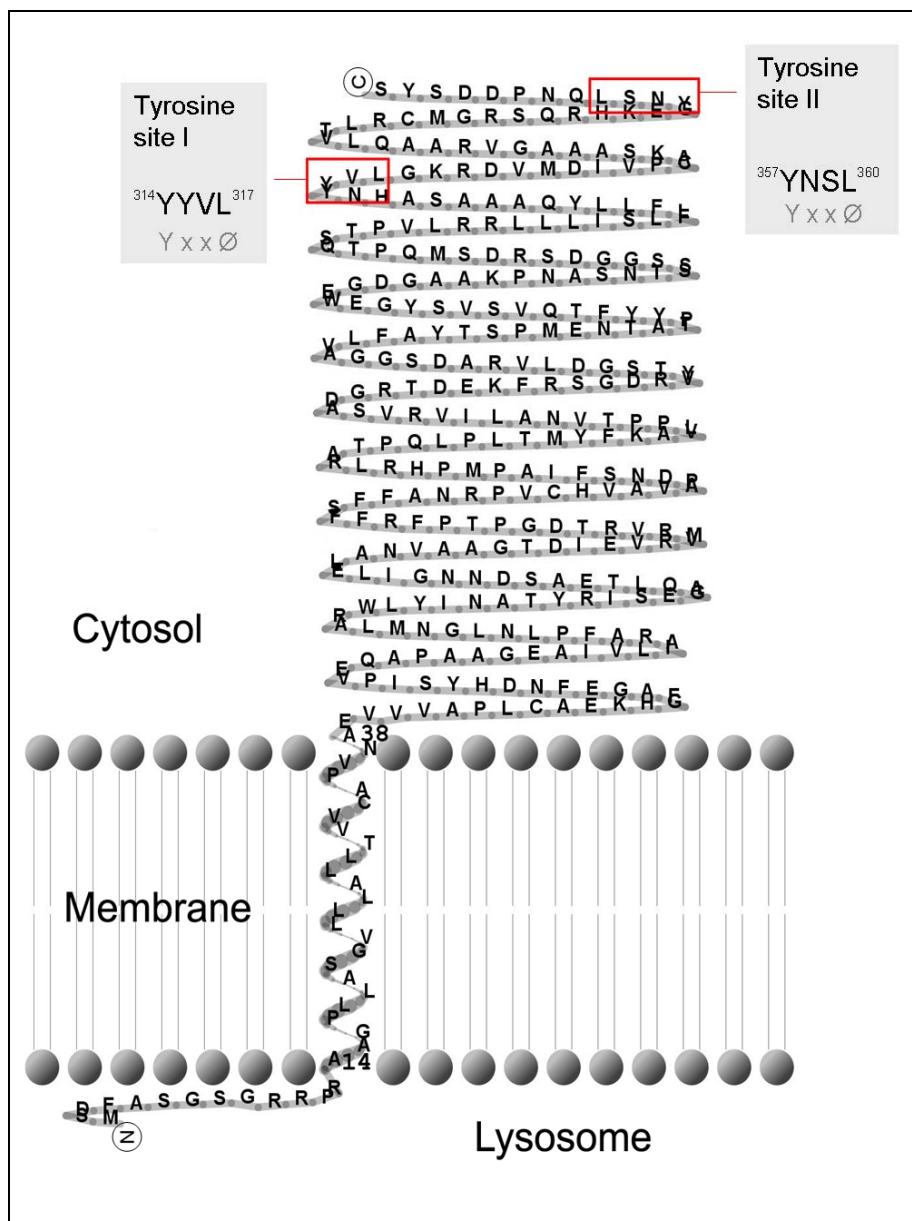


Figure 5-7: Prediction of *L. major* LMP protein topology, predicted using the HMMTOP algorithm and visualised using TMPres2D. Predicted one transmembrane domain at amino acids 14-38. N: N-terminus, C: C-terminus. Red boxes: the two tyrosine motifs YYVL and YNSL.

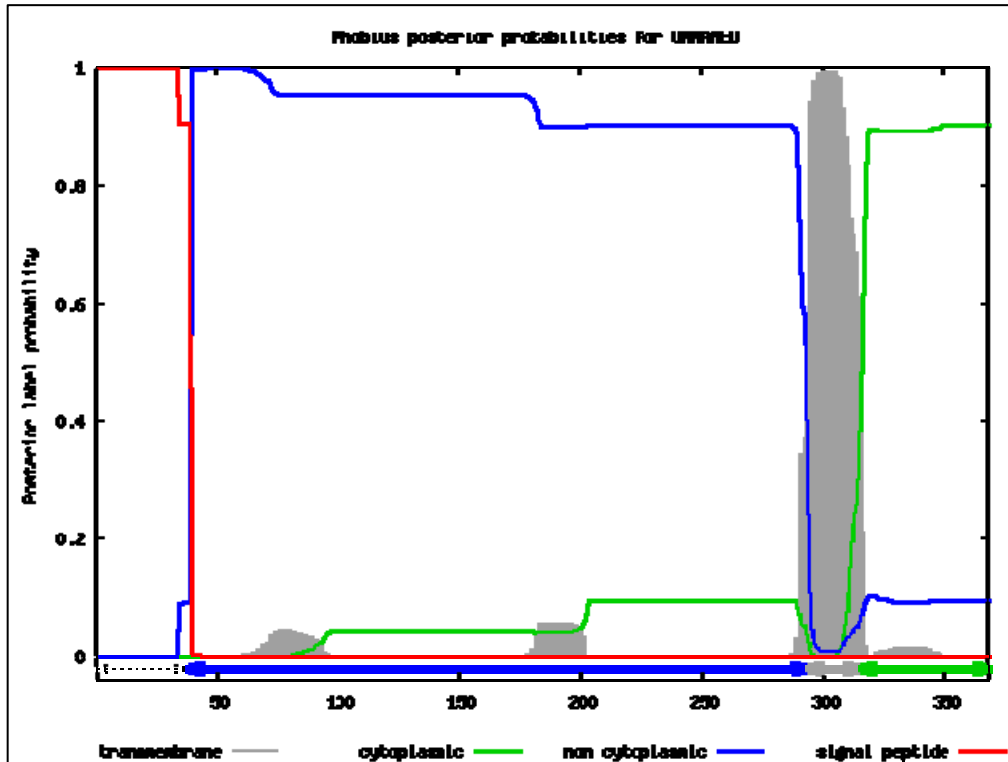


Figure 5-8: Prediction of *L. major* LMP protein topology, predicted using the Phobius algorithm. Predicted one transmembrane domain at amino acids 294-315. Red line: probability of a signal peptide (high at N-terminus), grey peak: predicted transmembrane domain.

```

MSDFASGSGRRPRAAGPLLASGVLLALLTVVCAPVNA↓EVVVAPLCAEKHGFAGEFNDYS
IPVEQAPAAGEAIVLIARAFPLNLGNMLARWLYINATYRISEGAQLTEASDNGILELANVAGT
DIEVRVMRVRTDGPTPFRFFSFFANRPVCHVAVAPDNSFIAPMPHRLRATPQLPLTMYFKAVL
PPTVNALIVRVSADGRTDEKFRSGDRVYTSGLVLRADSGGAVLFAYTSPMENTATPYTQVS
VSYGEWEGDGAAKPNASNTSSSGGDSRDSMQPTQSTPVLRRLLIISLFLFLLYQAAASAHN
YYVLGKRDVMDIVPCAASAAAGVRAAQLVTLRCMGRSQRHKEGYNSLQNPDDSYS
  
```

Figure 5-9: *L. major* LMP protein sequence with annotations. Yellow: regions of potential transmembrane domains, red: canonical tyrosine motifs (YXXØ), green: canonical dileucine motif [D/E]XXX[LL/LI], grey: potential N-glycosylation sites, black arrow: most likely signal peptide cleavage site.

Table 5-1: Characteristics of *L. major* LMP gene and protein

GeneDB gene ID	LmjF30.2670
Size	1.107 kb 368 aa 39.6 kDa
Predicted transmembrane domains	SOSUI: Two at aa 20-42 and 293-311 HMMP: One at aa 14-38 TMHMM: One at aa 294-316 Phobius: One at aa 294-315
Predicted N-terminal signal peptide (SignalP-HMM)	Yes. Signal peptide probability: 0.995 Most likely cleavage site: after aa 38
Tyrosine motifs	Two YXXØ tyrosine motifs: ³¹⁴ YYVL ³¹⁷ and ³⁵⁷ YNSL ³⁶⁰
Dileucine motifs	One [D/E]XXX[LL/LI] dileucine motif: ⁷² EAIVLI ⁷⁷

5.2.2 Cloning and GFP labelling of LAMP-like protein

The *L. major* LMP gene was cloned in full length and fused to GFP to label the C-terminus of the protein, resulting in plasmid pGL1682. A second construct was cloned to replace the middle domain of LMP with GFP and leave 46 amino acids of the N-terminus and 83 amino acids of the C-terminus intact on either side of GFP ("LAMPends" construct) for targeting and integration into a membrane (pGL1683). Both constructs were expressed extrachromosomally in *L. major* wild type and AP3 carrier-deficient ($\Delta ap3\delta$) cell lines. Transfectants were analysed by fluorescence microscopy to assess the intracellular localisation of the LMP protein in *L. major* and to evaluate the possible involvement of AP3 in the targeting of LMP to its destination membrane.

5.2.3 Fluorescence microscopy

5.2.3.1 GFP fusion protein expression in *L. major*

Expression of the GFP-tagged proteins was successful; both constructs resulted in a visible expression and localisation of GFP in *L. major*. The full length LMP tagged with GFP appeared to localise in an undefined area close to the flagellar pocket. The fluorescence signal was diffuse and distributed in no distinct pattern (Fig. 5-10). The fusion protein of the LMP protein ends on either side of GFP ("LAMPends") gave a more distinct fluorescence pattern. It localised to a small elongated structure close to the kinetoplast and just inwards from the flagellar pocket. In some cases, probably depending on the focal plane, the structure appeared almost doughnut-shaped, in some cells seemingly encircling the kinetoplast (Fig. 5-11). Dividing cells could occasionally be observed to contain two such green structures (Fig. 5-12).

Staining of the GFP cell lines with the endocytic stain FM4-64 showed that the GFP fusion proteins did not localise to the *L. major* MVT lysosome in any promastigote life stage. The full length LMP-GFP signal and the red fluorescent stain only partially co-localised in the area of the flagellar pocket and possibly early endosomes, but not further into the endocytic pathway (Fig. 5-10). For the LAMPends-GFP fusion protein there was no detectable overlap with the FM4-64 pattern (Fig. 5-13).

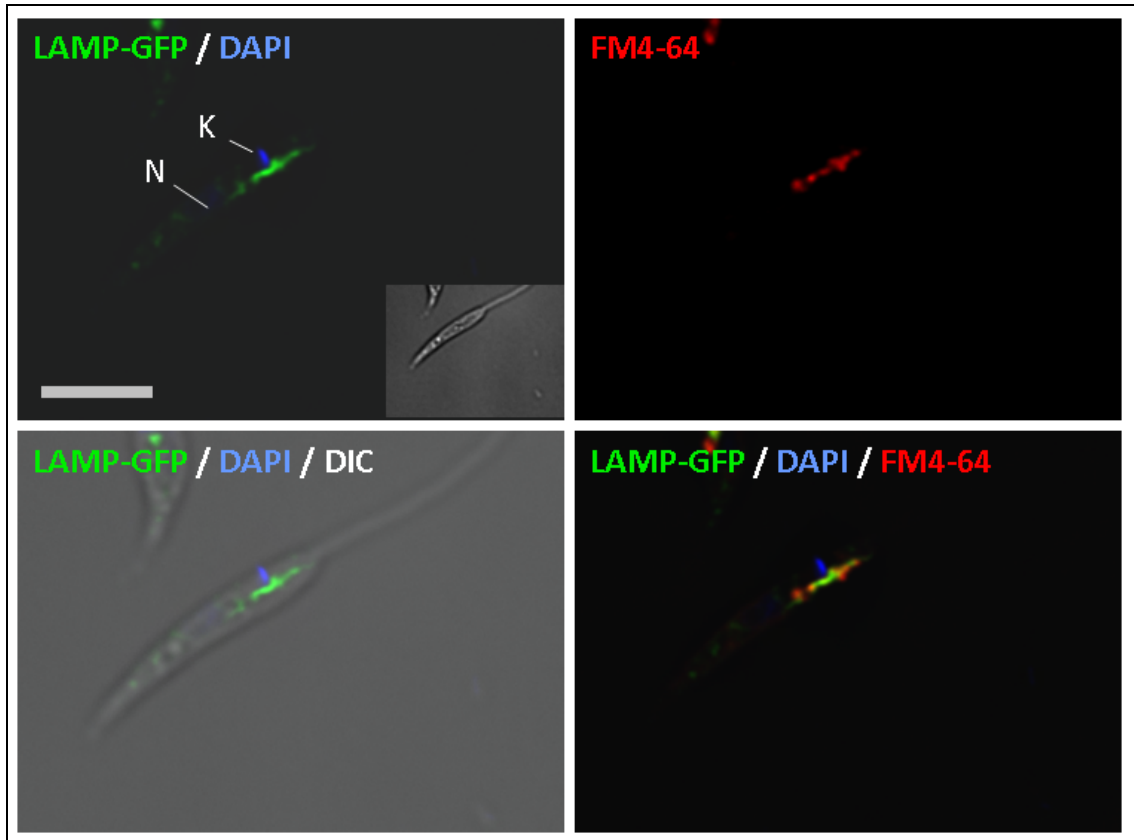


Figure 5-10: Live cell deconvolution fluorescence microscopy images of *L. major* expressing GFP-tagged full-length LMP protein (LmjF30.2670). Top left panel: GFP signal pattern. DIC image of cell shown as inset. Kinetoplast (K) and nucleus (N) stained blue with DAPI. Scale bar = 10 μm . Lower left panel: GFP and DAPI signals merged with DIC image to give outline of the cell. Top right panel: FM4-64 staining (~45 mins) of flagellar pocket and endosomes. Lower right panel: Merged image of GFP, DAPI and FM4-64 signal patterns.

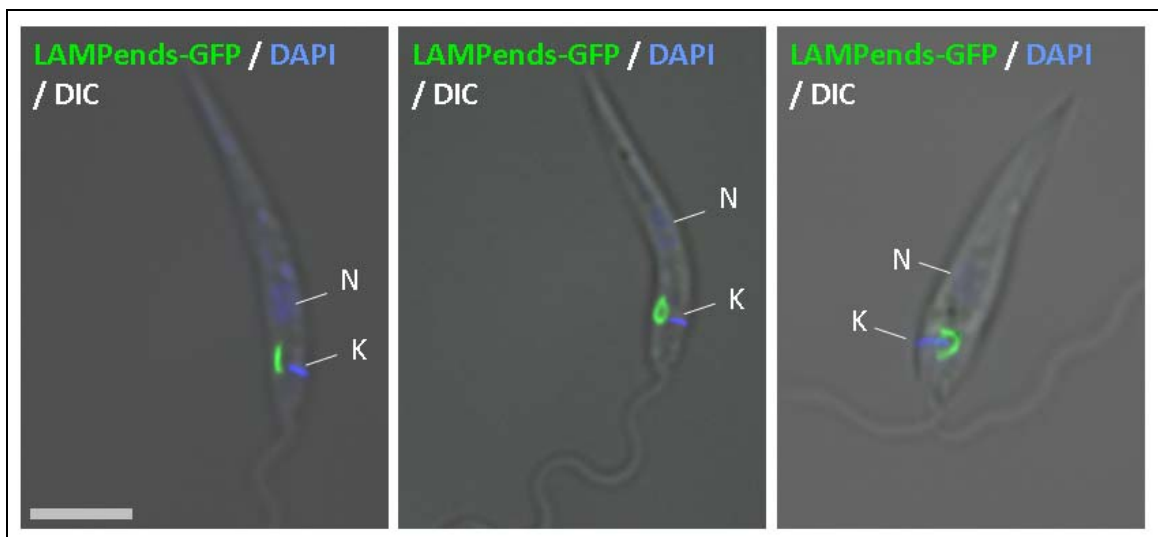


Figure 5-11: Live cell deconvolution fluorescence microscopy images of *L. major* expressing the "LAMPends" fusion protein (GFP between the C- and N-terminus of LMP (LmjF30.2670)), with three different GFP patterns observed. All images showing kinetoplast (K) and nucleus (N) stained blue with DAPI. Scale bar = 10 μm .

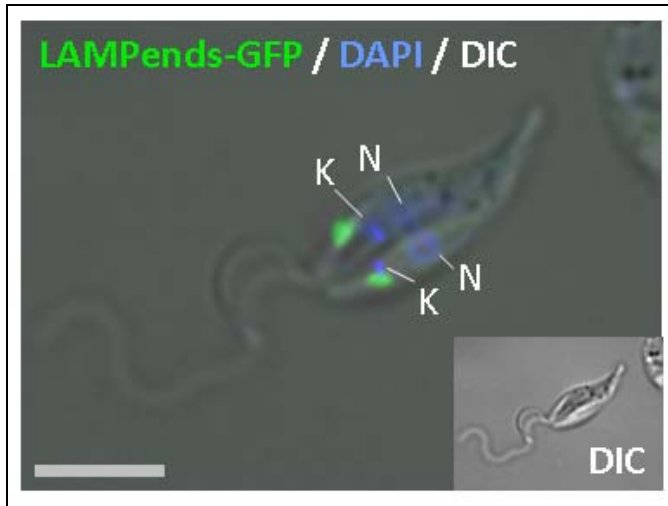


Figure 5-12: Live cell deconvolution fluorescence microscopy image of dividing *L. major* cell expressing the "LAMPends" fusion protein (GFP between the C- and N-terminus of LMP (LmjF30.2670)). Kinetoplasts (K) and nuclei (N) stained blue with DAPI. DIC image of cell shown as inset. Scale bar = 10 μ m.

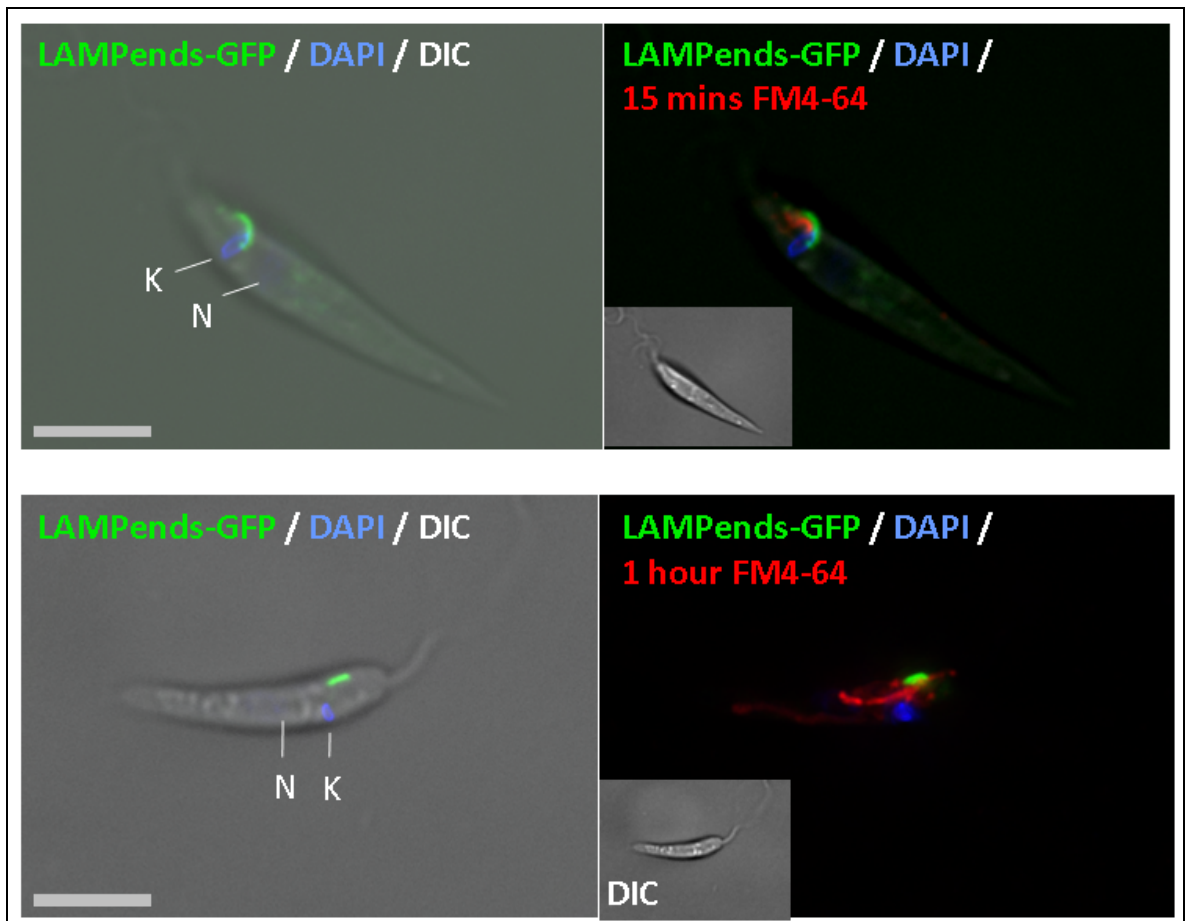


Figure 5-13: Live cell deconvolution fluorescence microscopy images of *L. major* expressing the "LAMPends" fusion protein (GFP between the C- and N-terminus of LMP (LmjF30.2670)). Left images: GFP signal and kinetoplast (K) and nucleus (N) stained blue with DAPI. Merged with DIC image to show outline of cell. Scale bar = 10 μ m. Right images: FM4-64 staining (top panel: 15 mins, bottom panel: 1 hour) of endo-/lysosomal system, as well as GFP and DAPI signals. DIC images of cells shown as inset.

The LAMPends GFP fusion protein was additionally co-localised with the red fluorescent surface marker HASPB-mCherry (as described in section 4.2.2 for Bem46). This experiment showed that the GFP-labelled structure was separate from the cell membrane. It could be observed that the GFP-labelled structure appeared to replicate during cell division (Fig 5-14).

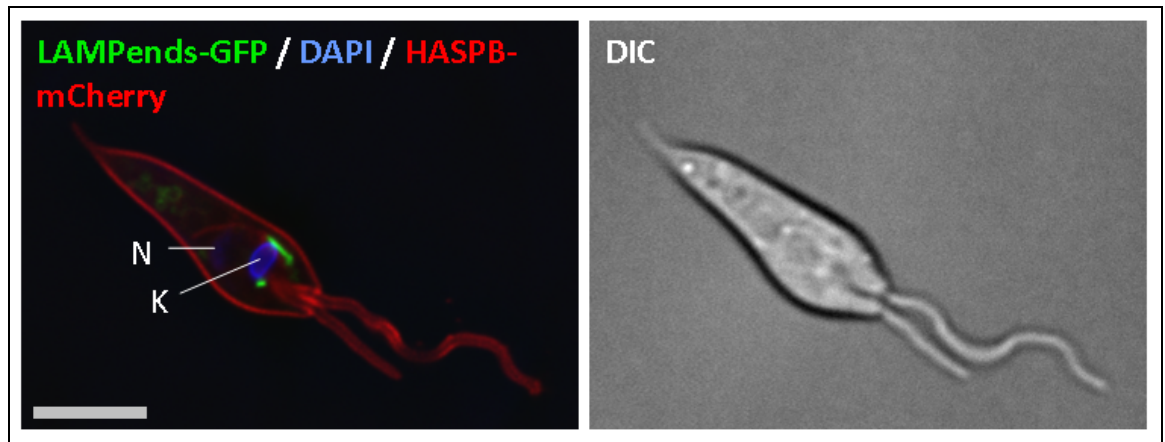


Figure 5-14: Live cell deconvolution fluorescence microscopy image of *L. major* co-expressing the "LAMPends" fusion protein (GFP between the C- and N-terminus of LMP (LmjF30.2670)) and a red fluorescent HASPB-mCherry fusion protein labelling the cell surface. Left panel: Merged image of GFP signal, kinetoplast (K) and nucleus (N) stained blue with DAPI and surface labelled with mCherry. Scale bar = 10 μ m. Right panel: DIC image of cell.

5.2.3.2 GFP fusion protein expression in $\Delta ap3\delta$ cells

The two GFP fusion proteins were also expressed in $\Delta ap3\delta$ cells, to investigate whether the absence of the adaptor complex AP3 affects the trafficking and localisation of the LMP protein. Expression in $\Delta ap3\delta$ resulted in the same fluorescence patterns as in wild type *L. major*. There was no detectable difference between the cell lines, either with the full length GFP-tagged LMP (Fig. 5-15), or with the LAMPends fusion protein (Fig. 5-16).

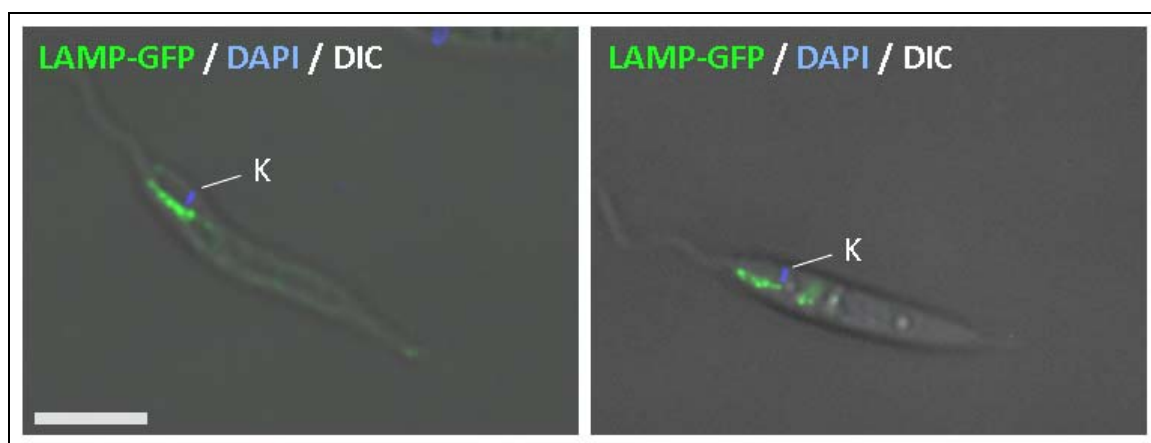


Figure 5-15: Live cell deconvolution fluorescence microscopy images of *L. major* $\Delta ap3\delta$ cells expressing GFP-tagged full-length LMP (LmjF30.2670). GFP and DAPI signals merged with DIC image to give outline of the cell. Kinetoplast (K) stained blue with DAPI. Scale bar = 10 μ m.

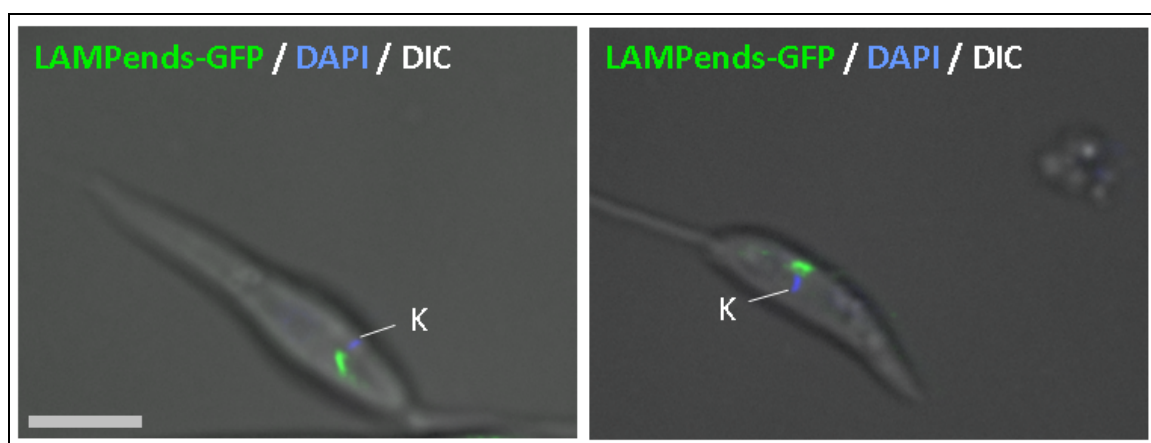


Figure 5-16: Live cell deconvolution fluorescence microscopy images of *L. major* $\Delta ap3\delta$ cells expressing GFP-tagged “LAMPends” fusion protein. GFP and DAPI signals merged with DIC image to give outline of the cell. Kinetoplast (K) stained blue with DAPI. Scale bar = 10 μ m.

5.2.4 Mutagenesis of tyrosine motifs

The LMP protein contains two canonical tyrosine motifs near its C-terminus, tyrosine site I ($^{314}\text{YYVL}^{317}$) and site II ($^{357}\text{YNSL}^{360}$) (Fig. 5-7 and 5-9), which may be involved in trafficking of the protein, possibly by AP3. The tyrosine residue of each site was changed into alanine by site-directed mutagenesis of the "LAMPends" GFP fusion plasmid pGL1683. Both tyrosine sites were mutated separately, resulting in plasmid pGL1957 with tyrosine site I mutated and pGL1958 with site II mutated. The plasmids were transfected into *L. major* wild type cells as before and transfectants analysed by fluorescence microscopy. The tyrosine mutant cell lines did not differ from the wild type fusion protein expressing lines, the fluorescence pattern observed was very similar.

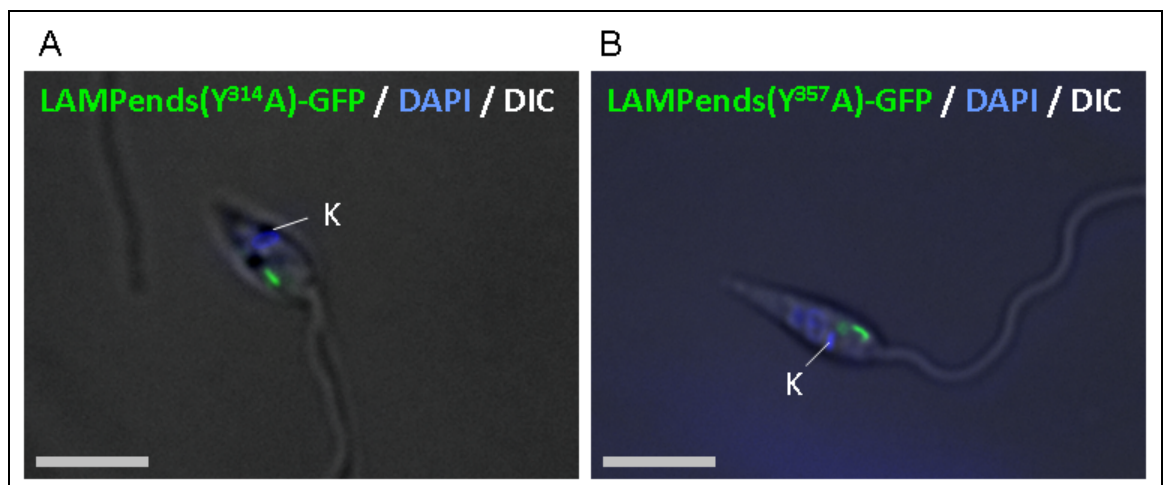


Figure 5-17: Live cell deconvolution fluorescence microscopy images of *L. major* wild type cells expressing GFP-tagged "LAMPends" fusion protein with C-terminal tyrosine motifs mutated. (A) Tyrosine site I ($^{314}\text{YYVL}^{317}$) mutated, with Y^{314} changed to alanine. (B) Tyrosine site II ($^{357}\text{YNSL}^{360}$) mutated, with Y^{357} changed to alanine. GFP and DAPI signals merged with DIC image to give outline of the cell. Kinetoplast (K) stained blue with DAPI. Scale bar = 10 μm .

5.2.5 Deletion of *LAMP*-like gene in *L. major*

L. major cell lines deficient in LMP protein (Δlmp) were generated by deleting both alleles of the wild type gene locus and replacing them with the antibiotic resistance marker cassettes for hygromycin and bleomycin. The initial round of transfections was carried out with both hygromycin and bleomycin resistance marker plasmids separately, yielding heterozygous cell lines resistant to the respective antibiotic. These were subsequently transfected again, to add the other antibiotic marker, in replacement of the second allele of the *LMP* gene. Twelve doubly resistant parasite cell lines were obtained after cloning out transfectants under antibiotic pressure. They were analysed for correct *LMP* gene deletion by PCR and Southern blot analysis. Four cell lines (BH3, BH4, HB1 and HB4, whereby names relate to the order in which the bleomycin or hygromycin cassettes were integrated) did not show a PCR product for the wild type *LMP* gene (1.1 kb), but products of the correct sizes for the integrated hygromycin (1.5 kb) and bleomycin (2.3 kb) resistance cassettes (Fig. 5-19 and Fig. 5-18 for strategy). All four cell lines could subsequently be confirmed to be Δlmp null mutants, by Southern blot probing for the 5' flanking region of the gene locus after digesting whole genomic DNA with *Hind*III and *Not*I. The four cell lines showed integration of both antibiotic resistance cassettes (fragment sizes were 6 kb for hygromycin integration and 5.3 kb for Bleomycin integration), but no wild type alleles (fragment size 3.5 kb) (Fig. 5-21 and Fig. 5-20 for strategy).

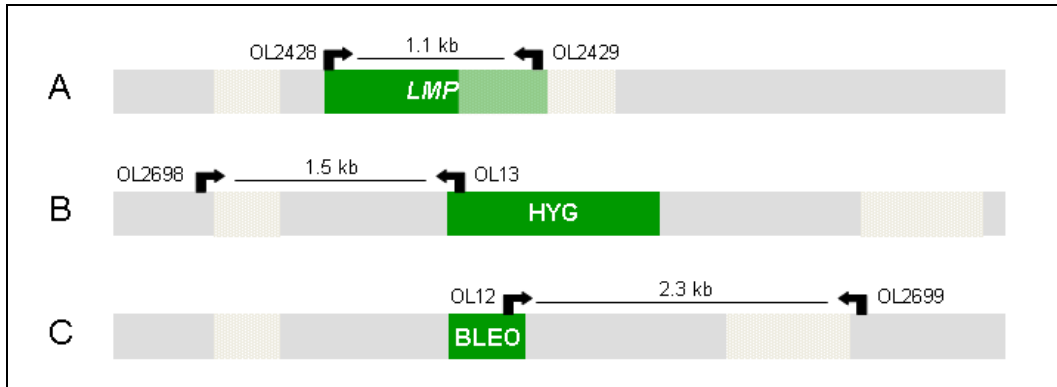


Figure 5-18: Strategy for PCR analysis of potential Δlmp clones. (A) *LMP* gene locus. (B) Hygromycin cassette integrated in *LMP*. (C) Bleomycin cassette integrated in *LMP*. Green: open reading frames; light grey: surrounding DNA sequence; dark grey: 5' and 3' gene deletion flanks (overlapping with wild type allele in A); arrows: primer binding sites, annotated with PCR product size and OL primer numbers.

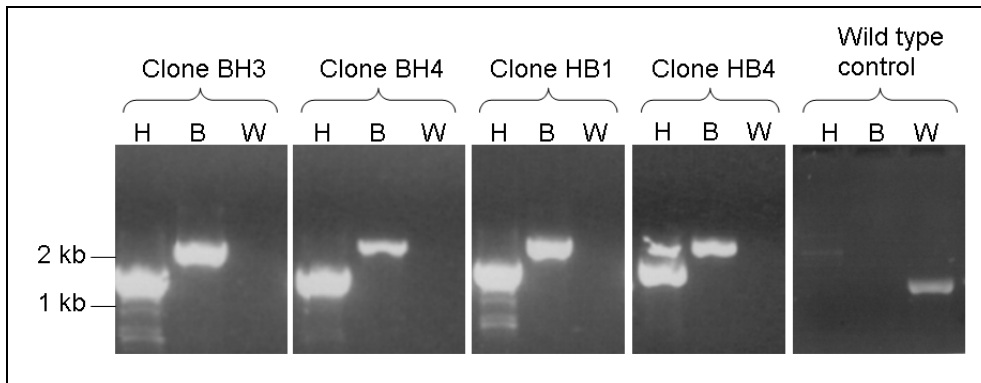


Figure 5-19: PCR analysis of potential Δlmp clones BH3, BH4, HB1 and HB4 and a wild type DNA control. H: PCR targeting hygromycin cassette using primers OL2698 and OL13 (product size 1.5 kb); B: PCR targeting bleomycin cassette using primers OL12 and OL2699 (product size 2.3 kb); W: PCR targeting *LMP* gene using primers OL2428 and OL2429 (product size 1.1 kb).



Figure 5-20: Strategy for Southern blot to be probed with 5' flank fluorescent probe (red box). (A) *LMP* gene locus, *HindIII* / *NotI* digest results in 3.5 kb product. (B) Hygromycin cassette in *LMP*, *HindIII* / *NotI* digest results in 6 kb product. (C) Bleomycin cassette in *LMP*, *HindIII* / *NotI* digest results in 5.3 kb product.

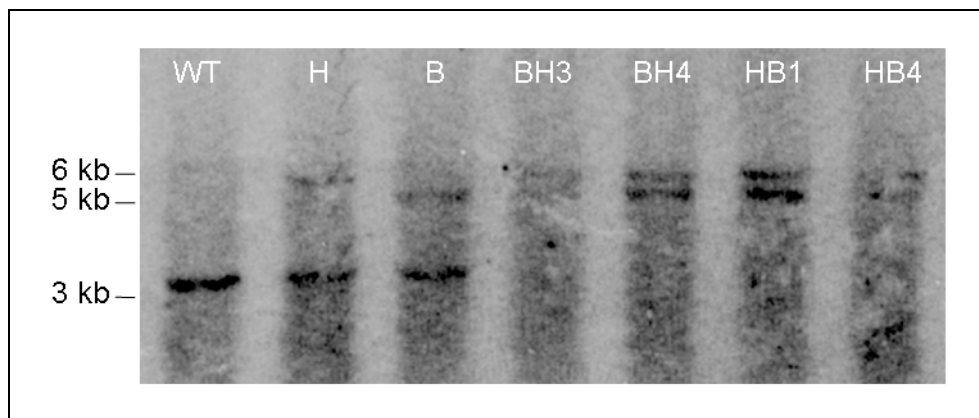


Figure 5-21: Southern blot analysis of Δlmp clones BH3, BH4, HB1 and HB4 as well as *L. major* DNA (WT) as control and both hygromycin (H) and bleomycin (B) heterozygous cell lines. Blot probed for the 5' flanking region of the gene locus after digest with *HindIII* and *NotI*. *L. major* locus fragment size 3.5 kb. Bleomycin cassette integration site fragment size 5.3 kb. Hygromycin cassette integration site fragment size 6 kb.

To elucidate the role of the *L. major* LMP protein in more detail, the Δlmp cell line BH3 was phenotypically analysed by assessing population growth *in vitro*, mouse footpad infectivity and lesion development. Promastigote growth was assessed in culture, by measuring population densities daily for 9 days. The Δlmp cell line grew at a normal rate in promastigote culture, similar to the wild type (Fig. 5-22). Unpaired t-tests showed no significant differences between the two cell lines, with all p-values above 0.3.

BALB/c mice were inoculated with Δlmp and wild type cells and footpad lesion development was monitored over a four week period. Unpaired t-tests showed a significantly slower lesion development in Δlmp -infected mice from week 2 onwards, in comparison to the wild type infection (p-values < 0.02) (Fig. 5-23).

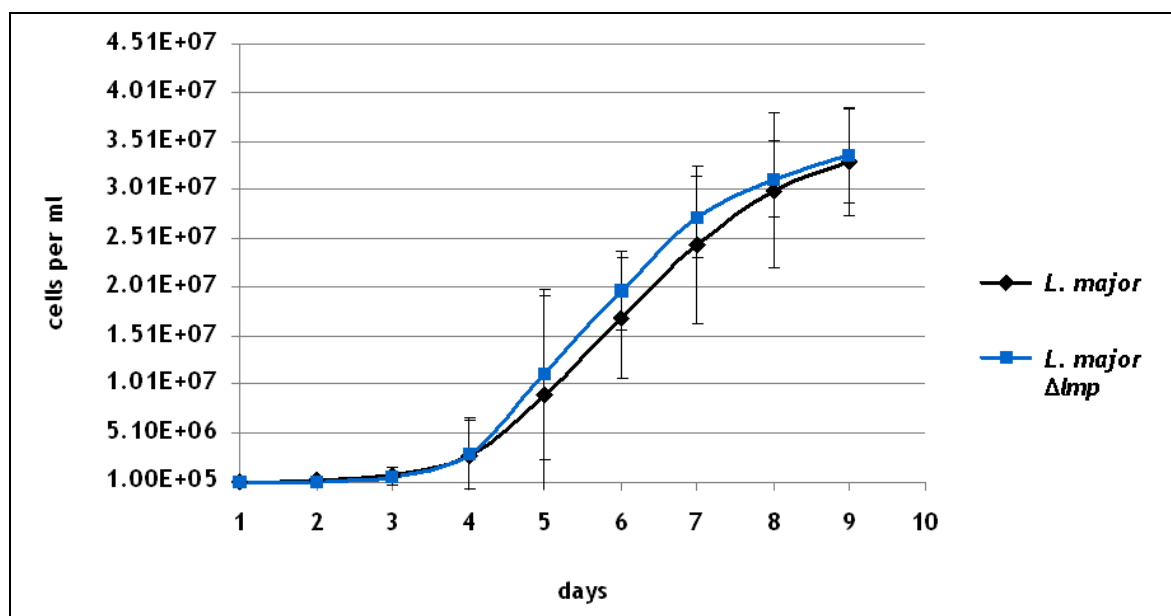


Figure 5-22: *In vitro* growth curve of promastigote cultures of wild type *L. major* and Δlmp cells. Daily cell counts, experiments done in triplicates. Error bars show +/- standard deviation of the mean.

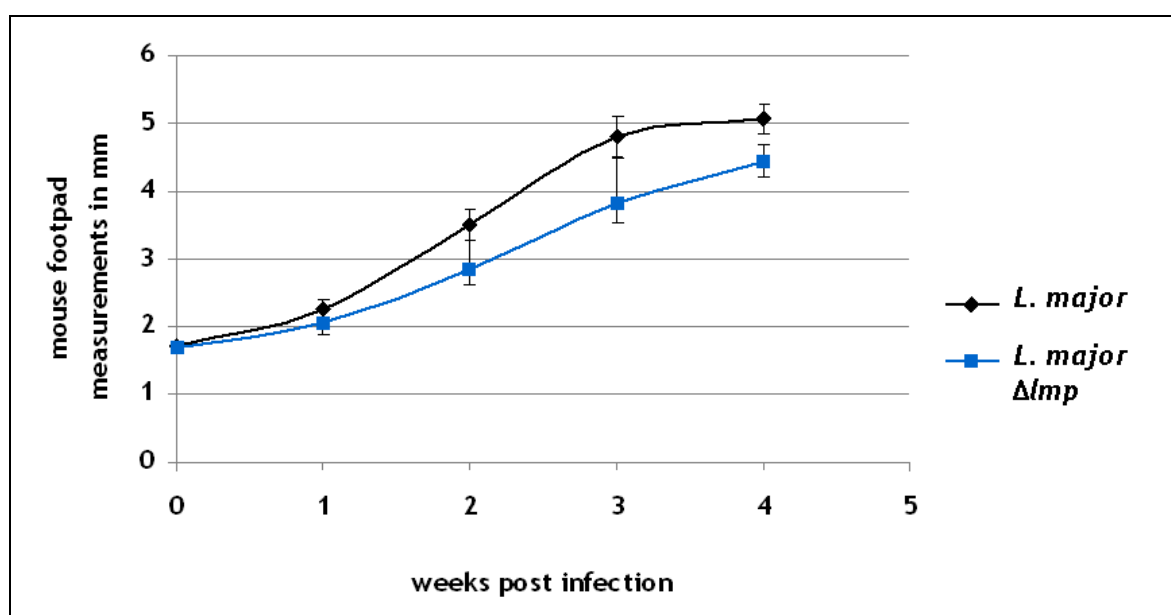


Figure 5-23: Measurements of footpad lesion development of BALB/c mice after infection with wild type *L. major* and Δlmp cells. Weekly measurements of footpad swelling in mm. Measurements of six mice per cell line. Error bars show +/- standard deviation of the mean.

5.3 Results: The *L. major* acidocalcisomal V-H⁺-PPase

5.3.1 Cloning and GFP labelling of V-H⁺-PPase

In order to investigate the intracellular localisation and function of the *L. major* acidocalcisomal V-H⁺-PPase (GeneDB gene ID LmjF31.1220), the full-length gene was cloned and fused to GFP at its 5' end using the pNUS-GFPcN vector, resulting in the plasmid pGL1681. This construct was transfected into *L. major* wild type and $\Delta ap3\delta$ cells and expressed extrachromosomally.

5.3.2 Fluorescence microscopy

The cell lines transfected with the GFP fusion plasmids were analysed by fluorescence microscopy. The GFP fusion protein was observed to localise to punctate structures in wild type cells. Co-localisation experiments with the acidocalcisome-labelling LysoTracker stain showed that the punctate structures were acidocalcisomes (Fig. 5-24). In *Leishmania*, LysoTracker has been found to preferentially stain acidocalcisomes rather than lysosomes, suggesting that the *Leishmania* lysosome is less acidic than the acidocalcisomes (Mullin et al., 2001h; Ghedin et al., 2001a). In contrast to the wild type results, the $\Delta ap3\delta$ cell line showed a consistent loss of all visible green fluorescence (Fig. 5-25).

These fluorescence microscopy experiments were carried out to confirm previous experiments using a specific antibody against the V-H⁺-PPase, which showed punctate structures of a highly similar size and distribution in the cell to those observed here (Besteiro et al., 2008h).

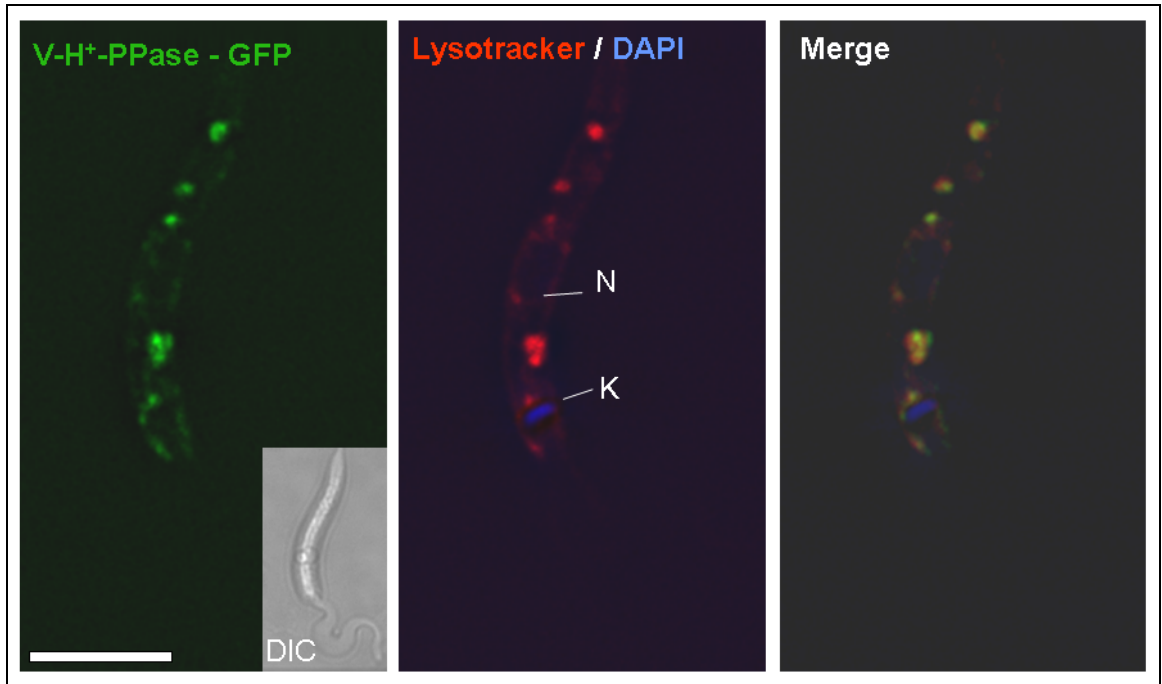


Figure 5-24: Live cell deconvolution fluorescence microscopy images of *L. major* expressing GFP-tagged V-H⁺-PPase (LmjF31.1220). Left panel: Punctate pattern of GFP signal, DIC image of cell shown as inset, scale bar = 10 μ m. Middle panel: LysoTracker staining the punctate acidocalcisomes; kinetoplast (K) and nucleus (N) stained blue with DAPI. Right panel: Merged image of DAPI and co-localising GFP and LysoTracker patterns.

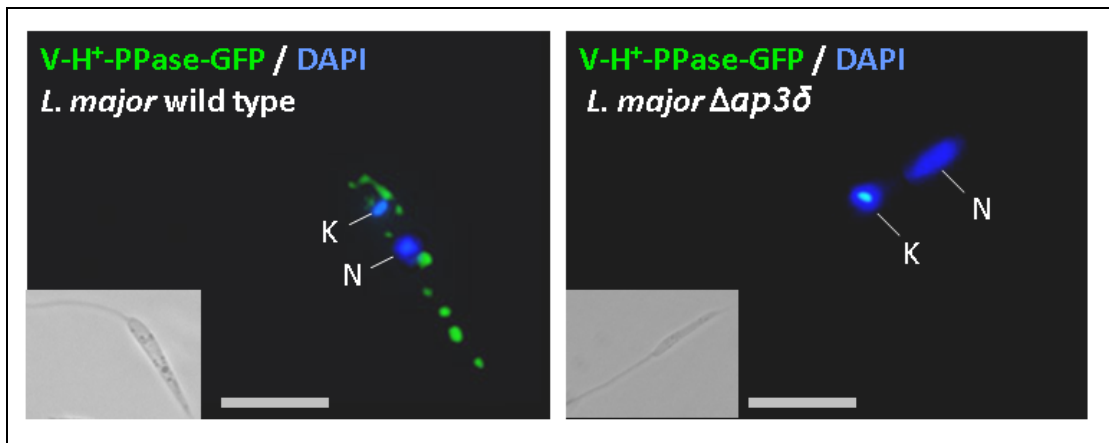


Figure 5-25: Live cell deconvolution fluorescence microscopy images of *L. major* wild type and $\Delta ap3\delta$ mutant cell lines, expressing GFP-tagged V-H⁺-PPase (LmjF31.1220). Left panel: Wild type cell line showing punctate pattern of GFP signal. Right panel: $\Delta ap3\delta$ mutant cell line showing no detectable GFP signal. DIC images of cells shown as inset. Kinetoplast (K) and nucleus (N) stained blue with DAPI. Scale bar = 10 μ m.

5.3.3 Mutagenesis of tyrosine motifs

Two of the tyrosine motifs found in the V-H⁺-PPase sequence (Fig. 5-3), tyrosine site III (⁴⁶⁷YRPV⁴⁷⁰) and site IV (⁵³⁹YGPI⁵⁴²) were mutated by site-directed mutagenesis, to investigate whether they play a role in the trafficking of newly synthesised V-H⁺-PPase to the acidocalcisomes. The mutageneses were performed on the GFP fusion plasmid (pGL1681), changing the respective tyrosine residues to alanine. Both tyrosine sites were mutated separately as well as together, resulting in the plasmids pGL1702 (Y⁴⁶⁷A, mutated tyrosine site III), pGL1703 (Y⁵³⁹A, mutated site IV) and pGL1704 (both sites mutated).

The plasmids were transfected into *L. major* wild type cells as before. Fluorescence microscopy showed that neither the single nor the double tyrosine mutation had a visible impact on the trafficking of the V-H⁺-PPase to the acidocalcisomes. The punctate acidocalcisomal GFP pattern was observed in all three mutant cell lines, with no detectable difference from the wild type fusion protein (Fig. 5-26).

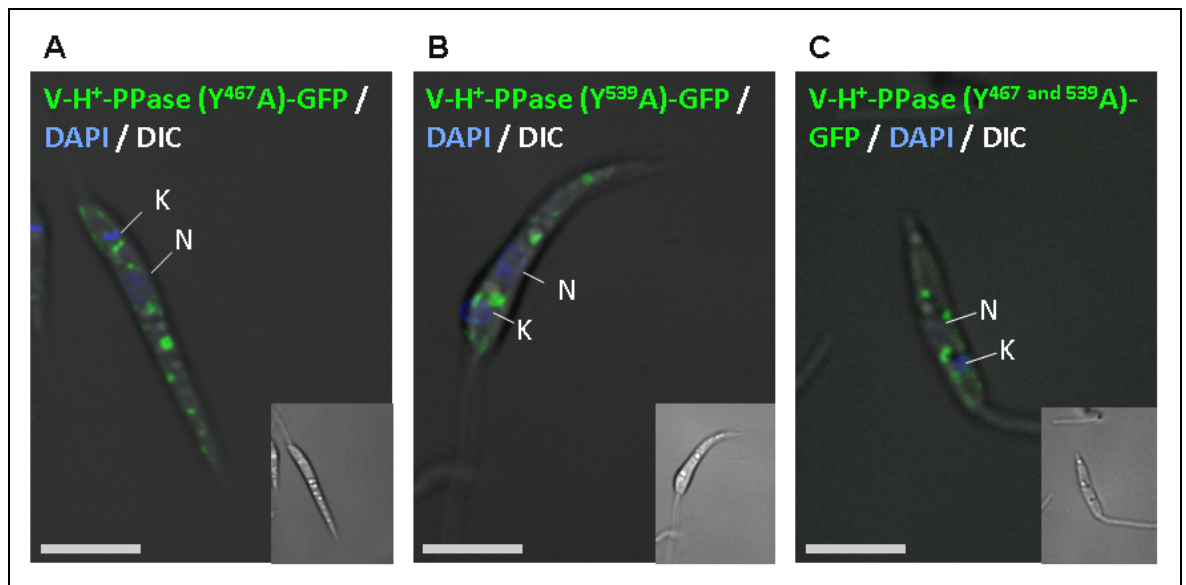


Figure 5-26: Live cell deconvolution fluorescence microscopy images of *L. major* expressing GFP-tagged V-H⁺-PPase (LmjF31.1220) with mutated tyrosine sites. (A) Tyrosine site III (⁴⁶⁷YRPV⁴⁷⁰) mutated, with Y⁴⁶⁷ changed to alanine. (B) Tyrosine site IV (⁵³⁹YGPI⁵⁴²) mutated, with Y⁵³⁹ changed to alanine. (C) Double mutant with both tyrosine site III and IV mutated. GFP and DAPI signals merged with DIC image to give outline of the cell, DIC images of cells shown as insets. Kinetoplast (K) and nucleus (N) stained blue with DAPI. Scale bar = 10 μ m.

5.3.4 Confirmation of GFP expression in all V-H⁺-PPase cell lines

To confirm that all V-H⁺-PPase-GFP cell lines were indeed expressing GFP, whether it was detectable by fluorescence microscopy or not (as observed in $\Delta ap3\delta$ cells), RT (reverse transcriptase)-PCRs targeting the GFP-fusion gene were performed. For this, RNA was isolated from the following cell lines: *L. major* wild type; wild type and $\Delta ap3\delta$ expressing V-H⁺-PPase-GFP; wild type expressing V-H⁺-PPase-GFP(Y⁴⁶⁷A) and V-H⁺-PPase-GFP(Y⁵³⁹A). cDNA was prepared from the RNA samples, including controls without Reverse Transcriptase (“-RT”). Using the cDNA as the template, primers binding within the GFP cassette (OL2639 and OL2640) were used to PCR-amplify a 500 bp part of GFP. All cDNA samples except the wild type gave the expected 500 bp PCR product, while the “-RT” controls did not (Fig. 5-27). This confirmed that GFP mRNA was present in all cell lines and that the GFP fusion genes were being transcribed.

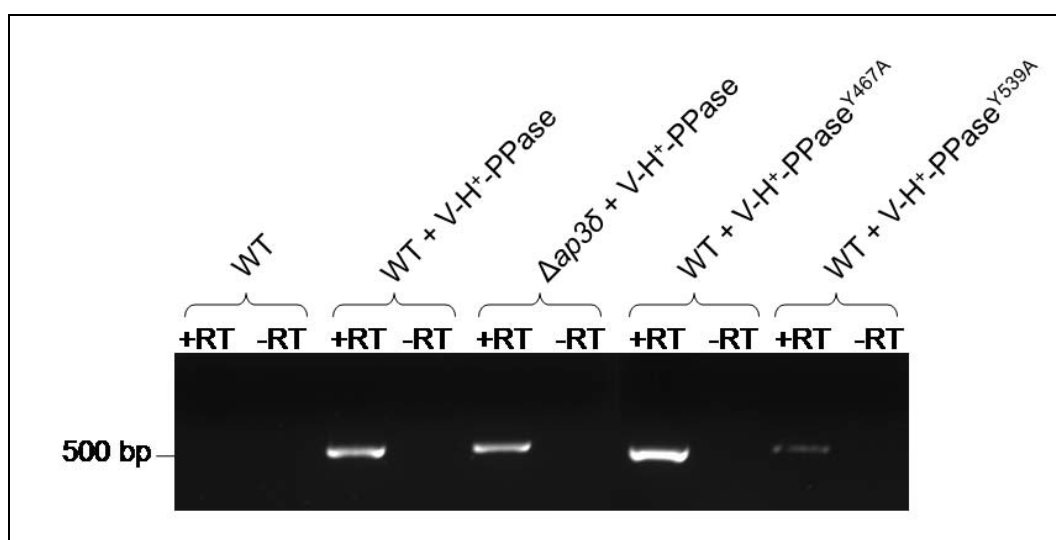


Figure 5-27: Agarose gel of RT-PCR products of GFP cDNA from wild type (WT) and $\Delta ap3\delta$ cells expressing GFP-tagged V-H⁺-PPase (wild type V-H⁺-PPase or with mutated tyrosine sites), to confirm translation of GFP cassette into mRNA. “+RT”: cDNA samples. “-RT”: control samples not treated with reverse transcriptase. WT: wild type DNA as control.

5.4 Discussion

5.4.1 The LAMP-like protein (LMP)

The *Leishmania* LMP protein that was identified after a genome database search does not appear to have a lysosome-associated localisation after all. Its predicted structure suggested a similarity to the mammalian LAMPs and also the trypanosome LAMP-like protein p67, although the topology prediction softwares used gave varying results. It could not be established *in silico* whether the *L. major* LMP contains one or two transmembrane domains and, if there is only one, at which terminus of the protein. The sequence of LMP and its low number of potential glycosylation sites were considerably different from other LAMP-like proteins. However, the number of glycosylation sites may not be important, as trypanosomatids can form very large glycans from one N-glycosylation site (Atrih *et al.*, 2005).

GFP-labelling experiments showed that the protein did not localise to or close to the lysosome in *L. major*; no co-localisation could be observed with FM4-64-stained endo- or lysosomes. Instead, the GFP fusion protein was observed in the region of the flagellar pocket and the kinetoplast. The two different GFP fusion constructs, a full-length construct and one consisting of the C- and N-terminus of the protein surrounding GFP ("LAMPends"), resulted in different GFP patterns. Both localised to the same area of the cell, just inwards of the flagellar pocket, but the full-length protein gave a more diffuse pattern with no clear shape, in close proximity to the endocytic stain FM4-64 but with no clear overlap with it. The "LAMPends" fusion protein on the other hand could be observed in a very clearly delineated structure next to the kinetoplast. The GFP pattern was observed to take an elongated rod-shape or a doughnut shape in close juxtaposition to the kinetoplast, sometimes even encircling it. These different shapes may solely reflect different perspectives or focal planes of the images, though, and the GFP-labelled compartment may always be circular. A structure of this shape and position has not been described in *Leishmania* so far. In *T. brucei*, the protein BILBO1 takes a very similar doughnut- or horseshoe-like shape, but is localised around the collar of the trypanosome flagellar pocket and functions as a cytoskeletal scaffolding protein involved in flagellar pocket

biosynthesis (Bonhivers *et al.*, 2008). *L. major* LMP bears no homology to BILBO1 and appears to be in a distinctly different position in the cell. The *T. brucei* protein XMAP215, when tagged with YFP, shows a circular fluorescence pattern similar to that of LMP, too. This is a microtubule plus end binding protein and it is thought to define the posterior end of procyclic cells (Vaughan *et al.*, 2009), but details of this work are not published yet.

Because the LAMPends fusion protein was observed in a much more defined and clear-cut structure in the cell than the full-length fusion, it may be a better indicator of the natural localisation of LMP. The C-terminus of LMP may be important for the correct trafficking of the protein or the correct anchoring of it in a membrane, especially as it contains two tyrosine motifs that could be sorting signals. In the full-length GFP fusion protein, the C-terminus may be blocked by the relatively large GFP and this may interfere with the targeting of the protein. Although site-directed mutageneses of the tyrosine sites did not lead to a visible disturbance of LMP protein trafficking, the possibility remains that these sites are important, perhaps in conjunction with other signals. There is, for example, one dileucine site towards the N-terminus of the protein, which may play a role. Alternatively, the tyrosine sites may have some redundancy and only simultaneous deletion of both tyrosine sites may lead to an effect on trafficking. So although the LAMPends protein is missing a large proportion of LMP, its targeting may be more reliable because it still contains both its termini intact and unobstructed.

Tyrosine motifs of lysosomal membrane proteins in other organisms interact with the AP3 adaptor complexes for targeting (Dell'Angelica *et al.*, 1999b). It is thought that the main function of AP3 is the transport of membrane proteins to the lysosome (Nakatsu and Ohno, 2003c), but there is also evidence that AP3 might be involved in targeting proteins to the lysosome-like acidocalcisomes (Besteiro *et al.*, 2008g). The LMP-GFP fusion proteins were expressed in $\Delta ap3\delta$ mutants in addition to wild type cells, to investigate if AP3 is responsible for targeting of LMP. The $\Delta ap3\delta$ cells exhibited the same GFP pattern as the wild type. The localisation studies suggest that LMP is not lysosomal or acidocalcisomal, so AP3 may not be the adaptor complex responsible for LMP trafficking. However, as it appears to be a membrane protein it may still be targeted to its destination by one of the other AP complexes. To my knowledge,

L. major deletion mutants of AP1, -2 and -4 do not currently exist, but it would be interesting to express the LAMPends protein in such cell lines to investigate a possible AP complex interaction. However, there is an avirulent AP1-deficient *L. mexicana* mutant cell line (Gokool, 2003), which may be suitable for expression and further localisation studies of LMP-GFP. AP1 is generally thought to be important for protein traffic between the trans-Golgi network and endosomes as well as the plasma membrane. There is evidence that *Leishmania* AP1 is important for traffic to the lysosome, too (Vince *et al.*, 2008), but its function remains unclear. As LMP appears to localise close to the flagellar pocket and, therefore, close to the endo- and exocytic pathways and the trans-Golgi network, a possible interaction of LMP and AP1 may be worth investigating.

It is worth noting that it is not clear whether LMP is indeed a membrane protein. It may only have one transmembrane domain and it is possible that it is cleaved. Furthermore, the predictions of transmembrane domains are just that, predictions, and a predicted N-terminal transmembrane domain can, in reality, be a signal peptide (Emanuelsson *et al.*, 2007; Lao *et al.*, 2002a). The Phobius algorithm has been trained to distinguish these two domains with more accuracy (Kall *et al.*, 2004d), so its prediction of a highly likely N-terminal signal peptide and only one transmembrane domain towards the C-terminus may be the most reliable. Nevertheless, the possibility remains that the HMMTOP prediction with one transmembrane domain at the N-terminus is the best prediction, that this transmembrane domain is actually a signal peptide and that LMP is soluble.

To investigate whether LMP is membrane-bound, cellular fractionation experiments may be useful. Cytoplasmic and organellar fractions of the cell can be separated by differential centrifugation or digitonin extraction (Coombs *et al.*, 1982; Hide *et al.*, 2008). LMP can then be detected on a Western immunoblot of the fractions, ideally using an LMP-specific antibody. Alternatively, the experiment can be performed with LMP-GFP expressing cells and an anti-GFP antibody.

To confirm the localisation of the native LMP protein, immunofluorescence experiments with specific antibodies could be useful. Thus far, all results were obtained using overexpressed GFP fusion proteins. The observed GFP patterns

were concentrated in small, distinct areas and therefore likely not artefacts. Misfolding, mislocalisation or exaggerated overexpression levels could be expected to cause accumulation of the GFP protein in the cytosol or in the lysosome for degradation. Nevertheless, the GFP data require confirmation by alternative experiments, ideally immunofluorescence or transmission electron microscopy (immuno-TEM) using a specific anti-LMP antibody. Such an antibody was raised against a recombinant LMP protein fragment (the predicted soluble proportion of the protein), but could not be utilised. The affinity-purified antibody cross-reacted with many other proteins, on Western immunoblots of *Leishmania* cell extracts as well as in whole cell immunofluorescence analyses, and was thus not useful for further experiments.

So far, the nature of the subcellular structure that is labelled by the LAMPends-GFP protein could not be determined. It does not appear to be part of the endosomal system and some observations suggest that the structure replicates during cell division. The latter notion could be studied in more detail by immunofluorescence analyses of all promastigote cell cycle stages, to establish at what time during cell division this structure replicates. Co-expression of the LAMPends-GFP protein with the surface-labelling HASPB-mCherry protein showed that the GFP-labelled structure is not directly attached to the cell surface, but appears to lie further inwards. Its position in relation to the kinetoplast appears variable; it can lie closer to the nucleus or closer to the flagellar pocket, and sometimes it appears to encircle the kinetoplast.

The area around the flagellar pocket and the kinetoplast is an area of high activity; the endo- and exocytic pathways converge here, the mitochondrion as well as the Golgi and the ER can extend towards the pocket (Correa et al., 2007; McConville et al., 2002l; Lacomble et al., 2009b), as well as barely known structures like membrane whorls. LMP does not co-localise with the endocytic dye FM4-64 and it is predicted by the Mitoprot algorithm not to be targeted to the mitochondrion (with a low probability of 0.09 for mitochondrial export). Nevertheless, an association with any of these organelles is possible. Alternatively, LMP may localise to a novel structure or a specific type or area of a known compartment. In trypanosomes, specialised “quartet” bundles of microtubules have been found associated with the flagellar pocket (Lacomble et al., 2009a), so it may be interesting to investigate whether the LMP structure is

associated with microtubules in this area. Treatment of cells with a microtubule-disruptor like thioridazine (Ilgoutz *et al.*, 1999; Seebeck and Gehr, 1983) may be useful here, to investigate if this has an effect on the localisation of LMP-GFP.

Deletion of the *LMP* gene did not appear to have a strong impact on viability and general morphology of *L. major*. However, mouse footpad infections with Δlmp progressed significantly slower than wild type infections from week 2 onwards, after an initially normal infection development. So the lack of LMP appears to have some effect on virulence. Further experiments will be necessary to analyse the phenotype of the Δlmp cell line, including macrophage infection assays in comparison to wild type *L. major*. Additionally, transmission electron microscopy of the flagellar pocket area may reveal morphological defects in the Δlmp cells.

5.4.2 The acidocalcisomal V-H⁺-PPase

The investigation of the acidocalcisomal V-H⁺-PPase confirmed and supported previous findings by S. Besteiro (Besteiro *et al.*, 2008f). The GFP-fused V-H⁺-PPase localised to the acidocalcisomes, as shown by co-localisation with the acidocalcisome-staining LysoTracker dye. The same punctate pattern had previously been shown for the native V-H⁺-PPase when detected by specific antibodies in wild type cells (Besteiro *et al.*, 2008e). The pattern was very different for the $\Delta ap3\delta$ cells, where no GFP signal could be detected, although Reverse Transcription PCRs showed that GFP was being expressed at a comparable level to that of wild type cells expressing V-H⁺-PPase-GFP. This, again, corroborates the results from experiments using the V-H⁺-PPase-specific antibody on $\Delta ap3\delta$ cells, which also showed a strong decrease in detection of V-H⁺-PPase and, therefore, intact acidocalcisomes (Besteiro *et al.*, 2008d). This is strong evidence that the *L. major* V-H⁺-PPase is trafficked to the acidocalcisomal membrane through the carrier complex AP3 or another process that depends on AP3. Nevertheless, acidocalcisomes were still present in $\Delta ap3\delta$ cells, suggesting that AP3 is not involved in their biogenesis, but rather supplies these organelles with certain membrane proteins (Besteiro *et al.*, 2008c).

In the $\Delta ap3\delta$ cells, the V-H⁺-PPase is being expressed but does not appear to reach the acidocalcisomes. The fact that it could not be detected when labelled with GFP and only a very small proportion could be detected by immuno-

staining, leaves the question what happens to the V-H⁺-PPase in $\Delta ap3\delta$ cells. It is not merely mislocalised, because it could not be detected elsewhere in the cell. A protein that is expressed but cannot be transported to its destination is most likely rapidly degraded, in the lysosome or in the cytosolic proteasome. Especially the proteasomal degradation machinery of eukaryotic cells has been investigated and it was found that many newly synthesised proteins can be degraded very quickly if they are misfolded or superfluous (Goldberg, 2003a; Schubert et al., 2000). This can take place directly after biosynthesis at the ER, where the ER-associated protein degradation (ERAD) machinery identifies and labels proteins for proteasomal degradation. If the V-H⁺-PPase can not be trafficked away from the ER in AP3-deficient cells, the ERAD pathway may be involved in rapid degradation of this protein. It is thought that kinetoplastids may have an active ERAD pathway, but no details are known (Engstler *et al.*, 2007). Apart from the non-lysosomal degradation at the proteasome, some proteins can alternatively be digested in the lysosome. In trypanosomes, proteins with disrupted targeting signals have been observed to be taken to the lysosome and be degraded there (Triggs and Bangs, 2003).

Studies on the *T. brucei* V-H⁺-PPase showed how this protein is synthesised but not targeted correctly when the SRP (signal recognition particle) machinery for ER import is silenced. In this case, the nascent V-H⁺-PPase is likely degraded before entering the ER and this degradation appears to be neither lysosomal nor proteasomal, but dependent on an unknown, possibly ER membrane-associated mechanism (Lustig *et al.*, 2007). In the *L. major* experiments presented here, the situation appears different and the *L. major* V-H⁺-PPase is likely to enter the ER and be mistargeted or degraded at a later stage, where the lysosome or proteasome could indeed play a role again.

To elucidate the fate of the V-H⁺-PPase in $\Delta ap3\delta$ cells, future experiments could involve treating the cells with inhibitors of lysosomal peptidases, like K11777 (Mahmoudzadeh-Niknam and McKerrow, 2004) or proteasome inhibitors like lactacystin (Fenteany *et al.*, 1995) or MG132 (Robertson, 1999a). Ideally, such inhibitors will stop or delay degradation of the GFP-labelled V-H⁺-PPase, allowing its detection in the lysosome or, if it is targeted to the proteasome, in the cytosol.

The V-H⁺-PPase has several tyrosine-based motifs that could serve as interaction sites for AP3 (Ohno et al., 1998e). To elucidate this, the two tyrosine sites (III and IV) that were predicted to be most exposed in the cytosol, as well as being conserved among kinetoplastids, were mutated individually as well as simultaneously. None of these manipulations led to consistent changes in the GFP distribution in wild type cells expressing the GFP-labelled V-H⁺-PPase with the respective mutations. This suggests that the tyrosine sites III and IV are not or not solely responsible for interacting with AP3. The other tyrosine sites, or indeed altogether different motifs like a dileucine site, may be important for AP3 binding. Alternatively, the V-H⁺-PPase may not bind directly to AP3 itself, or other carrier complexes take over the function of AP3 when it is absent from the cell. A yeast-two-hybrid assay may help to elucidate whether AP3 and the V-H⁺-PPase are binding partners.

6. Final Conclusions

Intracellular protein trafficking is important for virulence of *Leishmania*. The exo- and endocytic pathways, which converge in the flagellar pocket area, allow secretion of virulence factors as well as the uptake of host components into the parasite for lysosomal degradation (de Souza et al., 2009; McConville et al., 2002m). Additionally, the lysosome is also crucial for *Leishmania* protein turnover and, therefore, cellular remodelling and adaptation to different host organisms. As the flagellar pocket is the sole site of endo- and exocytosis in kinetoplastids, the area around this pocket is of particular importance for the trafficking of potential virulence factor proteins. The aims of the study presented here were the identification of a potentially secreted *L. major* peptidase that may act as a virulence factor, as well as the identification of an *L. major* lysosomal membrane protein and the elucidation of AP3-dependent protein trafficking to the lysosome and the lysosome-like acidocalcisomes.

For the identification of both the potentially secreted peptidases and the potential lysosomal membrane protein, a bioinformatics approach was taken and candidate proteins were chosen based on predictions of protein properties and targeting signals. These predictions proved not very reliable. There were discrepancies between results from different algorithms and the experimental localisations of the proteins only partially agreed with the predictions. The rhomboid peptidase LmjF02.0430, for example, localised to the mitochondrion despite all employed algorithms predicting a secretory signal and a very low probability of mitochondrial import. Furthermore, different transmembrane topology prediction programmes sometimes yielded differing predictions, like for Bem46, which was calculated to have from one to three transmembrane domains, depending on the algorithm used.

The prediction programmes were developed either for proteins from a very broad spectrum of organisms or trained on mammalian / higher eukaryote proteins. Thus, predicting protein properties for an ancient and divergent eukaryote like *Leishmania* was unreliable with these programmes and

predictions had to be treated with care. It is likely that *Leishmania* has retained or developed kinetoplastid-specific protein targeting signals and pathways, in addition to or instead of those found in mammalian cells (Marin-Villa *et al.*, 2008; Silverman *et al.*, 2008). In fact, an analysis of the *L. donovani* secreted / released proteins (the “secretome”) revealed that only two of 151 apparently secreted proteins (a putative beta-fructofuranosidase and a putative eukaryotic translation initiation factor 3 subunit) carried a classical N-terminal secretory signal peptide (Silverman *et al.*, 2008); Silverman and colleagues combined a mass spectrometry analysis of *L. donovani* culture supernatants with a bioinformatics screen of the *L. major* genome database and the two resulting sets of proteins showed no overlap except for the two proteins mentioned above. Silverman *et al* identified only 50 proteins with a known classical eukaryotic secretion signal by bioinformatics analyses, whilst ruling out proteins with multiple transmembrane domains. Of the candidate peptidases analysed in the study presented here, only Bem46 and the serine carboxypeptidase LmjF18.0450 were identified in the bioinformatics screen by Silverman *et al.* The lack of overlap between the *in vitro* and *in silico* approaches appears too striking to be explained by very conservative experimental thresholds or the differences between the *L. major* and *L. donovani* genomes (Silverman *et al.*, 2008). Another, recent publication by Cuervo and colleagues (2009) analysed the secretome of *L. braziliensis*, using 2D electrophoresis and mass spectrometry on culture supernatants, as well as subsequently analysing the identified proteins for secretory signals by bioinformatics. 35 different proteins were found to be secreted / released by *L. braziliensis*, only three of which contained a classical N-terminal secretion signal (a protein disulfide isomerase, an elongation factor 1-beta and a mitochondrial precursor of a HSP70-related protein 1) (Cuervo *et al.*, 2009b).

None of the *L. major* peptidases analysed in the work presented here were found in either the *L. donovani* or the *L. braziliensis* supernatant secretomes, despite the fact that at least Silverman *et al* found an abundance of peptidases and proteolysis-related proteins to be secreted, including the family S9 oligopeptidase B (OPB) (Silverman *et al.*, 2008). Thus, bioinformatics analyses of classical secretion signals may not be particularly useful for *Leishmania*, a notion that was corroborated by the partially unreliable prediction results obtained in

the study presented here. It appears that alternative mechanisms to classical secretion, for example secretion through microvesicles or exosome-like blebs, are important in *Leishmania*. This is supported by the findings that some of the *L. donovani* secreted proteins are orthologues of proteins secreted in microvesicles by higher eukaryotic cells and that small vesicle-like blebs have been observed in the area of the *L. donovani* promastigote flagellar pocket as well as on the surface of amastigotes (Silverman *et al.*, 2008). From the results obtained in the study presented here, the conclusion that *Leishmania* secretory pathways seem to differ from those of higher eukaryotes may be extended to other trafficking signals and pathways, like mitochondrial targeting peptides. These could not be predicted reliably for *Leishmania* proteins either and may also differ from classical eukaryotic mechanisms. Such specialisations are of particular interest, as kinetoplastid-specific pathways and protein functions can be useful drug targets.

Of the eight candidate peptidases that were predicted to be secreted and subsequently tagged with GFP for localisation studies, only one, the Bem46 serine peptidase, accumulated in the flagellar pocket. Deletion of Bem46 did not affect promastigote growth or infectivity in mice significantly, but it is possible that other peptidases compensated for the loss of Bem46 or that the effect was too subtle to be detected thus far. However, Bem46 appears not to be a major virulence factor and further investigations will help to elucidate its function as well as clarify whether it is released. As the bioinformatics predictions of transmembrane domains appear to favour a model of one transmembrane domain at the N-terminus of Bem46, it may be anchored in the flagellar pocket membrane and not released. This conclusion is supported by the fact that Bem46 was not found in *Leishmania* secretome analyses so far (Silverman *et al.*, 2008; Cuervo *et al.*, 2009a). Thus, Bem46 may be a resident protein of the *Leishmania* flagellar pocket.

A bioinformatics approach was also taken to try and identify a membrane protein of the *Leishmania* lysosome, which would be a useful marker for an in depth investigation of this important organelle. For this, the *L. major* genome was screened for proteins with one or two transmembrane domains as well as tyrosine or dileucine motifs that may interact with AP3, a trafficking complex that delivers membrane proteins to the lysosome in other organisms. The

selected candidate protein LMP showed low sequence identity to mammalian lysosome-associated proteins, but structural similarities. The bioinformatics analyses performed on the LMP protein to predict transmembrane domains did not yield consistent results, with different algorithms predicting different topologies. This further supports the notion that generic eukaryotic protein prediction algorithms are of limited usefulness for *Leishmania* proteins. Labelling the N- and C-terminus of LMP protein with GFP showed that it did not localise to the lysosome, but to a small elongated or circular structure close to the kinetoplast, in the flagellar pocket area. As this is an area of particularly high activity with endo- and exocytic pathways converging, a novel compartment or complex here, like the LMP-labelled structure, might be involved in either of these processes and may give insight into previously unknown pathways. It appears unlikely that the LMP structure is part of the endocytic pathway, as it does not co-localise with the endocytic stain FM4-64, but it could be involved in sorting proteins for exocytosis. Another possibility is an association with the mitochondrion in some way, as the LMP structure was always observed close to the kinetoplast, which is incorporated into the *Leishmania* mitochondrion. Further analyses of the phenotype of LMP-deficient *L. major* should shed light on this protein's function. The data presented here show a lag in mouse footpad lesion development after infection with Δlmp parasites, which may be caused by a disturbance in mammalian host cell invasion. Thus, macrophage infection assays may yield useful results. LMP is highly conserved among the kinetoplastids, which suggests a somewhat important function for this protein. Whilst there are no close homologues of LMP in *L. major*, it is possible that a divergent but maybe structurally similar protein compensated for LMP loss in the Δlmp mutant.

The identification of a resident protein of the *Leishmania* lysosomal membrane remains a useful goal for future projects. Such a protein will allow further investigations of the lysosome, an organelle that probably plays an important role in parasite virulence and survival. The previous finding that *Leishmania* lysosomes are intact in AP3-deficient cells (Besteiro et al., 2008b) points to differences in AP3 function or AP3 pathways between *Leishmania* and higher eukaryotes. A lysosomal membrane marker would be very useful in shedding light on AP3 function in *Leishmania*. The protein CLN3 (ceroid lipofuscinosis

neuronal protein 3, also Battenin) is a glycosylated multispanning transmembrane domain of mammalian lysosomal membranes (Nugent *et al.*, 2008; Storch *et al.*, 2004; Phillips *et al.*, 2005; Kyttala *et al.*, 2004) that possibly depends on the AP3 carrier for lysosomal trafficking (Mao *et al.*, 2003; Kyttala *et al.*, 2005). It has an *L. major* homologue with only 15 % sequence identity, but a similar predicted topology with several transmembrane domains. Preliminary GFP-tagging experiments have suggested a lysosomal localisation for the *L. major* CLN3 and this protein may be worth investigating further as a potential lysosomal marker.

For LMP as well as for Bem46 it will be interesting to explore protein localisation as well as the effects of the respective gene deletions in the amastigote life cycle stage, for example by macrophage infection studies. Whilst promastigotes are a relevant study object and virulence factors identified here can play an important role not only in the sand fly infection stage but also in the initial phase of the mammalian infection, amastigotes are the cells that mainly interact with mammalian macrophages and they possibly differ from promastigotes in their secretome to some extent (Silverman *et al.*, 2008).

Finally, the results for the intracellular localisation and AP3 traffic-dependence of the V-H⁺-PPase corroborate previous results and strengthen the notion that AP3 and / or the acidocalcisomes are important for *Leishmania* virulence (Besteiro *et al.*, 2008a). If AP3 directly interacts with the V-H⁺-PPase, further site- directed disruptions of potential binding sites should elucidate this pathway. Furthermore, the fate of the V-H⁺-PPase in AP3-deficient cells remains unclear and it will be interesting to discover how and where it is degraded. It appears unlikely that the mistargeting of the V-H⁺-PPase itself and on its own is responsible for the avirulent phenotype and defective acidocalcisomes observed in AP3-deficient *Leishmania*. Thus, other proteins of the acidocalcisomes will be of interest, too, as well as finding out more about the origin and biosynthesis pathway of acidocalcisomes in general.

8. References

A

- Aguilar, R.C., Boehm, M., Gorshkova, I., Crouch, R.J., Tomita, K., Saito, T., Ohno, H., and Bonifacino, J.S. (2001). Signal-binding specificity of the mu4 subunit of the adaptor protein complex AP-4. *J Biol Chem.* 276, 13145-13152.
- Akopyants, N.S., Kimblin, N., Secundino, N., Patrick, R., Peters, N., Lawyer, P., Dobson, D.E., Beverley, S.M., and Sacks, D.L. (2009). Demonstration of genetic exchange during cyclical development of *Leishmania* in the sand fly vector. *Science* 324, 265-268.
- Alberts, B., Johnson, A., Lewis, J., Raff, M., Roberts, K., and Walter P. (2002). *Molecular Biology of the Cell.* Garland Science).
- Alexander, D.L., Schwartz, K.J., Balber, A.E., and Bangs, J.D. (2002). Developmentally regulated trafficking of the lysosomal membrane protein p67 in *Trypanosoma brucei*. *J Cell Sci* 115, 3253-3263.
- Alexander, J. and Bryson, K. (2005). T helper (h)1/Th2 and *Leishmania*: paradox rather than paradigm. *Immunol. Lett.* 99, 17-23.
- Alexander, J., Coombs, G.H., and Mottram, J.C. (1998). *Leishmania mexicana* cysteine proteinase-deficient mutants have attenuated virulence for mice and potentiate a Th1 response. *J. Immunol.* 161, 6794-6801.
- Alexander, J. and Vickerman, K. (1975). Fusion of host cell secondary lysosomes with the parasitophorous vacuoles of *Leishmania mexicana*-infected macrophages. *J. Protozool.* 22, 502-508.
- Allen, C.L., Liao, D., Chung, W.L., and Field, M.C. (2007). Dileucine signal-dependent and AP-1-independent targeting of a lysosomal glycoprotein in *Trypanosoma brucei*. *Mol Biochem Parasitol.* 156, 175-190.
- Alvar, J., Canavate, C., GutierrezSolar, B., Jimenez, M., Laguna, F., LopezVelez, R., Molina, R., and Moreno, J. (1997). *Leishmania* and human immunodeficiency virus coinfection: The first 10 years. *Clinical Microbiology Reviews* 10, 298-308.
- Antoine, J.C., Lang, T., Prina, E., Courret, N., and Hellio, R. (1999). H-2M molecules, like MHC class II molecules, are targeted to parasitophorous vacuoles of *Leishmania*-infected macrophages and internalized by amastigotes of *L. amazonensis* and *L. mexicana*. *J Cell Sci* 112, 2559-2570.
- Atrih, A., Richardson, J.M., Prescott, A.R., and Ferguson, M.A. (2005). *Trypanosoma brucei* glycoproteins contain novel giant poly-N-acetyllactosamine carbohydrate chains. *J Biol Chem.* 280, 865-871.

Azizi,H., Hassani,K., Taslimi,Y., Najafabadi,H.S., Papadopoulou,B., and Rafati,S. (2009). Searching for virulence factors in the non-pathogenic parasite to humans *Leishmania tarentolae*. *Parasitology* 136, 723-735.

B

Bangs,J.D., Uyetake,L., Brickman,M.J., Balber,A.E., and Boothroyd,J.C. (1993). Molecular cloning and cellular localization of a BiP homologue in *Trypanosoma brucei*. Divergent ER retention signals in a lower eukaryote. *J Cell Sci* 105 (Pt 4), 1101-1113.

Banuls,A.L., Hide,M., and Prugnolle,F. (2007). *Leishmania* and the leishmaniasis: a parasite genetic update and advances in taxonomy, epidemiology and pathogenicity in humans. *Adv. Parasitol.* 64, 1-109.

Barois,N. and Bakke,O. (2005). The adaptor protein AP-4 as a component of the clathrin coat machinery: a morphological study. *Biochem J* 385, 503-510.

Barr,S.D. and Gedamu,L. (2003). Role of peroxidoxins in *Leishmania chagasi* survival. Evidence of an enzymatic defense against nitrosative stress. *J Biol Chem.* 278, 10816-10823.

Bates,P.A. and Dwyer,D.M. (1987). Biosynthesis and Secretion of Acid-Phosphatase by *Leishmania donovani* Promastigotes. *Molecular and Biochemical Parasitology* 26, 289-296.

Bates,P.A., Hermes,I., and Dwyer,D.M. (1989). *Leishmania donovani* - Immunochemical Localization and Secretory Mechanism of Soluble Acid-Phosphatase. *Experimental Parasitology* 68, 335-346.

Bendtsen,J.D., Jensen,L.J., Blom,N., von Heijne,G., and Brunak,S. (2004a). Feature-based prediction of non-classical and leaderless protein secretion. *Protein Eng Des Sel* 17, 349-356.

Bendtsen,J.D., Nielsen,H., von Heijne,G., and Brunak,S. (2004b). Improved prediction of signal peptides: SignalP 3.0. *J Mol Biol* 340, 783-795.

Benzel,I., Weise,F., and Wiese,M. (2000). Deletion of the gene for the membrane-bound acid phosphatase of *Leishmania mexicana*. *Mol Biochem Parasitol.* 111, 77-86.

Berman,J. (2003). Current treatment approaches to leishmaniasis. *Current Opinion in Infectious Diseases* 16, 397-401.

Berriman,M., Ghedin,E., Hertz-Fowler,C., Blandin,G., Renault,H., Bartholomeu,D.C., Lennard,N.J., Caler,E., Hamlin,N.E., Haas,B., Bohme,W., Hannick,L., Aslett,M.A., Shallom,J., Marcello,L., Hou,L.H., Wickstead,B., Alsmark,U.C.M., Arrowsmith,C., Atkin,R.J., Barron,A.J., Bringaud,F., Brooks,K., Carrington,M., Cherevach,I., Chillingworth,T.J., Churcher,C., Clark,L.N., Corton,C.H., Cronin,A., Davies,R.M., Doggett,J., Djikeng,A., Feldblyum,T., Field,M.C., Fraser,A., Goodhead,I., Hance,Z., Harper,D., Harris,B.R., Hauser,H., Hostetter,J., Ivens,A., Jagels,K., Johnson,D., Johnson,J., Jones,K.,

Kerhornou,A.X., Koo,H., Larke,N., Landfear,S., Larkin,C., Leech,V., Line,A., Lord,A., MacLeod,A., Mooney,P.J., Moule,S., Martin,D.M.A., Morgan,G.W., Mungall,K., Norbertczak,H., Ormond,D., Pai,G., Peacock,C.S., Peterson,J., Quail,M.A., Rabbinowitsch,E., Rajandream,M.A., Reitter,C., Salzberg,S.L., Sanders,M., Schobel,S., Sharp,S., Simmonds,M., Simpson,A.J., Talton,L., Turner,C.M.R., Tait,A., Tivey,A.R., Van Aken,S., Walker,D., Wanless,D., Wang,S.L., White,B., White,O., Whitehead,S., Woodward,J., Wortman,J., Adams,M.D., Embley,T.M., Gull,K., Ullu,E., Barry,J.D., Fairlamb,A.H., Opperdoes,F., Barret,B.G., Donelson,J.E., Hall,N., Fraser,C.M., Melville,S.E., and El Sayed,N.M. (2005). The genome of the African trypanosome *Trypanosoma brucei*. *Science* 309, 416-422.

- Besteiro,S., Coombs,G.H., and Mottram,J.C. (2004). A potential role for ICP, a Leishmanial inhibitor of cysteine peptidases, in the interaction between host and parasite. *Mol. Microbiol.* 54, 1224-1236.
- Besteiro,S., Coombs,G.H., and Mottram,J.C. (2006a). The SNARE protein family of *Leishmania major*. *Bmc Genomics* 7.
- Besteiro,S., Williams,R.A., Coombs,G.H., and Mottram,J.C. (2007). Protein turnover and differentiation in *Leishmania*. *Int. J Parasitol.* 37, 1063-1075.
- Besteiro,S., Williams,R.A., Morrison,L.S., Coombs,G.H., and Mottram,J.C. (2006b). Endosome sorting and autophagy are essential for differentiation and virulence of *Leishmania major*. *J. Biol. Chem.* 281, 11384-11396.
- Besteiro,S., Tonn,D., Tetley,L., Coombs,G.H., and Mottram,J.C. (2008). The AP3 adaptor is involved in the transport of membrane proteins to acidocalcisomes of *Leishmania*. *J Cell Sci* 121, 561-570.
- Beverley,S.M. (2003). Protozoomics: Trypanosomatid parasite genetics comes of age. *Nature Reviews Genetics* 4, 11-19.
- Blobel,G. and Dobberstein,B. (1975). Transfer of proteins across membranes. I. Presence of proteolytically processed and unprocessed nascent immunoglobulin light chains on membrane-bound ribosomes of murine myeloma. *J Cell Biol* 67, 835-851.
- Blott,E.J. and Griffiths,G.M. (2002). Secretory lysosomes. *Nat Rev Mol Cell Biol* 3, 122-131.
- Boehm,M. and Bonifacino,J.S. (2001). Adaptins - The final recount. *Molecular Biology of the Cell* 12, 2907-2920.
- Boehm,M. and Bonifacino,J.S. (2002). Genetic analyses of adaptin function from yeast to mammals. *Gene* 286, 175-186.
- Bonhivers,M., Nowacki,S., Landrein,N., and Robinson,D.R. (2008). Biogenesis of the trypanosome endo-exocytotic organelle is cytoskeleton mediated. *PLoS Biol* 6, e105.

- Bonifacino, J.S. and Dell'Angelica, E.C. (1999). Molecular bases for the recognition of tyrosine-based sorting signals. *J Cell Biol* 145, 923-926.
- Bonifacino, J.S. and Traub, L.M. (2003). Signals for sorting of transmembrane proteins to endosomes and lysosomes. *Annu. Rev Biochem* 72, 395-447.
- Bonifacino, J.S. and Weissman, A.M. (1998). Ubiquitin and the control of protein fate in the secretory and endocytic pathways. *Annu. Rev Cell Dev. Biol* 14, 19-57.
- Bright, N.A., Gratian, M.J., and Luzio, J.P. (2005). Endocytic delivery to lysosomes mediated by concurrent fusion and kissing events in living cells. *Curr. Biol* 15, 360-365.
- Brittingham, A., Chen, G., McGwire, B.S., Chang, K.P., and Mosser, D.M. (1999). Interaction of *Leishmania* gp63 with cellular receptors for fibronectin. *Infection and Immunity* 67, 4477-4484.
- Broadhead, R., Dawe, H.R., Farr, H., Griffiths, S., Hart, S.R., Portman, N., Shaw, M.K., Ginger, M.L., Gaskell, S.J., Mckean, P.G., and Gull, K. (2006). Flagellar motility is required for the viability of the bloodstream trypanosome. *Nature* 440, 224-227.
- Brooks, D.R., Tetley, L., Coombs, G.H., and Mottram, J.C. (2000). Processing and trafficking of cysteine proteases in *Leishmania mexicana*. *J. Cell Sci.* 113 (Pt 22), 4035-4041.
- Burchmore, R.J.S. and Barrett, M.P. (2001). Life in vacuoles - nutrient acquisition by *Leishmania* amastigotes. *International Journal for Parasitology* 31, 1311-1320.
- Buxbaum, L.U., Denise, H., Coombs, G.H., Alexander, J., Mottram, J.C., and Scott, P. (2003). Cysteine protease B of *Leishmania mexicana* inhibits host Th1 responses and protective immunity. *Journal of Immunology* 171, 3711-3717.

C

- Cabib, E., Drgonova, J., and Drgon, T. (1998). Role of small G proteins in yeast cell polarization and wall biosynthesis. *Annu. Rev Biochem* 67, 307-333.
- Cameron, P., McGachy, A., Anderson, M., Paul, A., Coombs, G.H., Mottram, J.C., Alexander, J., and Plevin, R. (2004). Inhibition of lipopolysaccharide-induced macrophage IL-12 production by *Leishmania mexicana* amastigotes: the role of cysteine peptidases and the NF-kappaB signaling pathway. *J Immunol.* 173, 3297-3304.
- Campbell, D.A., Thomas, S., and Sturm, N.R. (2003). Transcription in kinetoplastid protozoa: why be normal? *Microbes and Infection* 5, 1231-1240.
- Carrera, L., Gazzinelli, R.T., Badolato, R., Hieny, S., Muller, W., Kuhn, R., and Sacks, D.L. (1996). *Leishmania* promastigotes selectively inhibit interleukin 12 induction in bone marrow-derived macrophages from susceptible and resistant mice. *J Exp. Med.* 183, 515-526.

- Castro,H., Romao,S., Gadelha,F.R., and Tomas,A.M. (2008). *Leishmania infantum*: provision of reducing equivalents to the mitochondrial trypanredoxin/trypanredoxin peroxidase system. *Exp. Parasitol.* 120, 421-423.
- Cazzulo,J.J., Hellman,U., Couso,R., and Parodi,A.J. (1990). Amino acid and carbohydrate composition of a lysosomal cysteine proteinase from *Trypanosoma cruzi*. Absence of phosphorylated mannose residues. *Mol. Biochem. Parasitol.* 38, 41-48.
- Chan,J., Fujiwara,T., Brennan,P., Mcneil,M., Turco,S.J., Sibille,J.C., Snapper,M., Aisen,P., and Bloom,B.R. (1989). Microbial Glycolipids - Possible Virulence Factors That Scavenge Oxygen Radicals. *Proceedings of the National Academy of Sciences of the United States of America* 86, 2453-2457.
- Chang,K.P., Reed,S.G., McGwire,B.S., and Soong,L. (2003). *Leishmania* model for microbial virulence: the relevance of parasite multiplication and pathoantigenicity. *Acta Tropica* 85, 375-390.
- Chenik,M., Lakhal,S., Ben Khalef,N., Zribi,L., Louzir,H., and Dellagi,K. (2006). Approaches for the identification of potential excreted/secreted proteins of *Leishmania major* parasites. *Parasitology* 132, 493-509.
- Claros,M.G. and Vincens,P. (1996). Computational method to predict mitochondrially imported proteins and their targeting sequences. *Eur. J Biochem* 241, 779-786.
- Clayton,C. and Shapira,M. (2007). Post-transcriptional regulation of gene expression in trypanosomes and leishmanias. *Mol Biochem Parasitol.* 156, 93-101.
- Clayton,C.E. (2002). Life without transcriptional control? From fly to man and back again. *Embo Journal* 21, 1881-1888.
- Coetzer,T.H., Goldring,J.P., and Huson,L.E. (2008). Oligopeptidase B: a processing peptidase involved in pathogenesis. *Biochimie* 90, 336-344.
- Coombs,G.H., Craft,J.A., and Hart,D.T. (1982). A comparative study of *Leishmania mexicana* amastigotes and promastigotes. Enzyme activities and subcellular locations. *Mol Biochem Parasitol.* 5, 199-211.
- Coombs,G.H., Tetley,L., Moss,V.A., and Vickerman,K. (1986). 3-Dimensional Structure of the *Leishmania* Amastigote As Revealed by Computer-Aided Reconstruction from Serial Sections. *Parasitology* 92, 13-23.
- Corell,R.A., Feagin,J.E., Riley,G.R., Strickland,T., Guderian,J.A., Myler,P.J., and Stuart,K. (1993). *Trypanosoma brucei* minicircles encode multiple guide RNAs which can direct editing of extensively overlapping sequences. *Nucleic Acids Res.* 21, 4313-4320.

- Correa, J.R., Brazil, R.P., and Soares, M.J. (2007). *Leishmania (Viannia) lainsoni* (Silveira *et al.* 1987): ultrastructural aspects of the parasite and skin lesion in experimentally infected hamster (*Mesocricetus auratus*). *Parasitology Research* 100, 1227-1232.
- Costa-Pinto, D., Trindade, L.S., McMahon-Pratt, D., and Traub-Cseko, Y.M. (2001). Cellular trafficking in trypanosomatids: a new target for therapies? *Int. J. Parasitol.* 31, 536-543.
- Couvreux, B., Wattiez, R., Bollen, A., Falmagne, P., Le Ray, D., and Dujardin, J.C. (2002). Eubacterial HslV and HslU subunits homologs in primordial eukaryotes. *Mol Biol Evol.* 19, 2110-2117.
- Cowles, C.R., Odorizzi, G., Payne, G.S., and Emr, S.D. (1997). The AP-3 adaptor complex is essential for cargo-selective transport to the yeast vacuole. *Cell* 91, 109-118.
- Croall, D.E. and Ersfeld, K. (2007). The calpains: modular designs and functional diversity. *Genome Biology* 8.
- Croft, S.L. and Coombs, G.H. (2003). Leishmaniasis - current chemotherapy and recent advances in the search for novel drugs. *Trends in Parasitology* 19, 502-508.
- Cuervo, A.M. and Dice, J.F. (1996). A receptor for the selective uptake and degradation of proteins by lysosomes. *Science* 273, 501-503.
- Cuervo, P., De Jesus, J.B., Saboia-Vahia, L., Mendonca-Lima, L., Domont, G.B., and Cupolillo, E. (2009). Proteomic characterization of the released/secreted proteins of *Leishmania (Viannia) braziliensis* promastigotes. *J Proteomics*.
- Cutler, D.F. (2002). Introduction: lysosome-related organelles. *Semin. Cell Dev. Biol* 13, 261-262.

D

- De Souza, L.S., Lang, T., Prina, E., Hellio, R., and Antoine, J.C. (1995). Intracellular *Leishmania amazonensis* amastigotes internalize and degrade MHC class II molecules of their host cells. *J. Cell Sci.* 108 (Pt 10), 3219-3231.
- de Souza, W. (2002). Special organelles of some pathogenic protozoa. *Parasitol. Res.* 88, 1013-1025.
- de Souza, W., Sant'Anna, C., and Cunha-e-Silva NL (2009). Electron microscopy and cytochemistry analysis of the endocytic pathway of pathogenic protozoa. *Prog. Histochem. Cytochem.* 44, 67-124.
- Dell'Angelica, E.C., Aguilar, R.C., Wolins, N., Hazelwood, S., Gahl, W.A., and Bonifacino, J.S. (2000). Molecular characterization of the protein encoded by the Hermansky-Pudlak syndrome type 1 gene. *Journal of Biological Chemistry* 275, 1300-1306.

- Dell'Angelica, E.C., Klumperman, J., Stoorvogel, W., and Bonifacino, J.S. (1998). Association of the AP-3 adaptor complex with clathrin. *Science* 280, 431-434.
- Dell'Angelica, E.C., Mullins, C., and Bonifacino, J.S. (1999a). AP-4, a novel protein complex related to clathrin adaptors. *Journal of Biological Chemistry* 274, 7278-7285.
- Dell'Angelica, E.C., Ohno, H., Ooi, C.E., Rabinovich, E., Roche, K.W., and Bonifacino, J.S. (1997). AP-3: an adaptor-like protein complex with ubiquitous expression. *EMBO J* 16, 917-928.
- Dell'Angelica, E.C., Shotelersuk, V., Aguilar, R.C., Gahl, W.A., and Bonifacino, J.S. (1999b). Altered trafficking of lysosomal proteins in Hermansky-Pudlak syndrome due to mutations in the beta 3A subunit of the AP-3 adaptor. *Molecular Cell* 3, 11-21.
- Denny, P.W., Field, M.C., and Smith, D.F. (2001). GPI-anchored proteins and glycoconjugates segregate into lipid rafts in Kinetoplastida. *Febs Letters* 491, 148-153.
- Denny, P.W., Gokool, S., Russell, D.G., Field, M.C., and Smith, D.F. (2000). Acylation-dependent protein export in *Leishmania*. *J Biol Chem.* 275, 11017-11025.
- Denny, P.W., Lewis, S., Tempero, J.E., Goulding, D., Ivens, A.C., Field, M.C., and Smith, D.F. (2002). *Leishmania* RAB7: characterisation of terminal endocytic stages in an intracellular parasite. *Mol Biochem Parasitol.* 123, 105-113.
- Denny, P.W., Morgan, G.W., Field, M.C., and Smith, D.F. (2005). *Leishmania major*: clathrin and adaptin complexes of an intra-cellular parasite. *Experimental Parasitology* 109, 33-37.
- Desjardins, M. and Descoteaux, A. (1997). Inhibition of phagolysosomal biogenesis by the *Leishmania* lipophosphoglycan. *Journal of Experimental Medicine* 185, 2061-2068.
- Dhir, V., Goulding, D., and Field, M.C. (2004). TbRAB1 and TbRAB2 mediate trafficking through the early secretory pathway of *Trypanosoma brucei*. *Mol Biochem Parasitol.* 137, 253-265.
- Docampo, R., de Souza, W., Miranda, K., Rohloff, P., and Moreno, S.N. (2005). Acidocalcisomes - conserved from bacteria to man. *Nat. Rev. Microbiol.* 3, 251-261.
- Docampo, R. and Moreno, S.N.J. (1999). Acidocalcisome: A novel Ca²⁺ storage compartment in trypanosomatids and apicomplexan parasites. *Parasitology Today* 15, 443-448.
- Docampo, R. and Moreno, S.N.J. (2001). The acidocalcisome. *Molecular and Biochemical Parasitology* 114, 151-159.

- Doyle,P.S. and Dwyer,D.M. (1993). *Leishmania* - Immunochemical Comparison of the Secretory (Extracellular) Acid-Phosphatases from Various Species. *Experimental Parasitology* 77, 435-444.
- Drake,M.T., Zhu,Y., and Kornfeld,S. (2000). The assembly of AP-3 adaptor complex-containing clathrin-coated vesicles on synthetic liposomes. *Mol Biol Cell* 11, 3723-3736.

E

- Eisenhaber,B., Bork,P., and Eisenhaber,F. (1999). Prediction of potential GPI-modification sites in proprotein sequences. *J Mol Biol* 292, 741-758.
- El Sayed,N.M., Myler,P.J., Blandin,G., Berriman,M., Crabtree,J., Aggarwal,G., Caler,E., Renauld,H., Worthey,E.A., Hertz-Fowler,C., Ghedin,E., Peacock,C., Bartholomeu,D.C., Haas,B.J., Tran,A.N., Wortman,J.R., Alsmark,U.C.M., Angiuoli,S., Anupama,A., Badger,J., Bringaud,F., Cadag,E., Carlton,J.M., Cerqueira,G.C., Creasy,T., Delcher,A.L., Djikeng,A., Embley,T.M., Hauser,C., Ivens,A.C., Kummerfeld,S.K., Pereira-Leal,J.B., Nilsson,D., Peterson,J., Salzberg,S.L., Shallom,J., Silva,J.C., Sundaram,J., Westenberger,S., White,O., Metville,S.E., Donelson,J.E., Andersson,B., Stuart,K.D., and Hall,N. (2005). Comparative genomics of trypanosomatid parasitic protozoa. *Science* 309, 404-409.
- Emanuelsson,O., Brunak,S., von Heijne,G., and Nielsen,H. (2007). Locating proteins in the cell using TargetP, SignalP and related tools. *Nat Protoc.* 2, 953-971.
- Emanuelsson,O., Nielsen,H., Brunak,S., and von Heijne,G. (2000). Predicting subcellular localization of proteins based on their N-terminal amino acid sequence. *J Mol Biol* 300, 1005-1016.
- Engstler,M., Bangs,J.D., and Field,M.C. (2007). Intracellular transport systems in trypanosomes: Function, evolution, and virulence. *Trypanosomes - After the genome* (Barry D, McCulloch R, Mottram J, Acosta-Serrano A). Horizon Bioscience press, 281-317.
- Eschenlauer,S.C., Faria,M.S., Morrison,L.S., Bland,N., Ribeiro-Gomes,F.L., DosReis,G.A., Coombs,G.H., Lima,A.P., and Mottram,J.C. (2009). Influence of parasite encoded inhibitors of serine peptidases in early infection of macrophages with *Leishmania major*. *Cell Microbiol.* 11, 106-120.
- Eskelinen,E.L. (2006). Roles of LAMP-1 and LAMP-2 in lysosome biogenesis and autophagy. *Mol. Aspects Med.*
- Eskelinen,E.L., Cuervo,A.M., Taylor,M.R., Nishino,I., Blum,J.S., Dice,J.F., Sandoval,I.V., Lippincott-Schwartz,J., August,J.T., and Saftig,P. (2005). Unifying nomenclature for the isoforms of the lysosomal membrane protein LAMP-2. *Traffic* 6, 1058-1061.

- Eskelinen, E.L., Schmidt, C.K., Neu, S., Willenborg, M., Fuertes, G., Salvador, N., Tanaka, Y., Lullmann-Rauch, R., Hartmann, D., Heeren, J., von Figura, K., Knecht, E., and Saftig, P. (2004). Disturbed cholesterol traffic but normal proteolytic function in LAMP-1/LAMP-2 double-deficient fibroblasts. *Mol Biol Cell* 15, 3132-3145.
- Eskelinen, E.L., Illert, A.L., Tanaka, Y., Schwarzmann, G., Blanz, J., von Figura, K., and Saftig, P. (2002). Role of LAMP-2 in Lysosome Biogenesis and Autophagy. *Molecular Biology of the Cell* 13, 3355-3368.
- Espiau, B., Lemercier, G., Ambit, A., Bringaud, F., Merlin, G., Baltz, T., and Bakalara, N. (2006). A soluble pyrophosphatase, a key enzyme for polyphosphate metabolism in *Leishmania*. *Journal of Biological Chemistry* 281, 1516-1523.
- Evans, J.S. and Turner, M.D. (2007). Emerging functions of the calpain superfamily of cysteine proteases in neuroendocrine secretory pathways. *Journal of Neurochemistry* 103, 849-859.

F

- Feng, L.J., Seymour, A.B., Jiang, S., To, A., Peden, A.A., Novak, E.K., Zhen, L.J., Rusiniak, M.E., Eicher, E.M., Robinson, M.S., Gorin, M.B., and Swank, R.T. (1999). The beta 3A subunit gene (Ap3b1) of the AP-3 adaptor complex is altered in the mouse hypopigmentation mutant pearl, a model for Hermansky-Pudlak syndrome and night blindness. *Hum. Mol. Genet.* 8, 323-330.
- Fenteany, G., Standaert, R.F., Lane, W.S., Choi, S., Corey, E.J., and Schreiber, S.L. (1995). Inhibition of proteasome activities and subunit-specific amino-terminal threonine modification by lactacystin. *Science* 268, 726-731.
- Field, M.C. and Carrington, M. (2004). Intracellular membrane transport systems in *Trypanosoma brucei*. *Traffic.* 5, 905-913.
- Freeman, M. (2004). Proteolysis within the membrane: rhomboids revealed. *Nat Rev Mol Cell Biol* 5, 188-197.
- Frommel, T.O., Button, L.L., Fujikura, Y., and McMaster, W.R. (1990). The major surface glycoprotein (GP63) is present in both life stages of *Leishmania*. *Mol Biochem Parasitol.* 38, 25-32.
- Fukuda, M. (1991). Lysosomal membrane glycoproteins. Structure, biosynthesis, and intracellular trafficking. *J Biol Chem.* 266, 21327-21330.
- Fulop, V., Bocskei, Z., and Polgar, L. (1998). Prolyl oligopeptidase: an unusual beta-propeller domain regulates proteolysis. *Cell* 94, 161-170.

G

- Gallusser, A. and Kirchhausen, T. (1993). The beta 1 and beta 2 subunits of the AP complexes are the clathrin coat assembly components. *EMBO J* 12, 5237-5244.

- Germain,D. (2008). Ubiquitin-dependent and -independent mitochondrial protein quality controls: implications in ageing and neurodegenerative diseases. *Mol Microbiol.* 70, 1334-1341.
- Ghedin,E., Debrabant,A., Engel,J.C., and Dwyer,D.M. (2001). Secretory and endocytic pathways converge in a dynamic endosomal system in a primitive protozoan. *Traffic.* 2, 175-188.
- Ghosh,S., Goswami,S., and Adhya,S. (2003). Role of superoxide dismutase in survival of *Leishmania* within the macrophage. *Biochem J* 369, 447-452.
- Giot,L., Bader,J.S., Brouwer,C., Chaudhuri,A., Kuang,B., Li,Y., Hao,Y.L., Ooi,C.E., Godwin,B., Vitols,E., Vijayadamodar,G., Pochart,P., Machineni,H., Welsh,M., Kong,Y., Zerhusen,B., Malcolm,R., Varrone,Z., Collis,A., Minto,M., Burgess,S., McDaniel,L., Stimpson,E., Spriggs,F., Williams,J., Neurath,K., Ioime,N., Agee,M., Voss,E., Furtak,K., Renzulli,R., Aanensen,N., Carrola,S., Bickelhaupt,E., Lazovatsky,Y., DaSilva,A., Zhong,J., Stanyon,C.A., Finley,R.L., Jr., White,K.P., Braverman,M., Jarvie,T., Gold,S., Leach,M., Knight,J., Shimkets,R.A., McKenna,M.P., Chant,J., and Rothberg,J.M. (2003). A protein interaction map of *Drosophila melanogaster*. *Science* 302, 1727-1736.
- Gluezn,E., Smith,A., Hoog,J., Dawe,H., Heah,C., Shaw,M., and Gull,K. (2009). Structure and function of the *Leishmania* amastigote flagellum. Abstract, Kinetoplastid Molecular Cell Biology conference (Woods Hole, April 2009).
- Gokool,S. (2003). Sigma 1- and mu 1-Adaptin homologues of *Leishmania mexicana* are required for parasite survival in the infected host. *J Biol Chem.* 278, 29400-29409.
- Goldberg,A.L. (2003). Protein degradation and protection against misfolded or damaged proteins. *Nature* 426, 895-899.
- Gossage,S.A., Rogers,M.E., and Bates,P.A. (2003). Two separate growth phases during the development of *Leishmania* in sand flies: implications for understanding the life cycle. *International Journal for Parasitology* 33, 1027-1034.
- Goto,Y., Bogatzki,L.Y., Bertholet,S., Coler,R.N., and Reed,S.G. (2007). Protective immunization against visceral leishmaniasis using *Leishmania* sterol 24-c-methyltransferase formulated in adjuvant. *Vaccine* 25, 7450-7458.
- Gottlieb,M. and Dwyer,D.M. (1982). Identification and partial characterization of an extracellular acid phosphatase activity of *Leishmania donovani* promastigotes. *Mol Cell Biol* 2, 76-81.

- Gough, N.R., Zweifel, M.E., Martinez-Augustin, O., Aguilar, R.C., Bonifacino, J.S., and Fambrough, D.M. (1999). Utilization of the indirect lysosome targeting pathway by lysosome-associated membrane proteins (LAMPs) is influenced largely by the C-terminal residue of their GYXXphi targeting signals. *J Cell Sci* 112, 4257-4269.
- Granger, B.L., Green, S.A., Gabel, C.A., Howe, C.L., Mellman, I., and Helenius, A. (1990). Characterization and cloning of lgp110, a lysosomal membrane glycoprotein from mouse and rat cells. *J Biol Chem.* 265, 12036-12043.
- Gregory, D.J. and Olivier, M. (2005). Subversion of host cell signalling by the protozoan parasite *Leishmania*. *Parasitology* 130, S27-S35.

H

- Haile, S., Dupe, A., and Papadopoulou, B. (2008). Deadenylation-independent stage-specific mRNA degradation in *Leishmania*. *Nucleic Acids Res.* 36, 1634-1644.
- Handman, E. and Bullen, D.V. (2002). Interaction of *Leishmania* with the host macrophage. *Trends Parasitol.* 18, 332-334.
- Hannavy, K., Rospert, S., and Schatz, G. (1993). Protein import into mitochondria: a paradigm for the translocation of polypeptides across membranes. *Curr. Opin. Cell Biol* 5, 694-700.
- Hart, D.T. and Opperdoes, F.R. (1984). The occurrence of glycosomes (microbodies) in the promastigote stage of four major *Leishmania* species. *Mol Biochem Parasitol.* 13, 159-172.
- Harter, C. and Mellman, I. (1992). Transport of the lysosomal membrane glycoprotein lgp120 (lgp-A) to lysosomes does not require appearance on the plasma membrane. *J Cell Biol* 117, 311-325.
- Hermansky, F. and Pudlak, P. (1959). Albinism associated with hemorrhagic diathesis and unusual pigmented reticular cells in the bone marrow: report of two cases with histochemical studies. *Blood* 14, 162-169.
- Hertz-Fowler, C., Ersfeld, K., and Gull, K. (2001). CAP5.5, a life-cycle-regulated, cytoskeleton-associated protein is a member of a novel family of calpain-related proteins in *Trypanosoma brucei*. *Molecular and Biochemical Parasitology* 116, 25-34.
- Hide, M., Ritleng, A.S., Brizard, J.P., Monte-Allegre, A., and Sereno, D. (2008). *Leishmania infantum*: tuning digitonin fractionation for comparative proteomic of the mitochondrial protein content. *Parasitol. Res.* 103, 989-992.
- Hilley, J.D., Zawadzki, J.L., McConville, M.J., Coombs, G.H., and Mottram, J.C. (2000). *Leishmania mexicana* mutants lacking glycosylphosphatidylinositol (GPI): Protein transamidase provide insights into the biosynthesis and functions of GPI-anchored proteins. *Molecular Biology of the Cell* 11, 1183-1195.

- Hirokawa, T., Boon-Chieng, S., and Mitaku, S. (1998). SOSUI: classification and secondary structure prediction system for membrane proteins. *Bioinformatics* 14, 378-379.
- Hirst, J., Bright, N.A., Rous, B., and Robinson, M.S. (1999). Characterization of a fourth adaptor-related protein complex. *Mol Biol Cell* 10, 2787-2802.
- Hirst, J. and Robinson, M.S. (1998). Clathrin and adaptors. *Biochim. Biophys. Acta* 1404, 173-193.
- Hommel, M. (1999). Visceral leishmaniasis: biology of the parasite. *J. Infect.* 39, 101-111.
- Honing, S., Sandoval, I.V., and von Figura, K. (1998). A di-leucine-based motif in the cytoplasmic tail of LIMP-II and tyrosinase mediates selective binding of AP-3. *Embo Journal* 17, 1304-1314.
- Hsiao, C.H., Yao, C., Storlie, P., Donelson, J.E., and Wilson, M.E. (2008). The major surface protease (MSP or GP63) in the intracellular amastigote stage of *Leishmania chagasi*. *Mol Biochem Parasitol.* 157, 148-159.
- Huete-Perez, J.A., Engel, J.C., Brinen, L.S., Mottram, J.C., and McKerrow, J.H. (1999). Protease trafficking in two primitive eukaryotes is mediated by a prodomain protein motif. *Journal of Biological Chemistry* 274, 16249-16256.
- Hunziker, W. and Geuze, H.J. (1996). Intracellular trafficking of lysosomal membrane proteins. *Bioessays* 18, 379-389.
- Huynh, K.K., Eskelinen, E.L., Scott, C.C., Malevanets, A., Saftig, P., and Grinstein, S. (2007). LAMP proteins are required for fusion of lysosomes with phagosomes. *EMBO J* 26, 313-324.

I

- Ihrke, G., Kyttala, A., Russell, M.R., Rous, B.A., and Luzio, J.P. (2004). Differential use of two AP-3-mediated pathways by lysosomal membrane proteins. *Traffic* 5, 946-962.
- Ilg, T. (2000a). Lipophosphoglycan is not required for infection of macrophages or mice by *Leishmania mexicana*. *EMBO J* 19, 1953-1962.
- Ilg, T. (2000b). Proteophosphoglycans of *Leishmania*. *Parasitology Today* 16, 489-497.
- Ilg, T., Fuchs, M., Gnau, V., Wolfram, M., Harbecke, D., and Overath, P. (1994). Distribution of parasite cysteine proteinases in lesions of mice infected with *Leishmania mexicana* amastigotes. *Mol Biochem Parasitol.* 67, 193-203.
- Ilgoutz, S.C., Mullin, K.A., Southwell, B.R., and McConville, M.J. (1999). Glycosylphosphatidylinositol biosynthetic enzymes are localized to a stable tubular subcompartment of the endoplasmic reticulum in *Leishmania mexicana*. *EMBO J* 18, 3643-3654.

Ivens,A.C., Peacock,C.S., Worthey,E.A., Murphy,L., Aggarwal,G., Berriman,M., Sisk,E., Rajandream,M.A., Adlem,E., Aert,R., Anupama,A., Apostolou,Z., Attipoe,P., Bason,N., Bauser,C., Beck,A., Beverley,S.M., Bianchetti,G., Borzym,K., Bothe,G., Bruschi,C.V., Collins,M., Cadag,E., Ciarloni,L., Clayton,C., Coulson,R.M., Cronin,A., Cruz,A.K., Davies,R.M., De Gaudenzi,J., Dobson,D.E., Duesterhoeft,A., Fazelina,G., Fosker,N., Frasc,A.C., Fraser,A., Fuchs,M., Gabel,C., Goble,A., Goffeau,A., Harris,D., Hertz-Fowler,C., Hilbert,H., Horn,D., Huang,Y., Klages,S., Knights,A., Kube,M., Larke,N., Litvin,L., Lord,A., Louie,T., Marra,M., Masuy,D., Matthews,K., Michaeli,S., Mottram,J.C., Muller-Auer,S., Munden,H., Nelson,S., Norbertczak,H., Oliver,K., O'neil,S., Pentony,M., Pohl,T.M., Price,C., Purnelle,B., Quail,M.A., Rabinowitsch,E., Reinhardt,R., Rieger,M., Rinta,J., Robben,J., Robertson,L., Ruiz,J.C., Rutter,S., Saunders,D., Schafer,M., Schein,J., Schwartz,D.C., Seeger,K., Seyler,A., Sharp,S., Shin,H., Sivam,D., Squares,R., Squares,S., Tosato,V., Vogt,C., Volckaert,G., Wambutt,R., Warren,T., Wedler,H., Woodward,J., Zhou,S., Zimmermann,W., Smith,D.F., Blackwell,J.M., Stuart,K.D., Barrell,B., and Myler,P.J. (2005). The genome of the kinetoplastid parasite, *Leishmania major*. *Science* 309, 436-442.

J

- Jahn,R. and Scheller,R.H. (2006). SNAREs - engines for membrane fusion. *Nature Reviews Molecular Cell Biology* 7, 631-643.
- Janvier,K. and Bonifacino,J.S. (2005). Role of the endocytic machinery in the sorting of lysosome-associated membrane proteins. *Mol Biol Cell* 16, 4231-4242.
- Jhingran,A., Chatterjee,M., and Madhubala,R. (2008). Leishmaniasis: Epidemiological Trends and Diagnosis. *Leishmania - After the genome* (Myler PJ, Fasel N), Caister Academic Press, 1-14.
- Jochim,R.C. and Teixeira,C. (2009). *Leishmania* commandeers the host inflammatory response through neutrophils. *Trends Parasitol.* 25, 145-147.
- John,B. and Hunter,C.A. (2008). Immunology. Neutrophil soldiers or Trojan Horses? *Science* 321, 917-918.
- Joshi,M.B. and Dwyer,D.M. (2007). Molecular and functional analyses of a novel class I secretory nuclease from the human pathogen, *Leishmania donovani*. *J Biol Chem.* 282, 10079-10095.
- Joshi,M.B., Mallinson,D.J., and Dwyer,D.M. (2004). The human pathogen *Leishmania donovani* secretes a histidine acid phosphatase activity that is resistant to proteolytic degradation. *Journal of Eukaryotic Microbiology* 51, 108-112.

Joshi,P.B., Kelly,B.L., Kamhawi,S., Sacks,D.L., and McMaster,W.R. (2002). Targeted gene deletion in *Leishmania major* identifies leishmanolysin (GP63) as a virulence factor. *Molecular and Biochemical Parasitology* 120, 33-40.

Joshi,P.B., Sacks,D.L., Modi,G., and McMaster,W.R. (1998). Targeted gene deletion of *Leishmania major* genes encoding developmental stage-specific leishmanolysin (GP63). *Molecular Microbiology* 27, 519-530.

K

Kall,L., Krogh,A., and Sonnhammer,E.L. (2004). A combined transmembrane topology and signal peptide prediction method. *J Mol Biol* 338, 1027-1036.

Kantheti,P., Qiao,X.X., Diaz,M.E., Peden,A.A., Meyer,G.E., Carskadon,S.L., Kapfhamer,D., Sufalko,D., Robinson,M.S., Noebels,J.L., and Burmeister,M. (1998). Mutation in AP-3 delta in the mocha mouse links endosomal transport to storage deficiency in platelets, melanosomes, and synaptic vesicles. *Neuron* 21, 111-122.

Katayama,H., Yamamoto,A., Mizushima,N., Yoshimori,T., and Miyawaki,A. (2008). GFP-like proteins stably accumulate in lysosomes. *Cell Struct. Funct.* 33, 1-12.

Kelley,R.J., Alexander,D.L., Cowan,C., Balber,A.E., and Bangs,J.D. (1999). Molecular cloning of p67, a lysosomal membrane glycoprotein from *Trypanosoma brucei*. *Mol Biochem Parasitol.* 98, 17-28.

Khamesipour,A., Rafati,S., Davoudi,N., Maboudi,F., and Modabber,F. (2006). Leishmaniasis vaccine candidates for development: a global overview. *Indian J Med. Res.* 123, 423-438.

Killick-Kendrick,R., Molyneux,D.H., and Ashford,R.W. (1974). Ultrastructural observations on the attachment of *Leishmania* in the sandfly. *Trans. R. Soc. Trop. Med. Hyg.* 68, 269.

Kissinger,J.C. (2006). A tale of three genomes: the kinetoplastids have arrived. *Trends Parasitol.* 22, 240-243.

Koonin,E.V., Makarova,K.S., Rogozin,I.B., Davidovic,L., Letellier,M.C., and Pellegrini,L. (2003). The rhomboids: a nearly ubiquitous family of intramembrane serine proteases that probably evolved by multiple ancient horizontal gene transfers. *Genome Biol.* 4, R19.

Krogh,A., Larsson,B., von Heijne,G., and Sonnhammer,E.L. (2001). Predicting transmembrane protein topology with a hidden Markov model: application to complete genomes. *J Mol Biol* 305, 567-580.

Kundra,R. and Kornfeld,S. (1999). Asparagine-linked oligosaccharides protect Lamp-1 and Lamp-2 from intracellular proteolysis. *J Biol Chem.* 274, 31039-31046.

- Kyttala,A., Ihrke,G., Vesa,J., Schell,M.J., and Luzio,J.P. (2004). Two motifs target Batten disease protein CLN3 to lysosomes in transfected nonneuronal and neuronal cells. *Mol Biol Cell* 15, 1313-1323.
- Kyttala,A., Yliannala,K., Schu,P., Jalanko,A., and Luzio,J.P. (2005). AP-1 and AP-3 facilitate lysosomal targeting of Batten disease protein CLN3 via its dileucine motif. *J Biol Chem.* 280, 10277-10283.

L

- Lacomble,S., Vaughan,S., Gadelha,C., Morphew,M.K., Shaw,M.K., McIntosh,J.R., and Gull,K. (2009). Three-dimensional cellular architecture of the flagellar pocket and associated cytoskeleton in trypanosomes revealed by electron microscope tomography. *J Cell Sci* 122, 1081-1090.
- Landfear,S.M. and Ignatushchenko,M. (2001). The flagellum and flagellar pocket of trypanosomatids. *Mol. Biochem. Parasitol.* 115, 1-17.
- Lao,D.M., Arai,M., Ikeda,M., and Shimizu,T. (2002). The presence of signal peptide significantly affects transmembrane topology prediction. *Bioinformatics* 18, 1562-1566.
- Laskay,T., van Zandbergen,G., and Solbach,W. (2008). Neutrophil granulocytes as host cells and transport vehicles for intracellular pathogens: apoptosis as infection-promoting factor. *Immunobiology* 213, 183-191.
- Le Borgne,R., Alconada,A., Bauer,U., and Hoflack,B. (1998). The mammalian AP-3 adaptor-like complex mediates the intracellular transport of lysosomal membrane glycoproteins. *Journal of Biological Chemistry* 273, 29451-29461.
- Lefurgey,A., Gannon,M., Blum,J., and Ingram,P. (2005). *Leishmania donovani* amastigotes mobilize organic and inorganic osmolytes during regulatory volume decrease. *J Eukaryot. Microbiol.* 52, 277-289.
- Lemberg,M.K. and Freeman,M. (2007). Cutting Proteins within Lipid Bilayers: Rhomboid Structure and Mechanism. *Molecular Cell* 28, 930-940.
- Lemercier,G., Espiau,B., Ruiz,F.A., Vieira,M., Luo,S.H., Baltz,T., Docampo,R., and Bakalara,N. (2004). A pyrophosphatase regulating polyphosphate metabolism in acidocalcisomes is essential for *Trypanosoma brucei* virulence in mice. *Journal of Biological Chemistry* 279, 3420-3425.
- Lemercier,G., Dutoya,S., Luo,S., Ruiz,F.A., Rodrigues,C.O., Baltz,T., Docampo,R., and Bakalara,N. (2002). A Vacuolar-type H⁺-Pyrophosphatase Governs Maintenance of Functional Acidocalcisomes and Growth of the Insect and Mammalian Forms of *Trypanosoma brucei*. *Journal of Biological Chemistry* 277, 37369-37376.
- Levine,B. and Klionsky,D.J. (2004). Development by self-digestion: molecular mechanisms and biological functions of autophagy. *Dev. Cell* 6, 463-477.

- Levine, B. and Yuan, J. (2005). Autophagy in cell death: an innocent convict? *J Clin. Invest* 115, 2679-2688.
- Li, Z., Lindsay, M.E., Motyka, S.A., Englund, P.T., and Wang, C.C. (2008). Identification of a bacterial-like HslVU protease in the mitochondria of *Trypanosoma brucei* and its role in mitochondrial DNA replication. *PLoS Pathog.* 4, e1000048.
- Lopez, C., Chevalier, N., Hannaert, V., Rigden, D.J., Michels, P.A., and Ramirez, J.L. (2002). *Leishmania donovani* phosphofructokinase. Gene characterization, biochemical properties and structure-modeling studies. *Eur. J Biochem* 269, 3978-3989.
- Lustig, Y., Vagima, Y., Goldshmidt, H., Erlanger, A., Ozeri, V., Vince, J., McConville, M.J., Dwyer, D.M., Landfear, S.M., and Michaeli, S. (2007). Down-regulation of the trypanosomatid signal recognition particle affects the biogenesis of polytopic membrane proteins but not of signal peptide-containing proteins. *Eukaryot. Cell* 6, 1865-1875.
- Luzio, J.P., Poupon, V., Lindsay, M.R., Mullock, B.M., Piper, R.C., and Pryor, P.R. (2003). Membrane dynamics and the biogenesis of lysosomes. *Mol. Membr. Biol.* 20, 141-154.
- Luzio, J.P., Pryor, P.R., and Bright, N.A. (2007). Lysosomes: fusion and function. *Nat Rev Mol Cell Biol* 8, 622-632.
- Lynn, M.A. and McMaster, W.R. (2008). *Leishmania*: conserved evolution--diverse diseases. *Trends Parasitol.* 24, 103-105.

M

- Mahmoudzadeh-Niknam, H. and McKerrow, J.H. (2004). *Leishmania tropica*: cysteine proteases are essential for growth and pathogenicity. *Experimental Parasitology* 106, 158-163.
- Mao, Q., Xia, H., and Davidson, B.L. (2003). Intracellular trafficking of CLN3, the protein underlying the childhood neurodegenerative disease, Batten disease. *FEBS Lett.* 555, 351-357.
- Marin-Villa, M., Sampaio, M.G., Roy, D., and Traub-Cseko, Y.M. (2008). *Leishmania* lysosomal targeting signal is recognized by yeast and not by mammalian cells. *Parasitol. Res.* 103, 983-988.
- Marotta, D.E., Gerald, N., and Dwyer, D.M. (2006). Rab5b localization to early endosomes in the protozoan human pathogen *Leishmania donovani*. *Mol Cell Biochem* 292, 107-117.
- Martinez-Calvillo, S., Yan, S.F., Nguyen, D., Fox, M., Stuart, K., and Myler, P.J. (2003). Transcription of *Leishmania major* Friedlin chromosome 1 initiates in both directions within a single region. *Molecular Cell* 11, 1291-1299.

- Matos Guedes,H., Carneiro,M., Gomes,D., Rossi-Bergmanmn,B., and de Simone,S. (2007). Oligopeptidase B from *L. amazonensis* : molecular cloning, gene expression analysis and molecular model. *Parasitology Research* 101, 853-863.
- Matthews,K.R., Tschudi,C., and Ullu,E. (1994). A Common Pyrimidine-Rich Motif Governs Transsplicing and Polyadenylation of Tubulin Polycistronic Pre-Messenger-Rna in Trypanosomes. *Genes & Development* 8, 491-501.
- McConville,M.J. and Blackwell,J.M. (1991). Developmental changes in the glycosylated phosphatidylinositols of *Leishmania donovani*. Characterization of the promastigote and amastigote glycolipids. *J Biol Chem.* 266, 15170-15179.
- McConville,M.J., De Souza,D., Saunders,E., Likic,V.A., and Naderer,T. (2007). Living in a phagolysosome; metabolism of *Leishmania* amastigotes. *Trends Parasitol.* 23, 368-375.
- McConville,M.J., Ilgoutz,S.C., Teasdale,R.D., Foth,B.J., Matthews,A., Mullin,K.A., and Gleeson,P.A. (2002a). Targeting of the GRIP domain to the trans-Golgi network is conserved from protists to animals. *Eur. J Cell Biol* 81, 485-495.
- McConville,M.J., Mullin,K.A., Ilgoutz,S.C., and Teasdale,R.D. (2002b). Secretory pathway of trypanosomatid parasites. *Microbiol. Mol. Biol. Rev.* 66, 122-154.
- McGwire,B.S., Chang,K.P., and Engman,D.M. (2003). Migration through the extracellular matrix by the parasitic protozoan *Leishmania* is enhanced by surface metalloprotease gp63. *Infect. Immun.* 71, 1008-1010.
- McNeely,T.B., Rosen,G., Londner,M.V., and Turco,S.J. (1989). Inhibitory Effects on Protein Kinase-C Activity by Lipophosphoglycan Fragments and Glycosylphosphatidylinositol Antigens of the Protozoan Parasite *Leishmania*. *Biochem J* 259, 601-604.
- McQuibban,G.A., Saurya,S., and Freeman,M. (2003). Mitochondrial membrane remodelling regulated by a conserved rhomboid protease. *Nature* 423, 537-541.
- Medina-Acosta,E., Karess,R.E., Schwartz,H., and Russell,D.G. (1989). The promastigote surface protease (gp63) of *Leishmania* is expressed but differentially processed and localized in the amastigote stage. *Mol Biochem Parasitol.* 37, 263-273.
- Mehul,B. and Hughes,R.C. (1997). Plasma membrane targetting, vesicular budding and release of galectin 3 from the cytoplasm of mammalian cells during secretion. *J Cell Sci* 110 (Pt 10), 1169-1178.
- Melby,P.C. (2002). Recent developments in leishmaniasis. *Curr. Opin. Infect. Dis.* 15, 485-490.

- Mercker,M., Kollath-Leiss,K., Allgaier,S., Weiland,N., and Kempken,F. (2009). The BEM46-like protein appears to be essential for hyphal development upon ascospore germination in *Neurospora crassa* and is targeted to the endoplasmic reticulum. *Curr. Genet.* 55, 151-161.
- Miranda,K., Benchimol,M., Docampo,R., and de Souza,W. (2000). The fine structure of acidocalcisomes in *Trypanosoma cruzi*. *Parasitol. Res.* 86, 373-384.
- Miranda,K., Docampo,R., Grillo,O., Franzen,A., Attias,M., Vercesi,A., Plattner,H., Hentschel,J., and de Souza,W. (2004). Dynamics of polymorphism of acidocalcisomes in *Leishmania* parasites. *Histochem. Cell Biol* 121, 407-418.
- Mochizuki,S., Harada,A., Inada,S., Sugimoto-Shirasu,K., Stacey,N., Wada,T., Ishiguro,S., Okada,K., and Sakai,T. (2005). The Arabidopsis WAVY GROWTH 2 protein modulates root bending in response to environmental stimuli. *Plant Cell* 17, 537-547.
- Moreno,S.N. and Docampo,R. (2009). The role of acidocalcisomes in parasitic protists. *J Eukaryot. Microbiol.* 56, 208-213.
- Morgan,G.W., Hall,B.S., Denny,P.W., Carrington,M., and Field,M.C. (2002a). The kinetoplastida endocytic apparatus. Part I: a dynamic system for nutrition and evasion of host defences. *Trends Parasitol.* 18, 491-496.
- Morgan,G.W., Hall,B.S., Denny,P.W., Field,M.C., and Carrington,M. (2002b). The endocytic apparatus of the kinetoplastida. Part II: machinery and components of the system. *Trends Parasitol.* 18, 540-546.
- Mottram,J.C., Brooks,D.R., and Coombs,G.H. (1998). Roles of cysteine proteinases of trypanosomes and *Leishmania* in host-parasite interactions. *Curr. Opin. Microbiol.* 1, 455-460.
- Mottram,J.C., Coombs,G.H., and Alexander,J. (2004). Cysteine peptidases as virulence factors of *Leishmania*. *Curr. Opin. Microbiol.* 7, 375-381.
- Mottram,J.C., Frame,M.J., Brooks,D.R., Tetley,L., Hutchison,J.E., Souza,A.E., and Coombs,G.H. (1997). The multiple cpb cysteine proteinase genes of *Leishmania mexicana* encode isoenzymes that differ in their stage regulation and substrate preferences. *J. Biol. Chem.* 272, 14285-14293.
- Mottram,J.C., Souza,A.E., Hutchison,J.E., Carter,R., Frame,M.J., and Coombs,G.H. (1996). Evidence from disruption of the lmcpb gene array of *Leishmania mexicana* that cysteine proteinases are virulence factors. *Proc. Natl. Acad. Sci U. S A* 93, 6008-6013.
- Mullin,K.A., Foth,B.J., Ilgoutz,S.C., Callaghan,J.M., Zawadzki,J.L., McFadden,G.I., and McConville,M.J. (2001). Regulated degradation of an endoplasmic reticulum membrane protein in a tubular lysosome in *Leishmania mexicana*. *Mol. Biol. Cell* 12, 2364-2377.

Murray,H.W., Berman,J.D., Davies,C.R., and Saravia,N.G. (2005). Advances in leishmaniasis. *Lancet* 366, 1561-1577.

Myler,P.J. (2008). Genome structure and content. *Leishmania* - After the genome (Myler PJ, Fasel N), Caister Academic Press, 15-28.

Myler,P.J., Audleman,L., Devos,T., Hixson,G., Kiser,P., Lemley,C., Magness,C., Rickel,E., Sisk,E., Sunkin,S., Swartzell,S., Westlake,T., Bastien,P., Fu,G., Ivens,A., and Stuart,K. (1999). *Leishmania major* Friedlin chromosome 1 has an unusual distribution of protein-coding genes. *Proc. Natl. Acad. Sci U. S A* 96, 2902-2906.

N

Naderer,T., Vince,J.E., and McConville,M.J. (2004). Surface determinants of *Leishmania* parasites and their role in infectivity in the mammalian host. *Curr. Mol Med.* 4, 649-665.

Nakamura,N. and Hirose,S. (2008). Regulation of mitochondrial morphology by USP30, a deubiquitinating enzyme present in the mitochondrial outer membrane. *Mol Biol Cell* 19, 1903-1911.

Nakamura,N., Rabouille,C., Watson,R., Nilsson,T., Hui,N., Slusarewicz,P., Kreis,T.E., and Warren,G. (1995). Characterization of a cis-Golgi matrix protein, GM130. *J Cell Biol* 131, 1715-1726.

Nakatsu,F. and Ohno,H. (2003). Adaptor protein complexes as the key regulators of protein sorting in the post-Golgi network. *Cell Struct. Funct.* 28, 419-429.

Newell-Litwa,K., Seong,E., Burmeister,M., and Faundez,V. (2007). Neuronal and non-neuronal functions of the AP-3 sorting machinery. *J Cell Sci* 120, 531-541.

Nielsen,H., Engelbrecht,J., Brunak,S., and von Heijne,G. (1997). Identification of prokaryotic and eukaryotic signal peptides and prediction of their cleavage sites. *Protein Eng* 10, 1-6.

Nishino,I., Fu,J., Tanji,K., Yamada,T., Shimojo,S., Koori,T., Mora,M., Riggs,J.E., Oh,S.J., Koga,Y., Sue,C.M., Yamamoto,A., Murakami,N., Shanske,S., Byrne,E., Bonilla,E., Nonaka,I., DiMauro,S., and Hirano,M. (2000). Primary LAMP-2 deficiency causes X-linked vacuolar cardiomyopathy and myopathy (Danon disease). *Nature* 406, 906-910.

Nugent,T., Mole,S.E., and Jones,D.T. (2008). The transmembrane topology of Batten disease protein CLN3 determined by consensus computational prediction constrained by experimental data. *FEBS Lett.* 582, 1019-1024.

O

- Oberholzer, M., Marti, G., Baresic, M., Kunz, S., Hemphill, A., and Seebeck, T. (2007). The *Trypanosoma brucei* cAMP phosphodiesterases TbrPDEB1 and TbrPDEB2: flagellar enzymes that are essential for parasite virulence. *FASEB J* 21, 720-731.
- Odorizzi, G., Cowles, C.R., and Emr, S.D. (1998). The AP-3 complex: a coat of many colours. *Trends Cell Biol.* 8, 282-288.
- Ohno, H., Aguilar, R.C., Yeh, D., Taura, D., Saito, T., and Bonifacino, J.S. (1998). The medium subunits of adaptor complexes recognize distinct but overlapping sets of tyrosine-based sorting signals. *J Biol Chem.* 273, 25915-25921.
- Ohno, H., Fournier, M.C., Poy, G., and Bonifacino, J.S. (1996). Structural determinants of interaction of tyrosine-based sorting signals with the adaptor medium chains. *J Biol Chem.* 271, 29009-29015.
- Ohno, H., Stewart, J., Fournier, M.C., Bosshart, H., Rhee, I., Miyatake, S., Saito, T., Gallusser, A., Kirchhausen, T., and Bonifacino, J.S. (1995). Interaction of tyrosine-based sorting signals with clathrin-associated proteins. *Science* 269, 1872-1875.
- Olivier, M., Gregory, D.J., and Forget, G. (2005). Subversion mechanisms by which *Leishmania* parasites can escape the host immune response: a signaling point of view. *Clin. Microbiol. Rev.* 18, 293-305.
- Ollis, D.L., Cheah, E., Cygler, M., Dijkstra, B., Frolow, F., Franken, S.M., Harel, M., Remington, S.J., Silman, I., Schrag, J., and . (1992). The alpha/beta hydrolase fold. *Protein Eng* 5, 197-211.
- Opperdoes, F. and Michels, P.A. (2008). The metabolomic repertoire of leishmania and implications for drug discovery. *Leishmania - After the genome* (Myler PJ, Fasel N), Caister Academic Press, 124-158.
- Otto, J.C., Kim, E., Young, S.G., and Casey, P.J. (1999). Cloning and characterization of a mammalian prenyl protein-specific protease. *J. Biol. Chem.* 274, 8379-8382.
- Ouellette, M., Drummelsmith, J., Leprohon, P., El Fadili, K., Foucher, A., Verges, B., and Legare, D. (2008). Drug resistance in *Leishmania*. *Leishmania - After the genome* (Myler PJ, Fasel N), Caister Academic Press, 159-176.

P

- Pacaud, M. and Richaud, C. (1975). Protease II from *Escherichia coli*. Purification and characterization. *J Biol Chem.* 250, 7771-7779.

- Parmentier, M.L., Woods, D., Greig, S., Phan, P.G., Radovic, A., Bryant, P., and O'Kane, C.J. (2000). Rapsynoid/partner of inscuteable controls asymmetric division of larval neuroblasts in *Drosophila*. *J Neurosci.* 20, RC84.
- Parussini, F., Garcia, M., Mucci, J., Agüero, F., Sanchez, D., Hellman, U., Aslund, L., and Cazzulo, J.J. (2003). Characterization of a lysosomal serine carboxypeptidase from *Trypanosoma cruzi*. *Mol. Biochem. Parasitol.* 131, 11-23.
- Patel, N., Singh, S.B., Basu, S.K., and Mukhopadhyay, A. (2008). *Leishmania* requires Rab7-mediated degradation of endocytosed hemoglobin for their growth. *Proc. Natl. Acad. Sci U. S A* 105, 3980-3985.
- Peacock, C.S., Seeger, K., Harris, D., Murphy, L., Ruiz, J.C., Quail, M.A., Peters, N., Adlem, E., Tivey, A., Aslett, M., Kerhornou, A., Ivens, A., Fraser, A., Rajandream, M.A., Carver, T., Norbertczak, H., Chillingworth, T., Hance, Z., Jagels, K., Moule, S., Ormond, D., Rutter, S., Squares, R., Whitehead, S., Rabbinowitsch, E., Arrowsmith, C., White, B., Thurston, S., Bringaud, F., Baldauf, S.L., Faulconbridge, A., Jeffares, D., Depledge, D.P., Oyola, S.O., Hilley, J.D., Brito, L.O., Tosi, L.R., Barrell, B., Cruz, A.K., Mottram, J.C., Smith, D.F., and Berriman, M. (2007). Comparative genomic analysis of three *Leishmania* species that cause diverse human disease. *Nat Genet.* 39, 839-847.
- Peck, R.F., Shiflett, A.M., Schwartz, K.J., McCann, A., Hajduk, S.L., and Bangs, J.D. (2008). The LAMP-like protein p67 plays an essential role in the lysosome of African trypanosomes. *Mol Microbiol.* 68, 933-946.
- Peden, A.A., Oorschot, V., Hesser, B.A., Austin, C.D., Scheller, R.H., and Klumperman, J. (2004). Localization of the AP-3 adaptor complex defines a novel endosomal exit site for lysosomal membrane proteins. *J Cell Biol* 164, 1065-1076.
- Peters, N.C., Egen, J.G., Secundino, N., Debrabant, A., Kimblin, N., Kamhawi, S., Lawyer, P., Fay, M.P., Germain, R.N., and Sacks, D. (2008). In vivo imaging reveals an essential role for neutrophils in leishmaniasis transmitted by sand flies. *Science* 321, 970-974.
- Phillips, S.N., Benedict, J.W., Weimer, J.M., and Pearce, D.A. (2005). CLN3, the protein associated with batten disease: structure, function and localization. *J Neurosci. Res.* 79, 573-583.
- Pimenta, P.F., Turco, S.J., McConville, M.J., Lawyer, P.G., Perkins, P.V., and Sacks, D.L. (1992). Stage-specific adhesion of *Leishmania* promastigotes to the sandfly midgut. *Science* 256, 1812-1815.
- Plewes, K.A., Barr, S.D., and Gedamu, L. (2003). Iron superoxide dismutases targeted to the glycosomes of *Leishmania chagasi* are important for survival. *Infect. Immun.* 71, 5910-5920.
- Polgar, L. (2002). The prolyl oligopeptidase family. *Cell Mol Life Sci* 59, 349-362.

- Pollock, K.G., McNeil, K.S., Mottram, J.C., Lyons, R.E., Brewer, J.M., Scott, P., Coombs, G.H., and Alexander, J. (2003). The *Leishmania mexicana* cysteine protease, CPB2.8, induces potent Th2 responses. *J. Immunol.* *170*, 1746-1753.
- Porcel, B.M., Aslund, L., Pettersson, U., and Andersson, B. (2000). *Trypanosoma cruzi*: A putative vacuolar ATP synthase subunit and a CAAX prenyl protease-encoding gene, as examples of gene identification in genome projects. *Experimental Parasitology* *95*, 176-186.
- Proudfoot, L., Nikolaev, A.V., Feng, G.J., Wei, X.Q., Ferguson, M.A.J., Brimacombe, J.S., and Liew, F.Y. (1996). Regulation of the expression of nitric oxide synthase and leishmanicidal activity by glycoconjugates of *Leishmania* lipophosphoglycan in murine macrophages. *Proceedings of the National Academy of Sciences of the United States of America* *93*, 10984-10989.

R

- Ralston, K.S., Kabututu, Z.P., Melehani, J.H., Oberholzer, M., and Hill, K.L. (2009). The *Trypanosoma brucei* flagellum: moving parasites in new directions. *Annu. Rev. Microbiol.* *63*, 335-362.
- Rangarajan, D., Gokool, S., McCrossan, M.V., and Smith, D.F. (1995). The gene B protein localises to the surface of *Leishmania major* parasites in the absence of metacyclic stage lipophosphoglycan. *J Cell Sci* *108 (Pt 11)*, 3359-3366.
- Rawlings, N.D., Morton, F.R., Kok, C.Y., Kong, J., and Barrett, A.J. (2008). MEROPS: the peptidase database. *Nucleic Acids Res.* *36*, D320-D325.
- Requena, J.M., Alonso, C., and Soto, M. (2000). Evolutionarily conserved proteins as prominent immunogens during *Leishmania* infections. *Parasitol. Today* *16*, 246-250.
- Robertson, C.D. (1999). The *Leishmania mexicana* proteasome. *Mol Biochem Parasitol.* *103*, 49-60.
- Robinson, M.S. (2004). Adaptable adaptors for coated vesicles. *Trends Cell Biol* *14*, 167-174.
- Rodrigues, C.O., Scott, D.A., and Docampo, R. (1999a). Characterization of a vacuolar pyrophosphatase in *Trypanosoma brucei* and its localization to acidocalcisomes. *Mol Cell Biol* *19*, 7712-7723.
- Rodrigues, C.O., Scott, D.A., and Docampo, R. (1999b). Presence of a vacuolar H⁺-pyrophosphatase in promastigotes of *Leishmania donovani* and its localization to a different compartment from the vacuolar H⁺-ATPase. *Biochem J* *340 (Pt 3)*, 759-766.
- Rogers, K.A., Dekrey, G.K., Mbow, M.L., Gillespie, R.D., Brodskyn, C.I., and Titus, R.G. (2002a). Type 1 and type 2 responses to *Leishmania major*. *Fems Microbiology Letters* *209*, 1-7.

- Rogers, M.E., Chance, M.L., and Bates, P.A. (2002b). The role of promastigote secretory gel in the origin and transmission of the infective stage of *Leishmania mexicana* by the sandfly *Lutzomyia longipalpis*. *Parasitology* 124, 495-507.
- Rogers, M.E., Ilg, T., Nikolaev, A.V., Ferguson, M.A.J., and Bates, P.A. (2004). Transmission of cutaneous leishmaniasis by sand flies is enhanced by regurgitation of fPPG. *Nature* 430, 463-467.
- Rohloff, P. and Docampo, R. (2006). Ammonium production during hypo-osmotic stress leads to alkalinization of acidocalcisomes and cytosolic acidification in *Trypanosoma cruzi*. *Mol Biochem Parasitol.* 150, 249-255.
- Rous, B.A., Reaves, B.J., Ihrke, G., Briggs, J.A., Gray, S.R., Stephens, D.J., Banting, G., and Luzio, J.P. (2002). Role of adaptor complex AP-3 in targeting wild-type and mutated CD63 to lysosomes. *Mol Biol Cell* 13, 1071-1082.
- Rozenfeld, R. and Devi, L.A. (2008). Regulation of CB1 cannabinoid receptor trafficking by the adaptor protein AP-3. *FASEB J* 22, 2311-2322.
- Rubartelli, A., Cozzolino, F., Talio, M., and Sitia, R. (1990). A novel secretory pathway for interleukin-1 beta, a protein lacking a signal sequence. *EMBO J* 9, 1503-1510.
- Ruiz, F.A., Lea, C.R., Oldfield, E., and Docampo, R. (2004). Human platelet dense granules contain polyphosphate and are similar to acidocalcisomes of bacteria and unicellular eukaryotes. *Journal of Biological Chemistry* 279, 44250-44257.
- Ruiz, F.A., Rodrigues, C.O., and Docampo, R. (2001). Rapid changes in polyphosphate content within acidocalcisomes in response to cell growth, differentiation, and environmental stress in *Trypanosoma cruzi*. *J Biol Chem.* 276, 26114-26121.
- Russell, D.G. and Wilhelm, H. (1986). The Involvement of the Major Surface Glycoprotein (Gp63) of *Leishmania* Promastigotes in Attachment to Macrophages. *Journal of Immunology* 136, 2613-2620.

S

- Sacks, D.L., Brodin, T.N., and Turco, S.J. (1990). Developmental Modification of the Lipophosphoglycan from *Leishmania major* Promastigotes During Metacyclogenesis. *Molecular and Biochemical Parasitology* 42, 225-233.
- Sacks, D.L., Modi, G., Rowton, E., Spath, G., Epstein, L., Turco, S.J., and Beverley, S.M. (2000). The role of phosphoglycans in *Leishmania*-sand fly interactions. *Proc. Natl. Acad. Sci U. S A* 97, 406-411.
- Schubert, U., Anton, L.C., Gibbs, J., Norbury, C.C., Yewdell, J.W., and Bennink, J.R. (2000). Rapid degradation of a large fraction of newly synthesized proteins by proteasomes. *Nature* 404, 770-774.

- Scott,D.A., de Souza,W., Benchimol,M., Zhong,L., Lu,H.G., Moreno,S.N., and Docampo,R. (1998). Presence of a plant-like proton-pumping pyrophosphatase in acidocalcisomes of *Trypanosoma cruzi*. *J Biol Chem.* 273, 22151-22158.
- Scott,D.A. and Docampo,R. (2000). Characterization of isolated acidocalcisomes of *Trypanosoma cruzi*. *J. Biol. Chem.* 275, 24215-24221.
- Scott,D.A., Docampo,R., Dvorak,J.A., Shi,S., and Leapman,R.D. (1997). In situ compositional analysis of acidocalcisomes in *Trypanosoma cruzi*. *J Biol Chem.* 272, 28020-28029.
- Seay,M.B., Heard,P.L., and Chaudhuri,G. (1996). Surface Zn-proteinase as a molecule for defense of *Leishmania mexicana amazonensis* promastigotes against cytolysis inside macrophage phagolysosomes. *Infect. Immun.* 64, 5129-5137.
- Seebeck,T. and Gehr,P. (1983). Trypanocidal action of neuroleptic phenothiazines in *Trypanosoma brucei*. *Mol Biochem Parasitol.* 9, 197-208.
- Selzer,P.M., Pingel,S., Hsieh,I., Ugele,B., Chan,V.J., Engel,J.C., Bogyo,M., Russell,D.G., Sakanari,J.A., and McKerrow,J.H. (1999). Cysteine protease inhibitors as chemotherapy: lessons from a parasite target. *Proc. Natl. Acad. Sci. U. S. A* 96, 11015-11022.
- Sereno,D., Vanhille,L., Vergnes,B., Monte-Allegre,A., and Ouaisi,A. (2005). Experimental study of the function of the excreted/secreted *Leishmania* LmSIR2 protein by heterologous expression in eukaryotic cell line. *Kinetoplastid. Biol Dis.* 4, 1.
- Shakarian,A.M. and Dwyer,D.M. (2000). Structurally conserved soluble acid phosphatases are synthesized and released by *Leishmania major* promastigotes. *Exp. Parasitol.* 95, 79-84.
- Shakarian,A.M., Ellis,S.L., Mallinson,D.J., Olafson,R.W., and Dwyer,D.M. (1997). Two tandemly arrayed genes encode the (histidine) secretory acid phosphatases of *Leishmania donovani*. *Gene* 196, 127-137.
- Shaner,N.C., Campbell,R.E., Steinbach,P.A., Giepmans,B.N., Palmer,A.E., and Tsien,R.Y. (2004). Improved monomeric red, orange and yellow fluorescent proteins derived from *Discosoma sp.* red fluorescent protein. *Nat Biotechnol.* 22, 1567-1572.
- Silverman,J.M., Chan,S.K., Robinson,D.P., Dwyer,D.M., Nandan,D., Foster,L.J., and Reiner,N.E. (2008). Proteomic analysis of the secretome of *Leishmania donovani*. *Genome Biology* 9.
- Simpson,F., Peden,A.A., Christopoulou,L., and Robinson,M.S. (1997). Characterization of the adaptor-related protein complex, AP-3. *Journal of Cell Biology* 137, 835-845.
- Simpson,L. and Simpson,A.G. (1978). Kinetoplast RNA of *Leishmania tarentolae*. *Cell* 14, 169-178.

- Singh, S.B., Tandon, R., Krishnamurthy, G., Vikram, R., Sharma, N., Basu, S.K., and Mukhopadhyay, A. (2003). Rab5-mediated endosome-endosome fusion regulates hemoglobin endocytosis in *Leishmania donovani*. *EMBO J* 22, 5712-5722.
- Smith, D.F., Peacock, C.S., and Cruz, A.K. (2007). Comparative genomics: from genotype to disease phenotype in the leishmaniasis. *Int. J Parasitol.* 37, 1173-1186.
- Sorensen, A.L., Hey, A.S., and Kharazmi, A. (1994). *Leishmania major* Surface Protease Gp63 Interferes with the Function of Human Monocytes and Neutrophils In-Vitro. *Apmis* 102, 265-271.
- Spath, G.F., Epstein, L., Leader, B., Singer, S.M., Avila, H.A., Turco, S.J., and Beverley, S.M. (2000). Lipophosphoglycan is a virulence factor distinct from related glycoconjugates in the protozoan parasite *Leishmania major*. *Proceedings of the National Academy of Sciences of the United States of America* 97, 9258-9263.
- Stierhof, Y.D., Bates, P.A., Jacobson, R.L., Rogers, M.E., Schlein, Y., Handman, E., and Ilg, T. (1999). Filamentous proteophosphoglycan secreted by *Leishmania* promastigotes forms gel-like three-dimensional networks that obstruct the digestive tract of infected sandfly vectors. *European Journal of Cell Biology* 78, 675-689.
- Storch, S., Pohl, S., and Braulke, T. (2004). A dileucine motif and a cluster of acidic amino acids in the second cytoplasmic domain of the Batten disease-related CLN3 protein are required for efficient lysosomal targeting. *Journal of Biological Chemistry* 279, 53625-53634.
- Sturm, N.R. and Simpson, L. (1990). Kinetoplast DNA minicircles encode guide RNAs for editing of cytochrome oxidase subunit III mRNA. *Cell* 61, 879-884.
- Sun, F., Kanthasamy, A., Anantharam, V., and Kanthasamy, A.G. (2009). Mitochondrial accumulation of polyubiquitinated proteins and differential regulation of apoptosis by polyubiquitination sites Lys-48 and -63. *J Cell Mol Med.*

T

- Tazeh, N.N. and Bangs, J.D. (2007). Multiple motifs regulate trafficking of the LAMP-like protein p67 in the ancient eukaryote *Trypanosoma brucei*. *Traffic* 8, 1007-1017.
- Tetaud, E., Lecuix, I., Sheldrake, T., Baltz, T., and Fairlamb, A.H. (2002). A new expression vector for *Crithidia fasciculata* and *Leishmania*. *Mol. Biochem. Parasitol.* 120, 195-204.
- Thomas, S., Green, A., Sturm, N.R., Campbell, D.A., and Myler, P.J. (2009). Histone acetylations mark origins of polycistronic transcription in *Leishmania major*. *Bmc Genomics* 10, 152.

- Thompson,W.E., Ramalho-Santos,J., and Sutovsky,P. (2003). Ubiquitination of prohibitin in mammalian sperm mitochondria: possible roles in the regulation of mitochondrial inheritance and sperm quality control. *Biol Reprod.* 69, 254-260.
- Tobin,J.F. and Wirth,D.F. (1993). Mutational analysis of a signal sequence required for protein secretion in *Leishmania major*. *Mol Biochem Parasitol.* 62, 243-249.
- Torrentera,F.A., Glaichenhaus,N., Laman,J.D., and Carlier,Y. (2001). T-cell responses to immunodominant LACK antigen do not play a critical role in determining susceptibility of BALB/c mice to *Leishmania mexicana*. *Infect. Immun.* 69, 617-621.
- Triggs,V.P. and Bangs,J.D. (2003). Glycosylphosphatidylinositol-dependent protein trafficking in bloodstream stage *Trypanosoma brucei*. *Eukaryot. Cell* 2, 76-83.
- Turco,S.J. and Descoteaux,A. (1992). The Lipophosphoglycan of *Leishmania* Parasites. *Annual Review of Microbiology* 46, 65-94.
- Turco,S.J. and Sacks,D.L. (1991). Expression of a stage-specific lipophosphoglycan in *Leishmania major* amastigotes. *Mol Biochem Parasitol.* 45, 91-99.
- Turco,S.J., Spath,G.F., and Beverley,S.M. (2001). Is lipophosphoglycan a virulence factor? A surprising diversity between *Leishmania* species. *Trends in Parasitology* 17, 223-226.
- Tusnady,G.E. and Simon,I. (1998). Principles governing amino acid composition of integral membrane proteins: application to topology prediction. *J Mol Biol* 283, 489-506.
- Tusnady,G.E. and Simon,I. (2001). The HMMTOP transmembrane topology prediction server. *Bioinformatics* 17, 849-850.

U

- Ueda-Nakamura,T., Attias,M., and de Souza,W. (2001). Megasome biogenesis in *Leishmania amazonensis*: a morphometric and cytochemical study. *Parasitology Research* 87, 89-97.

V

- Vannier-Santos,M.A., Martiny,A., Lins,U., Urbina,J.A., Borges,V.M., and de Souza,W. (1999). Impairment of sterol biosynthesis leads to phosphorus and calcium accumulation in *Leishmania* acidocalcisomes. *Microbiology* 145 (Pt 11), 3213-3220.
- Vaughan,S., Wheeler,R., Palmer,R., and Gull,K. (2009). How do procyclic and bloodstream form *T. brucei* trypomastigotes divide? Abstract, Kinetoplastid Molecular Cell Biology conference (Woods Hole, April 2009).

- Vercesi,A.E., Moreno,S.N., and Docampo,R. (1994). Ca²⁺/H⁺ exchange in acidic vacuoles of *Trypanosoma brucei*. *Biochem J* 304 (Pt 1), 227-233.
- Vergnes,B., Sereno,D., Madjidian-Sereno,N., Lemesre,J.L., and Ouaiissi,A. (2002). Cytoplasmic SIR2 homologue overexpression promotes survival of *Leishmania* parasites by preventing programmed cell death. *Gene* 296, 139-150.
- Vince,J.E., Tull,D.L., Spurck,T., Derby,M.C., McFadden,G.I., Gleeson,P.A., Gokool,S., and McConville,M.J. (2008). *Leishmania* adaptor protein-1 subunits are required for normal lysosome traffic, flagellum biogenesis, lipid homeostasis, and adaptation to temperatures encountered in the mammalian host. *Eukaryot. Cell* 7, 1256-1267.
- von Heijne,G., Steppuhn,J., and Herrmann,R.G. (1989). Domain structure of mitochondrial and chloroplast targeting peptides. *Eur. J Biochem* 180, 535-545.
- Vowels,J.J. and Payne,G.S. (1998). A dileucine-like sorting signal directs transport into an AP-3-dependent, clathrin-independent pathway to the yeast vacuole. *EMBO J* 17, 2482-2493.

W

- Waller,R.F. and McConville,M.J. (2002). Developmental changes in lysosome morphology and function *Leishmania* parasites. *Int. J. Parasitol.* 32, 1435-1445.
- Wang,C.C., Bozdech,Z., Liu,C.L., Shipway,A., Backes,B.J., Harris,J.L., and Bogyo,M. (2003). Biochemical analysis of the 20 S proteasome of *Trypanosoma brucei*. *J Biol Chem.* 278, 15800-15808.
- Warburg,A., Tesh,R.B., and McMahon-Pratt,D. (1989). Studies on the attachment of *Leishmania* flagella to sand fly midgut epithelium. *J Protozool.* 36, 613-617.
- Webster,P. and Russell,D.G. (1993). The flagellar pocket of trypanosomatids. *Parasitol. Today* 9, 201-206.
- Weinheber,N., Wolfram,M., Harbecke,D., and Aebischer,T. (1998). Phagocytosis of *Leishmania mexicana* amastigotes by macrophages leads to a sustained suppression of IL-12 production. *European Journal of Immunology* 28, 2467-2477.
- Weise,F., Stierhof,Y.D., Kuhn,C., Wiese,M., and Overath,P. (2000). Distribution of GPI-anchored proteins in the protozoan parasite *Leishmania*, based on an improved ultrastructural description using high-pressure frozen cells. *J Cell Sci* 113, 4587-4603.
- Weise,F., Thilo,L., Engstler,M., Wiese,M., Benzel,I., Kuhn,C., Buhning,H.J., and Overath,P. (2005). Binding affinity and capacity of putative adaptor-mediated sorting of a Type I membrane protein in *Leishmania mexicana*. *Mol Biochem Parasitol.* 142, 203-211.

- Wen, W., Chen, L., Wu, H., Sun, X., Zhang, M., and Banfield, D.K. (2006). Identification of the yeast R-SNARE Nyv1p as a novel longin domain-containing protein. *Mol Biol Cell* 17, 4282-4299.
- Williams, M.A. and Fukuda, M. (1990). Accumulation of membrane glycoproteins in lysosomes requires a tyrosine residue at a particular position in the cytoplasmic tail. *J Cell Biol* 111, 955-966.
- Williams, R.A., Tetley, L., Mottram, J.C., and Coombs, G.H. (2006). Cysteine peptidases CPA and CPB are vital for autophagy and differentiation in *Leishmania mexicana*. *Mol. Microbiol.* 61, 655-674.
- Williams, R.A., Woods, K.L., Juliano, L., Mottram, J.C., and Coombs, G.H. (2009). Characterization of unusual families of ATG8-like proteins and ATG12 in the protozoan parasite *Leishmania major*. *Autophagy* 5, 159-172.
- Winter, G., Fuchs, M., McConville, M.J., Stierhof, Y.D., and Overath, P. (1994). Surface antigens of *Leishmania mexicana* amastigotes: characterization of glycoinositol phospholipids and a macrophage-derived glycosphingolipid. *J Cell Sci* 107 (Pt 9), 2471-2482.
- Worthey, E.A., Martinez-Calvillo, S., Schnauffer, A., Aggarwal, G., Cawthra, J., Fazelinia, G., Fong, C., Fu, G., Hassebrock, M., Hixson, G., Ivans, A.C., Kiser, P., Marsolini, F., Rickel, E., Salavati, R., Sisk, E., Sunkin, S.M., Stuart, K.D., and Myler, P.J. (2003). *Leishmania major* chromosome 3 contains two long convergent polycistronic gene clusters separated by a tRNA gene. *Nucleic Acids Res.* 31, 4201-4210.

Y

- Yang, W., Li, C.Y., Ward, D.M., Kaplan, J., and Mansour, S.L. (2000). Defective organellar membrane protein trafficking in Ap3b1-deficient cells. *J Cell Sci* 113, 4077-4086.
- Yonashiro, R., Ishido, S., Kyo, S., Fukuda, T., Goto, E., Matsuki, Y., Ohmura-Hoshino, M., Sada, K., Hotta, H., Yamamura, H., Inatome, R., and Yanagi, S. (2006). A novel mitochondrial ubiquitin ligase plays a critical role in mitochondrial dynamics. *EMBO J* 25, 3618-3626.
- Yoshimori, T. (2004). Autophagy: a regulated bulk degradation process inside cells. *Biochem. Biophys. Res. Commun.* 313, 453-458.

Z

- Zhang, K., Hsu, F.F., Scott, D.A., Docampo, R., Turk, J., and Beverley, S.M. (2005). *Leishmania salvage* and remodelling of host sphingolipids in amastigote survival and acidocalcisome biogenesis. *Mol Microbiol.* 55, 1566-1578.

